Identification and analysis of a novel nuclear role of Fibroblast Growth Factor 10 (FGF10)

Marta Mikolajczak

Candidate registration number: 100020636

Thesis submitted for the degree of Doctor in Philosophy

School of Biological Science
University of East Anglia
Norwich Research Park
Norwich, Norfolk
NR4 7TJ

June 2016

Dedication

To my dearest family,

who are always with me every step of the way.

Abstract

Fibroblast growth factor 10 (FGF10) is a paracrine molecule, serving crucial mesenchymal-to-epithelial signalling roles during development and postnatally. FGF10 binds specifically to FGF-receptor 2 IIIb (FGFR2-IIIb) and their interaction results in signal transduction pathways, which promote epithelial proliferation, motility and survival. Human heterozygous mutations in the Fgf10 gene result in LADD (lacrimo-auriculo-dento-digital) and ALSG (aplasia of lacrimal and salivary glands) syndromes, which to date have been solely attributed to perturbed FGF10 paracrine function. However, the molecular dynamics undelaying LADD-causing G138E FGF10 mutation, which falls outside its receptor interaction interface, has remained enigmatic. Moreover, Fgf10 is expressed within mouse hypothalamus, which is not accompanied by expression of its cognate receptor, signifying FGF10 may have additional intracrine function. In this study, FGF10 was investigated in a context of nuclear translocation and putative endogenous function within mesenchymal and hypothalamic cells. Through interrogation of FGF10's sequence and subcellular distribution, the protein was found to possess two putative nuclear localization sequences, termed NLS1 and NLS2, which were shown implicated in nuclear translocation of FGF10. Furthermore, the protein was found localising to the cell nucleolus. Subsequent examination of the LADD-causing G138E, through site-directed mutagenesis, revealed its curious positioning within NLS1 and its role in abrogation of both, nuclear and secretory function of the FGF10. Additionally, specific combinatorial mutations within NLS2 abolished the protein's nuclear translocation, yet did not diminish the protein's progression through the secretory pathway, showing importance of this motif in the nuclear transport of FGF10. Interestingly, endogenous FGF10 was shown to disrupt differentiation of mesenchymal chondrogenitors, whereas externally applied protein caused the opposite effect, promoting cell differentiation, suggesting contrary function of paracrine and nuclear FGF10. Moreover, novel culture of hypothalamic Fgf10 expressing tanycytes derived from transgenic mice was generated and characterised, showing that intracrine FGF10 may be potentially implicated in control of cell cycle of neural stem cells.

Acknowledgments

I feel very lucky as throughout my PhD I have received support and help from many people. They are all extremely important to me and I don't think I can express enough how much they mean to me and how much I value what they have done for me. I feel grateful to have you all in my life.

First and foremost, I would like to thank my supervisor Dr Mohammad Hajihosseini for his guidance, advice and enormous effort to support me throughout sometimes difficult times. I am grateful for his inspiring discussions and encouragement to reach higher than I thought I am capable of. His endless strength and determination were a constant source of inspiration to me and I feel privileged to be his student.

I would like to thank my colleague and dearest friend Dr Tim Goodman, who shared with me the best times as well as helped me to push through the challenges. His extensive knowledge, dedication to science and always positive spirit has been the biggest inspiration to me. I will be forever grateful for the many stimulating discussions, wiping of my tears, as well as time spent playing board games and eating pizza. I feel fortunate to have him as a friend. I would also like to thank my past and current lab members, Dr Christina Stratford and Ben Kaminskas, who have been absolute pleasure to work and socialize with. Thank you for your advice and help, all the fun times will not be forgotten and you will be very much missed. I also would like to thank amazing technical staff, with whom I had a pleasure to work: Benita Turner-Bridger, Andy Loveday and Shaun Clare. Thank you for your efforts to make my work run faster and smoother as well as for providing me with all these favours.

I am very grateful to my secondary supervisor Dr Mark Williams for many valuable comments and constant source of encouragement throughout all of my PhD studies. My sincere thanks to Professors Saverio Bellusci (Giessen, Germany), Tom Wileman, Penny Powell, Andrew Chantry (UEA, Norwich) for sharing constructs and antibodies. Thank you to past and current individuals working in BioMedical Research Centre (BMRC) and School of Biological Sciences, especially to Dr Jelena Gavrilovic, Dr Mette Mogensen and their lab teams, and all people from the "MED" group on floor 01, for their most generous attitude to share reagents, ideas and lab struggles. Thank you to Mr Georgios Iakovou and Dr Steven Hayward for their help with molecular docking system. Thank you to Dr Lee Wheldon for valuable input into last stages of my work and the wisdom he has passed onto me. Thank you to Paul Thomas for never failing to help with any microscope related issues and staff in DMU for their help to maintain our mice stock.

My special thanks to my great friends Ania Kowalewska, Camille Viaut, James O'Mullane and Kadri Oras. Thank you for always being here for me, listening to my

troubles and never failing to make me laugh. Thank you for all the lovely dinners, all those nights solving Sherlock's murder mysteries, sharing my passion for Agatha Christie novels and playing board games. Thank you for all these sparks of joy you have delivered to my PhD life.

From the bottom of my heart I would like to thank my family, who always have been supporting me at any stage of my life. Thank you for being with me every step of the way and always believing in me. Thank you for being understanding and massively supportive of all of my decisions. Thank you for giving me the strength to push on. I know that I have the best family anyone could have and would not be able to achieve what I have so far without them.

Last but not least, I would like to thank my partner Lukasz Czapranski, who has had invaluable input into my work. Thank you for being everything to me, thank you for being my strength, my support, thank you for your patience, for being my inspiration, for lifting me when I was low and for many other things I will not be able to express in words.

List of Figures

Chapter 1:

Chapter 2:

Chapter 3:

Chapter 4:

Chapter 5:

Chapter 6:

Chapter 7:

Chapter 1

Introduction

Cell activities and functions are governed by a complex system of communication and signals received from environment or generated intrinsically. Each cell possesses the ability to perceive and respond to their microenvironment, which is the sole basis of development and adult tissue homeostasis, and malfunctions result in syndromes, diseases and cancer. Biochemical signals (i.e. proteins, lipids, ions as well as gases) can be categorised basing on the distance between signalling and responder cells. Cells can communicate with each other via direct contact or over short distances, where signals are secreted into the extracellular matrix (ECM) and subsequently binding to a receptor present on a surface of an adjacent cell. Normally, thus activated receptor generates transduction signals, which often result in alteration of gene expression affecting cell survival, proliferation or motility. This is known as paracrine signalling, as the signals target cells in the vicinity of the emitting cell (Fig. 1.1A). In similar fashion cells can receive signals arising in distal parts of the body and travelling with the blood stream, which is referred to as endocrine signalling, typically associated with hormones. Additionally, cells can signal in an autocrine fashion (which is also known as self-signalling), through secretion of ligands that bind to the cell's own receptors (Fig. 1.1B).

Moreover, during autocrine signalling the ligands can also be endocytosed into the cell cytoplasm, either with or without its corresponding receptor, resulting in cytoplasmic signalling. Additionally, the secretory ligands can be translocated directly from the cytoplasm into the cell nucleus, acting in the intracrine fashion (Fig. 1.1C).

There is a broad range of signalling molecules and their target cells can be diverse. Malfunction and disruption to signalling pathways result in a variety of syndromes and disorders as well as cancer and aging. Therefore, detailed knowledge of the cell signalling mechanisms could result in identification of novel drug targets, treatment and prevention of diseases and cancer.

One of the major groups of signalling molecules are Fibroblast Growth Factors, known as FGFs.

Part 1.1 Introduction to the family of Fibroblast Growth Factors (FGFs)

1.1.1 Overview of FGFs

Fibroblast Growth Factors (FGFs) are known for their regulatory functions during development, tissue homeostasis and repair as well as maintenance of cell metabolism. They were first identified in early 70s, from pituitary extracts and shown to

stimulate proliferation in the 3T3 mouse fibroblast cell culture (Armelin, 1973, Gospodarowicz, 1974). FGFs are now known to belong to a large family of signalling molecules, comprised of 22 members (Fig. 1.2). They range in molecular mass from 17 to 34kDa and can be characterised by 13-74% amino acid conservation (Ornitz and Itoh, 2001). The protein sequence of the FGFs has a homologous core region that consists of 120–130 amino acids, ordered into 12 antiparallel β-strands (β1–β12) and flanked by divergent amino and carboxyl termini.

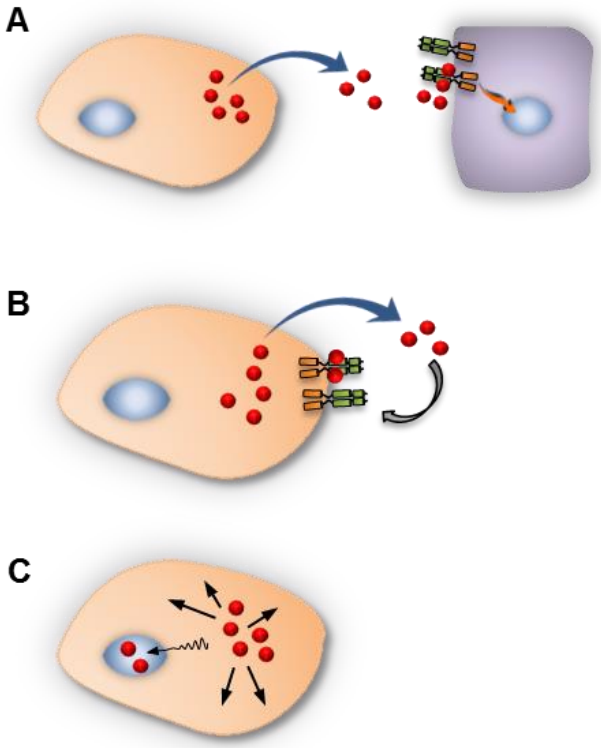

Figure 1.1 Schematic representations of cell signalling variations of secreted molecules. (A) Paracrine and endocrine signalling signifies secretion of a ligand by one cell targeting a receptor present on a surface of a different cell, triggering downstream signal transduction events. (B) During autocrine signalling a cell's receptors are activated by ligands they have secreted themselves. (C) Intracrine signalling takes place, when signals are produced within the cell itself, either within the cytoplasm or nucleus.

Importantly these flanking N- and C-terminal tails show the greatest sequence variation between FGFs, and therefore are responsible for the differences in biological properties of the ligands (Beenken and Mohammadi, 2009).

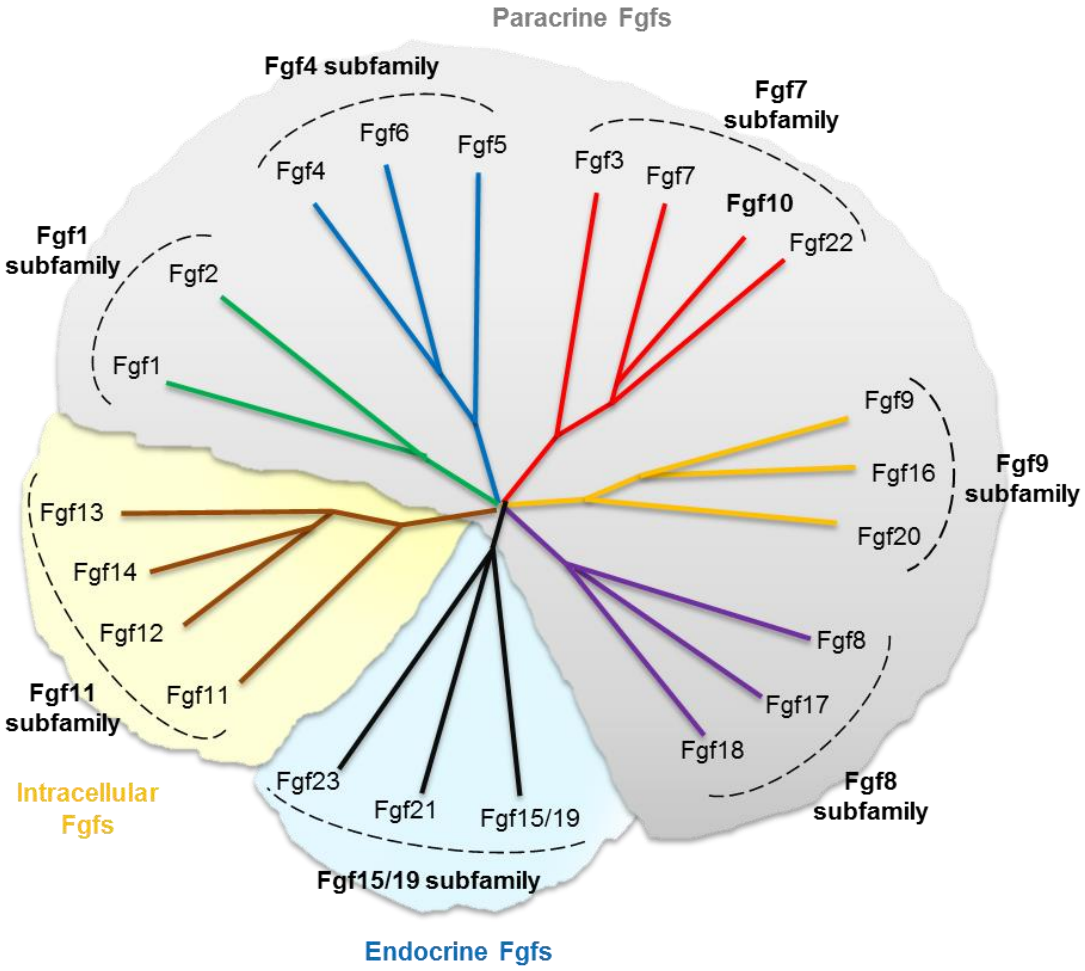

Figure 1.2 Schematic of phylogenetic tree of the Fgf family. The 22 members can be arranged into seven subfamilies. The members of Fgf1, Fgf4, Fgf7, Fgf8, and Fgf9 subfamily genes encode secreted paracrine ligands, which bind to and activate FGF receptors (FGFRs) with heparin as a cofactor, whereas members of the Fgf15/19 subfamily encode endocrine proteins, which bind to and activate FGFRs with the Klotho family protein as a cofactor. Members of the Fgf11 subfamily encode intracellular FGFs; contrary to others, these are non-signalling proteins, and majorly serve as cofactors for voltage gated sodium channels. Figure adapted from (Ornitz and Itoh, 2015).

Based on their biochemical, structural and functional properties, as well as sequence homology and phylogeny, FGF proteins are grouped into six subfamilies: Fgf1, Fgf4, Fgf7, Fgf9, Fgf8, Fgf15/19 (species specific) and Fgf11 (Fig. 1.2). Subfamilies of FGFs tend to have similar patterns of expression however each FGF has also some unique sites of expression. Moreover FGFs 3, 4, 8, 15, 17 and 19 are present mainly during embryonic development whilst others also function in the adult tissue (Ornitz and Itoh, 2001).

Most of the FGFs mediate biological responses by binding to and activating cell surface tyrosine kinase receptors, known as the FGFRs. The specific binding of a ligand to the receptor triggers particular downstream signalling pathways leading to expression of different genes (Fig. 1.4). Only the intracrine FGFs (FGF11, FGF12, FGF13 and FGF14), also known as FGF homologous factors 1-4 (FHF1-FHF4), act in the FGFR-independent manner. They are not secreted (Smallwood et al., 1996), therefore function intracellularly and are predominately expressed within the nervous system where they regulate diverse functions, such as the control of the voltage gated sodium channels (Goldfarb et al., 2007, Zhang et al., 2012).

1.1.2 Evolution of FGFs

FGFs are found in species of invertebrates and vertebrates but not in the single cell organisms like bacteria or yeast. While vertebrates are characterised by a large number of Fgf genes, only one Fgf-like gene (*branchless*) have been identified in *Drosophila melanogaster* (Sutherland et al., 1996) and two (egl-17 and let-756) in *Caenorhabditis elegants* (Burdine et al., 1997, Roubin et al., 1999).

Fgf genes tend to be scattered around the genome and distributed variably across multiple chromosomes, which are often not conserved among species. Several Fgfs however, have been found clustered on the same chromosomes, for example, Fgf3, Fgf4 and Fgf19 in humans are located on the 11q13 chromosome (Kim and Crow, 1998, Yoshida et al., 1988, Xie et al., 1999) and in mice on chromosome 7F (Peters et al., 1989); and are separated by no more than 40 to 80 kb. Similarly, Fgf6 and Fgf23 are both positioned on chromosome 12p13 in humans (Marics et al., 1989, Yamashita et al., 2000), separated by only 55 kb; and in mice on the chromosome 6F3-G1 (de Lapeyriere et al., 1990, Yamashita et al., 2000). Moreover human Fgf17 and Fgf20 are both present on chromosome 8p12-p22 (Xu et al., 1999, Kirikoshi et al., 2000). It has been suggested that such a gene clustering is a result of a historical gene duplication and translocation (Ornitz and Itoh, 2001).

Interestingly Fgf7, located in humans on chromosome 15, has been found amplified to approximately 16 highly related copies, which are dispersed around human genome. Moreover, they are transcriptionally active and undergo a tissue dependent regulation (Kelley et al., 1992). Similar number of copies Fgf7 were also found in several species of apes and monkeys suggesting implications of Fgfs during human evolution (Kelley et al., 1992).

The large gene number, their curious clustering on the chromosomes and variations in copy numbers has led to hypothesis that many Fgf genes arose due to

global gene duplications that took place during evolution of vertebrates (Ornitz and Itoh, 2001). Moreover, it is postulated that, FGFs did not arise from local duplication events, because FGFs which belong to same subfamilies and share most similarities are not clustered on the same chromosomes (Ornitz and Itoh, 2001).

1.1.3 Gene and protein organisation of FGFs

Most FGFs are encoded by three exons, where exon1 contains the AUG initiation start site. However there are several variations from this general pattern. Fgf2 and Fgf3 genes are transcribed from additional CUG codon, located in the 5' upstream region, generating proteins of various molecular weight, with different intracellular distribution and sometimes serving opposite function (Florkiewicz and Sommer, 1989, Arnaud et al., 1999, Kiefer et al., 1994a). In addition to the UTR, the exon1 itself can be a subject of multiple splicing variations as observed in Fgf8. In human and mice, the exon1 of Fgf8 is further subdivided into four sub-exons that undergo alternative splicing producing eight possible FGF8 isoforms (named "a-h"), that differ at their N-terminus. The FGF8 isoforms show diverse biological activity, are often expressed in different tissues and range in binding affinities to the receptors (Sunmonu et al., 2011). Similarly the intracellular Fgf11-14 (the FHFs) have two or more transcription initiation sites within their exon1, that give rise to proteins with different amino-terminal sequences (Goldfarb, 2005).

Conservation of Fgfs is reflected in proteins' structure and they share an internal core region characterised by 28 highly conserved residues of which at least six are invariant (Ornitz, 2000). Therefore, most FGFs adopt a β trefoil structure where approximately 12 β-sheets are arranged into four-stranded triangular manner (Ornitz, 2000). Most FGF molecules usually contain N-terminally located signal peptide (SP) sequence that targets the molecule to the secretory pathway. FGFs 1, 2, 9, 16 and 20 lack obvious secretory signals but are nevertheless secreted in a nonconventional manner (Miyamoto et al., 1993, Miyake et al., 1998, Barak et al., 2012, Kirov et al., 2015, Zacherl et al., 2015). Furthermore, the paracrine FGFs possess a receptor binding site and an additional region that is responsible for heparin binding.

Recent studies revealed that most secreted FGF proteins, at physiological conditions, exist mainly as unstable protein variants. FGF1 has been shown to have a limited half-life *in vivo* and about 50% of the protein exists in its unfolded state, prone to proteolytic degradation (Copeland et al., 1991), although introduction of specific mutations, was shown to increase the stability of the protein structure (Culajay et al., 2000, Zakrzewska et al., 2004). Limited ligand stability is thought to be linked to protein's biological activity, by restricting it to the neighbouring tissue and therefore

regulating the signalling potential through constraining the time of signal production. Additionally heparin sulphate was shown to influence FGF's turnover and in a pre-conditioned tissue culture medium at physiological temperature, binding of heparin stabilises the protein structure in majority of paracrine FGFs (FGF1–4/6–9/16–18/20/22), in the exception of FGF10, which rapid degradation is independent of the presence of heparin (Buchtova et al., 2015). However heparin and other polyanions, such as sucrose octasulfate (SOS), and inositol hexaphosphate (IHP), as well as negatively charged liposomes, increase thermo-unfolding of FGF10 by 9-15ºC, which was proposed to play a role in a protein transport events (Derrick et al., 2007).

The importance of appropriate regulation of FGF stability is further shown by the pathological signalling of FGF23. Mutations within FGF23 that generate protein resistant to degradation, result in human hypophosphatemic rickets (ADHR) (White et al., 2001) and familial tumoral calcinosis (FTC) (Kato et al., 2006).

1.1.4 The FGF Receptors

Secreted FGF ligands bind to and activate FGF Receptors (FGFRs). There are 4 known FGFRs, that belong to the family of tyrosine kinase (TK) transmembrane receptors, which are composed of ~800 amino acids and located within cell membrane. The extracellular, ligand binding part of the FGFRs is composed of three immunoglobulin (Ig)–like domains (D1-D3) and a heparin binding region. FGFRs are anchored within the cell membrane by a single transmembrane helix and extend into the cell cytoplasm with a split TK domain (Fig. 1.3 & 1.5).

The Ig-like domains play a crucial role in FGF signalling. The D2 and D3 form the ligand-binding pocket and determine the affinity and specificity for the FGF and heparan sulphate proteoglycans (HSPGs) (Chellaiah et al., 1999). On the other hand, D1 is considered a negative regulator of the FGF signalling. It was shown that mutant receptors, lacking the D1 module, show higher affinity for the ligand and heparin binding than the full 3 domain receptors (Olsen et al., 2004). Moreover, D1 domain is an auto-inhibitor of FGFR-FGF signalling, as it binds the D2 in the ligand/heparin pocket thus competing with the FGF molecules for the D2 interaction. This auto-inhibition serves two roles: primarily it further regulates FGF signalling and secondary, it prevents receptor self-activation through spontaneous FGFR dimerization through D2-D2 interaction (Kiselyov et al., 2006).

Moreover, FGFRs contain an acidic amino acid motif, called an 'acid box', which is a serine rich sequence in the linker region between the D1 and D2 domain (Fig. 1.3). Presence of the receptor's acidic box aids the ligand binding regulation function of the D1 domain. Its importance is highlighted in neural cells, where it is

involved in the stabilisation of a cell surface receptor, providing interaction with N-cadherin and neural cell adhesion molecules (NCAMs) (Sanchez-Heras et al., 2006), and modulating neurite outgrowth (Cavallaro et al., 2001).

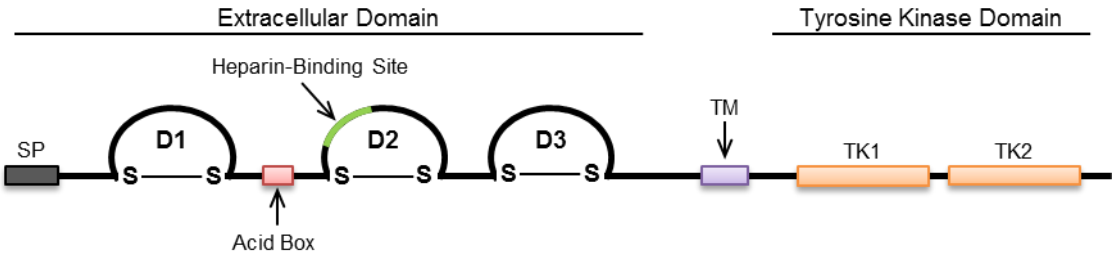

Figure 1.3 Representation of the basic structure of FGFR, showing the three extracellular immunoglobulin-like domains (D1, D2 and D3), indicating the position of the acid box (red) and heparin binding site (green). FGFR possesses a cleavable signal peptide (SP) targeting the protein to the membrane, anchored there via transmembrane domain (TM) and leaving two intracellular tyrosine kinase domains (TK1 and TK2) located within cell cytoplasm.

The D3 domain is encoded by three exons named the IIIa, IIIb and IIIc. The exon IIIa is invariant, but exons IIIb and IIIc undergo alternative splicing, resulting in two different isoforms of the receptor (Fig. 1.4A). The isoforms differ significantly in their ligand binding specificity and are transcribed in a tissue-specific manner. In general the IIIb isoform is expressed on a surface of epithelial cells, whilst the IIIc isoforms is present on the mesenchymal cells (Miki et al., 1992, Orr-Urtreger et al., 1993, Ornitz and Itoh, 2015). Each FGF binds to either, epithelial or mesenchymal FGFR, with the exception of FGF1 that interacts with both receptor splice isoforms (Zhang et al., 2006) (Fig. 1.4B). There are four FgfR genes but only FGFR1-3 are alternatively spliced (Partanen et al., 1991).

Other identified splice variants of FGFRs include Fgfr1 encoding only D2 and D3, generating a secreted protein which was shown to act as FGF signalling inhibitor (Duan et al., 1992). Moreover, an isoform of Fgfr3, lacking the transmembrane domain encoding exons 8 to 10, also generates a secreted protein variant, that inhibits the signalling pathways through binding the FGF ligands (Terada et al., 2001, Tomlinson et al., 2005). Furthermore, a novel membrane bound FGFR was identified, called the FGFR5 or FGFRL1 (Fig. 1.5), that contains either three (FGFR5β) or two (FGFR5γ) extracellular Ig domains, but lacks the TK domain. It is able to bind with low affinity the

FGF2 ligand (but not members of the FGF7 subfamily) (Sleeman et al., 2001). Moreover, FGFRL1 has been found expressed in the adult pancreatic tissue, where it enhances ERK1/2 signalling (Silva et al., 2013).

A

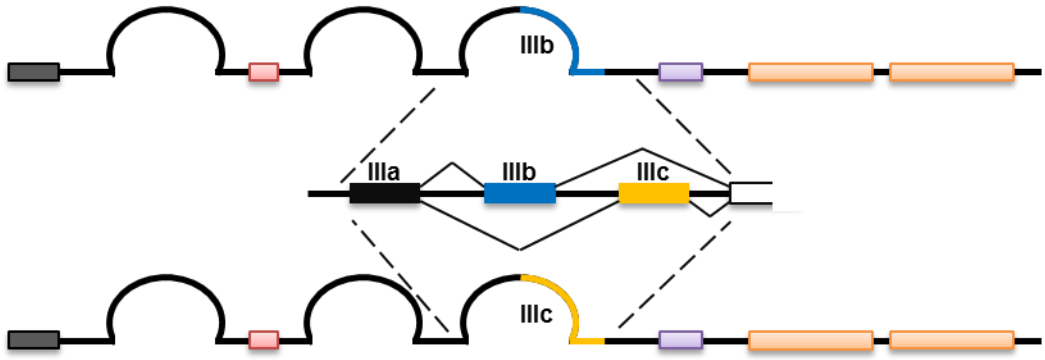

B

FGF subfamily	FGF	Cofactor	Receptor specificity
FGF1 subfamily	FGF1		All FGFRs
	FGF2		FGFR 1c, 3c > 2c, 1b, 4Δ
FGF4 subfamily	FGF4		
	FGF5		FGFR 1c, 2c > 3c, 4Δ
	FGF6		
FGF7 subfamily	FGF3	+ Heparin or Heparan Sulphate	
	FGF7		FGFR 2b > 1b
	FGF10		
	FGF22		
FGF8 subfamily	FGF8		
	FGF17		FGFR 3c > 4Δ > 2c > 1c >> 3b
	FGF18		
FGF9 subfamily	FGF9		
	FGF16		FGFR 3c > 2c > 1c,3b >> 4Δ
	FGF20		
FGF15/19 subfamily	FGF15/19	+β Klotho	FGFR 1c, 2c > 3c, 4Δ
	FGF21		FGFR 1c, 3c
	FGF23	+α Klotho	FGFR 1c, 3c, 4

Figure 1.4 Specificity of the ligands to the receptors. (A) The immunoglobulin-like domain 3 (D3) of the receptors Fgfr1–Fgfr3 is encoded by three exons (a,b and c), where the first (a) is invariant, but second and third are alternatively spliced, generating either IIIb or IIIc isoforms. These are major determinants of ligand-binding specificity and expressed in a tissue specific manner. (B) Table showing the ligand to receptor specificity, which use either heparin/Heparin Sulphate or Klotho molecules as cofactors for the binding. The FGF7 subfamily (red) shows exclusiveness to the FGFR2IIIb binding (and with a lesser degree binds to the FGFR1IIIb). Figure modified from (Ornitz and Itoh, 2015).

The FGF-FGFR form a 1:1 complex (Schlessinger et al., 2000) through a strong network of H-bonds. However, activation of the receptor takes place only when two units of FGF-FGFR form a dimer. These are juxtaposed in a symmetrical complex fortified by binding of heparan sulphate glycosaminoglycans (HSGAG), together generating a ratio of 2:2:1 of FGF-FGFR-HSGAG (Harmer et al., 2004). In the complex, the two receptors form direct bonds between each other; moreover, each FGF ligand interacts with both receptors – in addition to the main interaction with the primary receptor, each FGF was found to bind within D2 of the second receptor through the 'receptor secondary binding site'. The HSGAG facilitates formation of the complex by simultaneously binding the ligand and the receptor, through a canyon of basic residues shaped by the complex itself, therefore stabilizing the multivalent protein binding interactions (Ibrahimi et al., 2005). The dimerization of FGFRs enables their cytoplasmic TK domains to transphosphorylate (therefore activate) and interact with phospholipase C (PLC) γ1 (or FRS1) and FGFR substrate 2 (FRS2), triggering further downstream pathways, resulting in the modification in cells' gene expression (Fig. 1.5).

1.1.5 Major regulators of FGF signalling

The FGF signalling plays key regulatory roles during development and in the adult, therefore it requires a tight control itself, executed by a plethora of molecules. These can be promoting or inhibiting and can be either ligand or receptor specific as well as of a more general function.

One of the major regulators of the FGF signalling is protein expressed by the Kal1 gene, called anosmin-1 (An1). An1 binds to heparan sulphate (HS) present on cell surface within ECM. It has a dual effect on modulation of FGF signalling. In the presence of HS, An1 can act as an amplifier of the endogenous and exogenous FGF signals. However free An1 (not-bound to HS) directly interacts with FGFRs, which prevents formation of active FGF-FGFR complex (Hu et al., 2009, Korsensky and Ron, 2016).

Another important modulator of FGF signalling is FGF-binding protein (FGF-BP), known as a carrier and bio-activator of FGFs. It functions by releasing the ligands from the HSGAG binding, trapped within the ECM, therefore making them more accessible to the receptor. Its expression is closely regulated in a tissue specific manner and it plays main role during embryogenesis and wound healing. The importance of FGF-BP is highlighted by its high expression in most squamous cell carcinoma and upregulation in breast, colon and prostate cancer (Abuharbeid et al., 2006). FGF-BP binds to FGF2 in a specific dose-dependent manner that can be inhibited by FGF1, heparansulphate and heparinoids (Tassi et al., 2001).

Fibronectin leucine-rich transmembrane protein 3 (FLRT3), is also a protein known as a major activator of FGF signalling (Fig. 1.5). FLRT3 is co-expressed with the FGFs, meaning that its expression is induced during the FGF signalling and down-regulated when the FGF signalling is inhibited. FLRT3 interacts with the FGFRs and acts as the transmembrane facilitator of the FGF induced MAP kinase pathway (Bottcher et al., 2004).

An important inhibitor of the FGF signalling is protein similar expression to *fgf* genes (SEF) (Fig. 1.5). Although the expression of Sef gene itself is induced by the FGF signalling, it attenuates the FGF-induced Ras/MAPK pathway, in a species specific manner. SEF possesses two splice forms, both capable of inhibiting the ERK phosphorylation: one, membrane-bound, directly interacts with the FGFRs and acts independently of the ligand binding (Tsang et al., 2002) and second, which is confined to the cytoplasm and can inhibit FGF-mitogenic activity via an ERK-independent mechanism (Kovalenko et al., 2003, Tsang and Dawid, 2004). SEF-regulation of FGF signals plays key roles, for example during embryogenesis SEF is involved in establishment of the body axis, and postnatally SEF regulates FGF-mediated cell proliferation (e.g. of osteoprogenitors) (Korsensky and Ron, 2016).

Another key inhibitor of FGF induced MAPK signalling, is the sprouty family of proteins (SPRY), which act through generation of a negative feedback loop (Fig. 1.5). FGFs activate SPRYs, which indirectly prevent ERK phosphorylation through interaction with growth factor receptor-bound protein 2 (GRB2), son of sevenless (SOS1) and RAF1 (Ozaki et al., 2005, Mason et al., 2004). Moreover, the MAP kinase phosphatase 3 (MKP3), through dephosphorylation of ERK also antagonises the FGF signalling (Fig. 1.5). It is important regulator of the FGF and retinoic acid (RA) signalling during organogenesis (Le Bouffant et al., 2012, Li et al., 2007).

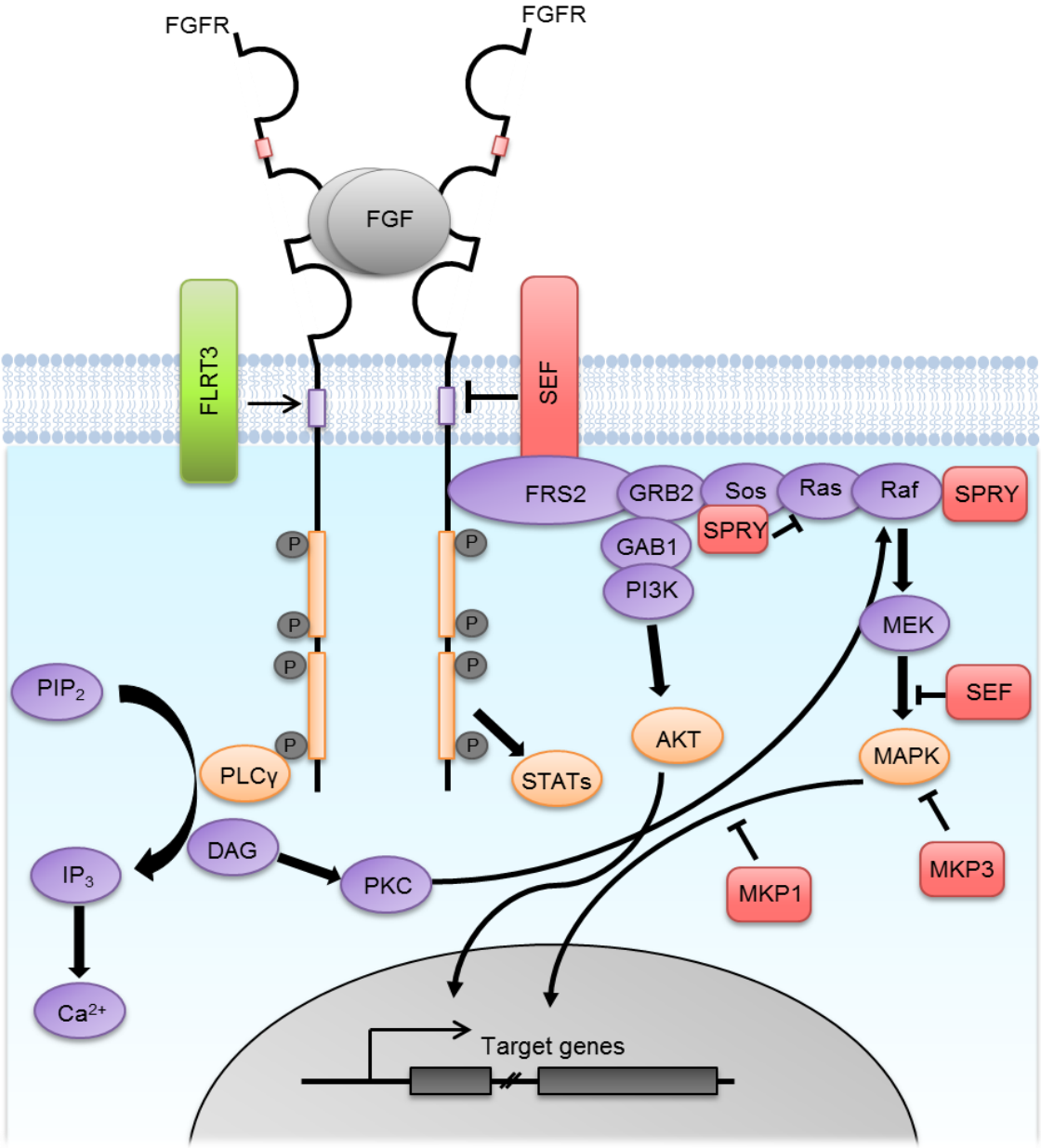

Figure 1.5 Schematic of intracellular signalling transduction pathways induced by FGF-FGFR. Ligand binding to the receptor promotes complex dimerization, resulting in the receptors' kinase domains mutual transphosphorylation. This activates RAS/MAPK and P13K-AKT signalling pathways (resulting in expression of target genes), as well as induction of signal transducer and activator of transcription (STAT) and phospholipase Cγ (PLCγ) (orange boxes). Negative regulation of the signalling is achieved through binding of SEF, SPRY, MAPK phosphatase 1 (MKP1) and MKP3 (red boxes). Other components of the pathways include: FRS2, GRB2, SOS, protein kinase C (PKC), inositol trisphosphate (IP3), phosphatidylinositol-4,5-bisphosphate (PIP2), diacylglycerol (DAG) (purple boxes). Figure adapted from (Turner and Grose, 2010).

Part 1.2 Introduction to Fibroblast Growth Factor 10 (FGF10)

1.2.1 Overview of FGF10's subfamily – the FGF7 subfamily

FGF10, together with FGF3, FGF7 and FGF22 forms the FGF7 subfamily of paracrine ligands (Fig. 1.2). FGF3 is considered a member of this subfamily, based on its phylogenetic and functional properties, however, interestingly its chromosome localisation indicates association with FGF4 and FGF6 (Itoh and Ornitz, 2004). FGF7 and FGF10 play a major role during wound healing, in the epidermal cells called Keratinocytes, and therefore they are also known as Keratinocyte Growth Factors (KGFs) (Marchese et al., 2001, Komi-Kuramochi et al., 2005). Importantly, unlike other FGFs, members of the FGF7 subfamily are expressed and secreted by mesenchymal cells and bind on the adjacent epithelial cells, generating (a unique to this subfamily) mesenchymal-to-epithelial (MTE) signalling (Nakao et al., 2013). Other paracrine FGFs act in an opposite fashion, creating an epithelial-to-mesenchymal (ETM) signals (Ornitz and Itoh, 2015). Moreover the characteristic of the FGF7 subfamily is an exclusive specificity of its ligands for the FGFR2IIIb and none of the other FGFs activate this receptor spliceform (Zhang et al., 2006) (Fig. 1.4). As most paracrine ligands, FGF7 subfamily members have high affinity for HSGAG, (hence act in a localized manner, near the source of their expression), but they differ between each other in the strength of that affinity, which is linked to their differential biological function (Beenken and Mohammadi, 2009, Makarenkova et al., 2009).

Despite high conservation and structure similarities, members of FGF7 subfamily possess individual biological functions and properties. FGF7 is implicated in wound healing, because in skin injury the Fgf7 expression becomes significantly upregulated (Werner et al., 1992) and it is thought to stimulate keratinocyte proliferation (Dlugosz et al., 1994) and migration (Karvinen et al., 2003) resulting in wound reepithelialization. Moreover, FGF7 is involved in growth, development and differentiation of hair follicle (Danilenko et al., 1995). Interestingly, FGF7 knockout mice are viable and fertile with minor abnormalities, i.e. matted hair (Guo et al., 1996) and reduction in nephron branching in kidney (Qiao et al., 1999).

FGF3 is a major player in inner ear development and homozygous deletions of FGF3 in humans lead to hereditary deafness and total inner ear agenesis (Tekin et al., 2007). Moreover knockout mice often do not survive till adulthood and also show severe defects in inner ear development as well as display tail abnormalities (Mansour et al., 1993).

Unlike other members of the family, the FGF22 knockout mice are viable and fertile, without any obvious abnormalities (Jarosz et al., 2012). In the adult mouse FGF22 is expressed in skin, tongue, as well as brain tissue (Beyer et al., 2003). Although FGF22 is dispensable within normal and “an unchallenged” tissue (Jarosz et al., 2012), it has a key regulatory role in synaptogenesis (Terauchi et al., 2010, Terauchi et al., 2015) and in circuit remodelling in the injured spinal cord (Jacobi et al., 2015).

Although each member of the FGF7 subfamily has a unique role, they display high level of redundancy and often compensate for the lack of one another; therefore FGF7 and FGF22 knock out mice do not display obvious defects. Moreover their function is often interlinked, e.g. FGF3 and FGF10 act collectively to induce the otic placode (Wright and Mansour, 2003).

1.2.2 Genomic localisation and control of Fgf10 expression

FGF10 was first identified in 1996 from a rat brain (Yamasaki et al., 1996), displaying high homology to FGF3 and FGF7 proteins. Soon after Fgf10 clones were also derived from human (Emoto et al., 1997) and mouse (Beer et al., 1997) genomes. The genomic localisation of Fgf10 is not conserved among vertebrate species – in humans it is found on a chromosome 5 (Emoto et al., 1997, Bagai et al., 2002), in mice on chromosome 13 (Crackower et al., 1998) and in rats on a chromosome 2. In all species however structure of the Fgf10 gene consists of three exons separated by one large and one small intron (Chioni and Grose, 2009) (Fig. 1.6).

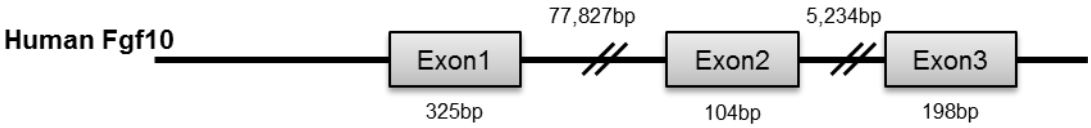

Figure 1.6 Representation of genomic structure of human Fgf10 locus positioned on a chromosome 5. The promoter region upstream of the ATG transcription site is still under scientific scrutiny however, it is known to comprise multiple regulatory enhancer elements (see text below). FGF10 is encoded by three exons, separated by two introns, which layout is conserved among vertebrate species.

There is a discrepancy within the scientific literature regarding the exact positioning of the Fgf10’s promoter. The genomic sequence upstream of the ATG transcription start site does not contain a canonical promoter TATA box. An insertion of

lacZ gene 114kb upstream of the Fgf10 translational start site generates an expression of the reporter within domains that correspond to the Fgf10 expression patterns. Therefore majority of the regulatory elements driving the Fgf10 expression were not disturbed and therefore are likely to be placed within this 114kb region (Kelly et al., 2001, Hajihosseini et al., 2008). There is a possibility that there is no unique promoter region and expression of Fgf10 is driven by a magnitude of specific enhancers acting in a spatio-temporal manner.

The 5' region, 6.6kb upstream of Fgf10 transcription start site is well conserved (up to 75%) between human, mouse and chicken genomes (Ohuchi et al., 2005). Moreover, bioinformatics tools predict that within this region lay multiple binding sites for at least 37 transcription factors, including MSX, SOX5, LHX3, NKX25, LEF1, AP1, PAX6, ISL1, FAST1, GATA2 and GATA3 (Ohuchi et al., 2005). Several other binding sites were recognised in human, mouse and chick Fgf10 promoter located 2kb upstream of the translational start site. These include NFAT, MYT1, COUP, CMYB, VMYB, ETSF, GFI1, PIT1, AP1F, MZF1, EGRF, AREB, AP4R, PAX5, OCT1, COMP, and FKHD. Moreover within the 0.7-0.2kb upstream region lays an enhancer specific for the limb cartilage expression (Sasak et al., 2002). The bioinformatics provides a strong research base; however the Fgf10 expression is mediated in a time and tissue specific manner, with a degree of tissue-related enhancer's sites redundancy, which requires experimental investigation.

The 5' RLM-RACE experiments investigating mouse embryonic RNA extracted from a lung tissue revealed, that a start site for the Fgf10 transcription is located 1001bp (~1kb) upstream of the protein translation start site, in a GC-rich region. This promoter region contains binding sites for polyoma enhancer activator 3 (PEA3), that was shown to negatively regulate expression of Fgf10. Authors of this work however, have not claimed this to be an exclusive regulatory region of the Fgf10 expression (Chioni and Grose, 2009) suggesting a possibility of additional regulatory sites for Fgf10's expression.

Moreover, within 6.5kb of genomic DNA upstream of the Fgf10 there are three T-box transcription factor 5 (TBX5) binding sites (GTGTGA), homologous between mouse and rat species. Moreover, TBX5 has been shown to directly activate the Fgf10 gene in order to drive the induction of an outgrowth of a limb bud (Agarwal et al., 2003). Interestingly, these TBX5 binding sites are utilised by the TBX1 to drive the Fgf10 expression during heart development, specifically during differentiation of myocardial precursors (Xu et al., 2004). Furthermore, a single consensus (β catenin activated) T-cell factor/lymphoid enhancer factor TCF1/LEF1 binding site (TTCAAAG) was discovered in mouse and human Fgf10, within the same 6.5kb promoter region, implicating Wnt signalling in a control of Fgf10 expression (Agarwal et al., 2003).

Interestingly, there have been identified numerous binding sites for a nuclear factor kappa-light-chain-enhancer of activated B cells (NF-κB), within region of 5.9kb upstream of the Fgf10, but the NF-κB does not interact with any of them (Benjamin et al., 2010). Furthermore, this Fgf10 genomic region also contains multiple guanosine-cytosine boxes (GC boxes), promoting binding of specificity protein 1 (Sp1) family transcription factors, and driving Fgf10 expression in the foetal lung mesenchyme, that is then in turn inhibited by NF-κB binding to Sp1 (Benjamin et al., 2010). Another protein that controls expression of Fgf10 within developing lung mesenchyme is Pre-B-cell leukaemia transcription factor 1 (Pbx1). The ChIP assay revealed five Pbx1 binding sites within 4kb upstream of Fgf10 and the gene activation is further enhanced by Pbx1 interactions with Meis and Hox proteins (Li et al., 2014b).

Furthermore, three binding sites of trans-acting T-cell-specific transcription factor GATA3 (GATA3) were found present within 1.4kb upstream of the Fgf10 (Economou et al., 2013), corresponding to the bioinformatics predictions (Ohuchi et al., 2005). Curiously, reporter assays analysis revealed that only one of these sites is crucial to control Fgf10 expression throughout the development of an inner ear (Economou et al., 2013), but the other two might be stimulated in different tissues. During limb development the transcription of Fgf10 was shown to be controlled through an evolutionarily conserved *cis*-regulatory 'AGAAAR' element. This cluster serves as binding site for the ETS translocation variant1 (Etv1) *trans*-acting factor, which in cooperation with EWS RNA-Binding Protein1 (Ewsr1), regulates Fgf10 promoter activity generating mesenchyme-specific expression of Fgf10 in the limb buds (Yamamoto-Shiraishi et al., 2014).

Expression of Fgf10 is differentially controlled in a spatio-temporal manner. For example artificially increased Wnt signalling from epithelium (through overexpression of β-catenin) was shown to reduce Fgf10 expression in in pancreatic mesenchyme (Heiser et al., 2006). However, in the lung tissue overexpression of Wnt5a within the epithelium increases the Fgf10 expression in the mesenchyme (Li et al., 2005). Furthermore, it was shown that in the developing prostate, treatment with TGFβ1 downregulated the expression of Fgf10 in the ventral mesenchymal pad, but not in the urethra. This regulation was achieved through TGFβ1-specific promoter element located between nucleotides -182 and -172, which additionally contained a consensus Sp1 binding site (Tomlinson et al., 2004).

Importantly, the regulatory elements driving the Fgf10 expression are also located downstream of the transcription start site, within the exonic and intronic regions. Several binding sites are located within the first intron, that allow interactions of Smad4, Nkx2.5, Tbx5 and Isl1 transcription factors. Disruption of these sites by insertion of Cre-ERT2 cassette reduces transcript levels of the Fgf10 (El Agha et al.,

2012). Furthermore, during development of human heart, the insulin gene enhancer protein 1 (Isl1) does not associate with the bioinformatics' predicted Isl1-binding sites within the Fgf10 promoter region (Ohuchi et al., 2005), but it does interact, in a tissue-specific manner, with a region within the first intron (327bp) (Golzio et al., 2012, El Agha et al., 2012). Treatment with retinoic acid (RA) was shown to increase expression of Fgf10 in mouse lung-specific mesenchymal cell line and decrease in non-lung-derived NIH3T3 cells, through selective activation of enhancer located within 1kb downstream and 3kb upstream of the putative transcription start site (Jean et al., 2008).

1.2.3 FGF10 protein structure

FGF10 displays high protein sequence homology between species of vertebrates, with 91-96% amino acid conservation between human, mouse and rat (Yamasaki et al., 1996, Beer et al., 1997, Igarashi, 1998). Full size of FGF10 protein ranges from 23-26kDa; human FGF10 corresponds to 208 amino acids (Igarashi, 1998), mouse FGF10 is 209 amino acids (Beer et al., 1997) and rat FGF10 protein is composed of 215 amino acids with an intriguing long serine-repeat positioned at the N-terminus (Emoto et al., 1997). The serine-repeat is a unique feature, not found in any other species however also noticed in FGF5 (Goldfarb et al., 1991); its function might be linked to regulation of *O*-type glycosylation status, but it requires further investigation (Yamasaki et al., 1996). Interestingly, it has been predicted that mRNA of FGF10 might possess a second translational site at Met position 42 (of rat sequence) generating a protein of 19.2kDa however, the potential function of this isoform has not been described yet (Lu et al., 1999).

FGF10's crystal structure was determined in 2003 from which it was established that the protein adopts a β-trefoil fold structure consisting of 12 β-strands (Yeh et al., 2003, Derrick et al., 2007). The first 35-40 amino acids of the FGF10 N-terminus are hydrophobic and correspond to a secretory signal peptide (SP) (Yamasaki et al., 1996, Emoto et al., 1997, Lu, 1999). FGF10 is unstable at physiological temperature (37.5ºC) and it undergoes thermal unfolding as well as shows presence of secondary and tertiary structures that change concurrently (Derrick et al., 2007). However, the protein structure is stabilised by binding to polyanions, such as heparin (Derrick et al., 2007, Buchtova et al., 2015). Low stability of all FGFs and limited half-life is thought to be a regulatory system, allowing time-restricted and therefore controlled signalling (Buchtova et al., 2015). Recombinant FGF10, stabilised by binding to heparan sulphate, can form dimers which show low stability at physiological temperature. The

stability of these dimers as well as other bigger aggregates (that have a potential of forming) increases with temperature below or above 37.5ºC however, it is unknown whether these have any functional properties (Derrick et al., 2007).

From comparison of protein structures it was shown that the β1 strand of FGF10 is longer than in FGF1 and FGF2. This extension provides a unique to FGF10 (as well as other members of its subfamily) conformation of the β1-β2 and β9-β10 loops, that is not found in other FGFs. Moreover the β10/β11 strand pair of FGF10 is defined by a single hydrogen bond between the two strands. The N-terminus of receptor-bound FGF10 is substantially more ordered than receptor bound N-terminus of FGF1 or FGF2, and the first five ordered residues in FGF10 form a short helix which connects to β1 via a short loop. These unique structural characteristics of the FGF7 subfamily members determine their specificity for the FGFR2IIIb splice isoform (Yeh et al., 2003).

Further analysis of human protein FGF10-FGFR2IIIb complex crystal structure revealed that FGF10 forms specific and extensive contacts with the cleft of the D3 domain of the FGFR2IIIb, of which most are direct or water mediated H-bonds. Sites of FGF10 that are known to interact with its cognate receptor are: the short helix at the N-terminus of the protein, the β1, β4 and β8 strands and the β7-β8 loop (Yeh et al., 2003). Furthermore, two highly specific bonds form between FGF10 Aspartate at position 76 (D76) and FGFR2IIIb Serine residue at position 315 (S315). The D76 is unique to FGF7 subfamily (being present also in FGF7 and FGF22) and the S315 is specific to the “b” isoform of the FGFR2, therefore bonds between these residues underscore the high specificity of the ligands to the receptor. Mutations of the D76 or S315 introduced to the ligand or receptor result in loss of the specificity and significant reduction or loss of the binding (Yeh et al., 2003). In addition, binding of FGF10 generates three H-bonds with the D2 domain of the receptor, simultaneously introducing a 40º rotation of the D2 domain, which further confers the ligand to receptor specificity (Yeh et al., 2003). Within a controlled system FGF10 and FGF7 exhibit similar affinity towards the receptor and compete with each other for the binding (Igarashi, 1998, Lu, 1999). Recombinant FGF10 and FGF7 ligands, applied at high concentration can also bind the FGFR1IIIb isoform, but with much lower affinity than other FGFs (Lu, 1999, Zhang et al., 2006). This interaction with FGFR1IIIb has not been confirmed to take place under the normal physiological conditions, yet.

The paracrine functioning of FGF10 is also linked to its affinity to herapan sulphate. This ubiquitously present component of proteoglycans is found on cell surfaces, in extracellular matrix as well as at basement membranes. It has divergent sulphation patterns (including 2-*O*-sulphation and 6-*O*-sulphation), which determine its binding properties with other molecules and can be directly translated onto a diverse

functions it serves (Ashikari-Hada et al., 2004). FGF10 is specific to the 6-*O*-sulphation of heparan but not the 2-*O*-sulphation, whereas FGF7 requires both (Ashikari-Hada et al., 2004). This might result in a fact that FGF10 has a higher affinity for immobilized heparin comparing to FGF7. Moreover the pericellular matrix of epithelial cells exhibits 4 times more heparan binding sites for FGF10 than for FGF7 (Lu et al., 1999). The difference in the affinity for heparan sulphate reflects the differential function these ligands serve. Mutations of Hs6st (a 6-*O*-sulfotransferase that adds sulfate groups to the C-6 carbon of the glucosamine residues of heparan) results in the lack of formation of lacrimal glands, a phenotype observed also in the FGF10 but not in FGF7 knockout mice, further suggesting that FGF10 and Hs6st operate in the same signalling pathway (Qu et al., 2011). During branching morphogenesis of the developing lacrimal and salivary gland epithelium buds, the variation of the binding affinity between FGF10 and FGF7 dictates their function. FGF10 is restricted to a domain adjacent to the tips of epithelial buds and is responsible for the bud elongation, whilst FGF7 is more diffuse and introduces branching (see section below) (Fig. 1.9). The distribution pattern and function of the proteins is controlled by the binding to heparan sulphate. FGF10 mutant in the heparan sulphate binding site, can mimic the expression pattern and function of FGF7 within the growing epithelial bud (Makarenkova et al., 2009).

Part 1.3 Tissue specific function of FGF10 during development and in an adult

Formation of a fully functioning organism from a single cell requires a tight spatio-temporal regulation of all the components involved. FGF10 is a well-known inducer of tissue morphogenesis during embryonic development. Particularly, FGF10 stimulates the limb outgrowth as well as branching morphogenesis of lungs, limbs, lacrimal and salivary glands, teeth as well as formation of inner ear, eye structures and many more. Importantly Fgf10 expression has been found in mouse hypothalamus, which is not accompanied by expression of its cognate receptor (Hajihosseini et al., 2008), and function of the protein in this tissue is still under investigation (see Chapter 6).

Fgf10 knockout mice do not survive beyond birth due to impaired lung development and additionally suffer from an absence of salivary, thyroid and pituitary glands, with minor defects in the formation of teeth, kidneys, hair follicles and digestive organs and are characterised by a lack of limbs (Min et al., 1998, Ohuchi et al., 2000, Sekine et al., 1999, Steinberg et al., 2005). Furthermore, insufficiency of FGF10 signalling affects lacrimal and salivary glands and ducts, ears, teeth, distal limb segments, which was shown both, in mice and humans. Heterozygous mutations within

the human FGF10 gene can result in an autosomal dominant aplasia of lacrimal and salivary glands (ALSG) and autosomal dominant lacrimo-auriculo-dento-digital (LADD) syndromes (Entesarian et al., 2007, Milunsky et al., 2006), which was explored further in Chapter 4 (see part 4.2).

Interestingly, elevated levels of FGF10 were also shown to cause several tissue defects. Higher than usual FGF10 transcript levels in adult eye sclera were found associated with extreme myopia (short-sightedness) in Chinese and Japanese populations (Yoshida et al., 2013, Hsi et al., 2013). The mechanisms underlying FGF10's overproduction, as well as molecular consequences that follow, are yet to be described, but they might be linked to alterations in extra-cellular matrix.

In order to understand the molecular reasons underlying the observed phenotypes generated through malfunction of FGF10, key roles of this protein in different tissues are still under scientific scrutiny. The most prominent function of FGF10 in limb and lung formation, has already been well summarised in several reviews (Volckaert and De Langhe, 2014, Itoh and Ohta, 2014, Yamamoto-Shiraishi et al., 2014), although it is still under constant further investigation. However, in order to understand the underlying causes of symptoms resulting from FGF10's malfunction, visible in LADD and ALSG, it is important to inspect the protein's role in the teeth, ear, eye as well as lacrimal and salivary glands during development and in the adult tissue.

1.3.1 Function of FGF10 in dental tissue and tooth formation

FGF10 knockout mouse embryos show dysgenesis of teeth and absence of epithelial stem cell loop, which maintains and regenerates mouse incisors (Ohuchi et al., 2000). Human individuals with haploinsufficiency of FGF10 suffer from hypoplastic teeth (Entesarian et al., 2005, Milunsky et al., 2006, Entesarian et al., 2007, McKenna et al., 2009). FGF10 therefore is crucial for the normal development and maintenance of teeth.

Odontogenesis (tooth development) is a complex process taking place during development as well as postnatally. The vertebrate teeth develop through inductive interactions between ectoderm of the first pharyngeal arch and the underlying ectomesenchyme derived from the neural crest (Fig. 1.7). This cross-talk between the two tissues results in formation of odontoblasts (derived from the mesenchyme), which further produces dentine, and ameloblasts (derived from the epithelium), that later generate enamel.

Briefly, the tooth development begins with the initiation stage, called the placode, with the distinction between the vestibular and the dental lamina. Then a group of epithelial cells, at the periphery of the dental lamina, proliferate into a bud

within the ectomesenchyme of the jaw. Each tooth bud is separated from the ectomesenchyme by a basement membrane. Later arises the dental papilla, which is created by ectomesenchymal aggregation, allowing the tooth bud to grow into a “cap” structure. This is succeeded by the early formation of enamel and dental sac. During the subsequent stage, called the “bell” several complex processes take place, involving proliferation of progenitor cells, their differentiation, matrix deposition, and subsequent mineralization, overall called the histo-differentiation and morpho-differentiation. These lead to final mature tooth shaping and its eruption (Fig. 1.7).

In mice, absence of FGF10 causes formation of hypoplastic teeth (Ohuchi et al., 2000) signifying that FGF10 is not required for the induction of a tooth formation. Furthermore, analysis of Fgf10-deficient mice revealed that FGF10 is not involved in the early signalling networks, at early morphogenesis of tooth initiation (Harada et al., 2002b).

In postnatal mice incisor (closely resembling the developmental stages) Fgf10 as well as Fgf3, are expressed within a restricted area of the dental mesenchyme of the apical end of the tooth. Fgf10 specifically is expressed in the mesenchyme under the inner enamel epithelium and extends into the mesenchyme surrounding the cervical loop, a zone underlying inner enamel epithelium (Harada et al., 1999, Tummers and Thesleff, 2003), which is known to expresses the cognate receptor FGFR2-IIIb (Fig. 1.7). Expression of Fgf3 closely resembles that of Fgf10 (Harada et al., 1999), and therefore it is not certain whether these two co-operate to regulate tooth formation, or are mutually redundant. However, expression of both Fgf10 and Fgf3 disappears when the tooth begins to form its root (Tummers and Thesleff, 2003) (Fig. 1.7). Another Fgf expressed during teeth formation and acting as a major player is FGF9, which unlike Fgf10 and Fgf3, is detected in both dental epithelium and mesenchyme, however the epithelial expression is more prominent (Zhao et al., 2011) (Fig. 1.7).

During the early tooth development FGF10 signalling is thought to activate cell proliferation in the inner dental epithelial cells (Kawano et al., 2004) via stimulation of the MAPK and pERK pathway, which subsequently leads to regulation of the PI3K activity (Cho et al., 2009). Interestingly, the pERK pathway was also activated in the mesenchymal cells expressing Fgf10 and inhibition of the FGF receptor does not reduce the levels of activated ERK in mesenchymal cells, however it does in the epithelium (Cho et al., 2009). Therefore potentially endogenous FGF10 could be responsible for the pERK stimulation in developing tooth mesenchymal cells.

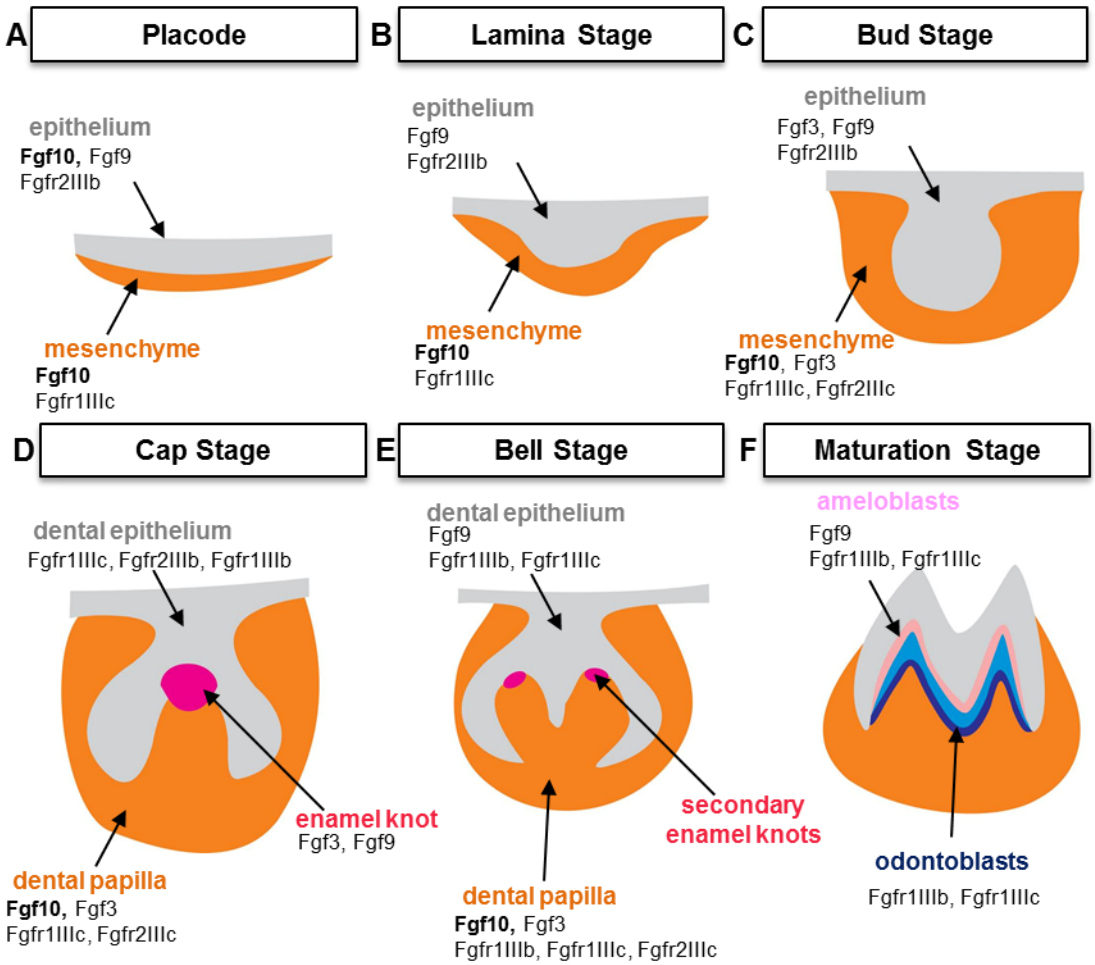

Figure 1.7 Schematic representation of molar development. (A) The primary (initiation) stage of tooth formation is 'the placode' where FGF10 is expressed predominantly within mesenchyme, however low levels can also be detected within the epithelium, together with Fgf9; the Fgfr2IIIb is also present within the epithelium. (B) When the dental lamina forms, expression of Fgf9 and Fgfr2IIIb is localized in epithelium and Fgf10, at this stage, is only found within mesenchyme, together with the Fgfr1IIIc. (C) At bud stage, expression of Fgf3 is detectable within the epithelium, as well as Fgf9 and Fgfr2IIIb, however the major expression of Fgf3 now closely resembles that of Fgf10 in underlying and surrounding mesenchyme, where the Fgfr1IIIc and Fgfr2IIIc are also present. (D) When cap stage is reached, the dental epithelium expresses mainly the receptors Fgfr1IIIb, Fgfr1IIIc and Fgfr2IIIb; the mesenchyme (expressing Fgf10, Fgf3 as well as Fgfr1IIIc, Fgfr2IIIc), forms the dental papilla underlying the enamel knot, where Fgf3 is also expressed. (E) During the bell stage, the dental epithelium still mainly expresses the Fgfr1IIIb and Fgfr1IIIc, whereas the expression of Fgf10 and Fgf3 is now restricted to the mesenchyme of the dental papilla, which also expresses the Fgfr1IIIb, Fgfr1IIIc and Fgfr2IIIc. (F) At the final, maturation stage, ameloblasts form from the epithelium and express Fgf9, Fgfr1IIIb and Fgfr1IIIc; whereas the mesenchymal cells give rise to odontoblasts that express Fgfr1IIIb and Fgfr1IIIc; Fgf10 and Fgf3 are no longer expressed. Figure based (Li et al., 2014a).

Furthermore, an externally applied FGF10 was shown to stimulate *in vitro* growth of a cervical loop epithelium of apical ends of the postnatal mouse incisors. Moreover FGF10 signalling regulates the expression of the lunatic fringe (Lfng) gene within the cervical loop epithelium and inner enamel epithelium (Harada et al., 1999). Lunatic fringe is a secretory molecule involved in the modulation of Notch signalling (Shifley and Cole, 2008). During tooth development, Notch signalling has been associated with the differentiation of dental epithelial and mesenchymal cells (Cai et al., 2011). Therefore, FGF10 secreted by the mesenchymal cells, acts on epithelium to stimulate LFNG protein production, that in turn, through inhibiting Notch, promotes cell proliferation (Harada et al., 1999).

Fgf10 is constantly expressed during development and postnatally (adult teeth that show constant growth, such as mouse incisors and vole molars) and in a dose-dependent manner FGF10 signalling is involved in maintaining proliferation of tooth epithelial cells (Kawano et al., 2004), as well as establishment and maintenance of the stem cell compartment (Harada et al., 2002b, Harada et al., 2002a, Yokohama-Tamaki et al., 2006). Direct evidence shows that within the mice incisors FGF10 prevents stem cell apoptosis, and mesenchymal FGF10 signals maintains them within their undifferentiated state (Harada et al., 2002b). Expression of Fgf10 disappears after the initiation of root development (Yokohama-Tamaki et al., 2006), where the cells begin to differentiate, which demonstrates that lack of FGF10 signal results in a lack of the stem cell niche.

Furthermore, FGF10 signalling controls the generation of the crown epithelium and FGF10 is required for the production of the stratum intermedium, which in turn produces enamel structures (Kawano et al., 2004). Lack of Fgf10 expression, during molar development leads to termination of formation of the crown and ablation of a stem cell compartment. Moreover, overexpression of Fgf10 causes formation of epithelial bulges resembling apical buds and the expansion of the crown epithelium of the tooth during molar development (Yokohama-Tamaki et al., 2006).

In conclusion, FGF10 signalling promotes crown formation and ablation of FGF10 allows formation of a root. The termination of cell division and differentiation of enamel epithelial cells is one of the most important events in the transition from crown to root development. Control of FGF10 signal is therefore crucial for this transition to take place. In addition the expression of Fgf10 can occur in a variety of patterns, which might be linked to the diversification of teeth, i.e. the size of the tooth, a number of cusps and whether the teeth are of continuous or limited growth (Yokohama-Tamaki et al., 2006).

Furthermore, within dental tissue the FGF10 signalling is negatively regulated by Sprouty proteins. Loss of sprouty genes (from both epithelium and mesenchyme)

causes hypersensitivity to FGF10 in the mouse dental epithelium, resulting in duplication and incisors oversize associated with abnormal subdivision of the epithelium. Reduction of FGF10 levels in the sprouty mutants partially rescues the normal phenotype. Moreover sprouty mutant mice show upregulation of Fgf10 expression, but expression of other Fgfs, such as Fgf9 was unaltered (Charles et al., 2011).

Another factor known to affect expression of Fgf10 as well as Fgf3 and Fgf9, is TGFβ type I receptor (Alk5). Loss of Alk5 results in significant reduction in expression of Fgfs in dental tissue, which is followed by reduced number of proliferating cells in developing tooth. However, expression of Fgf10 (but not Fgf3 or Fgf9) can be re-established by addition of external TGFβ2, which shows the direct control of TGFβ pathway over Fgf10 signalling. Moreover, FGF10 is able to rescue the dental epithelial stem cell defects in the Alk5 null mutant. On the contrary, FGF3 only partially and temporarily supports the teeth growth in the Alk5 null mice, stimulating only the transit-amplifying cell population but (unlike FGF10) fails to rescue the true stem cells proliferation. Concluding therefore, FGF10 is located downstream of TGFβ signalling, and interactions of these two pathways forms a signalling transduction cascade that mediates tissue-tissue interaction during teeth formation (Zhao et al., 2011). Interestingly, similar TGFβ-FGF pathways were shown crucial for development of a tongue and other craniofacial structures (Hosokawa et al., 2010, Sasaki et al., 2006).

1.3.2 Role of FGF10 in the inner ear

FGF10 is implicated in formation of the inner ear, where it acts, similarly to the tooth formation, in concert with the member of its subfamily FGF3. The mammalian inner ear arises from a simple epithelium, specifically the ectodermal placode, adjacent to the developing hindbrain. The otic placode is specified through multistep process of inductive interactions of endoderm, mesoderm and neural ectoderm. The endoderm and mesoderm generate the initial signals for placode induction, which subsequently invaginates and forms a closed vesicle in a process that is strictly controlled by the signals from neural ectoderm (i.e. the adjacent hindbrain). The otic vesicle initiates cellular differentiation and morphogenesis, resulting in mature and very complex inner ear containing sensory epithelia innervated by the cochlea-vestibular ganglion (Wright and Mansour, 2003, Alvarez et al., 2003).

Both Fgf10 and Fgf3 are expressed during the inner ear development and are thought to act in combination with each other as neural signals for otic vesicle formation. Both Fgf10 and Fgf3 are required for induction of the otic placode, because the knockout of both genes results in complete absence of otic vesicle. On the

contrary, defects caused by single knockouts of Fgf10 or Fgf3 have incomplete penetrance and variable expressivity, suggestive of gene redundancy (Wright and Mansour, 2003). Moreover, in the Fgf10 and Fgf3 double knockout mouse embryos, ectopically expressed Fgf10 in hindbrain, in the place where Fgf3 is usually expressed, rescues the formation of the otic vesicles (Alvarez et al., 2003). This further supports the idea that FGF10 and FGF3 display partial redundancy.

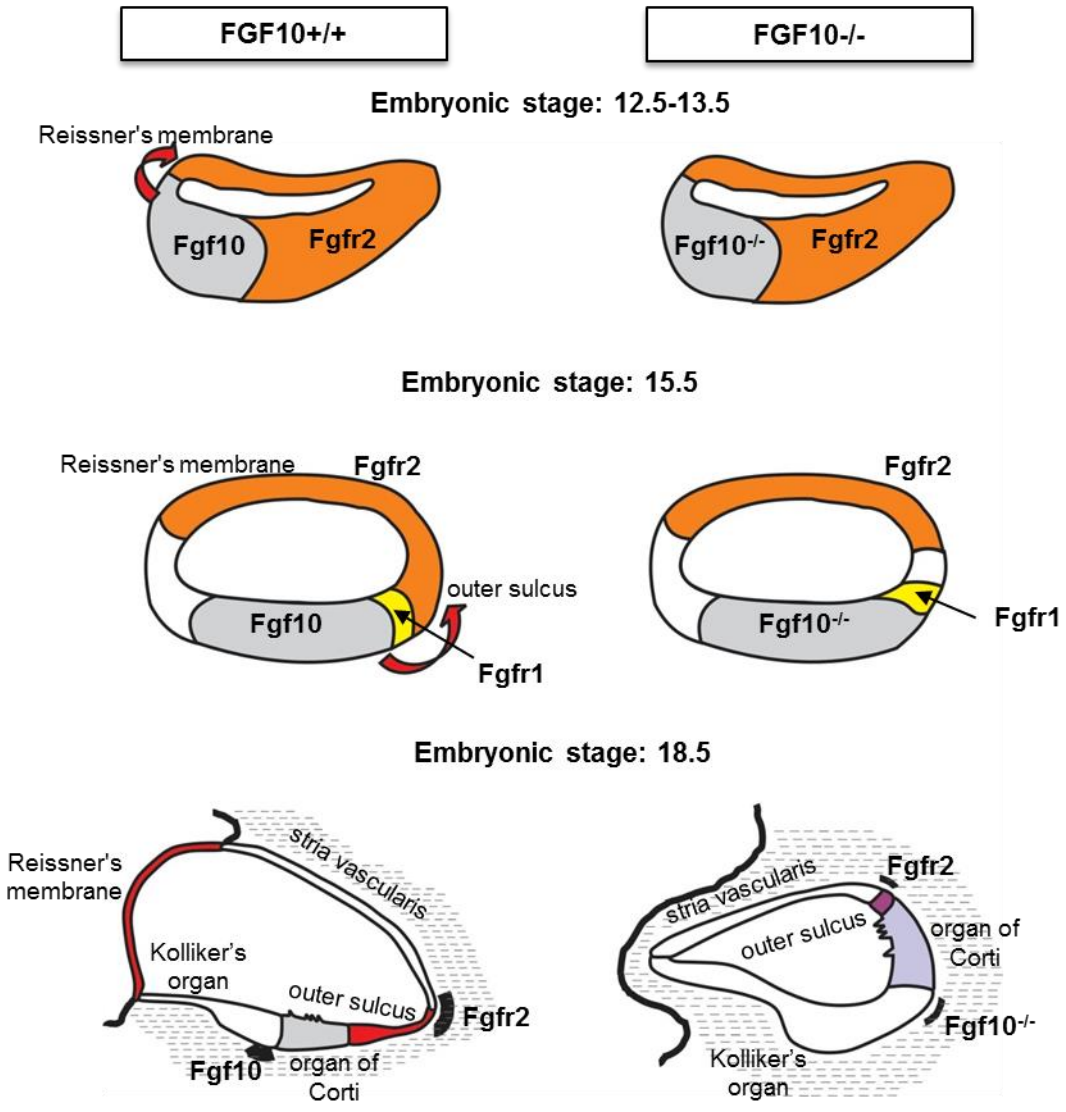

Figure 1.8 Schematic model illustrating the cochlear's developmental defects caused by knockout of FGF10. At the early stages of E12.5-E13.5 in the absence of FGF10, induction of Reissner's membrane is abolished and does not form. At the following stages of E15.5, in the FGF10's absence the outer sulcus fails to develop normally, which is clearly visible at the stage E18.5. Therefore, FGF10 plays a significant role in induction and development of non-sensory cochlear domains. Figure adapted from (Urness et al., 2015).

Importantly, each ligand is known to play individual roles, and FGF3 was shown to affect later stages of ear development, i.e. after formation of an otic vesicle and the later stages of vesicle morphogenesis. Fgf3 null mice form the otocyst as normal which subsequently fails to form an endolymphatic duct (Mansour et al., 1993). Similarly, the Fgf10 knockout mice display only a mild abnormality in the inner ear development and the ear appears morphologically normal during the early developmental stages, up to formation of the otic vesicle (Ohuchi et al., 2000). However, at the later developmental stages, lack of FGF10 leads to morphogenetic and innervation abnormalities of the inner ear (Fig. 1.8) (Pauley et al., 2003).

During development Fgf10 is expressed in the ventral part of the otic epithelium whereas its cognate receptor, the Fgfr2IIIb is activated within the dorsal side (Fig. 1.8). The expression of Fgf10 during the inner ear development is directly controlled by a GATA3 transcription factor (Economou et al., 2013). As the development progresses the FGF10 becomes confined to the presumptive cochlear and vestibular sensory epithelia and to the neuronal precursors and neuron. The receptor on the other hand, is found expressed in the non-sensory epithelium of the otocyst, which gives rise to structures such as the endolymphatic and semi-circular ducts. Therefore, FGF10-FGFR2IIIb signalling mediates inductive processes, from sensory to non-sensory epithelium, during semi-circular canal formation (Fig. 1.8) (Pirvola et al., 2000).

At the subsequent stages, Fgf10 is expressed within the mesenchyme underlying the prospective otic placode and signals to the receptor expressing epithelial cells (Wright and Mansour, 2003). Moreover, FGF10 is required for the removal of the fused cells after semi-circular plate formation, especially prominent at the posterior canal. Fgf10 null mice fail to develop the posterior crista and the posterior semi-circular canal and show deformations of the anterior and horizontal cristae as well as reduced formation of the anterior and horizontal canals (Ohuchi et al., 2005). In addition, the correct formation of this region is FGF10 dose-dependent, as mice heterozygous for Fgf10 also generate vestibular defects (i.e. a small or absent posterior semi-circular canal) (Urness et al., 2015). Moreover, ablation of Fgf10 expression affects the posterior canal sensory neurons, which form initially and project rather normally, but they quickly disappear (within 2 days) (Pauley et al., 2003).

In addition, recent studies show that removal of the Fgf10's expression in the inner ear results in complete absence of all of the vestibular membrane (membrane inside the cochlea) as well as a substantial portion of the outer sulcus. These two are non-sensory domains, not adjacent to each other, making the FGF10 a bi-directional signal that promotes sequential specification of the cochlear epithelium. Failure to generate these two non-sensory tissues in Fgf10 null mice is not linked to compromised cell proliferation or increased cell death and results from lack of

specification of the progenitor cells through compromised signalling (Fig. 1.8) (Urness et al., 2015). Unlike the typical mesenchymal-to- epithelial FGF10 signalling seen in other tissues, it was postulated that the non-sensory development of the inner ear could depend on intra-epithelial signalling of FGF10.

Furthermore, in a developing ear FGF10 induces expression of Fgf8. Misexpression of Fgf10, but not Fgf3, was shown to induce ectopic expression of Fgf8 in the hindbrain (Zelarayan et al., 2007). Similar processes occur during limb formation (Ohuchi et al., 1999)

1.3.3 FGF10 function in the development of an eyelid and an eye

Mammalian eyelids develop in a similar fashion among different species. During gestation human and mouse eyelids close and fuse temporarily. In human they reopen prior to birth, whilst mouse eyelids reopen shortly after birth. The eyelid forms in few stages, beginning with the initiation step, marked by an ectoderm morphogenesis and groove formation at E11.5. Then a mesenchymal protrusion of the eyelid extends (E13.5), which leads to formation of projecting epithelial ridge at the tip of the eyelid margin at E15. Subsequently at E15/16 epithelium of upper and lower eyelid extends and fuses together and this fusion process is followed by extension of the mesenchymal cells at E16.5/17.5.

One of the many characteristics of Fgf10 null mice is the open-eyelid phenotype exhibited at birth (Sekine et al., 1999, Tao et al., 2005). Moreover, a heterozygous mutation in Fgf10 that causes truncation of the protein and most likely leads to protein degradation, results in dominant slit-eye phenotype. It is characterised by abnormal eye-lids and atrophy of Harderian glands, but the eye displays normal size and morphology (Puk et al., 2009). Therefore, FGF10 is involved in normal formation of eye-lids in a dose sensitive manner.

Another aberration associated with abnormal eyelid development is the ‘eyes-open at birth’ phenotype, found in mice lacking: Activin βB (Vassalli et al., 1994), transforming growth factor α (TGFα) (Mann et al., 1993), epidermal growth factor receptor (EGFR) (Miettinen et al., 1999), aristaless-like homeobox protein (Alx4) (Curtain et al., 2015) and fibroblast growth factor receptor 2b (FGFR2b) (Li et al., 2001). Therefore, together with FGF10, these molecules are required for normal eyelid formation.

FGF10 is present during all of the stages of the eyelid development (Tao et al., 2005) and its expression is partially regulated by Alx4, putatively through binding to *cis* elements within Fgf10’s promoter region (Curtain et al., 2015). During the eyelid initiation Fgf10 is expressed in the mesenchyme residing underneath the epithelium of

the emerging eyelid groove, which expresses the FgfR2IIIb. At the later stages, the expression of Fgf10 becomes restricted to mesenchymal cells lying just beneath the epithelial tip and in the developing corneal stroma. At the final stages of eyelid formation, Fgf10 is expressed in the eyelid mesenchyme, around the whole eye (Tao et al., 2005).

FGF10 null mice show formation of the eyelid protrusion, therefore the protein expression is not essential for the initial stage of eyelid induction, similarly to the inner ear formation (see above). However, expression of Fgf10 is essential for the subsequent stages of morphogenic changes and maintenance of the epithelial grove. FGF10 signalling regulates the normal formation of mice eyelids by two means: maintenance of epithelial cell proliferation (at the early stages) and then stimulation of coordinated cell migration (at the later stages). Signalling of FGF10 regulates formation of actin stress fibres (F-actin) within epithelial leading edge cells of the developing eyelid, through activation of TGFα and Activin βB (Tao et al., 2005, Tao et al., 2006). Through regulation of these molecular pathways, FGF10 indirectly affects maintenance of epithelial cell polarisation and controls the reorganisation of the epithelial cytoskeleton. Moreover, when the primitive periderm cells start streaming onto the ocular surface, FGF10 opposes the SHH signals (arising at the leading tip) further promoting cell migration (Tao et al., 2005, Tao et al., 2006).

Furthermore, FGF10 might be implicated in the development on other eye compartments, such as the lens and retina, where it is expressed at an embryonic stage E12.5 in mice. Curiously, varying from its usual mesenchymal association, at the late embryonic stages (E15.5 - E17.5) expression of Fgf10 is restricted to the lens epithelial cells. Within retina FGF10 is found within the posterior parts of the inner and outer nuclear layers and then within the prospective photoreceptor cells. However, eyes of Fgf10 heterozygous and null embryos show only minor misshaping of the central lens area (Puk et al., 2009), suggesting that FGF10 function might be mostly redundant during lens and retina formation.

On the other hand overproduction of FGF10 causes implications in the formation of sclera, most likely through mediating TFGβ signalling and remodelling the extra-cellular matrix. In young adult mice with form deprivation myopia (FDM), i.e. a short sightedness, Fgf10 transcript levels are increased within the scleral cells, but not within retina, as compared to healthy individuals (Hsi et al., 2013). In addition, individuals within Chinese and Japanese population that suffer from extreme myopia, show overexpression of Fgf10 in eye sclera (Hsi et al., 2013, Yoshida et al., 2013). Moreover, abnormally expressed Fgf10 within the epithelium of cornea promotes cell proliferation and induces formation of ectopic ocular glands-like structures

(Govindarajan et al., 2000). Hence, main function of FGF10 within the ocular system is the formation of the lacrimal and Harderian glands (see below).

1.3.4 Role of FGF10 in lacrimal and salivary glands

Patients suffering from LADD and ALSG syndromes, caused by heterozygous mutations in FGF10, are characterised mainly by their defects affecting lacrimal and salivary glands and ducts (Milunsky et al., 2006, Entesarian et al., 2007). Moreover, the Fgf10 knockout mice do not form lacrimal and salivary glands (Min et al., 1998, Ohuchi et al., 2000), signifying that FGF10 is a key player in development and maintenance of these tissues.

The lacrimal glands are a pair of almond-shaped structures localised at each side of a head, by eyes, and are responsible for a production of tears. The lacrimal glands secrete a layer of tear film which then flows through tear canals into the lacrimal sacs that drain through the lacrimal duct into the nose. Formation of the lacrimal glands at the embryonic stages occurs via epithelial-to-mesenchymal interaction, in a very similar fashion to formation of limbs, lungs and teeth. At first a small bud-like epithelial structure arises which is surrounded by periocular mesenchymal cells of neural crest origin. A tubular invagination is then shaped and subsequently extends and branches to generate the lobular structure of the mature gland.

During embryogenesis Fgf10 is present in the mesenchyme adjacent to the budding lacrimal epithelium, where FGFR2IIIb is expressed. Analysis of the knockout mice revealed that, in the absence of FGF10 the mesenchyme forms as normal, however the epithelial component of the gland fails to develop. Similar results are obtained by inhibiting the FGFR2IIIb receptor, meaning that FGF10 induces the epithelium formation via its cognate receptor (Makarenkova et al., 2000, Govindarajan et al., 2000). The FGF10-FGFR2IIIb signalling within the lacrimal glands is controlled by the bifunctional heparan sulfate N-deacetylase/N-sulfotransferase 1 (NDST1) enzyme as mutations within the Ndst1 gene disrupt the Fgf10 dependent lacrimal gland induction. Ndst1 generates specific N-sulphation on the heparan sulphate, which in turn selectively potentiates the FGF10-FGFR2IIIb interaction at lacrimal gland bud. Activation of the receptor results in phosphorylation of ERK via Shp2 protein. Phospho-ERK signalling pathway stimulates the Pea3/Erm transcription and cell proliferation (Pan et al., 2008).

Interestingly, within the lacrimal bud region expression of Fgf7 is less distinctive than Fgf10, however both proteins FGF10 and FGF7, can stimulate ectopic lacrimal bud formation (Makarenkova et al., 2000), suggesting a degree of functional redundancy.

Salivary glands can be divided into few categories: submandibular, sublingual and parotid. These develop from neural crest derived mesenchyme and ectoderm derived epithelium. Salivary glands form in a series of stages: thickening of an oral epithelium, then forming a pre-bud that leads to initial bud and then pseudo-glandular, at the end generating a canalicular gland.

Fgf10 is expressed within the mesenchyme surrounding the salivary gland. Absence of FGF10 or its receptor results in aplasia of salivary glands, however a small invagination forms, suggesting that initiation of the bud formation is not dependent on FGF10-FGFR2IIIb signalling (Jaskoll et al., 2005). Moreover, heterozygosity of FGF10 and FGFR2IIIb leads to branching hypoplasia of the submandibular gland in mice (Jaskoll et al., 2005) and in humans (Entesarian et al., 2005, Entesarian et al., 2007). Similarly, excess of FGF10 signalling induces branching morphogenesis of the submandibular gland *in vivo* which is caused by increase in epithelial proliferation (Jaskoll et al., 2005). Furthermore, FGF10 induced branching of the salivary gland is potentially aided by the FGF8 signalling, but despite stimulation of similar intracellular cascades, the FGF10 and FGF8 act through different receptors and therefore cannot compensate *in vivo* for each other's loss (Jaskoll et al., 2005).

Similarly to the processes within lacrimal glands (Makarenkova et al., 2009), FGF10 promotes elongation of the salivary duct, without enlargement of the epithelial buds, whereas FGF7 causes budding of the epithelial rudiment, in a dose dependent manner (Steinberg et al., 2005). Moreover, FGF10 increases the length of the branches through activating the MEK1/2-dependent pathway and promoting cell proliferation at the tips of the growing ducts (Steinberg et al., 2005). On the other hand, the FGF7 promotes epithelial budding via PI3K- and MEK1/2-dependent signalling.

Regardless of activating the same receptor isoform, FGF10 and FGF7 differ in the effects they cause during formation and morphogenesis of lacrimal and salivary glands (Fig. 1.9). FGF10 and FGF7 generate varying morphogen patterns through the extra-cellular matrix (ECM) determined by the affinity towards the heparin sulphate (HS). FGF10 with higher than FGF7 binding affinity towards HS, diffuses locally, close to the source of its expression, i.e. mesenchymal cells domain adjacent to the tips of epithelial buds. The morphogenic gradient of FGF10 is defined as 'steep', in which the concentration of ligand falls off sharply, and results in promoting cell proliferation mainly at the tip of the bud, causing its elongation. FGF7 on the contrary, is characterised by lower HS affinity than FGF10, and therefore is able to diffuse more freely across the ECM, forming a shallow gradient in which the concentration of ligand falls off gradually, in a result triggering branching of the buds (Fig. 1.9). Interestingly, these morphogenic patterns are not receptor or dose mediated, as reducing the

strength of the FGFR2IIIb binding or varying the dose of the ligands regulates the extent but not the nature of the epithelial responses (Makarenkova et al., 2009).

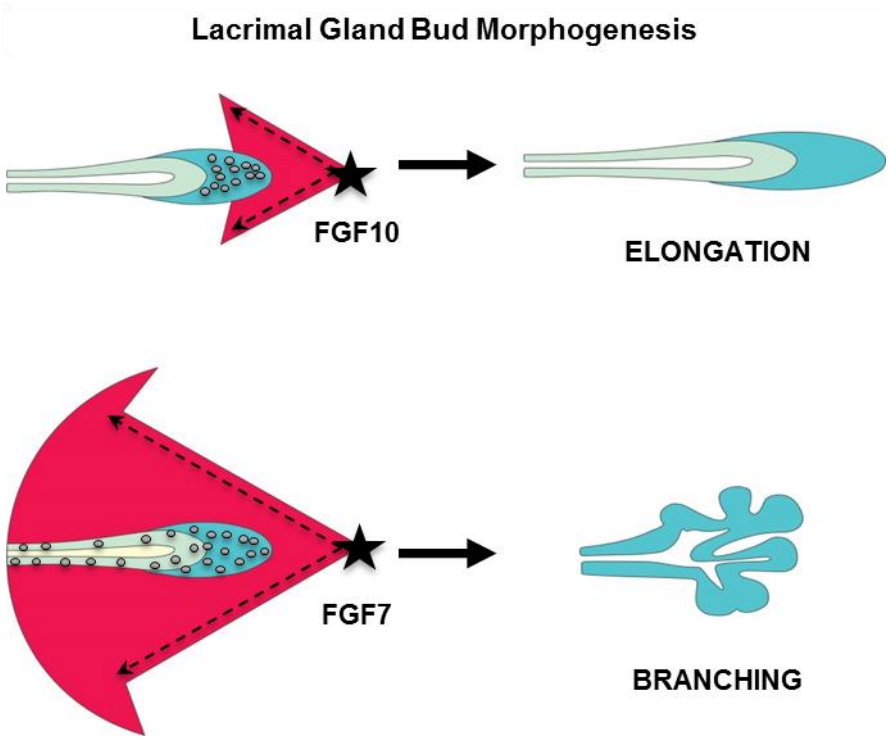

Figure 1.9 FGF10 and FGF7 regulate lacrimal gland bud morphogenesis. Branching morphogenesis is a multistep process that involves specification of the epithelium by the signals provided by surrounding mesenchyme. It begins by induction and shaping of a primary bud, which is followed by a repetitive bud elongation and cleft formation resulting in development of the mature and complex organ. A proposed model of FGF10 and FGF7 functioning in lacrimal gland bud demonstrates that FGF10, with high affinity to heparan sulfate, shows restricted diffusion through extra-cellular matrix, limited to the tip of the epithelial bud, resulting in bud elongation towards the FGF10 source. On the contrary, FGF7 with low affinity for heparan sulfate shows a wider and broader diffusion range, resulting in affecting cells residing in more distal parts of the epithelial bud, leading to bud branching. Figure adapted from (Makarenkova et al., 2009). This may serve as an example of branching morphogenesis taking place in other organs, such as lungs, pancreas, kidneys and salivary glands.

Interaction with HS is generated via four residues within FGF10, which in human protein sequence correspond to Arg187, Arg193, Lys195 and Thr197. Of these, the Arg187 and Arg193 were shown to be crucial for the HS binding. The R187V mutation abolished the interaction with HS groups, resulting in significant reduction of FGF10-to-HS binding in relation to wild type FGF10, whereas R193K substitution showed an immediate loss of heparin binding. Moreover, in lacrimal and salivary glands, the FGF10 R187V mutant mimics the function of FGF7 by inducing bud branching. Moreover, unlike wild type FGF10 but similarly to FGF7, the R187V mutant promotes cell proliferation in domains distal from the tip of the developing gland and triggers the same gene expression as FGF7 (Makarenkova et al., 2009). Furthermore, the FGF10 signalling during the formation of lacrimal glands is affected by modification of HS or other glycosaminoglycans (GAGs). Ablation of a UDP-glucose dehydrogenase (Ugdh) (which is an essential biosynthetic enzyme for GAGs), although does not affect the expression of Fgf10 in the periocular mesenchyme, leads to excessive dispersion of the FGF10 protein, which subsequently fails to stimulate the budding morphogenesis in the presumptive lacrimal gland epithelium (Qu et al., 2012).

Another molecule known to accompany the FGF signalling during the formation of lacrimal and salivary glands is paired box protein 6 (Pax6), which is a transcription factor that signals from the conjunctival epithelium to induce the outgrowth of the lacrimal bud. Expression of Pax6 is a primary signal of lacrimal gland development and even heterozygous mutations in Pax6 cause formation of vestigial lacrimal glands and lead to small eye phenotype (Sey) in mice. However, Pax6 does not affect the expression of FGF10 within mesenchymal cells, and FGF10 does not rescue the defects caused by Pax6 ablation. Therefore these two proteins indirectly co-regulate the normal development of lacrimal glands (Makarenkova et al., 2000).

Another molecule implicated in formation of ocular glands, alongside of FGF10, is Sry-related HMG box 9 (Sox9) transcription factor, and deletion of Sox9 within the ocular surface results in lack of formation of lacrimal gland. The FGF10 signalling was shown to regulate the expression of Sox9 gene, that in turn controls the initial budding and the elongation of the lacrimal bud, through regulation of production of the extra-cellular matrix. Subsequently, Sox9 activates Sox10 that further controls the elongation and branching of the lacrimal bud as well as the formation of secretory acini. Interestingly, in a Sox9 knockout mice, overexpression of FGF10 in a tissue specific manner, only partly rescues the formation of lacrimal gland. Furthermore, Sox9 indirectly regulates the FGF10 signalling through affecting the expression of heparan sulfate-synthesizing enzymes (HSSE), which are required for the synthesis and function of heparan sulfate (HS). Therefore, FGF10 and Sox9 generate a feedback loop mechanism during development of the ocular glands (Chen et al., 2014).

Furthermore, a homeobox protein Barx2, is expressed in the epithelium of lacrimal and salivary glands, and Barx2 null mice display a significant reduction and malformation of lacrimal glands, but not affecting the salivary glands formation. Barx2 is required for elongation of the FGF10 induced lacrimal bud. Expressed by surrounding mesenchyme FGF10 generates a transducing signal that guides the elongation of the Barx2 expressing epithelial bug, and stimulates its outgrowth. The exact relationship of Barx2 and FGF10 is still under scrutiny however, Barx2 null cells are unresponsive to FGF10 treatment, signifying Barx2 is downstream of FGF10. At the succeeding stages, Barx2 and FGF10 cooperatively regulate the expression of matrix metalloproteinases (MMPs), which are necessary for the epithelial bud outgrowth and cell proliferation. It has been proposed that MMPs control the signalling gradient of FGFs, through degradation of the extra-cellular matrix and release of these signalling ligands from binding to heparan sulphate and other proteoglycans, generating a regulatory feedback mechanism. Barx2, controlled by FGF10 signalling, binds directly to the promoter region of mouse MMP2, promoting gene expression. Surprisingly, this regulatory mechanism is unique to lacrimal glands, as despite the high levels of expression of Barx2 in the salivary glands, in the knockout mice salivary glands develop as normal, suggesting a redundant role of the protein in this tissue and highlights the tissue specificity of the FGF10 functioning (Tsau et al., 2011).

1.3.5 Overview of role and function of FGF10 in other tissues

Beyond those described above FGF10 is implicated in development and maintenance of multiple tissues and organs. For example, FGF10 is abundantly expressed within adult vascular-stromal fraction of a white adipose tissue, majorly composed of adipocyte precursors, raising interesting possibility of FGF10's involvement in adipogenesis (Sakaue et al., 2002). Moreover, FGF10 was shown to promote differentiation of the precursors into mature adipocytes (Zhang et al., 2010b). Importantly, in the FGF10 null mice embryos, development of the white adipose tissue is greatly impaired, displaying decreased proliferative activity of preadipocytes and greatly reduced expression of C/EBPβ and PPARγ transcription factors (Asaki et al., 2004).

FGF10 signalling plays also a crucial part in formation of heart's right ventricle and its outflow tract from myocardial progenitors (Urness et al., 2011). Fgf10 knockout mice show reduced proliferation of cardiomyocyte in heart's right ventricle. FGF10 signalling was shown to promote phosphorylation of forkhead box O 3 (FOXO3) transcription factor, which leads to decrease in expression of the cyclin-dependent kinase inhibitor $p27^{kip1}$ and promotes proliferation. Interestingly, in the adult tissue,

overexpression of Fgf10 generates rapid induction of cardiomyocyte cell cycle re-entry (Rochais et al., 2014).

Fgf10 knockout affects liver, through impairing the proliferation of hepatoblasts. The FGF10 signalling was shown to stimulate the embryonic stellate/myofibroblastic cells to promote β-catenin activation and survival of hepatoblasts (Berg et al., 2007). Furthermore, FGF10 is implicated in bladder formation and was shown to stimulate the differentiation of human stem cell into urothelial cells (Chung and Koh, 2013). Interestingly, FGF10 was found present in the nuclei of human urothelial cells (Kosman et al., 2007). Several other paracrine FGFs were shown to act from the cell nucleus, which is described in more detail below.

Part 1.4 Role and function of nuclear FGFs

1.4.1 General overview of nuclear proteins

In addition to an extracellular receptor-mediated signalling, several paracrine FGFs were shown to function in an intracellular fashion through direct interaction with cytosolic and/or nuclear proteins. For example, FGF1 and FGF2 both can bind to casein kinase 2 (CK2) protein, which is involved in control of a cell-cycle progression (Skjerpen et al., 2002). Furthermore, FGF1 binds to acidic FGF intracellular binding protein (FIBP) (Kolpakova et al., 1998) and mortalin (Mizukoshi et al., 1999), although the functional result of this interaction is yet not clear. FGF2 has been postulated to modulate a ribosomal activity via direct interaction with ribosomal proteins L6/TAXREB107 (Shen et al., 1998) and RPS19 (Soulet et al., 2001), postulating a role of FGF2 in preribosomal assembly and translational control of cell growth during viral infection.

Interestingly, FGF1, FGF2, FGF8 and FGF22 as well as FGFR1, FGFR2 and FGFR3 have been found translocating to and functioning from a cell nucleus, either individually or as a ligand-receptor complex.

1.4.2 Mediators of protein nuclear import

Cell nucleus encloses the genetic material and the transcriptional apparatus, separating it from the cytoplasmic translational and metabolic machinery via a double phospholipid membrane, that prevents larger molecules to freely shuttle across. Therefore, movement of proteins and other molecules across the nuclear envelope is

strictly controlled and takes place via nuclear pore complexes (NPCs). These are large macromolecular structures (~124MDa) (Reichelt et al., 1990), composed of at least 456 individual protein molecules and with a total diameter of ~120nm (Winey et al., 1997), spanning both nuclear membranes. NPCs are typically built from multiple copies of a protein termed nucleoporin (Nups). These nuclear channels are large enough to allow passive diffusion of proteins smaller than 40μm in diameter (or ~40kDa). However, it has been demonstrated that, even some of the smallest proteins in a cell, such as PTHrP (Cingolani et al., 2002) and histone H1 (Jakel et al., 1999), use specific carrier-mediated transport, demonstrating that, for the nuclear import, the rate at which cargos enter cell nucleus is more important factor than the protein's size. Therefore, it is thought that all proteins serving particular nuclear functions are selectively and actively uptaken into the nucleus, regardless of their size (Christie et al., 2015).

Carriers that mediate this nuclear protein transport belong to the β-karyopherin (β-Kap) superfamily of solenoid proteins, which is composed of importins and exportins. Structure of all β-Kap family members includes two tandem HEAT repeats (antiparallel α-helices of ~40–45 amino acids), named A and B and linked by a loop. Furthermore, the nuclear transport is dependent on a small GTPase named Ran (Fig. 1.10), which cycles between GDP/GTP-bound states, as determined by Ran regulatory proteins, such as nuclear located Ran guanine nucleotide exchange factor (RanGEF) and cytoplasmic Ran GTPase-activating protein (RanGAP) (Lui and Huang, 2009). Ran protein contains a small G-domain and two surface loops (switch-I and switch-II), which change conformation depending on the nucleotide-bound state of the protein. Importantly, the gradient of RanGDP/GTP generated by the regulatory proteins (RanGEF and RanGAP), establishes directionality in nucleocytoplasmic transport pathways (Gorlich et al., 1996).

There are few known pathways that provide protein's nuclear transport. Majority of proteins contain specific motifs on their surface called a Nuclear Localisation (NLS) or Nuclear Export Sequence (NES), and nuclear import and export are usually mediated via different pathways. NLSs are short peptide motifs, classified into classical (if consensus) and non-classical (if of unique pattern). Moreover, NLS can also be monopartite, consisting of a cluster of basic (Arginines/R and Lysines/K) amino acid residues and bipartite, where two smaller clusters of basic residues are separated by a stretch of about 10 amino acids, which typically fold into close proximity in the 3D structure of a protein.

Typically, the classical NLS is recognized by one of the isomers of importin-α (Imp-α) protein family, that serves as an adaptor linking the cargo to a carrier protein, i.e. one of the isoforms of the importin-β (Imp-β1) protein family, which transports the complex through the NPC (Fig. 1.10) (Christie et al., 2015). Alternatively, several

members of the importin-β family were shown to directly bind to cargo proteins, or use a different adaptor protein, called snurportin1 (SNP1) (Mitrousis et al., 2008, Marfori et al., 2011).

Importantly, the Imp-α possesses two functional and structurally distinctive domains. These are the N-terminal Impβ1-binding domain (αIBB), and a C-terminal armadillo (Arm) domain, which consists of 10 tandem Arm repeats, each generated by three α-helices (H1, H2 and H3) (Herold et al., 1998, Marfori et al., 2011). Structural studies revealed that cargo's classical NLS typically binds in a highly conserved concave groove on a surface of Imp-α. This groove typically contains an array of Tryptophan/W and Asparagine/N residues at the third and fourth turns of the H3 helices. Furthermore, the groove is divided into the high-affinity "major" (residues from Arm repeats 2–4) and the "minor" sites (Arm repeats 6–8). Monopartite NLSs can bind in either of the two sites, whereas the bipartite NLSs bind in an extended conformation to both major and minor binding sites, with the N-terminal basic cluster in the minor site, and the C-terminal basic cluster in the major site (Marfori et al., 2011).

Interaction of cargo protein's NLS with the Imp-α subsequently leads to further complex formation with the Imp-β1 (Fig. 1.10). Imp-β1 binds with high affinity the Imp-α, wrapping tightly around the Imp-α's αIBB domain and covering over 40% of its surface area (Cingolani et al., 1999). After complex formation, in order to pass through the nuclear pore the Impβ1 interacts directly with Nups, through the HEAT motif located on the importin and 'Phenylalanine-Glycine' ('FG') tandem repeats of nucleoporins (Marfori et al., 2011, Christie et al., 2015).

The family of the β-Kap proteins shows a large repertoire of proteins with low sequence conservation but high degree of structure similarity. In humans there have been identified around 20 β-Kaps, of which 10 are known to mediate transport of proteins into the nucleus, another 7 mediate the reverse, nucleus to the cytoplasm transport, other 2 were shown to mediate translocation in both directions and the remaining one is still not fully characterized. Different β-Kaps are known to be expressed in a tissue-specific manner and typically recognize different classes of cargo proteins. However, there is also a degree of redundancy present as several β-Kap receptors able to recognize the same cargoes (Chook and Suel, 2011, Christie et al., 2015).

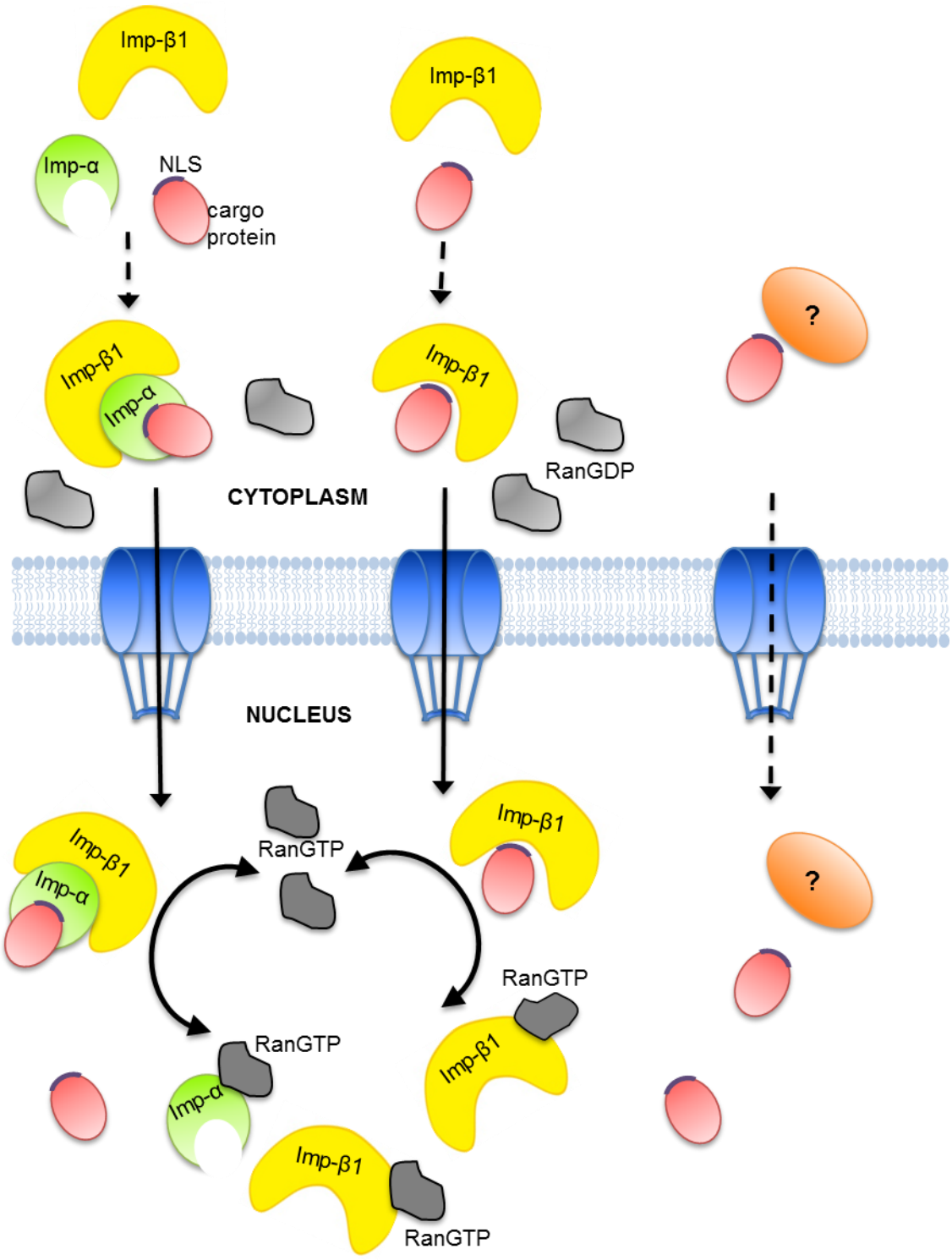

Figure 1.10 Model representing different nuclear import pathways. In the classical pathway, the nuclear localisation sequence (NLS) present on the cargo's surface binds to Importin-α (Imp-α) adaptor that subsequently interacts with the Importin-β (Imp-β1), resulting in the whole complex translocation through the nuclear pore (blue). Alternatively, Importin-β binds directly to the cargo protein allowing its nuclear import. The complexes dissociate in the nucleus in the presence of RanGTP (solid gray). Proteins may also be chaperoned into the nucleus through alternative pathways, not involving the classical imporin-mediated pathways, although these are not well described so far. Figure based on (Christie et al., 2015).

Many proteins shuttle in as well as out of the nucleus, and the nuclear export pathway is typically mediated via interaction between NES and exportins. There are seven identified exportins so far, among which the chromosomal maintenance 1 (CRM1) protein is the major nuclear export receptor for protein cargos (Xu et al., 2012). CRM1 transports not only proteins, but also mRNAs and rRNSs however, functions only in the form of a ternary complex, which also includes the RanGTP (Ishizawa et al., 2015).

1.4.3 Import and function of nuclear FGF1

Externally applied to eukaryotic cells FGF1 (also known as acidic FGF), was found to translocate into the cell nucleus (Wiedłocha et al., 1994, Klingenberg et al., 1998) where it was thought to stimulate DNA synthesis (Wesche et al., 2005a). The nuclear uptake of this paracrine molecule is preceded by an endocytosis of the protein through a cell membrane. FGF1 is able to interact with all of the FGFRs (Fig. 1.4B), located on a cell surface, but the endocytosis of the protein is stimulated only by binding to the FGFR1 or FGFR4 (Sorensen et al., 2006). This process was shown to be dependent on the receptor's C-terminal tail, although interestingly it is independent of the receptor's tyrosine kinase domain activity (also located within the receptor's C-terminus) (Sorensen et al., 2006). Endocytosis of the complex is further induced by a vesicular membrane potential (Malecki et al., 2002).

The internalised FGF1 translocates into the cell nucleus via the classical nuclear import pathway mediated by importins Kpnα1 & Kpnβ1, Ran GTPase as well as a leucine rich repeat containing 59 (LRRC59) protein (Sorensen et al., 2006, Nilsen et al., 2007). Interestingly, FGF1 contains two NLS sequences. One, a monopartite NLS is located within the N-terminal domain of the protein (Imamura et al., 1990), whereas the second, bipartite NLS resides within the C-terminus of the protein (Wesche et al., 2005a). Both NLSs are required for efficient nuclear transport of endocytosed FGF1. Interestingly, simultaneous mutation of both NLSs significantly reduces the FGF1 ability to stimulate DNA synthesis, while single mutations do not seem to have any considerable effect (Wesche et al., 2005a).

The comparison of the FGF1 primary sequences revealed that both of the NLSs are highly conserved across various vertebrate species (Wesche et al., 2005a), which further highlights importance of these motifs within the protein's sequence.

1.4.4 Overview of nuclear FGF2

FGF2 belongs to the same subfamily of FGF proteins as FGF1 (Fig. 1.2) however, the process of nuclear FGF2 translocation differs from the one associated with FGF1 (Bouche et al., 1987). Unlike other FGFs, the FGF2 does not contain the classical signal peptide motif and therefore is secreted out of the cell through unconventional pathway, which does not involve the Endoplasmic Reticulum and Golgi (Mignatti et al., 1992). Furthermore, there are 5 distinct forms of human FGF2 protein arising from differential translation of the mRNA. These so called “protein isoforms” are synthesised through an alternative translation initiation process rather than gene alternative splicing. Four of FGF2 isoforms are CUG-initiated, called high molecular weight (HMW) (22-34kDa) and found exclusively in the cell nucleus. The smaller AUG-initiated protein is called low molecular weight (LMW) (18kDa) and found in both the cytoplasm and nucleus (Renko et al., 1990).

The HMW protein isoforms contain an N-terminal NLS which confer their exclusive nuclear localisation (Quarto et al., 1991). Moreover, the nuclear accumulation of the HMW isoforms (but not the LMW) is further controlled by the post-translational modifications. It appears that methylation of specific arginine residues is essential for the nuclear localisation of the HMW isoforms. Treatment of fibroblast cells with Methyltransferase inhibitors prevents methylation of these arginine residues and results in significant reduction of the HMW FGF2 nuclear accumulation (Pintucci et al., 1996). The secreted LMW FGF2 binds and activates several isoforms of FGFRs (Fig. 1.4B) and interestingly, the ligand-receptor complex can be internalised into the cytoplasm, in a similar fashion to FGF1 (Malecki et al., 2004), and chaperoned by heat shock protein 90 (Hsp90) protein (Wesche et al., 2006). From the cytoplasm the endocytosed LMW FGF2, despite the lack of the N-terminal NLS, can translocate into the cell nucleus (Clarke et al., 2001), where it possibly functions to up-regulate the ribosomal RNA synthesis (Bouche et al., 1987). Interestingly, an endogenous LMW FGF2 is also uptaken into the cell nucleus. Inhibition of FGFR within epithelial cells, preventing the internalisation of the secreted molecule, did not abolish the nuclear localisation of the LMW protein (Dell'Era et al., 1991). The critical factor of the nuclear-cellular shuttling of LMW FGF2 is translokin/CEP57 protein (Bossard et al., 2003, Meunier et al., 2009) because decline in translokin levels leads to reduced translocation of FGF2 and affects its mitogenic function decreasing cell proliferation (Bossard et al., 2003).

FGF2 is thought to contain a second N-terminal NLS based on its sequence similarity to the NLS found within the FGF1 protein. Importantly, this sequence is present also within the LMW FGF2 (Presta et al., 1993). However, mutations of this NLS did not prevent the FGF2 from entering the cell nucleus, indicating that this is not

a unique motif that determines the intracellular localisation of the protein (Presta et al., 1993) but potentially aids the protein translocation. All forms of the FGF2 protein contain also a non-classical bipartite NLS within the C-terminus (Sheng et al., 2004). Mutating both NLS motifs (at the N and C terminus) fully prevents the nuclear localisation of the protein (Foletti et al., 2003). Moreover, the C-terminal NLS plays a significant role in the nucleolar targeting and localisation of FGF2 (Sheng et al., 2004). Overall, these studies show therefore that HMW FGF2 contains two NLSs at the N-terminus (of which one is a weak one) and one bipartite NLS at the C-terminus. The LMW FGF2 contains a weak NLS at the N-terminus and a bipartite NLS at the C-terminus, which is sufficient for their nuclear localisation.

The intracellular differences in distribution of FGF2 variants, HMW within the nucleus and LMW directed to the secretory pathway, is the major determinant of their functional diversity. The LMW FGF2 serves a paracrine function through activation of the transmembrane receptor, whereas the HMW FGF2 plays FGFR-independent intracellular role. This leads to differential routes of nuclear translocation, i.e. LMW FGF2 nuclear import is translokin and/or FGFR dependent, whereas the HMW FGF2 does not relay on the receptor complex formation and possesses the N-terminal NLS, absent in the LMW FGF2. These differences then reflect on the differential nuclear distribution of the FGF2 variants and lead to differential functions they serve within the nucleus.

The nuclear LMW FGF2 in Schwann cells (Claus et al., 2003) or the NIH3T3 cell line (Dini et al., 2002) is localised in nucleoli and Cajal bodies, which are a sub-organelles found in the nucleus of proliferative cells (Claus et al., 2004). This is reflected in the protein function, as LMW FGF2 has been found to stimulate rRNA synthesis, and induces cell proliferation and chemotactic movement (Dini et al., 2002).
The HMW FGF2 shows a punctuate pattern in the nucleoplasm and periphery of nucleoli, and co-localises with DNA and mitotic chromosomes (Claus et al., 2003). HMW FGF2 was detected in a variety of cultured cells, including osteoblasts (Sobue et al., 2001), cartilage (Krejci et al., 2007), epithelial (Galy et al., 1999), aortic endothelial (Couderc et al., 1991) cell lines as well as primary astrocytes (Li et al., 2006). The HMW FGF2 increases the proliferative potential of NIH3T3 and A31 cells, whilst the LMW FGF2 effect on cell proliferation of these cells is much lower. On the other hand, cells expressing the LMW FGF2 show higher migratory potential than cells expressing the HMW variants (Dini et al., 2002). Another difference is that the HMW FGF2 but not LMW variant is necessary for promoting estradiol dependent angiogenesis as well as endothelial cell migration and proliferation (Garmy-Susini et al., 2004).

1.4.5 Nuclear FGF3

FGF3 protein belongs to FGF7 subfamily of FGFs (Fig. 1.2). It was first identified as a secretory molecule acting as an oncogene in mouse mammary tumours (Muller et al., 1990), suggesting its role in cell proliferation. Nuclear FGF3 is thought to serve a quite opposite function, inhibiting DNA synthesis and reducing cell growth (Kiefer and Dickson, 1995b).

The unusual feature of FGF3 biosynthesis (similarly to FGF2) is the use of alternative initiation codon CUG. This generates different protein isoforms extended at the amino terminus (Dickson et al., 1989). Alike FGF2, the high molecular weight isoforms (HMW) of FGF3, with extended N-terminal, seem to accumulate directly in the cell nucleus (Acland et al., 1990).

FGF3 appears to be targeted in a similar proportion to the nucleus and to the secretory pathway. The signals responsible of directing the protein either for the nuclear import or endoplasmic reticulum (ER) entry are placed at the amino terminus within the protein sequence itself. Newly synthesised protein contains a hydrophobic signal peptide (SP) at its N-terminus that targets FGF3 for the vectorial transport across the ER (Dickson et al., 1991, Kiefer et al., 1994a). Next to the SP resides a classical, but relatively weak, bipartite NLS that allows protein entry to the cell nucleus (Kiefer et al., 1994a). This bipartite NLS is not crucial for the nuclear accumulation and nucleolar association of the protein. In the absence of the signal peptide mutations of this bipartite NLS did not prevent FGF3 from entering the nucleus (Kiefer and Dickson, 1995b). However this sequence is sufficient for the recognition and binding of an importin protein (karyopherin α/NPI-1) (Antoine et al., 1997) which is essential for the active transport of the complex through nuclear pores.

The weak signals at the N-terminus are thought to allow competition between the intracellular distributions of the protein. Weak NLS however, is not sufficient to cause nuclear transport of the protein, therefore FGF3 contains several additional weak NLS-like motifs which act to enhance nuclear uptake without affecting the balance between the two opposing trafficking pathways. These additional motifs are rich in basic residues and reside within the C-terminus of the FGF3 sequence. They act as fine tuning factors supporting the N-terminal NLS for the nuclear targeting of the protein when required but individually are not able to define the protein to the nucleus (Kiefer and Dickson, 1995b). Moreover, these factors also aid retaining the protein in the nucleus by facilitating binding to nucleolar proteins through (functionally conserved between mouse and human) nucleolar binding motifs (NBM) (Antoine et al., 1997). Interestingly, the nucleolar retention of FGF3 results in inhibition of cell growth and proliferation (Kiefer and Dickson, 1995b). Moreover, nucleolar FGF3 directly interacts

with nucleolar binding protein (NoBP), which might function to regulate division stage of cell cycle (Reimers et al., 2001).

1.4.6 Nuclear localisation of FGF8 and FGF22

FGF8 is known for its conventional mitogenic function during development and patterning of vertebrate embryo. FGF8 gene is alternatively spliced, in humans generating four protein isoforms (a-d), each serving different functions, for example during brain patterning (Olsen et al., 2006). Importantly, exogenously applied mouse FGF8b was observed to translocate into the nucleus of mouse fibroblast cells (Suzuki et al., 2012). The molecule is secreted out of the cell, then internalised by the surrounding cells (possibly through interaction with FGFRs) and incorporated into their nucleus, as demonstrated on the chick embryonic neural tube studies.

Sequence analysis revealed that FGF8 might potentially contain a NLS, although this point requires further investigation. Nonetheless FGF8b, that lacks signal peptide mostly localises to the cell nucleus of mouse fibroblast cells. Moreover endogenous FGF8 was detected *in vivo*, in the nuclei of the embryonic mouse isthmus (Suzuki et al., 2012). It was postulated that nuclear FGF8 directly induces expression of Sprouty2 gene (Suzuki et al., 2012).

FGF22 is a member of the FGF7 subfamily, to which FGF3 and FGF10 also belong (see Fig. 1.2). Transiently transfected FGF22 (fused to a small hemagglutinin A (HA) tag) into human breast adenocarcinoma MCF-7 cells was found localised to large nuclear bodies. Interestingly, transfection into monkey kidney, fibroblast-like COS-1 cells FGF22-HA was localising to the reticular and perinuclear cell compartments, indicating its association with ER and secretory pathway network (Beyer et al., 2003). The molecular mechanisms driving the nuclear import of FGF22 and its nuclear function are currently not described.

1.4.7 Nuclear FGF10

Interestingly recombinant FGF10 has been found in the nuclei of cultured urothelial cells (Bagai et al., 2002) and was postulated to contain a NLS, in human corresponding to residues 132MNKKGKL141 of a full protein sequence (Kosman et al., 2007). This NLS sequence was identified basing on its similarity to the NLS present in the FGF1 protein (21NYKKPKL27). Interestingly, mutation of this FGF10's NLS region, did not prevent the protein from localising within the nucleus however, it has shown that it might play a role in retaining FGF10 within the nucleus (Kosman et al., 2007).

Part 1.5 Introduction to hypothalamic stem cells and neurogenesis

Expression of Fgf10 was found in several brain regions, one of which is hypothalamus, where the protein is expressed mainly by cells named tanycytes (Hajihosseini et al., 2008, Haan and Hajihosseini, 2009). Although tanycytes that FGF10 demarcates were shown to possess neurogenic potential, the function of the protein itself within this these cells is currently unclear. Importantly, expression of FGF10's cognate receptor FGFR2IIIb was not detected in the adult mouse brain (Hajihosseini et al., 2008), suggesting an alternative mode of function of FGF10 protein. Therefore, studies of FGF10's mode of action within hypothalamus might generate interesting insight into intracellular/nuclear function of the protein.

1.5.1 Overview of hypothalamus

The hypothalamus is situated around the brain's third ventricle (3V), below thalamus and above pituitary gland (Fig. 1.11A). The hypothalamus is known as the centre of neuroendocrine and autonomic regulations that control the homeostatic body functions, which include: maintenance of body temperature, regulation of metabolic processes as well we coordination of hormonal and circadian cycles. Moreover, regions within hypothalamus were shown triggered during various emotional and instinctive activities, such as reproduction as well as aspects of parenting and attachment behaviours (Narita et al., 2012, Savic et al., 2005, Berglund et al., 2006). Importantly, hypothalamus is also the core regulator of appetite as well as energy uptake and expenditure (Sousa-Ferreira et al., 2011, Graham et al., 2003a).

Grossly, the hypothalamus is composed of three main structures referred to as the ependyma, the median eminence (ME) and the parenchyma (Fig. 1.11B). The parenchyma flanks the 3V and contains distinct 'neuronal nuclei' sharing neuronal interconnections. These are: the arcuate nucleus (ARC), the ventromedial (VMN), lateral (LHN), dorsomedial (DMN) and the paraventricular (PVN) nucleus (Fig. 1.11C). The median eminence (ME) is positioned on the ventral side of the hypothalamus (Fig. 1.11B), providing connection between hypothalamus and the pituitary gland and generating the hypophyseal portal system. One of the key functions of the median eminence is the transmission and secretion of hormones, such as corticotropin-releasing factor (CRF) (Romanov et al., 2015), gonadotropin-releasing hormone (GnRH) (Kenealy et al., 2015), thyrotropin-releasing hormone (TRH) (McKelvy et al., 1975), growth hormone-releasing hormone (GHRH) (Anderson et al., 2010) and dopamine (DA) (Arita and Kimura, 1986).

The ependyma corresponds to a single cell layer of epithelial-like cells that forms a boundary between the hypothalamus and the third ventricle (Fig. 1.11B). It is therefore also referred to as the ependymal wall of the third ventricle. Ciliated cells occupy the more dorsal parts of the ependymal whilst, non-ciliated cells with radial glial-like characteristics, such as tanycytes, reside in the floor and ventral lateral parts.

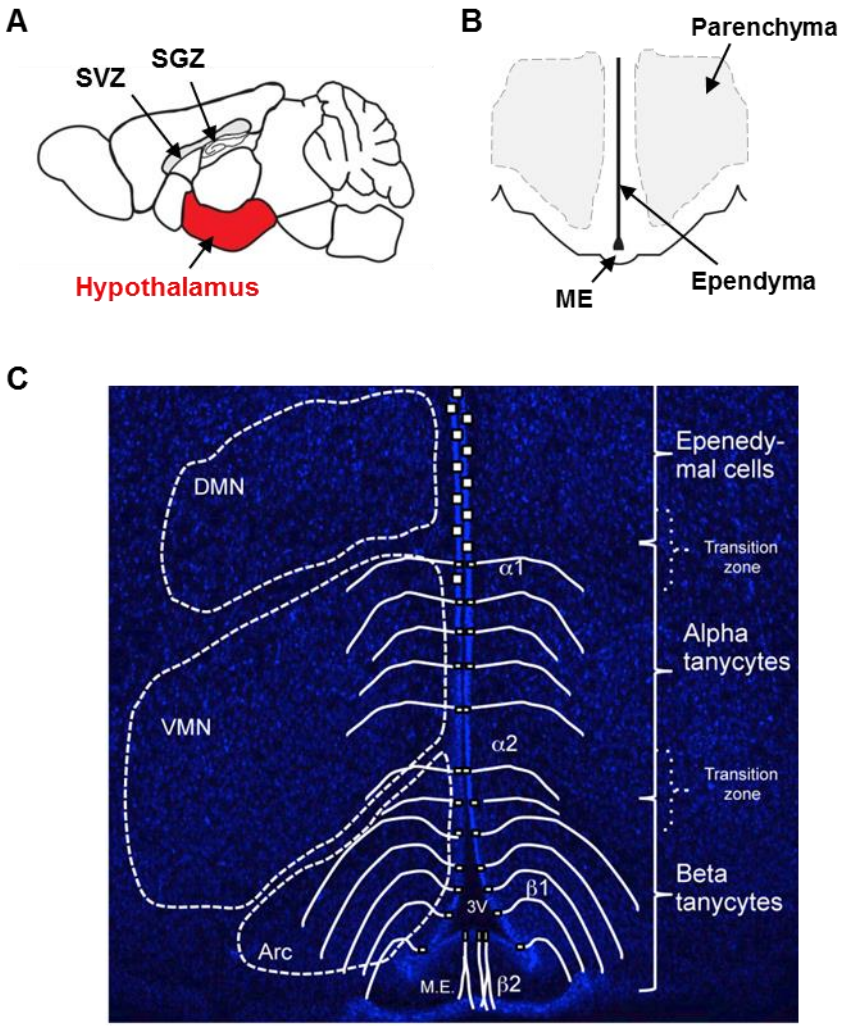

Figure 1.11 Localisation and structure of mouse hypothalamus. (A) Schematic drawing showing hypothalamus (red) located on a ventral side of mouse brain. (B) Schematic of hypothalamic coronal section showing the three main structures composing hypothalamus (C) Hypothalamic micrograph with superimposed schematic adapted from (Goodman and Hajihosseini, 2015), showing the organisation of tanycytes residing around the third ventricle (3V) and extending to the specific hypothalamic nuclei – α tanycytes reside medio-dorsally and extend mainly to the ventromedial (VMN) nucleus, while β tanycytes are located ventro-medially, within the median eminence (ME) and the arcuate nucleus (Arc).

1.5.2 Hypothalamic tanycytes – overview of the origin and organisation

The term “tanycytes” was first proposed by Horstmann in 1954 – it originates from the Greek word *tanus*, meaning “elongated”. Tanycytes are bipolar cells, known to be crucial connectors between hypothalamus and pituitary gland (Rodriguez et al., 2005). Tanycytes have a very distinctive elongated shape and can be distinguished from other ependymal cells by the lack of beating cilia. However, they possess a single, long basal process that projects to the VMN and ARC nuclei and to the median eminence (Fig. 1.11C). They emerge from a subpopulation of radial glial cells during the perinatal embryonic stages - E19 in rats and E17 in mice. In developing brain, these pre-tanycyte radial glial cells are regarded as neural stem/progenitor cells. In developing brain, radial glial cells are widely regarded as neural stem/progenitor cells. Tanycytes display several intriguing characteristics, such as ability to proliferate, short term signalling via changes in intracellular Ca^{2+} (Dale, 2011) and expression of specific markers (e.g. Nestin, Vimentin, Sox2 and Musashi) (Wei et al., 2002), which indicate that they have retained the properties of radial glial cells. The process of specification of tanycytes from the ciliated ependymal cells is regulated in part by transcription factor Lhx2 acting upstream of the gene Rax. It was shown that in the absence of Lhx2, the development of tanycytes is severely disrupted. Loss of Lhx2 resulted in lack of expression of tanycyte-specific genes and instead activation of ependymal-specific markers (Salvatierra et al., 2014).

Tanycytes are divided into two main groups (α and β), based on their positioning, morphology and function – cells located near to the dorso-ventral and ventro-medial hypothalamic nuclei are referred to as α1 and α2 tanycytes; and cells positioned more ventrally, close to the ARC and median eminence are known as β1 and β2 tanycytes (Fig. 1.11C). However, there is no clear boundary between the α and β tanycytes as cells of the different subtypes interdigitate forming a transition zone (Fig. 1.11C). For that reason reliable isolations of specific subtypes through microdissection of fresh brain extracts is particularly difficult (Goodman and Hajihosseini, 2015). In general, α tanycytes bridge the lumen of the third ventricle and terminate in close proximity of neurons within parenchyma, while β tanycytes establish a link between the ventricular cerebrospinal fluid (CSF) and the portal blood. Cell processes of the β1-tanycytes contact the parenchymal capillaries and segregate the ARC from the median eminence and the β2-tanycytes arch back medially and ventrally to contact the pial surface (Fig. 1.11C).

Anatomical tanycyte subdivisions have been additionally characterised by molecular markers, further highlighting differences between the subgroups. Although the α and β tanycytes share expression of Sox2 (Haan et al., 2013), Vimentin

(Brauksiepe et al., 2014) and Glucose transporter 1 (GLUT1) (Peruzzo et al., 2000), they also express cell-type specific genes/markers. For example, α tanycytes, express GFAP (Haan et al., 2013), GLAST (Robins et al., 2013), S-100β (Goodman and Hajihosseini, 2015) and Connexin43 (Rodriguez et al., 2010) which are also found within the dorsal ependymal cells, but not found in β tanycytes. On the other hand β tanycytes express BLBP (Haan et al., 2013), CNTFR (Kokoeva et al., 2005) and FGF10 (Hajihosseini et al., 2008) that are absent from the α tanycytes and the dorsal ependymal cells.

Moreover, there are further marker expression differences defining the specific tanycyte subtypes, for example the GLUT1 expression can be detected in the α and in the β1 tanycytes but it is absent from the β2 tanycytes (Peruzzo et al., 2000, Robins et al., 2013), and the adenosine triphosphate (ATP) is abundant in the α1 tanycytes (which are facing the VMN) and absent from all the other subtypes (Rodriguez et al., 2005).

The functions of the specific subtypes of tanycytes is still under investigation, however their strategic positioning at particular places around the 3V suggests their involvement in regulation of homeostasis (Fekete and Lechan, 2014) and control of appetite and energy expenditure (Frayling et al., 2011, Bolborea and Dale, 2013). Moreover tanycytes express several genes that have been linked to control of body weight and energy levels, including G protein-coupled receptor 50 (GPR50 receptor) (Sidibe et al., 2010), several genes involved in thyroid hormone signalling (Bolborea and Dale, 2013), Neuromedin U receptor (Graham et al., 2003a) and genes involved in the retinoic acid signalling pathway (Bolborea and Dale, 2013). Importantly, tanycytes have been shown implicated in generation of new neuronal cells, in a process of neurogenesis (Hajihosseini et al., 2008, Haan et al., 2013, Robins et al., 2013).

1.5.3 Overview of adult neurogenesis

The vast majority of neurons in the adult mammalian brain are terminally differentiated, post-mitotic cells, unable to renew themselves. This makes the brain particularly susceptible to effects of damage, cell death, neurodegenerative disease and ischemic stroke. However, the adult brain is not a static structure as it was once believed. In 1960, Altman and Das showed that generation of new neurons occurs in discrete areas of the postnatal and adult brain (Altman and Das, 1965). Subsequent studies confirmed this in a wide range of mammalian species, including humans (Zhao et al., 2008).

Neurogenesis is a multistep process production of new neurons from neural stem cells (NSCs). NSCs are undifferentiated cells with the ability to proliferate, self-

renew, and differentiate into not only neurons but also glial cells - astrocytes and oligodendrocytes. Although NSCs persist and can be found in the adult brain, they arise during embryonic development. In the adult brain, most NSCs are in a quiescent stage, except for few specific niches, where they have a very slow dividing turnover, which on average is approximately a few weeks. However, in an adult brain, beside the true stem cells, there is a population of neural progenitors, which are highly mitotic cells with the ability to give rise to terminally differentiated cells, but unlike NSCs, they are not capable of indefinite self-renewal, and their multipotency might be restricted (Abrous et al., 2005).

Adult neurogenesis closely resembles neurogenesis during embryonic development, which includes processes such as cell proliferation and cell fate specification of neural cell progenitors, followed by their differentiation, migration and functional incorporation into the existing neuronal circuitry *(*Ming and Song, 2005). The two main niches of adult neurogenesis are the subventricular zone (SVZ) of the lateral ventricles and the subgranular zone (SGZ) of the dentate gyrus in the hippocampus (Fig. 1.11A).

In the SVZ a niche of the NSC resides in a close proximity to the ventricular wall and similarly to hypothalamus, the ventricle is lined with ciliated ependymal cells. Although these ependymal cells themselves are not the NSC, the stem cells are closely associated with the ependyma (Zhao et al., 2003). The ependymal cells play important role in maintaining the stem cell niche by preventing their premature differentiation, for example through secretion of noggin (BMP antagonist) and FGF2 growth factor (Peretto et al., 2004). The proliferating stem cells possess radial glia-like characteristics and give rise to transient amplifying cells, which in turn generate neuroblasts (Fig. 1.12). The newly generated neuroblasts form a chain and migrate through the rostral migratory stream (RMS) to the olfactory bulb, where they migrate radially toward glomeruli and differentiate into different subtypes of interneurons (Ming and Song, 2011).

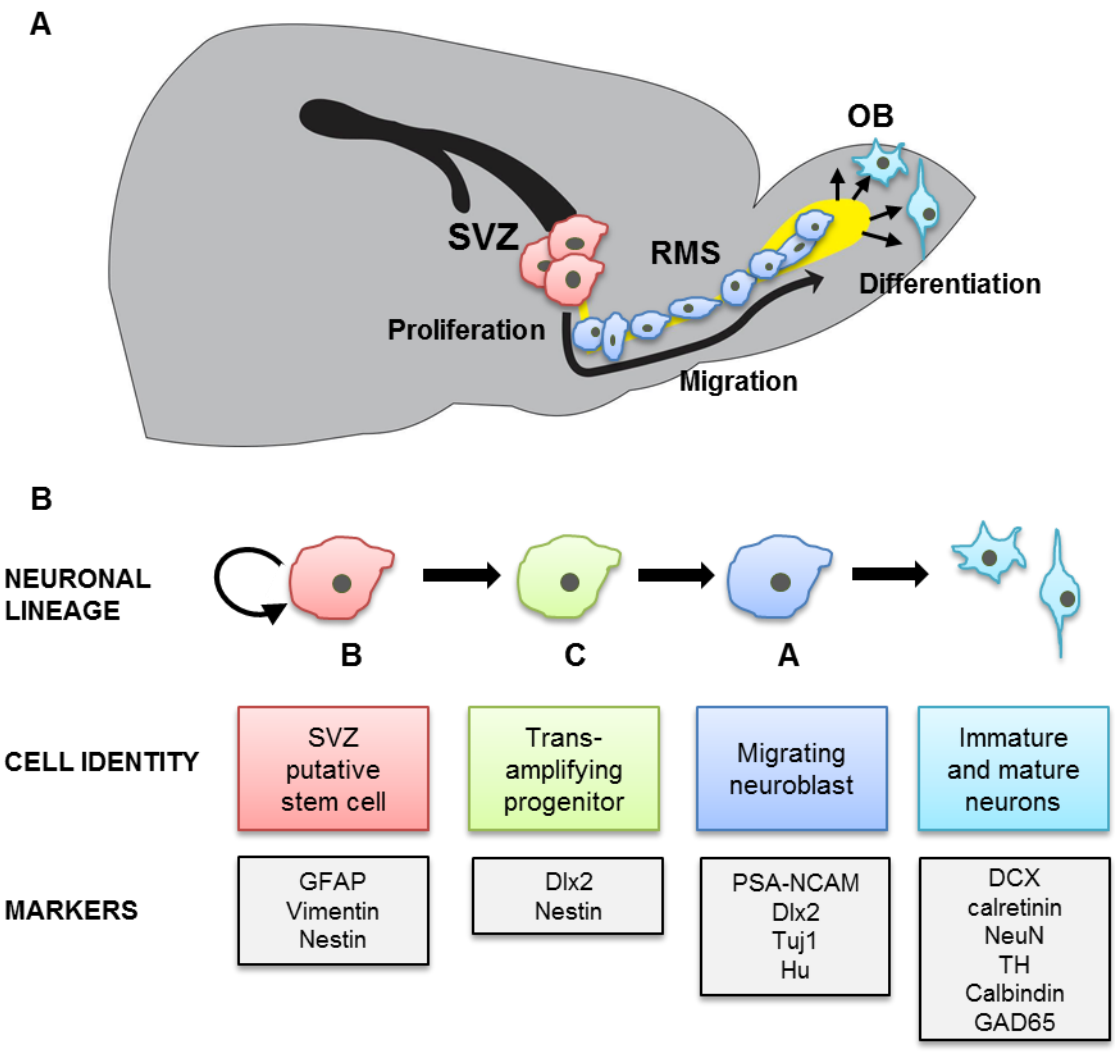

Figure 1.12 Schematic of the neurogenic processes taking place in the subventricular zone (SVZ). (A) Proliferative cells (red) reside around the ventricles of the SVZ, newly generated neuroblasts migrate along the rostral migratory stream (RMS) to reach the olfactory bulb (OB), where they migrate radially and undergo maturation. (B) Neurogenesis is a multistep process, during which, different types of cells express particular markers (shown in panels below) allowing their specification. Figure adapted from (Abrous et al., 2005).

In contrast to SVZ, the stem cell niche of SGZ does not reside in the vicinity of brain ventricles (Fig. 1.11A). Proliferating stem cells/precursors within the SGZ generate intermediate progenitors, which then give rise to neuroblasts (Fig. 1.13). These immature neurons then migrate into the granule cell layer of the dentate gyrus where they differentiate into neurons (Fig. 1.13), which follow processes for synaptic integration into the existing circuitry. In comparison to mature cells, these new neurons exhibit hyperexcitability and enhanced synaptic plasticity (Ming and Song, 2011).

Although the exact function of these new neurons is still under investigation, they seem to play a role in learning and memory (Deng et al., 2010).

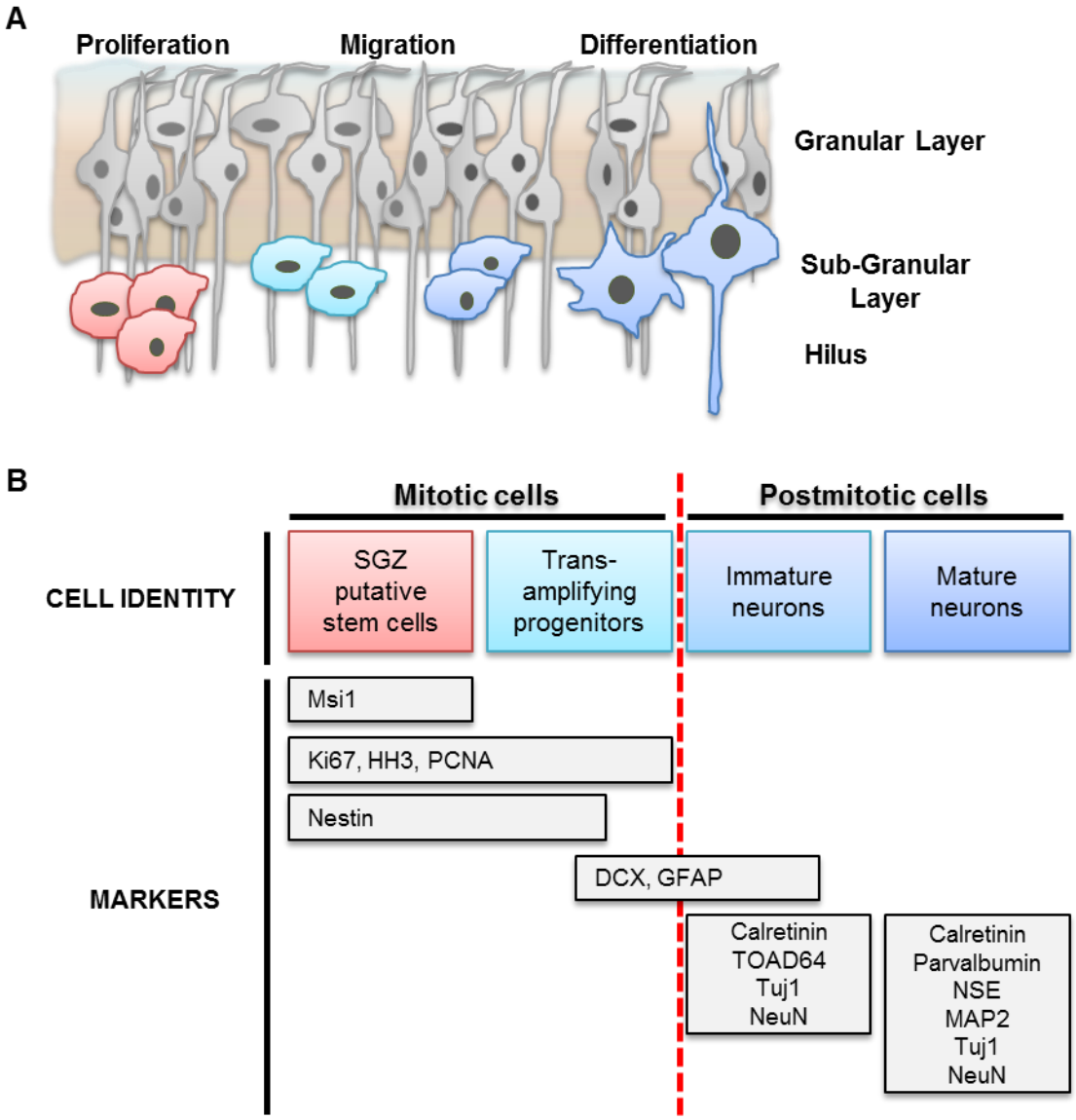

Figure 1.13 Schematic representation of neurogenesis within the subranular zone (SGZ). (A) Proliferative cells (red) reside within the sub-granular layer and the newly generated cells migrate to the granular layer, where they differentiate into mature neurons. (B) During neurogenesis the different cell types express specific lineage markers (shown in panels below) allowing their identification. Figure adapted from (Abrous et al., 2005).

Moreover, production of new neurons in the adult brain was also reported to take place in in the neocortex, the olfactory bulbs, the piriform cortex, the amygdala, the striatum, the substantia nigra, the dorsal vagal complex and the hypothalamus. However, neurogenic processes within these areas are under scientific debate due to discrepancy of results, and the fact that production of new cells is detectable only post injury or pharmacological treatments and manipulations (Migaud et al., 2010, Gould, 2007).

In the hypothalamus, the basis for the origin of the putative stem cell niche is established early during mammalian development, around the embryonic stage 10 (Shimada and Nakamura, 1973). The mouse hypothalamus has been found to contain a relatively quiescent resident stem cell population but cell proliferation can be stimulated by a number of factors and molecules, for example CNTF (Kokoeva et al., 2005), BDNF (Pencea et al., 2001) and IGF-I (Perez-Martin et al., 2010). There are still few discrepancies in terms of the exact location of the stem/progenitors cell niche: whether these reside within the hypothalamic parenchyma, its ependymal layer or within both. The hypothalamic parenchyma was shown to contain multipotent progenitor cells, expressing Sox2 and NG2 markers of proliferative cells and neuroglia respectively (Li et al., 2012a, Robins et al., 2013). However, their high mitotic activity and their punctate dispersal throughout the parenchyma suggest these are trans-amplifying progenitors rather than stem cells. The true stem cells are thought to reside within or in close proximity to the wall of the 3V (Haan et al., 2013, Robins et al., 2013).

In the postnatal hypothalamus, tanycytes are thought to act as bona fide stem cells, due to their strong resemblance to radial glial cells, their distinct arrangement within the third ventricle and their expression of neural stem/progenitor cell markers. The cells within the ependymo-tanycyte layer were shown to incorporate BrdU, a marker of proliferating cells (Kokoeva et al., 2005, Perez-Martin et al., 2010, Haan et al., 2013). Through lineage-tracing of GLAST-expressing α tanycytes it was shown that these cells are capable of expansion, even entering the domain of β tanycytes, contributing mostly however to the astroglial lineage within the parenchyma (Robins et al., 2013). By contrast, β tanycytes, marked by expression of Fgf10, were shown to proliferate, self-propagate within the ependyma and contribute to new neurons within the ARC nucleus as well as the VMN, DMN, and LHN. Furthermore the generated progeny continued to proliferate further within the parenchyma itself (Haan and Hajihosseini, 2009, Haan et al., 2013). However, the exact mechanisms controlling the hypothalamic stem cells are still under scrutiny, and involvement of FGF10 in hypothalamic tanycytes in general as well as within neurogenesis is still unclear.

1.5.4 Overview of FGFs in the central nervous system and neurogenesis

FGFs in general are implicated in development, patterning and maintenance of the nervous system. During early development at the stage of neural induction FGFs are essential for neural fate specification and act through antagonizing BMP signalling (Marchal et al., 2009). Then, throughout the whole embryonic development FGFs are involved in patterning of the neural plate, induction and patterning of the peripheral nervous system (PNS), as well as induction of the otic, epibranchial and olfactory placodes. Moreover FGF signalling contributes to shaping and forming of the brain and CNS, for example FGFs produced by the isthmic organizer, including FGF8, FGF17 and FGF18, collectively orchestrate the development of the midbrain anteriorly and the cerebellum posteriorly (Guillemot and Zimmer, 2011). Moreover, studies using Fgf8 hypomorphic mice have shown that this protein plays a prominent role during shaping and specification of developing neuroendocrine hypothalamus. Reduced levels of Fgf8 during hypothalamic development result in reduced number of PVN neurons as well as within hypothalamic region called the supraoptic nucleus (SON). However overall, the reduction of Fgf8 levels was shown to have a greater impact on the ventral hypothalamic structures, such as SON than the more dorsal nuclei, residing in a proximity to PVN (Tsai et al., 2011).

Importantly, FGFs play important roles in maintenance of survival, expansion and progression of neurogenic lineages from cortical neural stem/precursor cells, through immature trans-amplifying progenitors to mature neurons in the developing and adult brain. For example, FGF2 and FGF8 maintain the proliferative properties of neuroepithelial cells and onset of neurogenesis (Raballo et al., 2000, Storm et al., 2003). In the adult SVZ neurogenesis, FGF2 might promote stem/progenitor cell proliferation and maintain a slow-dividing stem cell pool postnatally (Zheng et al., 2004). FGF2 is thought to be a key factor regulating cortical neuro- and gliogenesis, as mice lacking Fgf2 expression contain even 50% less neurons than WT and show partially impaired neuronal migration (Vaccarino et al., 1999). Moreover FGF2 was shown to promote cell division, survival and neuronal differentiation of cell precursors (Tropepe et al., 1999, Hajihosseini and Dickson, 1999). Interestingly, FGF4 and FGF8 were shown to mimic the survival and mitogenic effect of FGF2 in a culture of neuronal precursors (Hajihosseini and Dickson, 1999), potentially suggesting a degree of redundancy between the signalling proteins. Furthermore, FGF8 was found to promote differentiation of a subpopulation of cortical neuronal precursors predominantly into the astrocyte lineage (Hajihosseini and Dickson, 1999). In hypothalamus FGF2 was also shown to promote proliferation of the α tanycytes *in vivo* (Robins et al., 2013).

FGF10 and other members of the FGF7 subfamily have a significant role within the nervous system, but most prominently are studied during embryogenesis. FGF7, FGF10 and FGF22 have been shown to promote neurite outgrowth (Umemori et al., 2004). FGF7 and FGF22 are expressed in the adult hippocampus where they function in formation of inhibitory and excitatory synapses (Terauchi et al., 2010). During corticogenesis, Fgf10 is transiently expressed by cell progenitors and was shown to determine the onset of cortical neurogenesis by promoting maturation of symmetrically dividing neuroepithelial cells into asymmetrically dividing radial glia cells. Although FGF10 regulates the radial glia differentiation, it does not affect proliferative capacity of the progenitors, nor their cell cycle or cell death (Sahara and O'Leary, 2009). Furthermore, FGF10 and FGF3 might have a role in innervation and vascularisation of the developing hypothalamus (Liu et al., 2013). Interestingly and importantly FGF10's cognate receptor, the FGFR2IIIb, is absent from the postnatal hypothalamus (Hajihosseini et al., 2008), which means that FGF10 may not be acting in a paracrine fashion in this brain region.

Part 1.6 General Aims

FGF10 is a paracrine molecule, serving crucial roles during embryonic development and within adult tissue. However, there are still unexplored areas of FGF10's function, which require further insight. Interestingly, several paracrine members of FGF family have been found to possess additional intracrine function, from a cell nucleus. FGF10 has been found present in a nucleus of urothelial cells (Kosman et al., 2007), but the molecular mechanisms underlying this process as well as its nuclear function are still unclear. In the light of the knowledge that paracrine FGF10 has been found translocating into cell nucleus, the main objective of this project was to determine whether there are additional factors, beyond the NLS proposed by Kosman et al. (Kosman et al., 2007), driving the nuclear translocation of the protein, as well as explore potential nuclear function of FGF10. These main aims were then subdivided further, as follows:

1. Using bioinformatics predictions determine whether FGF10 may possess any additional motifs providing its nuclear import. Furthermore, analyse FGF10's genomic and protein structure to gather knowledge of its putative mode of function alternative to the secretory pathway.
2. Through generation and use of a recombinant FGF10 detectable with antibodies, investigate whether FGF10 nuclear translocation is a cell type specific event and whether it is affected by reported protein mutations of human LADD and ALSG syndromes
3. Since FGF10 is typically produced by mesenchymal cells, determine, whether FGF10 serves an intracrine/nuclear role within mesenchymal cell line, affecting cell proliferation or differentiation
4. Fgf10 is expressed in hypothalamus, but expression of its cognate receptor is lacking (Hajihosseini et al., 2008), suggesting its intracrine/nuclear role may be of the most significance within this tissue. Therefore, the aim is to characterise the Fgf10-expressing hypothalamic cells *in vitro* and analyse putative function of FGF10 in the hypothalamus.

Chapter 2

Material and Methods

Part 2.1 Tools and software used for bioinformatics analysis

Human, mouse and rat genomic, cDNA and protein primary sequences were obtained from the NCBI website (http://www.ncbi.nlm.nih.gov/). Protein primary sequences in a 'FASTA' format were obtained from UniProt server (http://www.uniprot.org/). Unless specified otherwise, the primary sequence of mouse, rat and human FGF10 protein was analysed using the following, freely-available mathematical algorithms:

2.1.1 Prediction of Nuclear Localisation Sequence (NLS)

Programs such as WoLF PSORT: Advanced Protein Subcellular Localization Prediction Tool (http://wolfpsort.org) and PSORT II (http://psort.hgc.jp/cgi-bin/runpsort.pl) are commonly used to predict the putative localisation of a protein within a cell, including nuclear, cytoplasmic or membrane-bound position. These tools often can predict the classical type of NLSs. The programs are based on rules derived from experimental observations searching for the consensus motifs within a sequence. Briefly they operate by converting a protein's amino acid sequences into numerical localization features (based on sorting signals, amino acid composition and functional motifs).

In-depth analysis of non-classical NLSs was performed using NLStradamus (http://www.moseslab.csb) that is based on a simple Hidden Markov Model for nuclear localization signal prediction (Nguyen Ba et al., 2009) and NucPred (http://www.sbc.su.se) (Brameier et al., 2007). These programs analyse the composition of the basic residues within the protein sequence and able to predicts if the protein is likely to translocate to the nucleus.

2.1.2 Prediction of Nuclear Export Sequence (NES)

To determine if FGF10 is exported form the nucleus in the classical way the LocNes (http://omictools.com/locnes-s7902.html) tool was used. It is a Support Vector Machine (SVM) predictor, i.e. mathematical model that functions by locating classical nuclear export signals (NESs) in proteins that are cargoes of the Karyopherin β, called the chromosomal region maintenance 1 (CRM1). The CRM1 recognizes and exports from the nucleus hundreds of broadly functioning proteins (Ishizawa et al., 2015). Most CRM1 cargoes contain the classical leucine-rich NESs – a peptide of regularly spaced 8-15 conserved hydrophobic residues.

The obtained results were validated further using the ValidNESs (http://validness.ym.edu.tw/PREDICTION.php), a mathematical algorithm using regions of protein intrinsic disorder and other features such as the frequency of specific amino acids within particular regions, to predict leucine-rich NESs within protein sequence (Fu et al., 2011, Fu et al., 2013).

2.1.3 Predictions of putative post-translational modifications regarding FGF10

Analysis of protein SUMOylation was performed by a prediction algorithm GPS SUMO (http://sumosp.biocuckoo.org) that is based on experimental data, and able to determine the canonical consensus motifs as well as novel SUMO-interaction Motifs (SIMs) (Zhao et al., 2014). The PCI-SUMO (http://bioinf.sce.carleton.ca/SUMO) program on the other hand uses parallel cascade identification (PCI), a mathematical nonlinear system, that predicts the SUMO sites without any prior experimental knowledge regarding protein's subcellular localization.

Prediction of cut-off point of signal peptide (SP) of FGF10, was performed using SignalP 4.1 (http://www.cbs.dtu.dk), a program based on a combination of several artificial neural networks that incorporates a prediction of SP cleavage sites. Moreover the program can distinguish between the actual SP and protein transmembrane motifs (Petersen et al., 2011).

To prediction sites of glycosylation within FGF10 the NetNGlyc 1.0 Server (http://genome.cbs.dtu.dk) was applied. It predicts *N*-glycosylation sites in human proteins using artificial neural networks that examine the sequence in context of consensus motifs. Similarly the NetOGlyc 4.0 Server (http://www.cbs.dtu.dk) is based on same principles and generates neural network predictions of *O*-glycosylation sites in mammalian proteins. To further confirm the results, the GlycoEP (http://www.imtech.res.in) bioinformatics tool was used, that is a Support Vector Machine (SVM) predictor, trained and optimised using eukaryotic glycosites' datasets, performing stringent predictions of all types of glycosylation.

2.1.4 Searches of putative regulatory promoter sites of Fgf10

To determine any putative regulatory promoter sites, from human genomic sequence located on chromosome 13, a region was selected spanning from -77087 to -9000bp upstream of the Fgf10 translational start site. This region was then analysed using Promoter 2.0 Prediction (http://www.cbs.dtu.dk), program based on variation of neural networks and genetic algorithms; developed as an evolution of simulated

transcription factors that interact with sequences in promoter regions. It predicts specifically transcription start sites of vertebrate Polymerase II promoters in DNA sequences.

To enhance further the searches, the region between -1000 to +100 downstream of the ATG start site was analysed using Neural Network Promoter Prediction (http://www.fruitfly.org), and EPD - Eukaryotic Promoter Database (http://epd.vital-it.ch), two independent software tools that are based on collection of already discovered eukaryotic POL II promoters and comparing the existing knowledge to the sequence provided.

2.1.5 Other bioinformatics tools

Protein sequences were aligned using the CLUSTAL 2.1 multiple sequence alignment tool - Clustal Omega (http://www.ebi.ac.uk/Tools/msa/clustalo/). Sequencing data received from Source Bioscience was processed in SerialCloner1-3 and visualised in a form of peaks using ChromasLite program. Protein 3D structures were analysed and imagined using Chimera 1.9 (using protein structure data from Protein Data Bank - RCSB PDB). ImageJ and Photoshop programs were used to process images and generate cell counts. To calculate co-localisation of fluorescent markers on microscope images Volocity 6.3 software was used.

2.1.6 *In silico* Predictions of FGF10 binding to Importin using haptics-assisted molecular docking system

To determine if FGF10 is potentially able to interact with Importin molecules, the two proteins were fitted together *in silico* using a molecular docking system innovated with haptic system. Briefly, molecular docking systems generate predictions of the most plausible binding orientations of one protein to another. They aim to model and simulate *in silico* the intermolecular biochemical interactions, providing visual aid to the experimental studies. The haptics-assisted docking, in regards to rigid mathematical algorithms, enables the user to interact with the simulation via their sense of touch (Fig. 2.1). The repulsion forces arising between the two interacting proteins are calculated by the software, basing on the atoms coming into a close contact, and they determine the preferred orientation of the binding molecules. The closer the repulsion forces to zero, the more likely the interaction to occur in nature. Incorrect binding generate repulsing forces that can be sensed through the haptic device, avoiding misleading predictions and allowing quick adjustments of the molecules (Iakovou et al., 2015, Iakovou et al., 2014).

Within the tertiary structure of FGF10 (PDB 1NUN file), the NLS2 motif was selected, highlighted and fitted to isoforms of Importin-α (PDB 3WPT file) and Importin-β (PDB 1M5N file). Files showing the potential interactions were visualised, presented and imaged using Chimera 1.9 software (see Chapter 3). The molecular docking software with the haptic device was generated by Georgios Iakovou, who also kindly created the fittings of FGF10 to the Importins. Only cases that match specific repulse force requirements are assessed as probable "molecular fittings" (Iakovou et al., 2015).

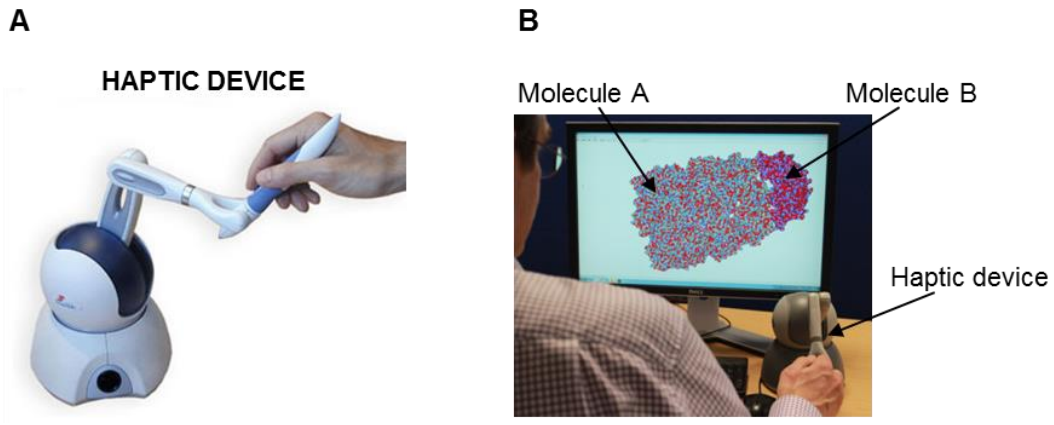

Figure 2.1 The haptics-assisted molecular docking system generates *in silico* predictions of protein-protein interactions (A) An example of the haptic device used for molecular docking (http://souvrsophie.blog.com) (B) Vibrations generated by the repulsion forces of the interacting proteins allow manual adjustment of the so called "molecular fittings" (Iakovou et al., 2014).

Part 2.2 Generation of Hemagglutinin A (HA) tagged rat FGF10 (rFGF10-HA) construct

2.2.1 PCR amplification of rFGF10-HA sequence

Rat FGF10 cDNA sequence was amplified from a rFgf10-pGEM-T vector (kind gift of Prof Saverio Bellusci) using forward primer with implemented EcoRI restriction enzyme site and reverse primer with implemented HA-tag DNA sequence and NotI restriction enzyme site (Fig. 2.2). The amplified PCR product was precipitated using Sodium Acetate (pH 5.2) and 100% EtOH, then treated with endonuclease restriction enzymes, EcoRI and NotI (NEBiolabs), at 37ºC overnight, to generate 'sticky ends' for following ligation into a vector. The digested DNA samples were then purified using GeneClean kit (MP bio).

Figure 2.2 Generation and amplification of HA tagged rat Fgf10 construct. (A) Sequence of rat Fgf10 (rFgf10) cDNA, incorporated within the pGEM-T vector between SphI and NdeI restriction sites, was provided as a kind gift of Prof S Bellusci. (B,C) Schematic diagram with a corresponding table of generation of HA-tagged rFgf10 through PCR amplification of the rFgf10 sequence using forward primer (FP) with incorporated EcoRI restriction enzyme binding site (purple) and reverse primer (RP) with incorporated HA tag DNA coding sequence (red) and NotI restriction enzyme (blue) binding site. (D) Schematic showing excision of mCherry sequence from the pmCherry-N1 vector (herein called “pmN1”) and substituting it with rFgf10-HA flanked by EcoRI and NotI restriction enzyme sites.

A

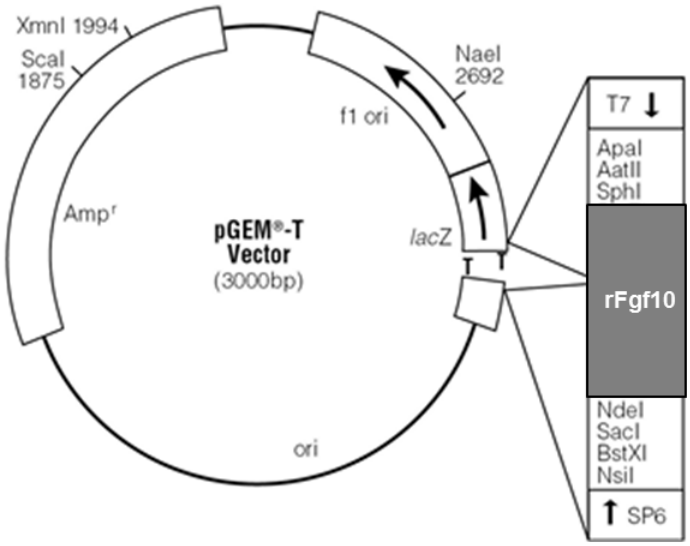

B

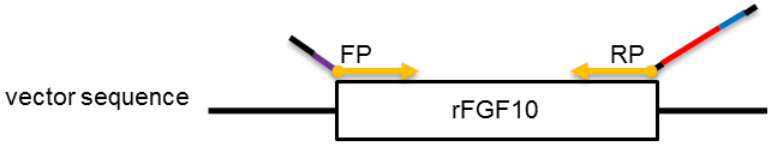

C

Primer	Primer Sequences (5'-3')
Forward Primer (FP)	5' GCTTCGAATTCAGATGTGGAAATGGATACTGACACATTG 3'
Reverse Primer (RP)	5'GTCAAGCGGCCGCTTAAGCGTAATCTGGAACATCGTATGGGT AACCAGCTGAGTGGACCACCATGGGGAGGAAGTG 3'

D

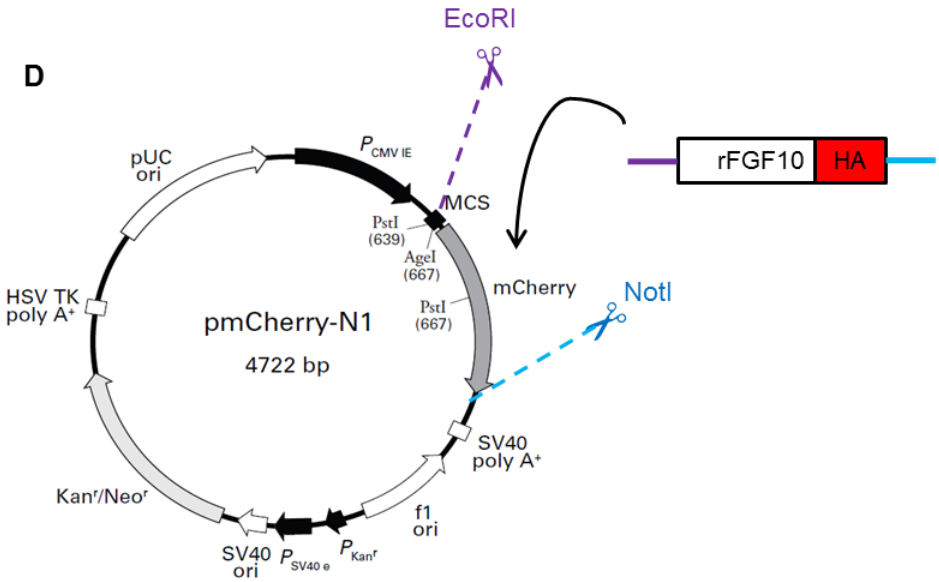

2.2.2 Preparation of the cloning vector

As a backbone vector, a pmCherry-N1 (Clontech Laboratories, Inc.) mammalian expression plasmid was used, from which the cDNA sequence of mCherry was removed between the EcoRI and NotI sites (Fig. 2.2D), by digestion with the restriction enzymes (NEBiolabs), at 37ºC overnight. Moreover treatment with enzymes generated 'sticky ends' allowing ligation of the PCR product of the rFGF10-HA sequence. The linearised vector sequence was separated from the residual mCherry DNA fragment by gel extraction from TAE 0.8% agarose gel (from now on called pmN1), where the band size was determined by comparing to 1kb Plus DNA Ladder (Thermo Scientific SM1331). To prevent re-circularization of linearized vector DNA, it was then treated with Calf-intestinal alkaline phosphatase (CIP) (Invitrogen 18009-027) for 1h and purified using GeneClean kit (MPbio).

2.2.3 Ligation and cloning of the rFGF10HA and vector sequence

The purified PCR product and vector sequences were ligated at ~18ºC overnight using T4 ligase (Sigma Aldrich) in a ratio 1:5 of 'pmN1' vector (20ng) to rFgf10-HA PCR insert (15ng), taking into account the length of both DNA strands, using following equation (providing a ratio 1:1 of vector to insert):

$$\frac{length\ of\ insert\ (kb)}{length\ of\ vector\ (kb)} \times Vng = Ing$$

Where: "kb" – kilo bases, "Vng" – nano-grams of vector, "Ing" – nano-grams of insert

Ligated product was transformed into DH5α competent cells, before culturing on Kanamycin antibiotic containing selection medium. 16 hours later, DNA was extracted from several selected colonies using mini and maxi-prep kits (Qiagen) according to the manufacturer's instructions. Concentration of the DNA was determined by conventional spectrophotometer or Nanodrop spectrophotometer.

2.2.4 Verification of the generated rFGF10HA construct

The presence of the rFgf10-HA insert within the pmN1 vector was verified by two means: (i) by digest with restriction nuclease enzymes (~200ng of DNA treated

with ScaI only or EcoRI and NotI for 1h 37ºC) and (ii) PCR reaction (see Chapter 4). For the diagnostic PCR (Table 2.1), the forward (5' CTACCGGACTCAGATCTCGAGCTC 3') and reverse (5' GCCTTAAGATACATTGATGAGTTTGG 3') primers bind to the vector sequence s flanking the insert. In the presence of an insert an expected band of 941bp would be observed, whilst in its absence, a 369bp band would be visible (see Chapter 4).

Cycle stage	Temperature (ºC)	Time	Number of cycles
Initial Denaturation	94	2'	x1
Denaturation	94	15''	x10
Annealing	65	30''	
Elongation	68	45''	
Denaturation	94	15'	x15
Annealing	63	30''	
Elongation	72	1'(+5'/cycle)	
Final Elongation	72	7'	x1
Cooling (End)	4	15'<	x1

Table 2.1 Cycles used for the diagnostic PCR of successful incorporation of rFgf10-HA insert into pm-N1 vector.

Samples carrying the correct, insert were then subjected to Sanger sequencing (Source Bioscience) to check for any PCR-introduced undesired mutations.

Part 2.3 Site-directed mutagenesis

All point mutation-bearing FGF10 products were generated by PCR (Fig. 2.3) using a QuikChange Lightning Site-Directed Mutagenesis Kit (Agilent Technologies) according to manufacturer's instructions with the relevant custom designed mutation-bearing primers (Table 2.2).

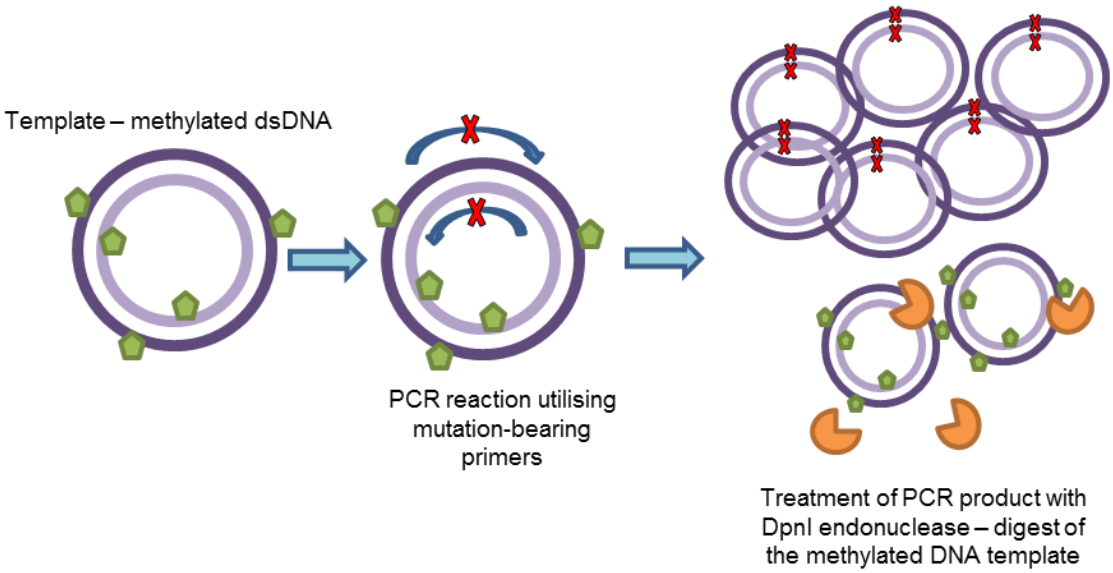

Figure 2.3 Schematic of site-directed mutagenesis procedure. The technique involves PCR reaction utilising a derivative of PfuUltra high-fidelity DNA polymerase, a pair of custom designed mutation-bearing primers and a dsDNA vector template (isolated from competent *E.coli* cells that caused its methylation). The obtained PCR product is subsequently treated with DpnI endonuclease enzyme, which recognises and digests methylated DNA, therefore removes the template. Green pentagon – DNA methylation; in orange – DpnI enzyme.

2.3.1 Primer design

In order to generate a double-stranded vector in PCR reaction, it was essential to design each pair of primers individually, ensuring that both (forward and backward) mutagenic primers contained the desired mutation and annealed to the same sequence on opposite strands of the plasmid (Fig. 2.3). Primers were designed for optimal PCR performance, by minimising primer dimer formation, ensuring balanced GC content and melting temperature (Tm) according to the 4+2 rule. Typically, a primer would consist of 25 base pairs, with a Tm of ~73 to 78°C. The desired point mutation was incorporated close to the middle of the primer with ~10–15 bases of template sequence flanking it. Typical GC content was 40% and primers terminated in one or more C or G bases at their 3' ends (Table 2.2). To generate a quadruple mutation within the NLS2 region, the R194T&R195T forward and reverse primers were used in conjunction with the R200T&K202T plasmid template. The technical limitations of the kit prevented generation of a triple mutation of R194T&R195T&K198T – such modification within primers disabled the PCR reaction.

Primer name	Sequence (5' to 3')
G145E (F)	GCCATGAACAAGAAGG**A**GAAACTCTATGGCTC
G145E (R)	GAGCCATAGAGTTTC**T**CCTTCTTGTTCATGGC
R194T (F)	GGAAAAGGAGCTCCCA**C**GAGAGGACAAAAAAC
R194T (R)	GTTTTTTGTCCTCTC**G**TGGGAGCTCCTTTTCC
R195T (F)	GGAGCTCCCAGGA**C**AGGACAAAAAACAAGAAGG
R195T (R)	CCTTCTTGTTTTTTGTCCT**G**TCCTGGGAGCTCC
K198T (F)	CCAGGAGAGGACAAA**C**AACAAGAAGGAAAAAC
K198T (R)	GTTTTTCCTTCTTGTT**G**TTTGTCCTCTCCTGG
R200T (F)	GAGGACAAAAAACAA**C**AAGGAAAAACACCTCCGC
R200T (R)	GCGGAGGTGTTTTTCCTT**G**TTGTTTTTTGTCCTC
R201T (F)	GGACAAAAAACAAGAA**C**GAAAAACACCTCCGCTC
R201T (R)	GAGCGGAGGTGTTTTTC**G**TTCTTGTTTTTTGTCC
K202T (F)	CAAAAAACAAGAAGGA**C**AAACACCTCCGCTCAC
K202T (R)	GTGAGCGGAGGTGTTT**G**TCCTTCTTGTTTTTTG
R194T&R195T (F)	GGAAAAGGAGCTCCCA**C**GA**C**AGGACAAAAAAC
R194T&R195T (R)	GTTTTTTGTCCT**G**TC**G**TGGGAGCTCCTTTTCC
R200T&R201T (F)	GAGGACAAAAAACAA**C**AA**C**GAAAAACACCTCCGC
R200T&R201T (R)	GCGGAGGTGTTTTTC**G**TT**G**TTGTTTTTTGTCCTC
R200T&K202T (F)	CAAAAAACAA**C**AAGGA**C**AAACACCTCCGCTCAC
R200T&K202T (R)	GTGAGCGGAGGTGTTT**G**TCCTT**G**TTGTTTTTTG
G145V (F)	GCCATGAACAAGAAGG**T**GAAACTCTATGGCTC
G145V (R)	GAGCCATAGAGTTTC**A**CCTTCTTGTTCATGGC
G145A (F)	GCCATGAACAAGAAGG**C**GAAACTCTATGGCTC
G145A (R)	GAGCCATAGAGTTTC**G**CCTTCTTGTTCATGGC

Table 2.2 Primer sequences with specific mutation incorporated shown in bold used to generate nucleotide substitution of rFGF10-HA.

2.3.2 PCR reactions of mutated constructs

The PCR reactions of the mutation-bearing constructs using the QuikChange Lightning were performed according to manufactures suggestions, as a 50µl reaction, using 50ng of the rFgf10-HA template, 5µl of 10x reaction buffer, 125ng of each of the primers, 1µl of QuickSolution reagent and 1µl of QuickChange Lightning Enzyme. The reactions were subsequently subjected to the specific PCR cycles (Table 2.3).

Cycle stage	Temperature (ºC)	Time	Number of cycles
Initial Denaturation	96	3’	x1
Denaturation	96	45’’	x18
Annealing	67-70*	30’’	
Elongation	72	5’	
Final Elongation	72	10’	x1
Cooling (End)	4	15’<	x1

Table 2.3 PCR cycles used for site-directed mutagenesis. Note the annealing temperature range (*), which was adjusted accordingly to the primers’ melting temperature.

2.3.3 PCR mutation-bearing construct processing and validation

Following the PCR reaction the obtained product was purified from the template (non-mutated) DNA, by treatment with DpnI endonuclease enzyme at 37ºC for 10min (Fig. 2.3). The template plasmid has been previously isolated from competent *E.coli* cells, where it became methylated by a ‘dam’ methylase. The DpnI enzyme is specific to methylated DNA (targets the 5’Gm^{6}ATC3’ sequence), and digests it, leaving purified mutation-bearing DNA product (Fig. 2.3), which was subsequently transformed into XL-10 Gold competent cells, through 30sec heat-shock at 42ºC. Several bacterial colonies, cultured on a Kanamycin selective medium, have been isolated, DNA extracted and the desired mutation-bearing products were selected by Sanger sequencing (Source Bioscience).

Part 2.4 Transgenic Animals

All animals used in this study were maintained, bred, treated and culled in strict compliance with terms of a Home Office licence granted to Dr Mohammad Hajihosseini. *In vivo* drug administrations, such as tamoxifen, were performed by Dr Timothy Goodman. For genotyping, DNA was extracted from tail biopsies and digested at 55ºC overnight, in a digest buffer (1M Tris, 0.5M EDTA, 5M NaCl, 2mg/mL SDS in ddH_20) containing 7µg/mL Proteinase K. Genomic DNA was then precipitated using isopropanol and subjected to Expand Long Template PCR (Roche) using gene-specific primers (Table 2.4) and PCR cycles (Table 2.5).

Allele	Primer Sequences (5'-3')	Product size (Kb)
$Fgf10^{nLacZ/+}$	GCATCGAGCTGGGTAATAAGCGTTGGCAAT	LacZ: 0.8
	GACACCGACACAACTGGTAATGGTAGCGAC	
	CGAGTGGAGCATGTACTTCCGTGTCCTGAA	WT: 0.5
	TCCCTACCCAGTCACAGTCACAGCTGCATA	
$Fgf10^{+/CreERT2}$	AGCAGGTCTTACCCTTCCAGTATGTTCC	Cre: 0.55
	TCCATGAGTGAACGAACCTGGTCG	
	AGCAGGTCTTACCCTTCCAGTATGTTCC	WT: 0.3
	CTCCTTGGAGGTGATTGTAGCTCCG	
$ROSA^{tomato}$	CTGTTCCTGTACGGCATGG	Tomato: 0.2
	GGCATTAAAGCAGCGTATCC	
	AAGGGAGCTGCAGTGGAGTA	WT: 0.3
	CCGAAAATCTGTGGGAAGTC	

Table 2.4 Primer sequences used for genotyping transgenic mice, with corresponding expected PCR product sizes shown in kilo-bases (kb)

Allele	Cycle stage	Temperature (ºC)	Time	Number of cycles
$Fgf10^{nLacZ/+}$	Denaturation	94	2’	x1
	Stage 1	94	30’’	x15
		62	45’’	
		68	1’	
	Stage 2	94	30’’	x17
		62	30’’	
		68	1’ (+40’’/cycle)	
	Final Elongation	68	7’	x1
	Cooling (End)	6	15’<	x1
$Fgf10^{+/CreERT2}$	Denaturation	94	2’	x1
	Stage 1	94	30’’	x10
		61	30’’	
		68	2’40’’	
	Stage 2	94	30’’	x17
		61	30’’	
		68	2’40’’ (+40’’/cycle)	
	Final Elongation	68	7’	x1
	Cooling (End)	6	15’<	x1
$ROSA^{tomato}$	Denaturation	94	2’	x1
	Stage 1	94	30’’	x10
		60	30’’	
		68	1’10’’	
	Stage 2	94	30’’	x17
		60	30’’	
		68	1’10’’ (+20’’/cycle)	
	Final Elongation	68	7’	x1
	Cooling (End)	6	15’<	x1

Table 2.5 PCR cycles used for genotyping transgenic mice using corresponding primers from Table 2.3

2.4.1 Fgf10$^{+/CreERT2}$ ::ROSA26R$^{tomato-DsRed}$ reporter mice

The Fgf10$^{+/CreERT2}$ ::ROSA26R$^{tomato-DsRed}$ mouse (Fgf10-tomato) is a conditional reporter allele, so that the system becomes activated only upon treatment with Tamoxifen drug. The mouse was generated by incorporating a Cre-ERT2-IRES-YFP into the end sequence of the first exon and beginning of the first intronic sequence of the Fgf10 gene (Fig. 2.4B). This insertion leaves the first exon dysfunctional and disrupts some regulatory *cis* sequences of the first Fgf10 intron leaving the allele non-functional and therefore mice were bread as heterozygotes – homozygous Fgf10^{CreERT2} mice are not viable (El Agha et al., 2012). The inserted construct encodes a Cre recombinase fused to the ERT2, becoming expressed in Fgf10-expressing cells only. This protein complex is retained in the cytoplasm in its inactive form. Treatment with the tamoxifen activates the Cre-ERT2 complex and allows its entry into the nucleus, where Cre binds to and excises loxP sites flanking a STOP cassette positioned ahead of transcription start site of red fluorescent protein, named tomato, (Fig. 2.4D), that is driven by a ROSA26 promoter.

In summary, upon treatment of the tamoxifen, all the Fgf10 expressing cells and their descendants, express also a tomato fluorescent reporter protein.

To activate tomato-DsRed (tomato) tamoxifen was administered via intraperitoneal injections of 20mg/mL solution (in 10%EtOH/corn oil mixed several hours at 55ºC) at 80-100mg/Kg mouse bodyweight. Depending on the experiment, mice were induced with tamoxifen at varying ages ranging from postnatal day 4 (P4) to postnatal day 40 (P40). Tamoxifen inductions were performed over a period of two days, and induced mice were culled, by cervical dislocation, 7 days later to allow for sufficient gene recombination.

2.4.2 Fgf10$^{nLacZ/+}$ (Fgf10-LacZ reporter) mice

Fgf10-lacZ mice had previously been generated by Kelly and colleagues though incorporation of nuclear targeted lacZ-transgene 114kb upstream of Fgf10 translational start site (Kelly et al., 2001) (Fig. 2.4C). Although this insertion does not disrupt the Fgf10's translation, it appears to impair some regulatory *cis* sequences generating a slight hypomorph of FGF10 (Mailleux et al., 2005). Hence, the mice were maintained as heterozygotes (Fgf10lacZ/+). The insertion of nLacZ is not a protein fusion and produces two separate transcripts. In tissues derived from this mouse, the product of the nLacZ gene, the β-galactosidase (β-gal) will appear mostly in the nucleus of Fgf10-expressing cells.

The generated β-galactosidase enzyme cleaves lactose into glucose and galactose. Upon treatment with X-gal solution (analogue of lactose, consists of galactose linked to a substituted indole) an intensely blue product is produced which is insoluble and can be easily visualised. The presence of β-galactosidase can also be detected through immunocytochemistry (ICC) upon treatment with anti β-galactosidase antibody.

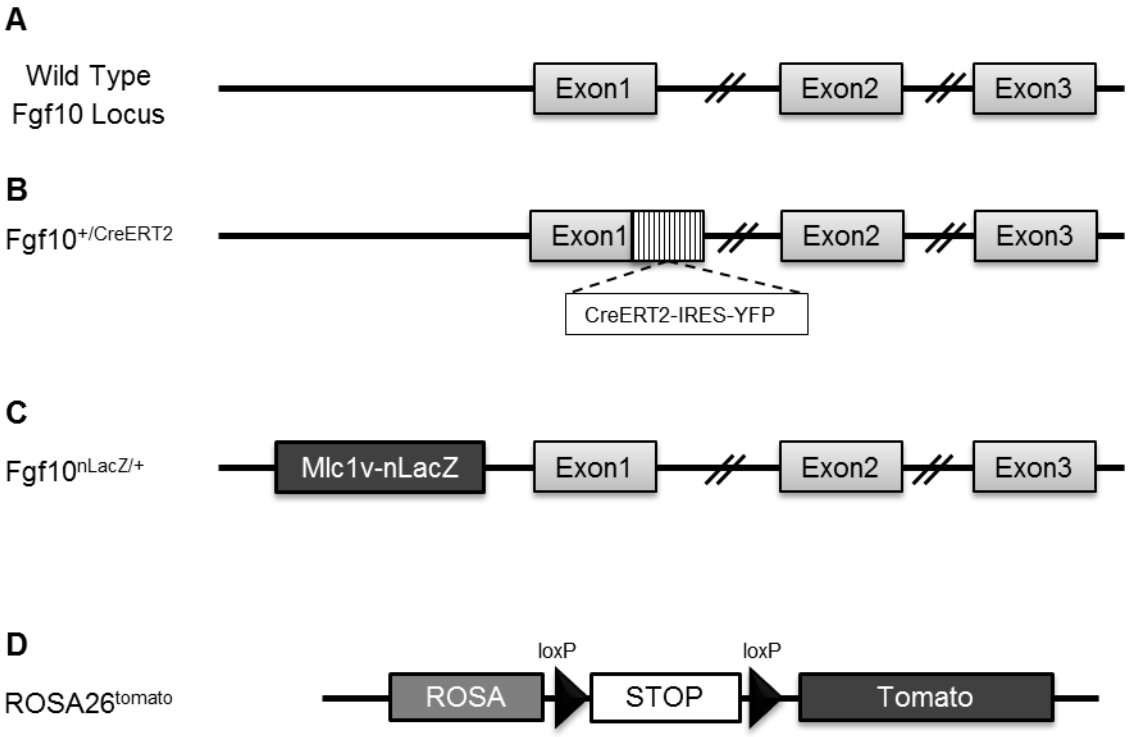

Figure 2.4 Schematic representation of genomic alleles of transgenic mice used. (A) Wild Type Fgf10 locus shows approximate positions of three exons and two introns. (B) In the $Fgf10^{+/CreERT2}$ line, the Cre-ERT2-IRES-YFP construct was inserted at the end of Exon1, disrupting beginning of the Intron1 sequence as well. (C) In the $Fgf10^{nLacZ/+}$ reporter, the nuclear LacZ (nLacZ) sequence was incorporated under the Fgf10 promoter, but upstream of the Exon1. (D) The ROSA26-tomato line has a STOP cassette, flanked by two loxP sites, incorporated upstream of the Tomato sequence but downstream of the ROSA26 promoter.

2.4.3 Dissection and preparation of hypothalamic cell suspension

Mice were sacrificed by cervical dislocation (in accordance to Schedule 1 Home Office Procedure), brains were removed from the skull and placed in Dulbecco's Phosphate Buffered Saline (DPBS) supplemented with 10% glucose and 5% HEPES

solution. The subventricular zone (SVZ) and hypothalamus regions were finely dissected out and then dissociated in a pre-warmed (37˚C) PPD digestion solution (comprised of 0.1mg/ml Papain; 1mg/ml Dispase II; 12.4 mM MgSO4 $7H_2O$ in HBSS) and incubated further at 37˚C for 2-5min. The tissue was gently triturated using a P1000 pipette tip until it was fully dissociated and clumps of cells were no longer visible. Dissociated cells were then centrifuged at 1000rpm, excess PPD solution was separated from the pellet and the cells were washed twice in a culture medium, by gentle dissociation and centrifugation. After the last wash, the pellet was resuspended in 2ml of a culture media and passed through 40µm nylon cell strainer to obtain a solution of single cells.

Part 2.5 Primary cell cultures

2.5.1 Establishment and growth of neurospheres

Single cell suspension of hypothalamic cells was seeded in a T25 flask in a NB-B27 medium (Neurobasal A medium (Gibco 10888-022) supplemented with 2% B27, 2µg/ml heparin, 1% Pen&Strep and 1% Glutamax solution). EGF and FGF2 growth factors were added fresh into the culture at a 20ng/µl concentration each. Cells were then incubated in 5% CO2 at 37ºC in a humidified chamber. Cultures were fed twice a week, supplying fresh amount of growth factors at each feed. Growth of the culture was monitored every 2-3 days and when spheres reached 300-400µm in a diameter, they were passaged.

To passage neurospheres, cells were dissociated by gentle trituration of spheres with P1000 pipette tip. Dissociated cells were then passed through a 40µm cell strainer to remove any cell aggregations and the resulting filtrate, containing single cells, was seeded at a clonal density of 50 cells/ml in a 50% conditioned NB-B27 medium.

2.5.2 Measuring growth rate of neurospheres

To determine the growth rate of neurospheres, single cells were seeded at clonal levels and the diameter of neurospheres was measured every 3-4 days. At each time point, 10 random neurospheres were measured. Since neurospheres do not grow

uniformly and small as well as big neurospheres are normally present in the same culture, to avoid cell death of an overgrown culture, the bigger spheres were measured.

Diameter measurements were taken until the spheres reached the passaging stage and care was taken to avoid measuring spheres that have clearly merged together (see Chapter 6). In a culture of neurospheres derived from the Fgf10$^{+/CreERT2}$ ::ROSA26R$^{tomato\text{-}DsRed}$ mouse, the expression of tomato was visualised using a fluorescent microscope. The growth rate was calculated using the following equation:

$$growth\,rate\ (\%) = (\frac{dn}{d0})^{\frac{1}{n}} - 1$$

Where "*d*0" is initial diameter, "*d*n" is diameter after "n" days in culture and growth rate is expressed as percentage.

When the neurospheres reached the passaging stage (ranging from 12-35 days depending on a passage number), the whole process was repeated. Cultures were passaged up to 6 times, until the passaged cells become quiescent and stopped forming neurospheres.

2.5.3 Induction of neurosphere differentiation into neurons and glial cells

Neurospheres were dissociated into single cell suspension by gently triturating with a P1000 pipette tip, and subsequently seeded at a 50x10^3 cells/well concentration on glass coverslips (placed in a 24 well plate and previously coated with 20µg/ml poly-D-lysine). To further stimulate differentiation, the NB-B27 growth medium was supplemented with 10% FBS and replaced every 3-4 days for 2 weeks. Differentiated cells were then fixed for 15min in 4% paraformaldehyde (PFA), immunolabelled with cell-type specific marker antibodies (see below) and mounted onto microscope slides.

2.5.4 Fluorescence-activated cell sorting (FACS) of primary hypothalamic cells

Several attempts were made to separate and isolate population of tomato fluorescence expressing cells from the remainder from the hypothalamic cell suspension. Cells were freshly dissected and dissociated from hypothalamic extract of the minimum number of two Fgf-tomato reporter and corresponding number of wild type control mice at the age of P8, pulsed *in vivo* with tamoxifen at the age of P4-P5. Cells were dissociated in a pre-warmed (37˚C) PPD digestion solution (comprised of

0.1mg/ml Papain; 1mg/ml Dispase II; 12.4 mM MgSO4 $7H_2O$ in HBSS) and incubated further at 37˚C for 2-5min. The tissue was gently triturated using a P1000 pipette tip until it was fully dissociated and clumps of cells were no longer visible. Subsequently cells were washed with HBSS supplemented with 0.01%BSA and 2mM EDTA, which was used to prevent cell aggregation, importing during the process of cell sorting. Cells were then passed through 40µm nylon cell strainer, to remove debris and ensure single cell suspension, which was then subjected to the FACS sorting machine operated by a qualified technician at Institute of Food Research, Norwich. Sorted cells were collected in 2ml of 100% FBS.

2.5.5 Establishment and growth of hypothalamic monolayer cell cultures

Mouse hypothalamus was freshly isolated from brains of 2-6 weeks old wild type (WT) or Fgf10-lacZ or tomato reporter mice. Hypothalamic cells were then dissociated and grown as a monolayer in DMEM/F12 HAMs media (Gibco 21331) supplemented with 5% FBS; 1% penicillin/streptomycin; 1% GlutaMAX; 1% B27 Supplement (Gibco); 35 µg/ml bovine pituitary extract (Invitrogen) and 20 ng/µl each of EGF and FGF2 (Peprotech).

The cells were seeded in a T25 flask or a six/ twelve-well plates at clonal densities (approximately $5x10^4$cell/ml), unless stated otherwise. The culture medium was replaced every 3-4 days and cells were maintained for either 6-10 days, or for the long term studies for >30 days. For the immunolabelling purposes cells were also seeded and cultured on PDL-coated glass coverslips.

2.5.6 Passaging of hypothalamic monolayer cell cultures

Sub-confluent cultures (~80% confluency) were passaged by treating cells with Trypsin-EDTA (0.05%) (Gibco). After removal of the growth media, cells were washed with Cell Harvest Buffer (0.02%EDTA Na_2^+, 0.9%NaCl, HEPES (free acid) 2.38g/L, 125µl/L Phenol Red, pH7.2) and then incubated with Trypsin at 37ºC for 2-5min. Removal of the cells from the bottom of the culture dish was aided by tapping on the side of the dish untill all cells had dislodged. Trypsin was inactivated by addition of the culture medium and cells were re-seeded (1 in 10 dilution) in a fresh container at clonal densities.

In order to determine the proportion of LacZ expressing cells, cultured from Fgf10-LacZ reporter, cells were obtained from eight mice at the age of P35, pulled together and cultured across 2 individual T25 dishes at semi-clonal densities. During

passaging, one of the dishes was stained with X-gal solution to determine the proportion of cells expressing β-gal, while the other was passaged according to the protocol, again providing at least 2 individual culture dishes.

2.5.7 X-gal staining of monolayer cell culture

Cells were rinsed with PBS and fixed with 0.5% glutaraldehyde (prepared in PBS) for 15min at RT. Then cells were rinsed three times with PBS and once with ddH_20 for 5min, and incubated for 30 min at 37ºC in (pre warmed) staining solution containing 2mM $MgCl_2$, 5mM $K_4Fe(CN)_6$, 5mM $K_3Fe(CN)_6$) and 0.5µg/ml X-gal (X-gal stock solution was prepared at 20mg/mL in 8% N,N Dimethylformamide and stored in aliquots at -20ºC). Once blue colour was evident, cells were rinsed several times in PBS and fixed for 10min with 4% PFA solution.

2.5.8 Measuring growth rate of LacZ positive patches

Cells derived from Fgf10-LacZ reporter mice (at the age of P8, P30 and P40) were cultured at semi-clonal densities, which gave rise to clonal patches of cells. Treatment with X-gal solution allowed to identify the LacZ expressing cell patches, within each number of cells was counted. From each culture 3 biggest patches were selected as an indication of the maximum propagation potential of the given culture. Therefore at P8, ‘n’ number of mice was equal to 3 and number of colonies analysed was 9. At P30, cells were derived from 10 mice and 30 colonies were analysed, whereas at P40, 9 mice were used and 27 colonies selected. It was assumed that the cells were undergoing symmetrical division and therefore the cell patches were growing exponentially. Therefore the growth rate of each patch was calculated according to the following equation:

$$P(t) = P_0e^{rt}$$

Where: P(t) = number of cells at time t

P_0 = initial amount of cells at time t = 0 (time of seeding) – because it was assumed each cell patch was a clonal cluster (due to seeding at semi-clonal density), it was presumed that each cell patch was derived from an individual proliferating cell, therefore $P_0 = 1$

r = the growth rate

t = time (number of days in culture) before fixing

2.5.9 Tamoxifen treatment of hypothalamic cell monolayers *in vitro*

Small patches of ~5 days old monolayer cultures of cells, derived from the Fgf10-tomato reporter mouse, were treated with 3µg/ml tamoxifen drug (kept in stock of 20mg/ml in DMSO), previously replacing the cell media 12-24h prior to drug treatment. To administer the drug, the culture media was briefly removed from the culture dish (leaving a small amount to prevent cells from drying) and placed in a Falcon tube, where tamoxifen was added to and mixed with. The drug containing media was re-applied to cells for 24h, then replaced with the fresh one and cultured for further 7-10 days or until confluent. The expression of the tomato protein in live cells was checked under the fluorescent inverted microscope. To account for possible cell death, the control cells were treated with corresponding amount of DMSO.

2.5.10 Differentiation of hypothalamic cell monolayers

Single cell suspensions derived from Fgf10-tomato reporter mouse hypothalamus were seeded on PDL-coated glass coverslips at a very high density (approximately $5x10^5$ cell/ml) and cultured for 10-30 day, until a top layer of differentiated neurons had emerged (see Fig. 6.16A) (Louis et al., 2013). Cultures were then fixed with 4% PFA 15min and immunolabelled with fluorescent antibodies.

2.5.11 Profiling of FGFs and FGFRs expression of cultured hypothalamic cell by RT-PCR

RNA was extracted from sub-confluent (~80%) culture of wild type (WT) hypothalamic cell monolayer grown in 10cm Petri dishes. Cultured cells were rinsed once with PBS and covered with 1ml of Trizol reagent, before being scraped off and, transferred to microcentrifuge tube. After 5 min incubation in Trizol at RT, 200µl chloroform was added to the tube, shaken vigorously for 15sec, incubated for a further 3min at RT and centrifuged at 12000rpm 15min 4ºC. Samples had separated into several layers and the top aqueous (clear) layer containing RNA was removed, RNA was precipitated by addition of 500µl Isopropanol for 10min at RT and sample was centrifuged at 12000rpm for 15min 4ºC, as a result of which a pellet formed on the side of the tube. After careful removal of the supernatant the pellet was washed with 1ml of 75% EtOH, vortexed for 5min 4ºC and centrifuged further 9000rpm 12min 4ºC. The supernatant was removed, and the pellet was briefly air-dried and re-suspended in 30µl of RNAse free ddH_20. To fully dissolve the RNA, the sample was incubated 10min at

55ºC. The Concentration and purity of RNA in the sample was determined using a Nanodrop spectrophotometer.

RT-PCR reaction was performed using the Illustra Ready-To-Go™ RT-PCR Beads (GE Healthcare) in accordance with the manufacturer's instructions. Briefly, lyophilized beads (containing M-MuLV Reverse Transcriptase, RNase Inhibitor, buffer, nucleotides, and Taq DNA Polymerase) were rehydrated with RNAse free water and kept on ice until the beads had fully dissolved. 1µg of sample RNA and 1µl of poly-$d(T)_{12\text{-}18}$ primers (Invitrogen 18418012) were added to each reaction tube and mixed gently. Samples were then subjected to the first stage of reverse transcription PCR cycle (see table). After the reaction was completed pairs of FGF and FGFR-specific primers (Hajihosseini and Dickson, 1999, Hajihosseini and Heath, 2002) was added each tube, which were then subjected to second phase of PCR cycle (Table 2.6). Detection of β-actin transcript was used as a general control for the PCR conditions. Following the completed two stage RT-PCR, the samples were resolved on a 1% agarose-TBE gel through electrophoresis and visualised with ethidium bromide under UV illumination.

RT-PCR Stage	Cycle stage	Temperature (ºC)	Time	Number of cycles
1) Reverse Transcriptase	Denaturation	42	15'	x1
	Annealing	95	5'	
	Cooling (End)	6	10'	
2) PCR	Denaturation	95	30''	x34
	Annealing	60	30''	
	Elongation	68	1'	
	Cooling (End)	6	12'<	x1

Table 2.6 RT-PCR cycles used for profiling of Fgf ligands and Fgf Receptors.

2.5.12 Establishment of primary astrocyte cultures

Brains were removed from 3-4 day old wild type (WT) mouse pups and placed in the Dulbecco's Phosphate Buffered Saline (DPBS) supplemented with 10% glucose, 0.02M HEPES solution. Cortices were removed from 5 brains, freed of meninges, transferred to 5ml (1ml/ 2 cortices) of DPBS containing 0.025% Trypsin-EDTA (pre-

warmed), minced by trituration with 1.6mm needle and incubated 10 min at 37ºC. Trypsin was then inactivated by addition of 10%FBS/DMEM. Cell clumps were further dissociated by subsequent trituration in a syringe fitted first with a 0.8mm and then 0.6mm sterile needle. Finally, cell suspension was passed through 40µm nylon membrane cell strainer, centrifuged for 5min at 1000rpm and the resulting cell pellet was re-suspended in 10%FBS/DMEM (supplemented with 1% penicillin/streptomycin, 1% GlutaMAX). Dissociated suspension of single cells were cultured in three T75 flasks and kept at 5% CO2 at 37ºC, in a humidified incubator. Cultures were fed with fresh 10%FBS/DMEM 24h after plating and then every 2-3 days, until confluent.

Part 2.6 Culture of cell lines

2.6.1 ARPE-19 cells

ARPE-19 a monolayer of uniform population of highly proliferative, polarised epithelial human retinal pigment epithelial (RPE) cells (Dunn et al., 1996). These cells were maintained in DMEM/F12 HAMs media (Gibco 31330) supplemented with 10%FBS, 0.001% Gentamicin (Sigma Aldrich G1397). Cells were fed every 2-3 days and passaged twice a week, by 1 in 4 dilution of a 70-80% confluent culture grown in T75 flasks. For experiments (immunolabelling, transfection etc.) cells were seeded at $5x10^4$ cells/well concentration, in 24-well plate, on PDL-coated glass coverslips.

2.6.2 ATDC5 cells

ATDC5 cells, originally cloned from the AT805 mouse embryonic teratocarcinoma cell line is a chondrogenic cell line that can go through a process analogous to chondrocyte differentiation (Yao and Wang, 2013). This cell line was obtained as a kind gift of Dr. Jelena Gavrilović (University of East Anglia).

In their undifferentiated state, ATDC5 cells are normally grown in ‘maintenance medium’ - DMEM/F12 HAMs media (Gibco 21331) containing 5% (v/v) FBS, 1% (v/v) L-glutamine and 1% (v/v) penicillin/streptomycin (Invitrogen) supplemented with 10 µg/ml Human Transferrin (Sigma Aldrich T8158) and 30nM Sodium Selenite (Sigma Aldrich). Cells within a culture normally divide once daily and the cultures were passaged twice a week at 1:8 or 1:16 of 70-80% confluent flask.

For experiments, undifferentiated ATDC5 cells were seeded on PDL-coated glass coverslips, placed in a 24 well plates, at the density of $15x10^3$ cells/well. These

cultures were then either used as undifferentiated cells in particular experiments (e.g. DNA transfection) or induced to differentiate.

In order to induce differentiation of ATDC5 cells, undifferentiated cells were grown for 1-2 days to sub-confluency in maintenance media and then stimulated with insulin (Atsumi et al., 1990, Temu et al., 2010). Briefly, the maintenance media was replaced with the 'differentiation media' - DMEM/F12 HAMs media (Gibco 21331) containing 5% (v/v) FBS, 1% (v/v) L-glutamine and 1% (v/v) penicillin/streptomycin (Invitrogen), supplemented with insulin, transferrin and sodium selenite (ITS) premix (Invitrogen 41400) and 50 µg/ml ascorbic acid sodium salt (Sigma Aldrich A4034). This was referred to as Day 0 of differentiation, and then cells were fed with fresh differentiation media every 2-3 days for up to 14 days. As a control, undifferentiated ATDC5 cells were grown for in parallel in maintenance media. The differentiating cells form 3D structures, referred here to 'differentiation nodules', that begin to be visible at Day 7 of differentiation and are clearly established at Day 14 (see Chapter 5).

2.6.3 293T-HEK cells

Human Embryonic Kidney 293T cells were maintained in DMEM/F12 HAMs media (Gibco 31330) supplemented with 10%FBS and 1% penicillin/streptomycin. Cells were fed every 2-3 days and the cultures were passaged three times a week at 1:10 of 70-80% confluent flask.

For experiments, (e.g. transfection) cells were seeded at $5x10^3$ cells/well concentration, on PDL/fibronectin-coated glass coverslips, placed in a 24 well plates, unless stated otherwise.

Part 2.7 Cell culture associated experimental methods

All cells (primary and cell lines) were maintained in a humidified incubator at 37°C with 5% CO_2. Cells were maintained and handled under sterile conditions and regularly screened for bacteria and mycoplasma infection.

2.7.1 Cell passaging and seeding

To maintain their proliferative state, cell were passaged at required confluency (typically at 70-80%) through treatment with 0.25% Trypsin-EDTA (Gibco 25200056). Briefly, after removal of the growth media, cells were washed with PBS or Cell Harvest

Buffer (0.02%EDTA Na_2^+, 0.9%NaCl, HEPES (free acid) 2.38g/L, 125µl/L Phenol Red, pH7.2) and then incubated with Trypsin (3ml/T75 culture flask) at 37ºC for 1-2 min. Dislodging of trypsinized cells was aided by gentle tapping on the side of the dish. Trypsin was inactivated by addition of the culture medium containing serum (FBS) and cells were re-seeded in a fresh container at required densities. Prior to plating, cell density in the suspension was measured using a haemocytometer.

2.7.2 Coating of glass coverslips with matrix molecules

When required, glass coverslips or plastic surfaces of the culture dishes were coated either with a poly-D-lysine hydrobromide (PDL) or fibronectin.

Poly-D-lysine is a positively charged amino acid polymer that improves the attachment of cultured cells, particularly neurons, glial cells and transfected cells to plastic or glass surfaces. To coat, PDL (Sigma Aldrich P6407) used at a final concentration of 20µg/ml solution, was applied to submerge glass coverslips or the required dish surface and incubated at 37ºC overnight. After removal of the PDL solution coverslips or dishes were washed with water and left in sterile environment to air-dry before applying cells to the coated surfaces. PDL coated dishes and coverslips, if not used immediately, were stored (sterilely packaged) at 4ºC for maximum of 3 weeks.

Fibronectin is a glycoprotein of the extracellular matrix (ECM), known to bind to integrins (membrane-spanning receptor proteins) thereby providing a potent physiological substrate for cell attachment. Fibronectin (Sigma Aldrich F1141) at 1mg/ml stock solution, was dissolved in PBS to 0.8 µg/mL, applied to a glass coverslip or dish surface and incubated 1h 37ºC. Fibronectin solution was then removed, the coated surface rinsed with PBS and used immediately for the cell culture.

2.7.3 Transfection of cultured cells

A variety of different transfection reagents, including JetPrime Reagent, Lipofectamine, Viromer, Fugene 6 and Calcium Phosphate method, were tested for optimal transfection of primary cells or cell lines with DNA plasmids. It was established that JetPrime Reagent and Calcium Phosphate provide the most efficient mode of DNA construct delivery, under the experimental procedures needed for this work.

The Jet Prime Reagent (Polyplus Transfections) transfection method was optimised for the best results using manufacturer's suggestions. Unless stated otherwise, for the routine transfections cells were cultured in a 24 well plate (on a

coated glass coverslips) till 70-80% confluency. In a microcentifuge tube, 100µl/well of the JetPrime Buffer and 0.8-1µg of plasmid DNA was mixed well and complemented with addition of The JetPrime Reagent (2µl/well) at 1:2 of DNA to JP Reagent ratio. Sample was mixed well and incubated 15min RT before applying to the cell media in the culture wells. Following 4h incubation, cells were washed and fed with fresh media. Typically transfected cells were fixed and immunolabelled 24h post transfection, unless stated otherwise. The same proportion of reagents was retained for different size culture dishes.

For the Calcium Phosphate ($CaPO_4$) precipitate transfection, cells were cultured to approximately 50-60% confluence in a T75 flask. To a microcentrifuge tube 62µl 2M $CaCl_2$.2H2O and 24 µg DNA (at concentration ≥ 1 µg/µl) were added sequentially and made up to 600 µl with ddH_2O. This mix was applied in drop-wise fashion, shaking vigorously, to 600 µl of 2xHEPES Buffered Saline (HBS) pH 7.02-7.12 (diluted from stock of 10xHBS - 8.18% NaCl (w/v (3.3g)); 5.94% HEPES (w/v (2.4g)); 0.2% Na_2HPO_4 (w/v (0.08g)) in 40ml ddH_2O; filter sterilised (0.2µm) and stored at 4°C) and allowed to stand at RT for 5 min. The formed precipitate was added drop-wise to the cells in normal growth media and incubated for 6-12h at 37ºC. Transfected cells were washed then cultured in UltraCHO (Lonza:12-724Q) for 24h, then used for further studies (e.g. fixed or lysed for protein extraction). The same proportion of reagents was retained for different size culture dishes (volumes were scaled depending on surface area of culture dish (cm^2)).

2.7.4 Glycerol shock mediated cell transfection

Glycerol shock is a technique used to increase the rate of cell transfection, by stimulating cells to uptake the plasmid DNA. Cells were cultured and transfected as per usual, using JetPrime Reagent. Four hours post incubation with the reagent, cells were washed with fresh cell culture media. Subsequently cells were submerged in 15% Glycerol (in PBS) and incubated for 2min at 37ºC, with was followed by immediate and thorough but gentle wash with media. Cells were then cultured as per usual.

2.7.5 Immunocytochemistry (ICC)

In preparation for immunolabelling, cultured cells (whether cell lines or primary cells) were rinsed in PBS to remove traces of culturing medium and fixed in 4% PFA solution for 15 min RT. Alternatively, cells were fixed using ice-cold 100% Methanol, incubated 5min -20ºC. Cells were then washed in PBS and treated with 1% NP-40

detergent to permeabilize the cell membranes, allowing antibody penetration. Subsequently cells were blocked in 10% normal goat serum (NGS) solution for 1h RT, to prevent non-specific binding of antibodies. Cells were then incubated with primary antibodies diluted in 0.2% NGS at 4ºC overnight, rinsed several times in 0.2% NGS solution and incubated for 1 hour at RT with the relevant species-specific secondary antibodies conjugated to Alexa 488 or 568 and diluted in 0.2% NGS, and in some cases also with phalloidin488 dye [1:1000] (Life Technologies A12379) to visualise cytoskeleton (as it binds to filamentous actin molecules). Full list of antibodies used and their concentration is shown in Table 2.7 and Table 2.8. Finally cells were rinsed in PBS and counterstained with nuclear dye Hoechst 33342 Trihydrochloride, Trihydrate (Hoechst) [1:10000] (Thermo Fisher Scientific H13399) for 10min at RT and rinsed with PBS and ddH_2O. Glass coverslips were mounted onto microscope slides using Vectrashield (Vector Laboratories) solution and sealed with clear nail varnish enamel to prevent cells from drying out.

Primary Antibodies					
Target	**Host**	**Source**	**Cat. Number**	**Purpose**	**Dilution**
β-actin	Ms	Abcam	ab3280	WB	1:1000
βCOP	Rb	custom made	n/a	ICC	1:500
β-gal	Chk	Abcam	ab9361	ICC	1:10 000
BLBP	Rb	Abcam	ab32423	ICC	1:300
BrdU	Rt	Thermo-Scientific	PA5-32256	ICC	1:1000
DsRed	Rb	CloneTech	63249	WB/ICC	1:1000
ERp60	Rb	custom made	n/a	ICC	1:500
Fibrillarin	Rb	abcam	ab5821	WB/ICC	1:1000
GFAP	Ms/Rb	Millipore	MAB360	ICC	1:1000
HA epitope	Ms	Cell Signalling Technology	2367S	WB/ICC	1:1000
Lamp2	Rb	Sigma Aldrich	L0668	ICC	1:500
Nestin	Ms	Developmental Studies Hybridoma Bank	Rat-401	ICC	1:200
NG2	Rb	Millipore	AB5320	ICC	1:200
Olig2	Rb	Millipore	AB9610	ICC	1:500
Sox2	Ms	R&D Systems	MAB 2018	ICC	1:50
TGN46	Rb	custom made	n/a	ICC	1:500
Tuj1	Ms	R&D Systems	MAB 1195	ICC	1:1500

Table 2.7 Primary antibodies used for either Immunocytochemistry (ICC) or Western Blotting (WB). Host species abbreviation: Chk – chicken; Ms – mouse; Rb – Rabbit; Rt – Rat.

Secondary Antibodies						
Target	**Host**	**Conjugation**	**Source**	**Cat No**	**Purpose**	**Dilution**
Gt	Ms	AlexaFluor® 488	Invitrogen	A-11001	ICC	1:1000
Gt	Ms	AlexaFluor® 568	Invitrogen	A-11004	ICC	1:1000
Gt	Rb	AlexaFluor® 488	Invitrogen	A-11008	ICC	1:1000
Gt	Rb	AlexaFluor® 568	Invitrogen	A-11011	ICC	1:1000
Gt	Chk	AlexaFluor® 568	Invitrogen	A-11041	ICC	1:1000
Gt	Ms	HRP	Sigma Aldrich	A-4416	WB	1:10 000
Gt	Ms	HRP IgG1	Santa Cruz Biotechnology, INC	SC-2060	WB	1:10 000
Gt	Rb	HRP	Sigma Aldrich	A-9169	WB	1:10 000
GAPDH	Ms	HRP	Abcam	ab9482	ICC	1:6000

Table 2.8 Secondary antibodies used for either Immunocytochemistry (ICC) or Western Blotting (WB). Host species abbreviation: Chk – chicken; Ms – mouse; Rb – Rabbit; Rt – Rat.

2.7.6 Analysis of cell transfection rate and intra-cellular protein distribution

For cell transfection experiments, a typical experiment (per construct) consisted of transfecting two coverslips, and taking measurements from five random fields of view (under 10x objective) on each coverslip (total of 10 measurements per sample). Within each photographed area, total number of cells as well as total number of transfected cells was quantified. The pattern of HA localization in each cell ('exclusively nuclear'; 'predominantly nuclear', 'predominantly cytoplasmic', 'exclusively cytoplasmic'; and 'equal distribution', where HA signal was as strong in the cytoplasm as it was in the nucleus) was expressed as a percentage of the number of transfected cells. The whole procedure was repeated 4 times using cell cultures of similar passage numbers.

2.7.7 Measurements of co-localisation of fluorescent markers

Co-localisation of two fluorescently labelled markers could signify protein-protein interaction. To determine whether given protein undergoes secretion from the cell, markers of secretory pathway were assessed for interaction with the HA-tagged protein, by determination of the level of co-localisation of two fluorescent channels – red and green.

From fluorescent images 10 random cells were analysed using Volocity 6.3 software (Fig. 2.5). Region of interest (ROI) corresponding to the area of the cell was selected and the co-localisation of markers was quantified by the software, selecting the appropriate channels: red (Alexa 568) as HA tag and green (Alexa 488) as the secretory pathway marker (either ERp60, βCOP or TGN46). Appropriate thresholds were set by the software, which calculations are based on the simultaneous estimations of the maximum threshold of intensity for each colour below which pixels do not show any statistical correlation (Costes et al., 2004). From performed calculations a scatter plot has been generated by the software of which each axis represents the ascending marker levels present within the two analysed channels, where two perfectly co-localized channels, generate a scatter plot where the points fall in a line at 45 degrees to either axis (Fig. 2.5A). On the contrary the horizontal line of scatter points signifies no correlation between the markers, therefore no co-localisation (Fig. 2.5B).

Furthermore from intensity values within thresholds the software generates calculations of the Pearson's Correlation coefficient (R_r) (Barlow et al., 2010), which describes the correlation of the intensity distribution between channels. Values range from -1.0 to 1.0, where values from 0 to 0.5 indicate no significant correlation between the given markers and values close to -1.0 indicate complete negative correlation. Importantly values that indicate co-localisation range from 0.5 to 1.0.

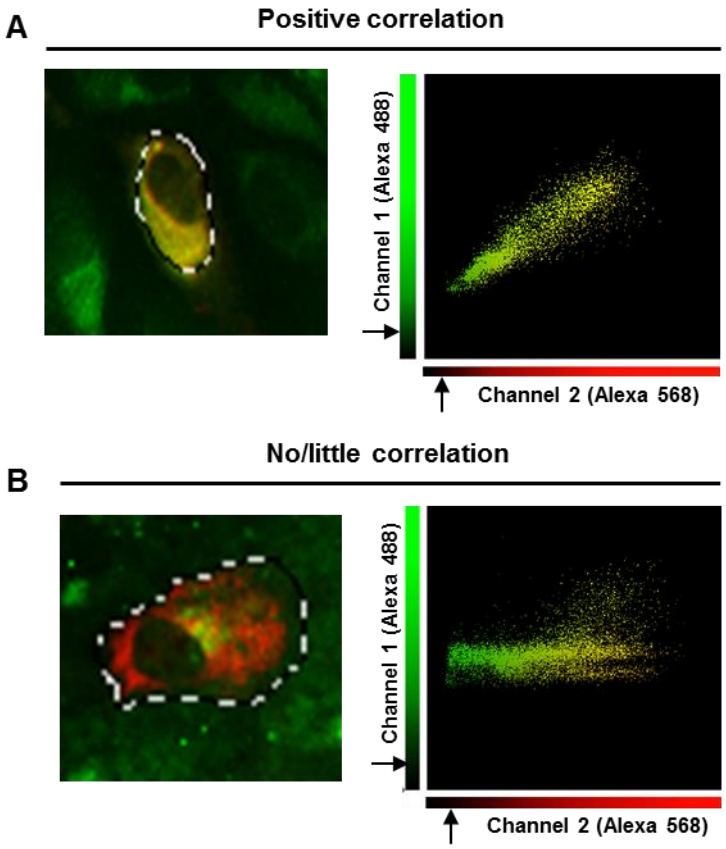

Figure 2.5 Representative images and graphs of quantification of co-localisation of two fluorescent markers using Velocity 6.3 software, where an area of the cell has been selected for analysis. (A) Image of G145E fluorescence and ERp60 marker, which serves as an example of positive correlation. (B) Image of G145E fluorescence and TGN46 marker, showing an example of no or very little correlation. Red channel (Alexa 568) corresponded to HA tagged protein expression and the green (Alexa 488) represented the secretory pathway markers. Black arrows point to the set thresholds generated by the software.

2.7.8 BrdU pulsing of cultured cells

To pulse cells with BrdU, cell media was removed from the culture and supplemented with BrdU (3µg/ml final concentration), mixed and promptly placed back onto cultured cells. Cells were incubated with BrdU for 4h and fixed immediately with 4%PFA for 15min at RT. Fixed cells were washed well with PBS and treated with 1M HCl (in ddH_2O) 30min 47°C to denature nuclear DNA thereby promoting anti-BrdU antibody access to DNA. Cells were subsequently washed once in ddH_2O for 5min, then three times in PBS for 5min, after which the immunohistochemistry was performed as usual.

2.7.9 Induced growth arrest and cell cycle inhibition of cell culture

In order to inhibit cell growth at specific cell cycle two methods were applied: drug treatment and serum starvation.

The drug Nocodazole (Sigma Aldrich M1404) which interferes with the polymerization of microtubules and formation of mitotic spindle, was used at a final concentration within a range of 0.2µg/ml (allowing the optimal inhibition but preventing cell stress) to arrest cells at G2/M phase of cell cycle. The drug was applied to cultures, 4h post application of DNA transfection reagents, and incubated for 12h followed by an immediate fixation with 4% PFA.

Serum-deprivation prevents cell growth and arrests cells at the G1/G0 phase of the cell cycle. Normal growth media was removed from sub-confluent cell culture (70%), cells were rinsed several times with culture media lacking serum and incubated with the same for 24-48h prior to transfection, then also throughout the whole DNA transfection procedure. Subsequently, cells were fixed and immunolabelled.

2.7.10 Alcian Blue and Alizarin Red staining of differentiated mesenchymal cells

Alcian Blue and Alizarin red are chemical dyes that mark chondrogenic differentiation. The Alcian Blue is a type of polyvalent dye, used to stain acidic polysaccharides such as glycosaminoglycans found in cartilage. The Alizarin Red is an organic compound of a red colour that stains the presence of calcific deposition present within cells of an osteogenic lineage. During each stage of this procedure a great care was taken and each solution was applied very gently as the cultures peel off easily of the bottom of the dish.

For Alcian Blue staining, differentiated ATDC5 cells which appear as ‘nodules’ were fixed with ice-cold 100% Methanol (5min -20°C) and incubated 30min RT with Alcian Blue dye (0.5%w/v, 0.1M HCl in ddH_2O). Alternatively, for Alizarin Red staining, the dye (2% solution prepared in ddH_2O pH 4.1-4.3) was applied for 10min at RT. Excess dyes were washed off with ddH_2O and cells were re-fixed for 10min 4%PFA at RT.

Part 2.8 Microscopy, imaging and image analysis

Fluorescently-labelled samples were visualised using a selection of microscopes (depending on the sample) including: Zeiss Axioimager M2 with an Apotome attachment, Zeiss Axioplan2 imaging and Zeiss LSM510 META confocal.

Live cell cultures as well as X-gal and Alcian Blue stained cells were imaged with Zeiss Axiovert40CFL microscope using phase contrast or fluorescent expression.

Images were acquired using Axiovision 4.8 software and then further processed using ImageJ and Adobe Photoshop CS4.

Part 2.9 Protein analysis

2.9.1 Protein extraction from cell lysate

For extraction of the protein from whole cell lysate, cells were cultured in a 100mm Petri dishes and transfected using the JetPrime Reagent. 24h post transfection cultures were placed on ice and washed several times with ice-cold PBS to remove traces of media. To each dish, 300µl of Modified RIPA cell lysis buffer (50mM Tris pH7.4, 150mM NaCl, 2.5mM $MgCl_2$, 1%(v/v) NP-40, 0.05%(v/v) Triton X-100, 0.5%(w/v) Na-deoxycholate) containing Halt Protease Inhibitors (1:100 dilution) (ThermoScientific 78430) was added, and cells were scraped off three times every 10min using a cell scraper.

To separate cell debris from the protein mixture, the scraped solution was transferred into a pre-chilled microcentrifuge Eppendorf tube and centrifuged at 12000rpm for 15min at 4°C. The resulting supernatant, containing protein, was then placed in a fresh, pre-chilled tube and used straight away or stored at -20°C for later use. Protein concentration in the sample was determined using Pierce™ BCA Protein Assay Kit (ThermoScientific 23225).

2.9.2 Trichloroacetic acid (TCA)-mediated protein precipitation

Cultures of cells grown in three 100mm diameter Petri dishes were transfected with plasmid DNA and after 4h incubation cells were rinsed twice with PBS to remove traces of serum, and cultured in 5ml of serum-free culture media. 24h-48h post transfection, the media was collected and centrifuged (1500rpm 10min) to remove cell debris. To maximise extracted protein yield, cultures cells were occasionally incubated with fresh serum-free media and supernatants were collected and pooled with previously collected samples.

Trichloroacetic acid (5% of final concentration) was added to the collected media and incubated overnight at 4°C. To pellet the precipitated protein, the samples were centrifuged at 12000rpm for 15min at 4°C, the supernatant was removed and the

protein pellet washed twice in ice-cold 150µl acetone at 4°C, finally transferring the sample into the microcentrifuge Eppendorf tube. Samples were centrifuged at 12000rpm for 15min at 4°C. The final pellet was re-suspended in 5X Sample Buffer and stored at -20°C.

2.9.3 SDS-PAGE and protein transfer

Proteins run through the polyacrylamide gel electrophoresis (PAGE) were first denaturated and reduced by the Sodium dodecyl sulphate (SDS). Binding of SDS disrupts non-covalent protein bonds through electrostatic repulsion, causing protein denaturation (loss of native molecular conformation) that results in proteins unfolding into a rod-like shape; thereby eliminates differences in protein shape as a factor for separation on the gel.

Typically 30µg of total protein from cell lysate was prepared for western blotting by mixing with 5X Sample Buffer (625mM TRIS-Base pH 6.8, 2%(w/v) SDS, 10%(v/v) glycerol, bromophenol blue and 5% β-mercaptoethanol) and ddH_20, bringing the total sample volume to 25µl Protein samples were further denaturated by boiling for 2min at 95˚C. Samples were loaded and run on a homemade gel – 10% resolving gel (40%(v/v) acrylamide, 375 mM Tris, 0.1% (v/v) Ammonium Persulphate, 0.25%(v/v) TEMED) and 5% stacking gel (40%(v/v) acrylamide, 125 mM Tris, 0.15%(v/v) Ammonium Persulphate, 0.4%(v/v) TEMED). Samples were run along with a protein ladder (PageRuler^{TM} Plus ThermoScientific 26619) at 200V per gel in running buffer (25 mM Glycine, 250 mM Tris, 1% (w/v) SDS) for 35 min. The resolving gel, transfer membrane and thick filter paper were soaked in a Transfer Buffer (39mM Glycine, 48mM Tri-HCl, 0.0375%SDS, pH8.3 and 20% methanol) for approximately 10 min. Protein was transferred using the semi-dry method, at 15V for 35min.

2.9.4 Western Blotting of protein samples

Following protein transfer, membranes were blocked in 10% (w/v) non-fat milk powder or in 3-5%(w/v) BSA in PBST (PBS and 0.5% Tween-20) at RT for 1-3h. Following blocking, the membranes were incubated in antibody solution (diluted in 0.5% milk/3%BSA in PBST) overnight at 4ºC and then washed excessively in 0.5% milk PBST over a period of 1h at RT. Membranes were then incubated with secondary antibody diluted in 0.5% milk/3%BSA in PBST for 1h RT, after which all membranes were washed multiple times in PBST for 30 min. Full list of antibodies used and their concentration is shown in Table 2.7 and Table 2.8.

For the antibody detection, membranes were incubated in ECL solution (100mM Tris pH8, 1.25mM Luminol, 0.2mM Coumaric Acid and 0.01% H_2O_2) for 5min and exposed to hyperfilm (GE Healthcare). Exposure times varied according to the sample from 15s -15min.

If required, membranes were stripped with Stripping Buffer (0.2M Glycine, 0.5M NaCl, pH 2.8) 2x 5min then washed 1x ddH_2O and 2x PBST, before they were re-blocked and reblotted according to the same protocol.

2.9.5 Protein deglycosylation

Protein glycosylation is a form of post-translational modification and can either occur on *N*-linked-glycosylation sites or *O*-linked-glycosylation sites, which is controlled by different enzymes and generated by different types of chemical bonds. In order to determine which protein sites are glycosylated the removal of protein glycosylation was obtained by two means: (1) treatment with Protein Deglycosylation Mix (New England BioLabs P6039S), which is a cocktail of enzymes designed to remove all types of glycosylation; and (2) treatment with PNGase F (New England BioLabs P0704S), an enzyme known to remove almost all *N*-linked oligosaccharides from proteins.

First ARPE cells were transfected with specific constructs and protein was obtained from the whole cell lysate. 25µg of protein was combined with 2µl of 10X Glycoprotein Denaturing Buffer and water, providing total reaction volume of 20µl. Protein samples were primarily denatured by heating for 10min at 100°C. For the removal of *N*-linked oligosaccharides to the samples 4µl of 10X G7 Reaction Buffer, 4µl of 10%NP40 and 2µl of PNGaseF enzyme was added, generating the reaction volume to 40µl in total by addition of ddH_2O. However for removal of all oligosaccharides, to the samples 5µl of 10X G7 Reaction Buffer, 5µl of 10%NP40 and 5µl of Deglycosylation Enzyme Coctail was added, generating the reaction volume to 50µl in total by addition of 15µl of ddH_2O.

2.9.6 Subcellular Fractionation

Cell fractionation (cytoplasmic versus nuclear) was carried out according to the protocol of Dimauro et al. (Dimauro et al., 2012). Briefly, 24 hours post transfection, HEK 293T cells were washed twice with cold PBS, and pelleted down at 4°C 500xg for 5min. The cytoplasmic fraction was then separated from the rest of the cell content by treating cells with STM buffer (250 mM sucrose; 50 mM Tris–HCl pH 7.4; 5 mM $MgCl_2$) in the presence of 1% Halt protease inhibitor cocktail (Thermo Fisher Scientific)

incubating on ice for 45min. The samples were centrifuged at 4°C 800xg for 15min and as a result of which the supernatant contained the cytosolic fraction whilst the remaining pellet contained the nuclear fraction.

To purify protein from cell debris, the cytoplasmic fraction was washed in STM buffer and protein content was precipitated in pre-cooled Acetone (4x sample volume) for 1h at -20°C. To remove the acetone, the sample was centrifuged at 4°C 12000xg for 5min and the obtained pellet was briefly air-dried for about 10min. Finally the cytosolic fraction was re-suspended in STM buffer (containing the protease inhibitors).

To remove any remaining cytoplasmic proteins, the nuclear fraction pellet was washed twice by subsequent re-suspension in the STM buffer 4°C 500xg, then for 15min. The washed pellet was treated with NET buffer (20 mM HEPES pH 7.9; 1.5 mM MgCl2; 0.5 M NaCl; 0.2 mM EDTA; 20% glycerol; and 1% TritonX-100) in the presence of 1% Halt cocktail, incubated on ice for 45 min. The debris was removed by pelleting it down through centrifugation at 9000xg and the obtained supernatant generated the nuclear fraction.

Part 2.10 Statistics

All statistical tests were performed using IMB SPSS Statistics 22. For normally distributed data with equal variances either independent sample Student t-test (if comparing two samples of equal variance) or ANOVA with post hoc Tukey (when comparing more than two samples of equal variance) were performed. For samples with varying variances Mann-Whitney U (comparing two-groups) or Krusal-Wallis (more than two samples) were used.

Within the figure legends, for each significance level ‘stars’ were used that refer to specific probability level ‘P’ precisely:

‘no stars’ corresponds to $P>0.05$ – no statistical significance

* denotes $P\leq0.05$

** denotes $P\leq0.01$

*** denotes $P\leq0.001$

**** denotes $P\leq0.0001$

Chapter 3

In silico analysis of the Fgf10 gene and protein structure

Part 3.1 Overview of bioinformatics

Secretory FGF10 molecule, upon release from the cell, binds with strong affinity to FGFR2IIIb (Fig. 1.4B) (see Chapter 1). However, recombinant rat FGF10 has been found in the nuclei of cultured cells (lacking endogenous expression of this protein) (Bagai et al., 2002), suggesting an alternative functioning pathway for the protein. Furthermore, FGF10 contains a putative nuclear localisation sequence (NLS)–like motif, that is based on a sequence homology to NLS found in FGF1 (Kosman et al., 2007, Zhan et al., 1992). However it is a 'weak' motif, that only partially influences FGF10's nuclear translocation (Kosman et al., 2007), suggesting the presence of other factors regulating localisation and function of FGF10. Moreover, Fgf10 is expressed in the mouse hypothalamus, which is not complemented by an expression of its cognate receptor FGFR2IIIb (Hajihosseini et al., 2008), suggesting alternative mechanisms of action of FGF10.

Bioinformatics (i.e. the *in silico* research method) is the application of computational techniques to understand and organise information associated with biological macromolecules and their mutual interactions. Advantages of the system include prediction with high probability of molecular models and hypotheses, as well as storage of vast amount of data and its quick and efficient processing. In the field of genetics freely available programs, including Basic Local Alignment Search Tool (BLAST) (Altschul et al., 1990) that allow comparison of nucleotide sequences, are essential tools in genome sequencing and annotating occurring mutations, such as in Genome Wide Association Studies (GWAS) (Londin et al., 2013). Bioinformatics is widely used in genomics and proteomics analysis, for example specific programs are designed to provide separation of the signal from noise in high-throughput gene expression studies, such as microarrays and mass spectrometry. Furthermore, computer algorithms and mathematical models are an indispensable part of systems biology, unravelling protein-protein interactions and their complicated networks (e.g. the metabolic pathway).

Importantly, bioinformatics is an essential and central part of structural biology, generating three dimensional visual models of nucleic acids and protein molecules. Those models are applied to simulate the intramolecular interactions, reducing time and costs of experimental procedures and are vital for drug targets identification and design. For example, crystal structure analysis of human recombinase Rad51 binding to BRC repeats of BRCA2, revealed specific binding residues potentially useful as targets of drugs that through disrupting the interaction could lead to cancer treatment (Blundell et al., 2006). Interestingly, bioinformatics has also been used to address biological activity of various molecules, including FGFs. Analysis of molecular model of

FGF1, FGFR2IIIc and heparan sulphate proteoglycan (HSPG) complex revealed the critical role of heparin in receptor activation. The receptor dimerization was shown to take place due to heparin-induced conformational change in the receptor itself (Pellegrini et al., 2000), which is likely to occur in other FGFRs. The progression from protein structure visualisation led to 'molecular dynamic simulation' (MDS), that is based on Newton's laws of motion and provides information about movement of atoms around rotatable bonds. Such programs are expanded further into computational algorithms termed 'docking algorithms', allowing *in silico* prediction of two molecules reacting together.

Advances in biology and computer sciences increase the resourcefulness of bioinformatics. Innovation in computer storage capabilities and improvements in mathematical models lead to more reliable results and allow valid predictions about the molecules that have not been experimentally addressed yet. Bioinformatics at the moment allows for the gathering of assumptions and predictions, providing a starting point to studies otherwise difficult to undertake.

FGF ligands, including FGF10, are the subject of intensive studies, providing a wide and in-depth knowledge, allowing a comprehensive base for further *in silico* analysis.

3.1.1 Aims

Although much is already known about Fgf10's genomic sequence and protein structure (see Chapter 1), recent advances in technology and bioinformatics tools provide novel approaches to further studies.

The aim of this part of the thesis is to examine FGF10's DNA and protein sequence, using *in silico* tools to analyse: (1) existence, positioning within the protein structure and functionality of potential NLS; (2) existence of putative post-translational modifications (PTM), i.e. SUMOylation and Glycosylation, that could affect nuclear import of FGF10; (3) and existence of putative regulatory sites within a promoter region of Fgf10 driving the expression of the protein. These will provide preliminary predictions of the protein's structure and function, as well as aid in determining the putative mode of FGF10's nuclear incorporation, which can be followed up with experimental approaches.

Part 3.2 Discovery and analysis of putative NLS within FGF10

3.2.1 Identification of a novel NLS within FGF10

FGF10 is found in the cell nucleus. However, the underlying mechanisms of its nuclear translocation remain unclear (Bagai et al., 2002, Kosman et al., 2007). The sequence proposed to act as NLS, within rat FGF10 corresponding to 142NKKGKLY148 (here on referred to NLS1) (Fig. 3.1B,C,E), was shown to be insufficient to act as a fully functioning nuclear import motif (Kosman et al., 2007). Therefore, FGF10 molecule was analysed in the context of additional non-classical NLS or NLS-like motifs necessary for the protein's nuclear transport.

Searches based on PSORT tools (WoLF PSORT and PSORT II), which use mathematical models to find consensus motifs within a sequence, predicted no classical NLS present within the rat FGF10 sequence and these results are in agreement with earlier literature (Kosman et al., 2007). However, both programs predicted stretches of basic residues within the rat FGF10, with overall content of 12.4% of the whole sequence, suggesting the possibility of existence of non-classical NLS. FGF molecules share up to 74% sequence similarity (Ornitz and Itoh, 2001) and FGF10 is well conserved between different species (Fig. 3.2A). However, providing that even slight structural differences, such as variation of a single residue, can determine the function of the protein (Makarenkova et al., 2009), the searches were also performed for primary human and mouse FGF10 sequences. Similarly, no classical NLS was found in human and mice. All of the following searches were then performed on human, mouse and rat sequences however, each time the three species displayed similar outcomes (data not shown). Therefore, the following results correspond to rat FGF10 sequence, particularly since recombinant rat protein was used in experimental work (see Chapters 4&5) and data shown here, unless stated otherwise, is a representative of all three species.

Examination of the non-classical NLS was performed using NLStradamus, a tool that analyses the composition of residues within the protein sequence and searches for specific clusters of basic residues rather than consensus motifs (Nguyen Ba et al., 2009). This approach allowed identification of a novel putative NLS-like motif, corresponding to rat 192APRRGQKTRRK202 sequence (Fig. 3.1A) (Appendix 1), residing close to the C-terminus of the protein (Fig. 3.2A). This prediction was then further confirmed by a NucPred, a genetic programming (GP) software (see Chapter 2). This is a machine-learning technique that automatically develops computer programs in an artificial evolutionary process, to analyse the protein sequence, compare to existing

nuclear proteins and classify parts of the protein sequence as “nuclear” or “not nuclear” (Brameier et al., 2007).

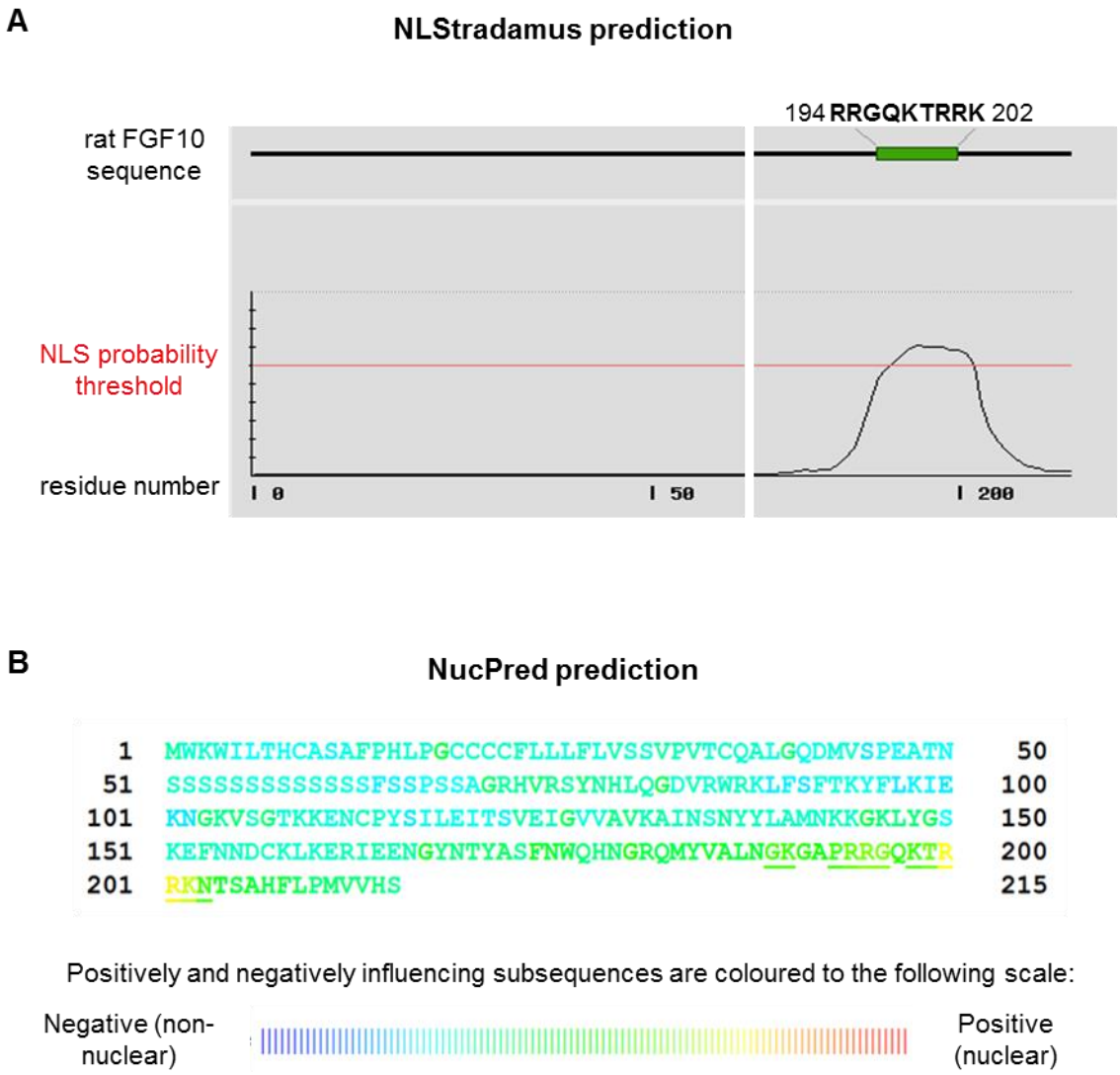

Figure 3.1 Identification of non-classical NLS2 within FGF10 sequence. (A) The NLStradamus predicts existence of a single NLS motif beyond its set probability threshold (red) based on clusters of basic residues. (B) NucPred results determine the NLS2 region as “likely/positive” to drive nuclear import of FGF10, as shown by the yellow-green colouring.

The NucPred’s analysis showed that within FGF10’s sequence, a stretch of amino acids spanning residues 194RRGQKTRRK202 displayed the highest positive

score for influencing the molecule's nuclear targeting (Fig. 3.1B). Therefore, the two NLS-prediction tools suggested the existence of a non-classical NLS within FGF10, which was then named NLS2. This sequence is located on the protein surface and resides outside of the receptor interacting interface (Fig. 3.2B). 50% of this NLS2 sequence is composed of basic amino acid residues (Arginine/R and Lysine/L) and the side chains are protruding out from the centre of the molecule, providing availability for putative interactions with Importin molecules (Fig. 3.2C).

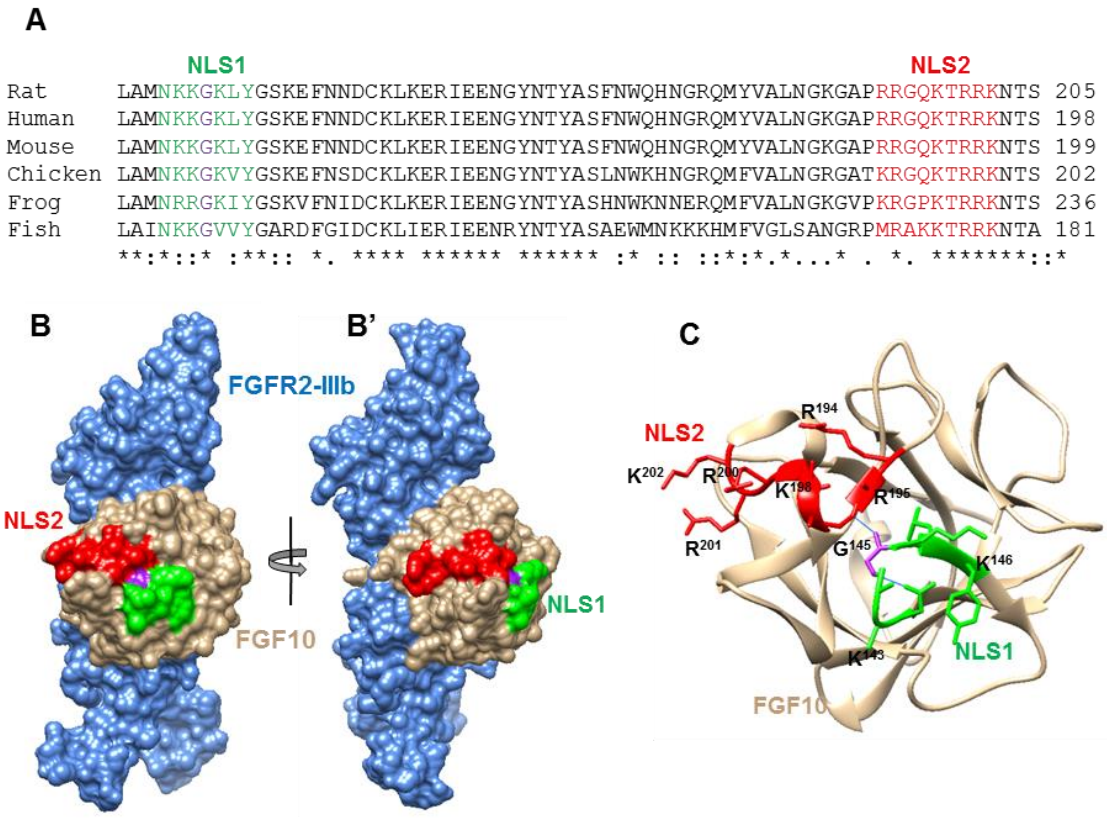

Figure 3.2 Conservation and position of NLS2 within primary and tertiary structure of FGF10. (A) NLS1 (green) and NLS2 (red) are well conserved between vertebrate species and reside about 44 residues apart within primary sequence of FGF10. (B) Both surface exposed NLS motifs come into close contact within the tertiary structure of the protein and positioned away from the FGF10 (light brown) and FGFR2IIIb (blue) interface; figures viewed from two angles. (C) NLSs directly interact through an H-bond between G145 residue (purple) and G196 in NLS2; figures drawn using 1NUN PDB file and Chimera 1.9 software.

Interestingly, in the protein's 3D structure, the NLS2 is positioned in a close proximity to the NLS1 (Fig. 3.2B). Moreover it was noted that a residue from NLS1, the

Glycine 145 forms an H-bond with a residue located in the NLS2, Glycine 196 (Fig. 3.2C). The tools predicted the NLS2 sequence as a “weak” NLS-like motif that might be similar to NLS1, which was experimentally shown to act as a “weak” NLS by Kosman et al. (Kosman et al., 2007). This raised the intriguing possibility that the two weak NLS motifs are advantageous to typical paracrine protein as they may act together to provide a stronger signal targeting FGF10 into the cell nucleus, allowing control over the levels of protein’s nuclear import.

Sequence alignments showed that NLS1 and NLS2 are well conserved within the primary sequence of FGF10 between various vertebrate species, ranging from fish to humans (Fig. 3.2A). A high level of species conservation could suggest that NLS1 and NLS2 regions were maintained by evolution, despite speciation, and therefore may be key aspects to the FGF10’s function. Furthermore, the sequence of FGF10 was aligned to sequences of known FGFs that translocate into the cell nucleus: FGF1 (Wesche et al., 2005b), FGF2 (Sheng, 2004) and FGF3 (Kiefer et al., 1994b) (Fig. 3.3).

```
FGF10  MWKWILTHCASAFPHLPGCCCCFLLLFLVSSVPVTCQALGQDMVSPEATNSSSSSSSSS 60
FGF3   --------------------MGLIWLLLLS------------LLEPGWPATGPGTRLRR- 27
FGF2   ----------------------------------------MAAGSITSLPALPEDGGG 18
FGF1   ----------------------------------------MAEGEITTFAALTERFN- 17
                                                 :    .   . .

FGF10  SSSFSSPSSAGRHVRSYNHLQGDVRWRKLFSFT-KYFLKIEKNGKVSGTKKENCPYSILE 119
FGF3   --------DAGGRGGVYEHLGGAPRRRKLYCAT-KYHLQLHPSGRVNGS-LENSAYSILE 77
FGF2   ----------------AFPPGHFKDPKRLYCKNGGFFLRIHPDGRVDGVREKSDPHVKLQ 62
FGF1   ----------------LPLGNYKKPKLLYCSNGGHFLRILPDGTVDGTRDRSDQHIQLQ 60
                              : *:. .  ..*::  .* *.*   ..  :  *:

FGF10  ITSVEIGVVAVKAINSNYYLAMNKKGKLYGSKEFNNDCKLKERIEENGYNTYAS--FNWQ 177
FGF3   ITAVEVGVVAIKGLFSGRYLAMNKRGRLYASEHYNAECEFVERIHELGYNTYASRLYRTG 137
FGF2   LQAEERGVVSIKGVCANRYLAMKEDGRLLASKCVTEECFFFERLESNNYNTYRS--RKYS 120
FGF1   LSAESAGEVYIKGTETGQYLAMDTEGLLYGSQTPNEECLFLERLEENHYNTYTS--KKHA 118
       : : . * * :*.  :. ****.  * * .*:  . :* : **:..  **** *   .

FGF10  HNG----------RQMYVALNGKGAPRRGQKTRRKNTSAHFLPMVVHS------------ 215
FGF3   PSGPGARRQPGAQRPWYVSVNGKGRPRRGFKTRRTQKSSLFLPRVLGHKDHEMVRLLQSG 197
FGF2   S--------------WYVALKRTGQYKLGSKTGPGQKAILFLPMSAKS------------ 154
FGF1   EKN------------WFVGLKKNGSCKRGPRTHYGQKAILFLPLPVSSD----------- 155
                     :*.:: .*  : * :*   :.:  ***

FGF10  ------------------------------------------------
FGF3   QPQAPGEGSQPRQRRQKKQSPGDHGKMEHLPTKATTSAQLDTGGLAMA 245
FGF2   ------------------------------------------------
FGF1   ------------------------------------------------
```

Figure 3.3 NLSs of different FGF proteins appear conserved within a N-terminal protein region. NLS2 (red) of FGF10 corresponds to one of the NLS-motifs of FGF3 (yellow) and resides in close proximity to NLS of FGF2 (brown) and FGF1 (blue); NLS1 of FGF10 shown in green. Figures drawn using Clustal 2.1 software.

The NLS2 motif of FGF10 corresponds to one of the NLS-motifs found within FGF3. Moreover, in close proximity to this region resides NLS of FGF2 and a bipartite NLS of FGF1 (Fig. 3.2). Similarly, conservation of the same region within proteins from different subfamilies could suggest that this particular region of FGF molecules is also important for their nuclear import.

FGF10 and FGF3 both belong to the FGF7 subfamily and share similar nuclear localisation motifs. It is likely therefore that these are also present in the remaining members of the subfamily. To determine if the NLS1 and NLS2 are conserved within FGF7 subfamily members, the sequences were aligned and assessed for presence of basic residues. Within all molecules the regions corresponding to NLS1 and NLS2 of FGF10 are well conserved, with a very high content of basic residues (Fig. 3.4). Moreover, besides FGF3, the NLS2 region of FGF10 shows high conservation within FGF22. Members of the same subfamily share structural and functional properties (see Chapter 1). High level of conservation of NLS motifs within all members could be linked to their structural or functional importance. Moreover, this raises an exciting possibility that all members of this subfamily may potentially be found in the cell nucleus. However testing this hypothesis is beyond the scope of this project and will not be explored further in this thesis.

```
FGF3   SGRYLAMNKRGRLYASEHYNAECEFVERIHELGYNTYASRLYRTG 137
FGF7   SEYYLAMNKQGELYAKKECNEDCNFKELILENHYNTSASAKWTHS 159
FGF10  SNYYLAMNKKGKLYGSKEFNNDCKLKERIEENGYNTYASFNWQHN 179
FGF22  SGFYVAMNRRGRLYGSRVYSVDCRFRERIEENGYNTYASRRWRHH 126
       *  *:***::*.**...  . :*.: * * *  *** **  :

FGF3   PSGPGARRQPGAQRPWYVSVNGKGRPRRGFKTRRTQKSSLFLPRV 182
FGF7   G-----------GEMFVALNQKGLPVKGKKTKKEQKTAHFLPMA 179
FGF10  G-----------RQMYVALNGKGAPRRGQKTRRKNTSAHFLPMV 200
FGF22  G-----------RPMFLALDSQGIPRQGRRTRRHQLSTHFLPVL 147
                     ::::: :* * :* :*:: : :: ***
```

Figure 3.4 Sequence alignments of FGF7 subfamily members (rat). The NLS1 (green) and NLS2 (red) of FGF10 show full conservation (blue) and high number of basic (purple) residues within corresponding regions of FGF3, FGF7 and FGF22. Figures drawn using Clustal 2.1 software

Proteins that are imported into the nucleus are also often exported out, and transport in either direction requires chaperone proteins. To facilitate protein's nuclear export these chaperones (known as karyopherins) often recognise and bind to specific

consensus motifs on the cargo proteins' surface, called nuclear export sequences (NES) (see Chapter 1). To predict existence of NES within FGF10 couple of bioinformatics tools was used such as LocNES, which is designed to search for consensus NESs, or ValidNESs, a program that determines presence of NES based on specific amino acid frequencies (see Chapter 2). However these could not detect existence of any NESs and most likely FGF10 is not transported out of the nucleus through classical pathway, or alternatively it is not transported out of the nucleus at all.

3.2.2 Potential interactions between FGF10's NLS2 and importins

Importins are nuclear transport chaperones that bind to NLS present on a protein's surface and guide the cargo protein through the molecular pores into cell's nucleus. Importins are distinguished as Importin α and Importin β subunits, each referring to a large family of molecules. The α and β subunits form a complex allowing transport of a cargo protein through the nuclear pore. Typically Importin-α binds the cargo protein and Importin-β interacts with the nuclear channel proteins (Fig. 1.10), although Importin-β is also found to bind non-classical NLS and transport proteins without the aid of Importin-α (see Chapter 1). It was therefore hypothesised that FGF10's NLS2 motif binds to an isoform of Importin in order to translocate into cell nucleus. To provide a basis for experimental approach, identification of putative FGF10(NLS2)-to-importin interactions was performed using a bioinformatics 'molecular docking' tool (see Chapter 2).

In collaboration with Mr Georgios Iakovou, who designed and generated molecular docking software based on haptic system (Iakovou et al., 2015), interactions between FGF10's NLS2 and Importin α or Importin β subunits were tested. The binding interactions of the two proteins were based on the repulsion forces generated between the two molecules, meaning that the closer the calculated repulsion force value to zero, the more likely the interaction to occur in nature (see Chapter 2). The *in sillico* results suggest that FGF10 utilising its NLS2 binds more strongly to an Importin-α isoform, with the repulsion force of -289.18 kcal/mol, than to an Importin-β, where a repulsion force ranges between -500 to -800 kcal/mol (Fig. 3.5A). Nonetheless the software predicts also a strong, non-chemical attraction towards Importin-β that attributes mainly to electrostatics forces. Four different attempts were made to determine the most likely binding of FGF10 to Importin-β, with the best (strongest) force prediction of -584.98 kcal/mol (Fig. 3.5B), the weakest of -717.97 kcal/mol (Fig. 3.5C) and two of middle range corresponding to -612.69 kcal/mol (Fig. 3.5D) and -649.88 kcal/mol (Fig. 3.5E).

Unfortunately, the system cannot adapt to conformational changes that the protein molecules might display during binding. Often, protein-protein interaction results in slight conformational changes to at least one of the protein's structure, providing flexibility that allows binding to occur. These however, cannot be predicted/designed and interpreted by the software without prior experimentally achieved knowledge of complex's crystal structure. Whilst the molecular docking system remains an aid to experimental studies, it cannot replace them.

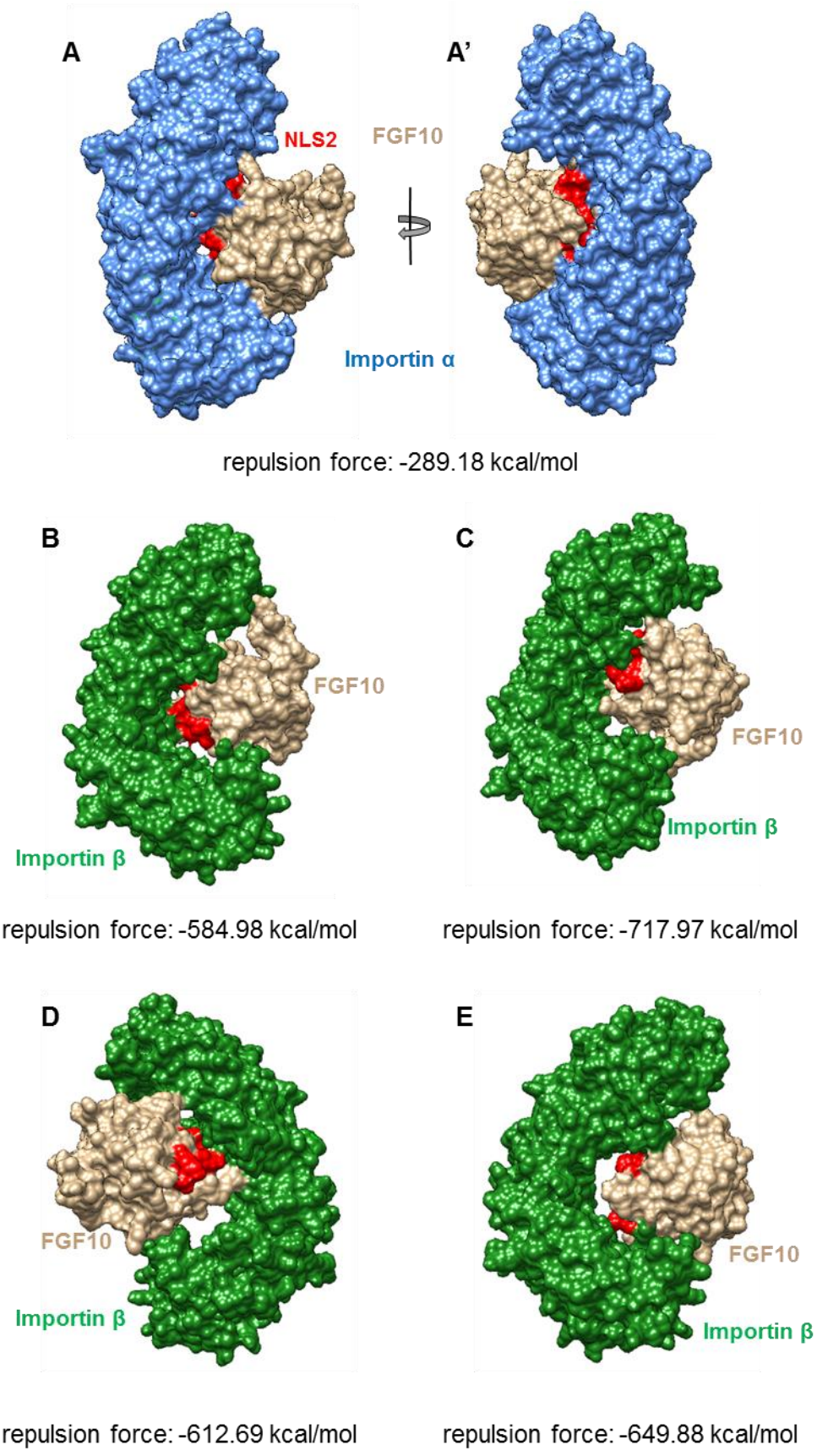

Figure 3.5 Molecular modelling of FGF10 binding predictions to Importins-α and -β. (A) The most likely prediction of naturally occurring interaction between FGF10 (light brown)-NLS2 (red) to Importin-α (blue), viewed from two angles. (B-E) Different variations of putative binding of Importin-β (green) to FGF10, all displaying higher repulsion forces than binding to Importin-α, hence less likely to occur.

Part 3.3 Analysis of putative post-translational modifications of FGF10

3.3.1 The influence of a putative SUMOylation site on nuclear import of FGF10

The family of Small Ubiquitin-like Modifier (SUMO) proteins modify function of other proteins by covalently attaching to or being removed from them, in a process of SUMOylation (Hay, 2005). The SUMOylation is a form of post-translational modification involved in multiple cellular processes. It can aid protein stability as in the case of Ago2 protein (Sahin et al., 2014, Lee and Kim, 2015) as well as affect gene expression and integrity of a genome as it regulates the PML/p53 tumour suppressor network (Muller et al., 2004). Moreover SUMOylation can affect progression through the cell cycle (Eifler and Vertegaal, 2015), for example the E2-conjugating enzyme Ubc9 was shown to be required for progression through mitosis by degrading M-phase cyclins (Seufert et al., 1995). Therefore, SUMOylation of FGF10 could impact the intra-cellular function of an otherwise secreted protein. Importantly SUMOylation is also involved in nuclear-cytosolic transport (Grunwald and Bono, 2011, Chen et al., 2013, Sedek and Strous, 2013) and enzymes involved in SUMO conjugation (Ubc9 and the E3-ligase RanBP2) are found at the nuclear pores in vertebrates (Melchior et al., 2003). Hence, putative SUMOylation of FGF10 could have a profound effect on its nuclear import. SUMO proteins, in a process of SUMOylation generate covalent interactions in an ATP-dependent reaction, forming an isopeptide bond with the amino group of a Lysine residue in the acceptor protein. Moreover the Lysine residue is positioned within a tetrapeptide consensus motif Ψ-K-x-D/E where Ψ is a hydrophobic residue; K is the lysine conjugated to SUMO; x is any amino acid; and D or E are an acidic residues (Melchior et al., 2003).

The primary sequence of FGF10 was tested for any putative SUMOylation sites. Application of two independent bioinformatics tools, GPS-SUMO and PCI-SUMO (see Chapter 2), predicted the existence of only one SUMOylation site within rat FGF10 corresponding to Lysine/K at position 98 (Fig. 3.6A&B). This site was also predicted in the human sequence at position K91 (Fig. 3.6D) (Appendix 2). The K98 resides on the protein surface and is positioned away from the NLS1 and NLS2 (Fig. 3.6C) as well as receptor binding site. Interestingly, within mouse FGF10 sequence Threonine (T92) replaces Lysine (Fig. 3.6D) resulting in the abrogation of SUMOylation (Appendix 2). Sequence alignment showed that SUMOylation may be also present in chicken, but is likely to be absent within frog and fish FGF10 sequences (Fig. 3.6D). Lack of conservation of this domain suggests that the putative SUMOylation site may not be a crucial element affecting function of FGF10 but it is possible that it generates slight,

species specific differences in the protein function. However to establish its true function (or lack thereof) it requires experimental testing.

A

ID	Position	Peptide	Score	Cutoff	Type
FGF10_rat	98	SFTKYFLKIEKNGKV	26.376	16	Sumoylation

B

rFGF10

Lysine Location	Window of Residues	Sumo/Not Sumo	Confidence	Part of a Motif
3	XXXXXXMWKWILTHCAS	NA	NA	No
88	LQGDVRWRKLFSFTKYF	NotSumo	0.2817	No
94	WRKLFSFTKYFLKIEKN	NotSumo	0.9714	No
98	FSFTKYFLKIEKNGKVS	Sumo	0.4724	Yes
101	TKYFLKIEKNGKVSGTK	NotSumo	0.4163	No
104	FLKIEKNGKVSGTKKEN	NotSumo	0.0098	No
109	KNGKVSGTKKENCPYSI	Sumo	0.5145	No
110	NGKVSGTKKENCPYSIL	Sumo	0.6153	No
131	VEIGVVAVKAINSNYYL	NotSumo	0.9258	No
143	SNYYLAMNKKGKLYGSK	NotSumo	0.4553	No
144	NYYLAMNKKGKLYGSKE	NotSumo	0.9636	No
146	YLAMNKKGKLYGSKEFN	NotSumo	0.7120	No
151	KKGKLYGSKEFNNDCKL	Sumo	0.3516	No
158	SKEFNNDCKLKERIEEN	Sumo	0.5837	No
160	EFNNDCKLKERIEENGY	Sumo	0.4773	No
190	QMYVALNGKGAPRRGQK	NotSumo	0.8241	No
198	KGAPRRGQKTRRKNTSA	NotSumo	0.3869	No
202	RRGQKTRRKNTSAHFLP	NotSumo	0.6641	No

C

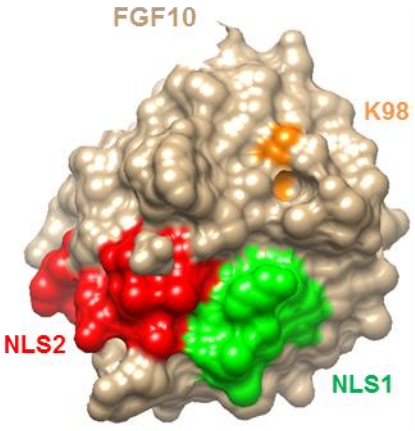

D

```
Rat      KLFSFTKYFLKIEKNGKVSGT 128
Human    KLFSFTKYFLKIEKNGKVSGT 121
Mouse    RLFSFTKYFLTIEKNGKVSGT 122
Chicken  KLYSYNKYFLKIEKNGKVSGT 125
Frog     KLFSYTKYFLQIDGNGTVSGT 161
Fish     KLFSYQKFFLRIDKNGKVNGT 112
         :*:*: *:** *: **.*.**
```

Figure 3.6 Predictions of FGF10's SUMOylation site. (A) GPS-SUMO prediction with medium stringency settings results in identification of K98 residue (B) Similarly the PCI-SUMO predicts K98 as putative SUMOylation site. (C) The K98 (in orange) resides on the protein's surface and away from the NLS1 and NLS2. (D) The SUMOylation site (orange) is present in rat, human and chicken sequences and is absent in other species (in purple corresponding residues).

3.3.2 Identification of putative glycosylation sites in FGF10 protein sequence

Upon translation, secreted proteins advance through the secretory pathway, towards the cell membrane from where they are secreted out. Most of these newly synthesised proteins contain a 'Signal Peptide' (SP) located at the N-terminus of the molecule, targeting the protein to the ER and towards the rest of the pathway. Upon protein maturation the signal peptide is removed and the protein becomes fully folded with the aid of chaperone proteins (see Chapter 1). As a typical secretory protein FGF10 was shown (using SignalP4.1 software) to contain a SP at its N-terminus (Fig. 3.7), that corresponds to the first 36-39 residues depending on the species, which is in line with data published in the literature (Yamasaki et al., 1996, Emoto, 1997).

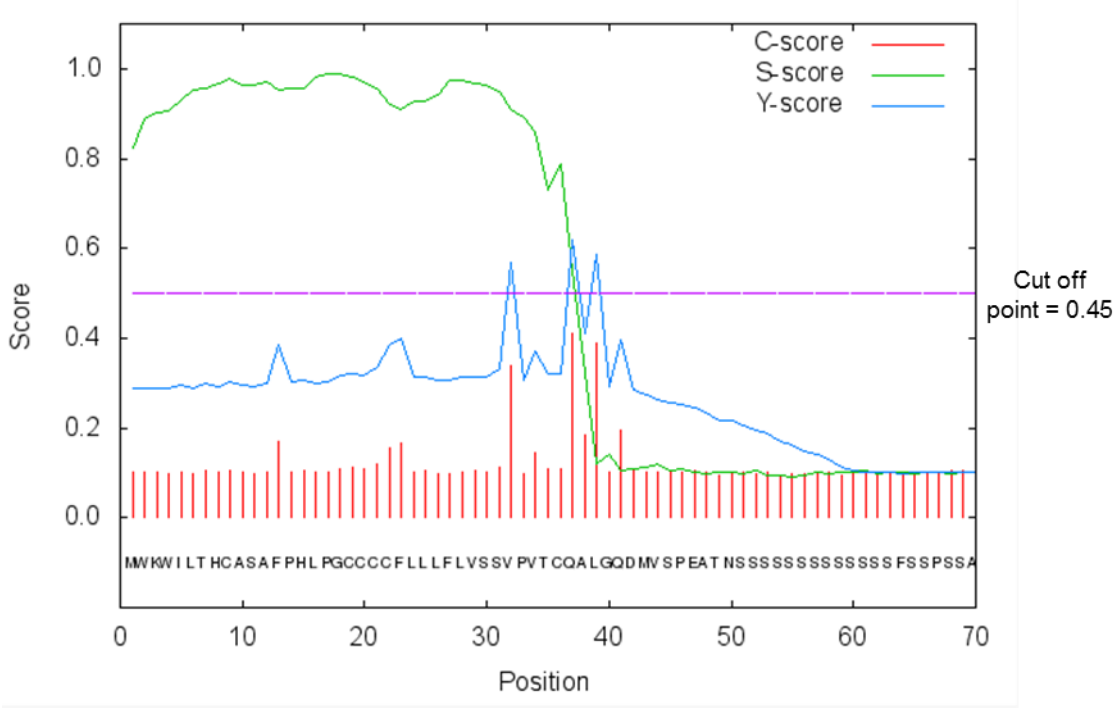

Figure 3.7 Predicted Signal Peptide (SP) of rat FGF10 according to SignalP4.1 – note the cleavage site located between residues 36 and 37. C-score - raw cleavage site score (output from networks trained to distinguish signal peptide cleavage sites); S-score - signal peptide score (output from networks trained to distinguish positions within SPs from positions in the mature part of the proteins and from proteins without signal peptides); Y-score - combined cleavage site score (combination of the C-score and the slope of the S-score).

Secretory proteins passing through the rough ER often undergo glycosylation - an enzymatic process during which glycans (sugars) are attached to specific sites on a protein structure. In the *N*-linked type of glycosylation, glycans are attached to a nitrogen atom found on the side-chains of Asparagine/N or Arginine/R residues. *N*-linked glycosylation is important for protein folding and stability (Tannous et al., 2015), and can affect protein function. For example, ablation of the glycosylation cassette in FGF4 results in the generation of two truncated protein isoforms, both showing higher biological activity than the full length FGF4 (Bellosta et al., 1993). The *O*-linked glycans are attached to the hydroxyl oxygen of Serine/S, Threonine/T, Tyrosine/Y, hydroxyl-Lysine, or hydroxyl-Proline. *O*-linked glycosylation also plays a role in protein folding, stability as well as degradation which translates onto protein function. For example, impairment of FGF23 *O*-glycosylation generates an inactive form of the protein that leads to Hyperostosis-hyperphosphatemia syndrome in humans (Frishberg et al., 2007). Importantly, there is evidence showing that glycosylation also influences protein nuclear import, even being sufficient to drive protein into the nucleus (Rondanino et al., 2003, Monsigny et al., 2004). However, certain types of glycosylation, especially those located in close proximity to a NLS, can prevent nuclear import (Schlummer et al., 2006). Since FGF10 is a secreted protein it is important to determine its putative sites of glycosylation.

A range of different bioinformatics tools predicting the glycosylation sites on a protein molecule are available online (see Chapter 2). Using different tools, there was a major similarity in the results searching for the *N*- and *O*-linked glycosylation within FGF10 rat sequence (Fig. 3.8A&B). Overall, taking into account small differences between the search tools, it was assumed that the rat FGF10 carries at least 2 putative *N*-linked and about 24 *O*-linked glycosylation sites (Fig. 3.8C). Interestingly two of those were located in close proximity to NLS2 sequence – the *N*-linked site 203 Asparagine/N and on *O*-linked site 204 Threonine/T. The significance of this is unknown but these sites could directly affect the functioning of NLS2, e.g. attract or prevent binding to Importin molecules. No glycosylation sites were found in close proximity of NLS1 site. Further searches showed that there was very little variation in predicted FGF10 glycosylation sites between different mammalian species (data not shown).

Glycosylation of FGF10 will be explored further, in the Chapter 4.

A **NetNGlyc 1.0 Server**

(Threshold=0.5)

SeqName	Position	Potential	Jury agreement	N-Glyc result
Sequence	50 NSSS	0.6578	(8/9)	+
Sequence	203 NTSA	0.5169	(3/9)	+

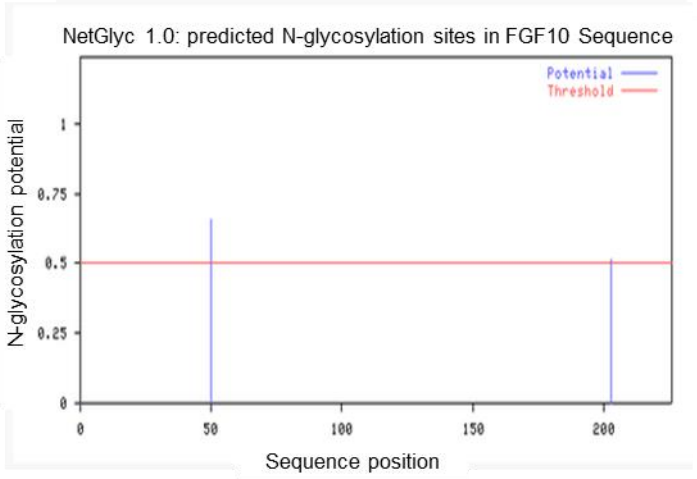

B **GlycoEP**

Position	Residue	Score	Prediction
50	NSS	0.91739417	Potential Glycosylated
78	NHL	-1.0099605	Non-glycosylated
102	NGK	-0.88443174	Non-glycosylated
179	NGR	-1.1911452	Non-glycosylated
188	NGK	-0.90478192	Non-glycosylated
203	NTS	0.76058536	Potential Glycosylated

C **Putative glycosylation sites within rFGF10HA**

MWKWILTHCASAFPHLPGCCCCFLLLFLVSSVPVTCQALGQDMVSPEATNSSS
SSSSSSSSSFSSPSSAGRHVRSYNHLQGDVRWRKLFSFTKYFLKIEKNGKVS
GTKKENCPYSILEITSVEIGVVAVKAINSNYYLAMNKKGKLYGSKEFNNDCKL
KERIEENGYNTYASFNWQHNGRQMYVALNGKGAPRRGQKTRRKNTSAHFLPMV
VHSAGYPYDVPDYA

Figure 3.8 Identification of putative rFGF10's glycosylation sites. Examples of identification of *N*-glycosylation by (A) NetNGlyc 1.0 Server and (B) GlycoEP software. (C) Collective predictions of bioinformatics tools – rFGF10 potentially carries 2 *N*-linked (purple) and 26 *O*-linked (blue) glycosylation sites; positions of NLS1 (green) and NLS2 (red) are also marked.

Part 3.4 Transcription of Fgf10 may be controlled by multiple promoters

The knowledge of mechanisms leading to a spatio-temporal transcription of Fgf10 could aid in resolving the function it serves. Genetically modified Fgf10-reporter mice, referred to as the Fgf10-LacZ mice, have a LacZ reporter placed within the Fgf10 promoter region and are used frequently to track the expression of the FGF10 protein (see Chapter 1, 2 and 6) (Kelly et al., 2001). These modifications to the promoter partially impair Fgf10 transcription (Mailleux et al., 2005). Therefore, using bioinformatics, possible promoter-positioning sites were proposed, that could be useful in future studies.

The Eukaryotic Promoter Database (EPD) tool was used to analyse a region spanning from 1000bp upstream of human Fgf10 translational start site to 100bp into the sequence of the first codon (-1000 to +100). The searches predicted five different sites for potential TATA-box positions (Fig. 3.9A), two sites for potential position of GC-box (Fig. 3.9B) and no sites for CAATT-box. Interestingly, none of these sites correspond to a promoter site predicted by a different bioinformatics tool, the Neural Network Promoter Prediction software, that predicted only one promoter site located at -243 to -293bp upstream of the Fgf10 translational start site.

Previous studies using Fgf10 LacZ-reporter mouse showed that the promoter (or some regulatory *cis*-elements) lay further upstream than 114kb from the Fgf10 ATG region (Kelly et al., 2001) (Chapter 2). Therefore an attempt was made to analyse the UTR region of Fgf10 genomic sequence further upstream than 114kb. The analysis of 7618 nucleotides of mouse genomic sequence located -900 to -77087bp on chromosome 13 upstream of the Fgf10 translational start site, using the Promoter 2.0 Prediction tool, resulted in identification of 17 putative promoter regions (Fig. 3.9C).

However, the functionality of these putative promoter regions requires experimental validation.

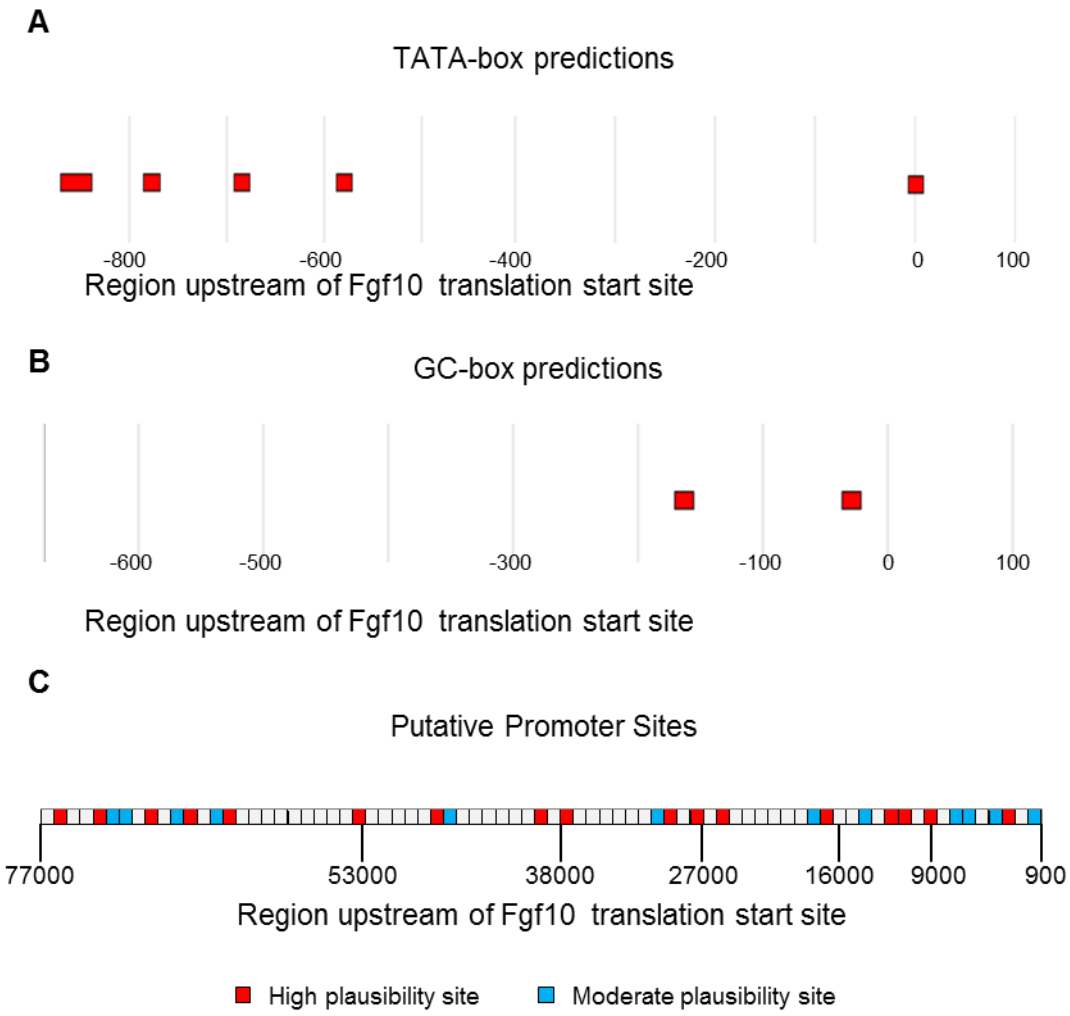

Figure 3.9 Putative promoter regions of Fgf10 gene. (A) there are 5 putative TATA box regions and (B) 2 putative GC-rich regions as determined by EPD software. (C) Further upstream of the Fgf10 translational start site there are several other putative promoter regions of high (red) and moderate (blue) plausibility as predicted by Promoter 2.0 software.

Part 3.5 Conclusion and Discussion

There is evidence that besides its secretory functions FGF10 can also translocate into a cell nucleus (Kosman et al., 2007, Bagai et al., 2002)(also shown later on in this thesis Chapter 4) through yet undescribed mechanisms (Kosman et al., 2007). In this study a range of bioinformatics tools was used to analyse FGF10 protein in context of nuclear translocation and establish possible basis for further studies.

It was found that FGF10 may contain two putative motifs, NLS1 and NLS2 that in the protein 3D structure reside in close proximity to each other (Fig. 3.1). Mutation of NLS1 does not prevent the protein from entering the nucleus. However, it causes a shift in the ratio of the nuclear-to-cytoplasmic protein presence, towards cytoplasmic (Kosman et al., 2007). Therefore, speculation has arisen that the two weak NLS motifs act together to generate a stronger signal driving protein's nuclear import. Presumably, at least one of the motifs is recognised by and interacts with an Importin chaperone, and this interaction is then further facilitated by the second NLS motif, promoting efficient nuclear transport. This arrangement of signals could provide the dual fate of the FGF10 – finely balanced opposing signals allow competition between the two intracellular trafficking pathways, either targeting the protein towards the secretory pathway or translocating it into cell nucleus. Similarly, multiple NLS-like motifs within FGF3 allow for the efficient protein import, competing with the signal peptide directing FGF3 to the secretory pathway. Moreover, alteration of the distance between the signal peptide cleavage site and one of the NLS motifs through introduction of a variable length spacer of random structure, negatively affected the nuclear import of the protein (Kiefer et al., 1994b). Therefore, the position of the motifs within the protein structure is crucial to the protein intracellular distribution, which perhaps also pertains to FGF10.

Furthermore, FGF3 belongs to the same subfamily as FGF10. Sequence alignments revealed a conservation between FGF10's putative NLS2 and one of the nuclear import motifs found within FGF3 (Fig. 3.2). Moreover, FGF7 and FGF22, both showed high content of basic residues within the NLS2 sequence region (Fig. 3.3). FGF22 was detected in the nucleus of human breast adenocarcinoma cells (MCF-7) however, the mechanisms leading to its nuclear import are not described (Beyer et al., 2003). Both NLS1 and NLS2 motifs have their paralogues in other FGF7 subfamily members and orthologues in other vertebrate species. These motifs therefore have been maintained throughout evolution, suggesting they might be of a structural or functional value to the protein. Sequence conservation was shown to determine its functional importance within a protein, and has been used to detect residues involved in ligand binding (Liang et al., 2006) and protein-protein interactions (Mintseris and Weng, 2005, Capra and Singh, 2007). Since three of the four members of the

subfamily have been detected in the cell nucleus, an interesting possibility could be raised that they all might serve an important nuclear role, which requires further investigation, beyond the scope of this project.

Interestingly, FGF10 was predicted to contain no Nuclear Export Sequences (NES). NES is a short stretch of 4 hydrophobic residues, usually Leucines/L, that bind to Exportins and targets the protein out from the nucleus into the cytoplasm. It is possible that FGF10 contains an atypical NES that cannot be detected by the limited capabilities of current software tools. It is also possible that FGF10 is exported out from the nucleus in an atypical fashion. For example, some isoforms of Importin proteins show bi-directional properties (Mingot et al., 2001). Another possibility is that FGF10 is not exported and possibly undergoes proteolytic degradation in the nucleus itself, for example by the nuclear ubiquitin-proteasome system (von Mikecz et al., 2008).

Importins belong to a large family of transport proteins, known as karyopherins. Both isoforms, α and β are able to transport their cargo proteins into cell nucleus. Specific interaction between FGF10 and a karyopherin requires experimental determination. For example, in a process of immunoprecipitation FGF10 in a complex with putative isoforms of importin could be isolated from a cell lysate FGF10. The specific Importin isoform could be further analysed through mass spectrometry. Bioinformatics predictions provide prior knowledge about certain protein interactions, which is advantageous to experimental procedures. Typically, Importin-α would bind to a classical NLS that promotes its interaction with Importin-β, and stimulates further incorporation of the whole complex into cell nucleus (see Chapter 1). Importin-β is also known to directly transport into cell nucleus proteins with an atypical NLS motif (Marfori et al., 2011). It was therefore predicted that FGF10, containing two non-consensus NLS-motifs, would implement only Importin-β as a nuclear import chaperone. Surprisingly, the results of the bioinformatics analysis show that, despite its atypical NLS motifs, FGF10 is more likely to interact with Importin-α, than Importin-β. The interaction site of FGF10-Importin α is predicted to occur within a minor site of the Importin-α. Typically interactions between Importin-α and its cargo happens within its major groove, and examples include human androgen receptor (Cutress et al., 2008), phospholipid scramblase 1 (PLSCR1) (Chen et al., 2005), c-Myc, SV40 and nucleoplasmin (Npl) (Marfori et al., 2011, Fontes et al., 2000). However, several proteins, for example nucleoporin Nup50 (Matsuura and Stewart, 2005), are known to bind within the minor groove (Kosugi et al., 2009). The selection of FGF10 NLS2-Importin-β predictions showed that these interactions were mainly generated by electrostatic forces (Fig. 3.4.). Large networks of electrostatic forces have already been shown essential and sufficient for other proteins (e.g. Parathyroid hormone-related protein (PTHrP) and Snurportin-1), providing their transport into cell nucleus by

Importin-β (Marfori et al., 2011). Although these are only predictions, they provide good basis to presume that FGF10 is able to interact with karyopherins.

In summary, bioinformatics tools suggested sites of FGF10, where putative post-translational modifications (PTM), such as SUMOylation and glycosylation could occur, which provided further implications to FGF10's nuclear transport mechanism. Both of these PTMs have been known to assist and even drive protein nuclear import and accumulation (Freiman and Tjian, 2003, Rondanino et al., 2003). Therefore, potentially they act to strengthen the weak NLS signal, facilitating the nuclear import. On the contrary, it is also possible that in specific cases the PTMs prevent the protein from entering the nucleus, for example through glycosylation of sites close to NLS2. However, the two protein PTMs showed species-specific differences (Fig. 3.5), and are therefore unlikely to be global regulators of the FGF10's intra-cellular distribution. Nonetheless, they could be responsible for minor species specific differences.

Chapter 4

Intra-cellular distribution of FGF10 reveals a putative novel endogenous function

This chapter is divided into several sections, where it will be investigated whether endogenously expressed Fgf10 can translocate into cell nucleus. Moreover, it will be studied, whether earlier identified NLS1 and NLS2 are involved in FGF10 nuclear trafficking. Additionally, mutation within FGF10 causing in humans LADD syndrome, which falls within NLS1, will be analysed in a context of nuclear trafficking of the protein. Lastly, the functional purpose of nuclear FGF10 will be addressed.

Part 4.1 Generation of recombinant FGF10 as a tool to study its endogenous function

Previous studies of externally applied FGF10's trafficking by Kosman and colleagues (Kosman et al., 2007) and bioinformatics analyses (see Chapter 3) collectively suggest that FGF10 may be transported into cell nucleus via two NLS-motifs. Endogenous detection of the protein is essential for its visual identification and determination of intra-cellular distribution. Several methods are already available, including FGF10-specific antibodies and transgenic reporter mice (see Chapter 2&6).

Currently several companies offer antibodies against FGF10, including Abcam, Abnova, R&D Systems and Santa Cruz. These antibodies have been used, for example, to show expression of FGF10 in mammary tumours, where it is meant to act as an oncogene (Theodorou et al., 2004); or within pancreatic cancer, where it induces cell migration and invasion (Nomura et al., 2008); and within an *in vitro* system, where excess of FGF10 was shown to stimulate maturation of bovine oocyte (Zhang et al., 2010a). However, these studies applied the antibody in the presence of high levels of FGF10, achieved either in overexpressed cancerous tissue or detecting accumulated recombinant protein. When tested on multiple occasions and under different settings, in order to detect endogenous FGF10 protein within cell culture and tissue sections, these antibodies yielded no signal or unreliable results (Hajihosseini's laboratory data not shown).

An alternative way to detect protein expression is through use of transgenic mice expressing reporter proteins driven by the Fgf10 promoter (Chapters 2&6). This allows visualising *in vivo* sites of Fgf10's expression, for example within ocular glands or mouse brain (Makarenkova et al., 2000, Hajihosseini et al., 2008), which allows study of the function it performs there. For example, FGF10 was shown to be an essential component of lacrimal gland development (see Chapter 1). Unfortunately the regulation of Fgf10 transcription and the exact positioning of Fgf10 promoter regions remain unclear (Chapters 1&3). Therefore, modification of the Fgf10 allele causes reduction of transcript levels, resulting in reporter mice being mildly hypomorphic for Fgf10 (Mailleux et al., 2005, El Agha et al., 2012). Moreover reporter proteins do not

provide information about intra-cellular localisation of the FGF10, as these are not FGF10-reporter fusions.

To overcome the above obstacles, a protein-to-tag fusion construct can be generated, expressed and then easily and reliably detected in a mammalian culture system. There are a variety of affinity tags available, including peptide tags such as His-tag, which corresponds to 5 to10 histidine amino acids bound by a nickel or cobalt chelate; and protein tags, such as Maltose binding protein-tag (MBP-tag), which is a protein that binds to amylose agarose. However, one of the commonly chosen tags is attachment of a fluorescent protein (Crivat and Taraska, 2012, Stadler et al., 2013), such as GFP and mCherry. Attachment of each tag presents its advantages and disadvantages. Fusion of FGF10 to a fluorescent protein can provide the possibility of detecting protein's localisation in live cell cultures and monitoring its dynamics over time. Importantly differences are noticed between different fluorescent proteins, for example, high photo-stability of mCherry protein makes it more desirable tag than GFP tag. Moreover, mCherry acts as a monomeric molecule as opposed to other fluorophores, such as GFP that often dimerise spontaneously (Shaner et al., 2004), which could result in changes to the protein function and localisation which does not correspond to processes happening *in vivo*.

On the contrary, linking another protein molecule to a small FGF10 (~20kDa) might obscure folding, stability and intra-cellular localisation of FGF10 within a cell (Lisenbee et al., 2003, Marks and Nolan, 2006), which constitutes a major drawback of the Fgf10-mCherry system. Therefore, FGF10 was fused to a very small Hemagglutinin A (HA) tag, which can be reliably detected by anti-HA antibodies. The small affinity tags, like the HA tag, have been shown to have a minimal effect on tertiary structure and biological activity of the protein they are fused to (Terpe, 2003). This system can therefore provide robust information about the FGF10 intra-cellular localisation.

Aims

This part of the study concentrates on visualising and tracking the intracellular trafficking of the FGF10 protein with the aid of stable recombinant Fgf10-reporter fusion construct.

4.1.1 Generation and validation of rFgf10-HA fusion construct

A rat Fgf10 cDNA sequence was amplified through a PCR reaction from the pGEM-T vector. Simultaneously, the sequence coding for HA tag was incorporated to the Fgf10's 3' end, through use of specific primers, generating a 707bp long cDNA strand (Fig. 4.1A). The amplified product was cloned into a mammalian expression vector, denoted pN1-rFgf10HA (see Chapter 2) (Fig. 4.1A).

To validate the successful incorporation of the Fgf10HA into the vector, the construct was digested with ScaI enzyme as Fgf10 carries a unique ScaI site, not found in the cloning vector backbone. Therefore, digestion of pN1-rFgf10HA with ScaI enzyme generated a linearized product of a 4633bp size (Fig. 4.1B). The original rFgf10-pGEM-T contains ScaI site within the vector backbone, additional to one found within Fgf10, which upon ScaI digestion generated two 2160bp and 1435bp DNA pieces (Fig. 4.1B).

Correct cloning of the Fgf10HA insert was also validated by PCR reaction using primers binding within the vector but flanking the rFgf10-HA sequence (Fig. 4.1A). The reactions generated a 941bp product showing successful incorporation of rFgf10-HA and a 369bp DNA fragment of the empty vector control (Fig. 4.1C).

Sanger sequencing of the of the PCR products revealed no mutations within the rFGF10-HA sequence, which was then used in further experiments (Fig. 4.1D).

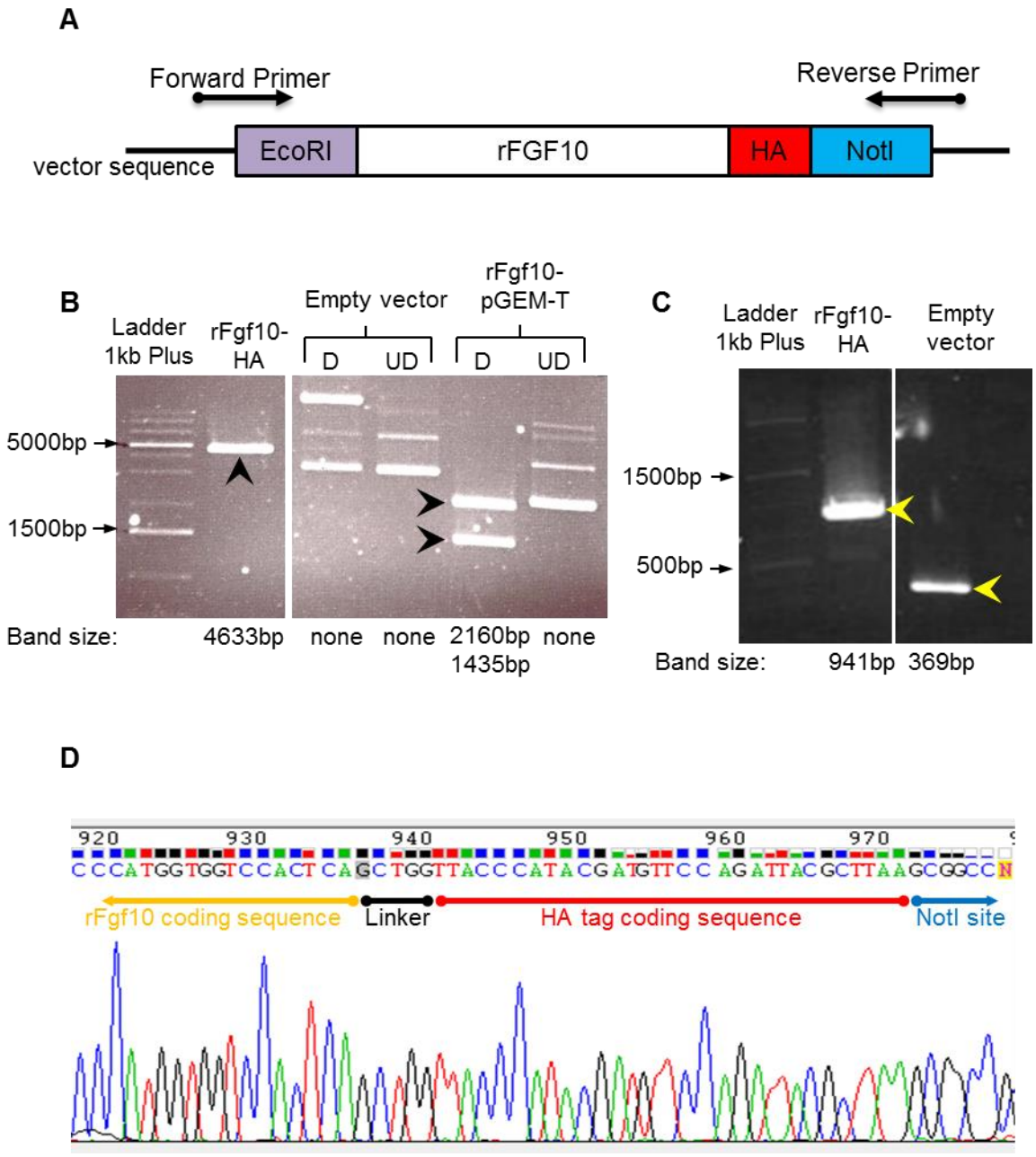

Figure 4.1 Generation of the pN1-rFgf10-HA construct. (A) Schematic representation of the pN1-rFgf10-HA, showing positions of forward and reverse primers used for PCR validation reactions. (B) ScaI restriction enzyme digest of the pN1-rFgf10-HA, and digested 'D' and undigested 'UD' controls; black arrowhead point to digested products. (C) Construct validation by PCR with yellow arrowheads pointing to two DNA pieces generated due to the presence/absence of the insert. (D) A fragment of Sanger sequence trace revealing no mutations within either the Fgf10 or HA coding sequence

4.1.2 Transient cell transfections reveal intra-cellular FGF10HA localisation

To determine the intracellular distribution of FGF10, the pN1-rFgf10HA construct was transiently transfected into human retinal pigment epithelial cells ARPE cell line. The cell line was chosen as a tool to study protein localisation due to their typical ease of accepting transfected DNA. Transfection was performed using JetPrime (Polypus), which is a polymer-based reagent that minimizes adverse cytotoxic effects triggered by transfection (see Chapter 2). The expression of the protein was visualised 24h post-transfection, by fluorescently immunolabelling with anti-HA antibody and scrutinised under high power confocal microscopy, which has shown the protein localising to specific nuclear loci (Fig. 4.2A). Moreover, co-labelling of HA with a nucleolar protein called Fibrillarin, has further demonstrated that FGF10HA was targeted to the nucleolus (Fig. 4.2B).

It was observed that from all of the transfected cells in a given culture only a subset demonstrated the nuclear HA label. Furthermore a variety of cellular distributions of FGF10HA were observed and these were categorised into five groups: (i) ‘exclusively nuclear’; (ii) ‘predominantly nuclear’, (iii) ‘predominantly cytoplasmic’, (iv) ‘exclusively cytoplasmic’; and (v) ‘equal distribution’ of the HA signal in both cytoplasm and the nucleus (Fig. 4.3A).

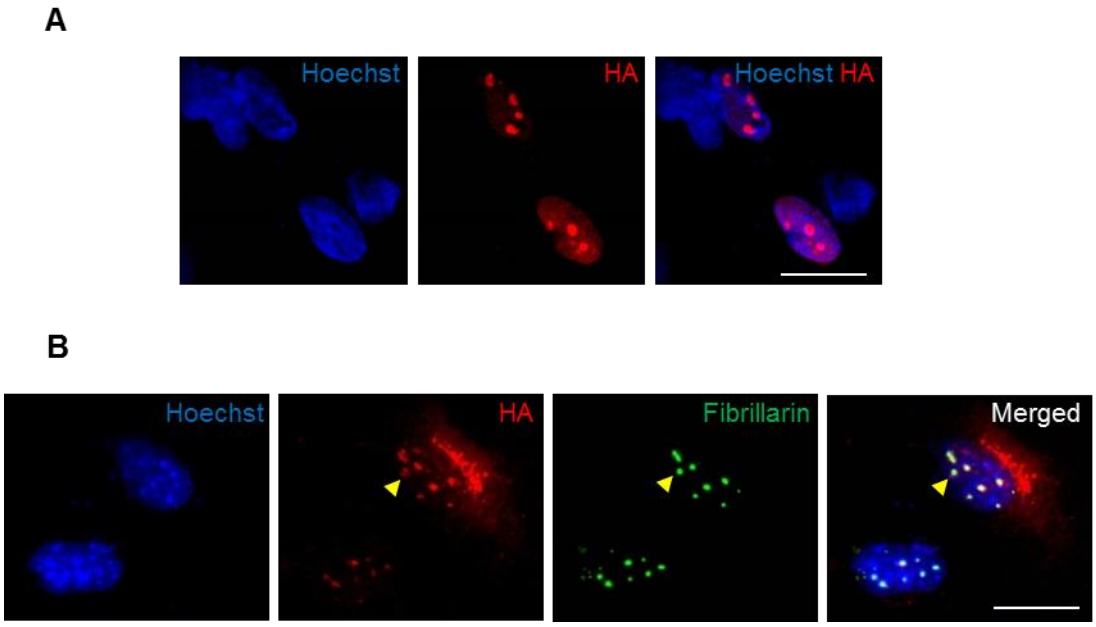

Figure 4.2 Detection and analysis of HA staining, indicative of FGF10 presence revealed nuclear protein localisation. (A) Staining was scrutinised under high power confocal microscopy; scale bar 20µm. (B) Co-localisation of HA staining with Fibrillarin marker (yellow arrowhead) revealed nucleolar localisation of FGF10HA within the cell nucleus; scale bar 20µm.

To analyse the intra-cellular distribution of the rFGF10-HA, ARPE cells, which were cultured on a 13mm diameter microscope glass coverslips and fixed 24h post transient transfection, subsequently immunofluorescently labelled and scrutinised by microscopy. Ten random fields of view were chosen across two different coverslips (5 from each coverslip), and the total number of cells present, as well as the total number of transfected cells and the cellular distribution of HA within each cell were determined. Cell transfection was performed on four separate occasions allowing reliable statistical analysis (see Chapter 2).

Importantly, in at least 15% of transfected cells rFGF10HA was found exclusively in the cell nucleus. Statistically, there is no significant difference between the different HA localisations (ANOVA $p=0.223$, $F=1.611$, $n=4$) and therefore it could be presumed that FGF10 is as likely to be found in cell nucleus as it is in the cytoplasm (Fig. 4.3B). To control for the transfection efficiency and HA visualisation, the ARPE cells were transfected simultaneously with a pmCherry-N1 vector - the backbone vector that was used to generate the pN1-rFgf10HA construct (see Chapter 2). Unlike rFGF10HA, the mCherry fluorescent protein was found ubiquitously present around the cell, and did not show predominant localisation within nucleus or cytoplasm (Fig. 4.3A). Moreover, it was noted that whereas nuclear FGF10HA was found within the nucleoli (Fig. 4.2&4.3), mCherry showed more diffused, non-specific pattern of expression, suggesting that it is not targeted to any particular site/loci within the nucleus or cytoplasm (Fig. 4.3A).

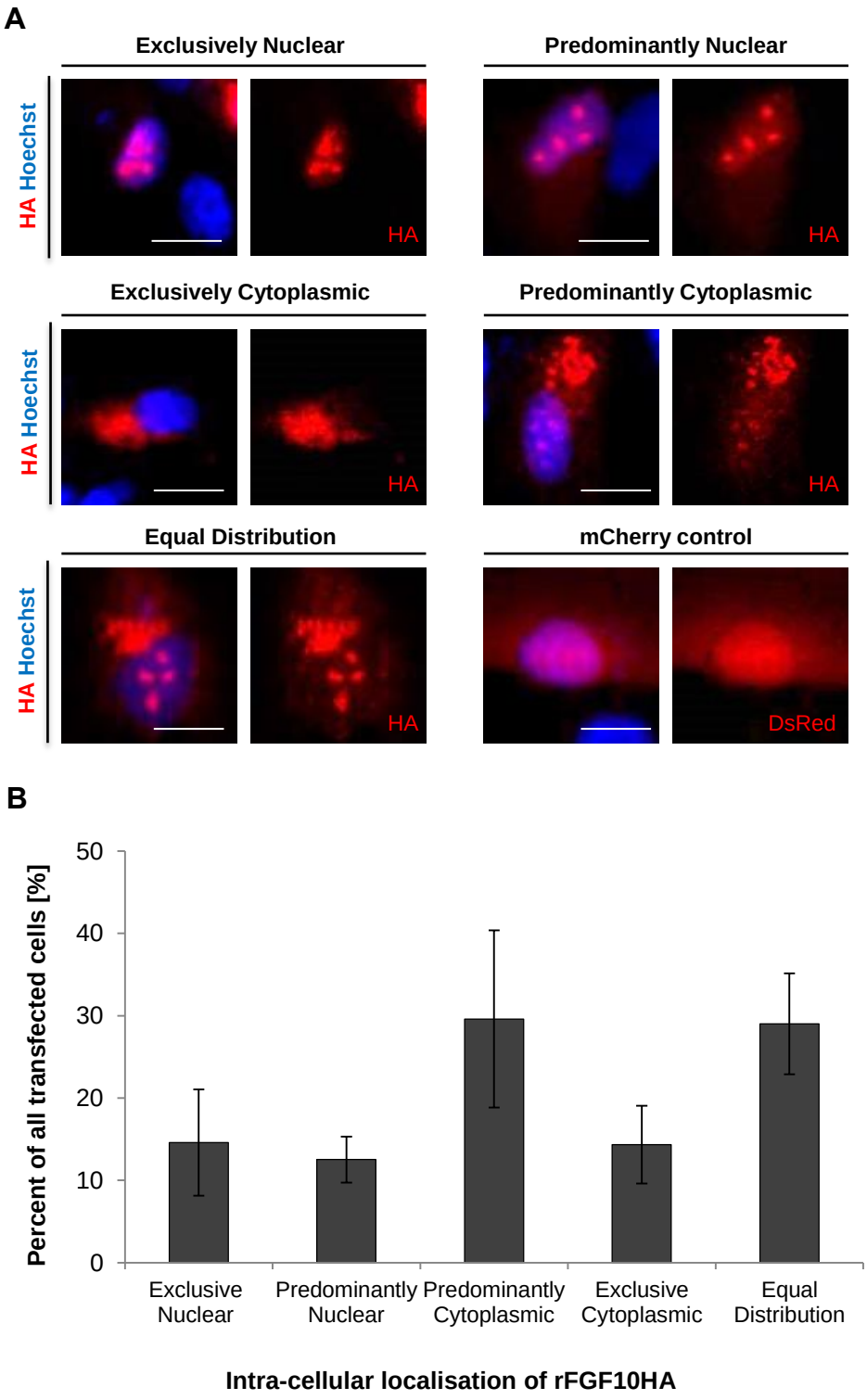

Figure 4.3 Intra-cellular distribution of rFGF10-HA in ARPE cell culture. (A) Detection of the HA (red) depending on the intensity of the staining was categorised into 5 categories, while mCherry is ubiquitously expressed around the cell; Scale bar 20µm. (B) Quantification of the percentage of cells expressing HA in any of the specific patterns shows that there is no statistically significant difference of FGF10's intra-cellular localisations (ANOVA p=0.223, F=1.611, n=4).

Detection of rFGF10HA in the nucleus was not specific to ARPE epithelial cells as transfection of the rFGF10HA construct into a variety of different cell types showed similar results. Hence, rFGF10HA was also found in the nucleus of mesenchymal (ATDC5), human embryonic kidney (HEK 293T), as well as primary astrocytes and hypothalamic neural cells (see Chapter 6) (Fig. 4.4). These results suggested that nuclear translocation of FGF10 may be a global phenomenon, putatively taking place in a variety of cell types expressing endogenously Fgf10 *in vivo*.

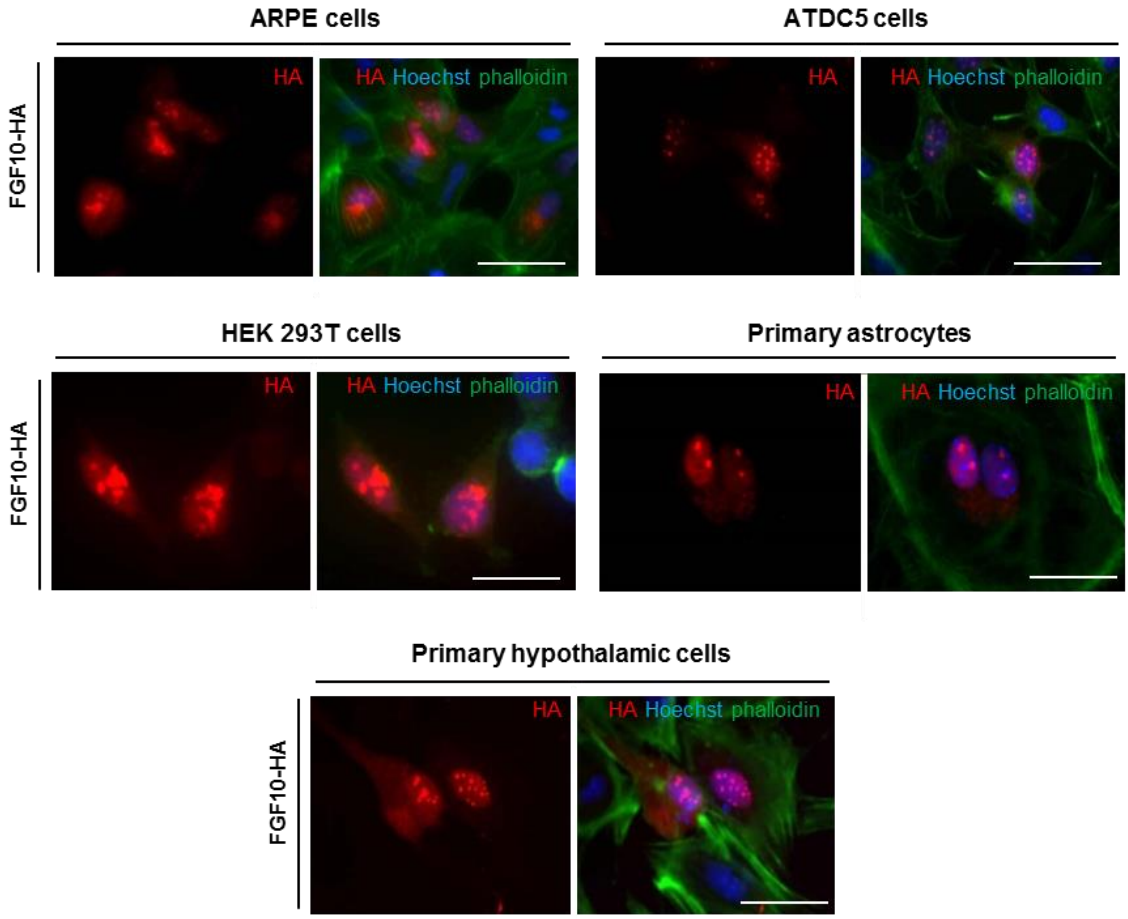

Figure 4.4 Different cell types show similar patterns of FGF10HA intracellular distribution. Micrographs showing examples of transiently transfected FGF10HA localised within the nucleus of epithelial (ARPE), mesenchymal (ATDC5), and human embryonic kidney (HEK 293T) cells as well as primary astrocytes and hypothalamic neural cells; Scale bar 50µm.

On average, regardless of the cell type analysed only about 10-30% of total transfected cells displayed rFGF10HA expression and 50-60% the control mCherry protein. Therefore, the achieved transfection rate - calculated as a percentage of total number of transfected cells from total number of cells present (see Chapter2), was reasonably low. A higher rate of transfection is desirable for overexpression studies, immunoprecipitation of a protein from the culture and any other required experiments. Several different transfection methods were tested, such as Calcium Phosphate precipitation; Lipofectamine® 3000 Reagent (Thermo Fisher Scientific); TurboFect Transfection Reagent (Thermo Fisher Scientific); and FuGENE®6 (Promega). However, none improve the transfection rate of <30% obtained with JetPrime Reagent. During transfection optimisation, factors such as cell density, amount of DNA and transfection reagent, incubation time and toxicity of the reagent, type of cells, time post transfection were taken into account and meticulously adjusted for each reagent every time. Furthermore, to enhance the transfection efficiency the method of 'glycerol shocking' was tested on several occasions, but with no significant improvement. The highest transfection rate of rFGF10HA was achieved in HEK 293T cells, ranging from 30-40%, while the mCherry's transfection ranged between 60-80% depending on the assay. This is not surprising, because HEK 293T cells are widely used for DNA transfection and mammalian protein expression, and with high transfection success rate, as demonstrated in a study analysing functional nuclear export signal (NES) in the green fluorescent protein asFP499 (Mustafa et al., 2006) or whilst determining the role of semaphorin-3F (s3f) on inhibition of FGF2 signalling during tumour angiogenesis (Kessler et al., 2004).

4.1.3 Conclusion

A recombinant rat FGF10 protein fused to small HA tag was detected in cells' nucleus where it localised to a subset of nucleoli. This appears to be a universal phenomenon, found across multiple cell types *in vitro*. Although a mouse recombinant Fgf10HA construct has been generated before, its intracellular distribution was not described (Beer et al., 1997). Therefore here for the first time it was shown that rFGF10HA is found in the nucleus of multiple types of cells.

In the absence of reliable FGF10-specific antibodies, the rFgf10-HA hence provides a good tool for further studies of FGF10 intracellular function.

Subsequently, it was investigated whether NLS1 and NLS2 drive the nuclear translocation of FGF10HA, either separately or in cooperation, analysing each motif individually.

Part 4.2 Mutation of NLS1-motif perturbs intracellular distribution of FGF10

The NLS1-motif of FGF10 (rat 142NKKGKLY148) has been proposed by Kosman and colleagues (Kosman et al., 2007) and analysed in the context of binding to importins through basic residues. The results showed that mutations of Lysines/K into neutral Threonine/T residues did not prevent FGF10 from entering the cell nucleus. However, it resulted in a higher than normal abundance of the cytoplasmic protein (Kosman et al., 2007). These experiments were based on exogenous application of the wild type and mutant protein to the cell culture, showing that the protein translocating into the nucleus was previously endocytosed.

Interestingly, analysis of human anomalies caused by Fgf10 mutations show that a single residue substitution within NLS1 – the G138E (rat G145E) causes LADD syndrome (Entesarian et al., 2007), which was omitted in the previous studies of the NLS1 (Kosman et al., 2007). The intriguing positioning of the G145E mutation within the NLS1 could suggest a role in the nuclear import of FGF10. In this part of the chapter, the effects of the mutation within NLS1 will be analysed in a context of endogenously produced protein, rather than exogenous treatment of a cell culture performed by Kosman et al. (Kosman et al., 2007).

4.2.1 Overview of human syndromes related to FGF10 function.

Aplasia of lacrimal and salivary glands (ALSG; OMIM 180920) and lacrimo-auriculo-dento-digital (LADD; OMIM 149730) syndromes are rare autosomal dominant disorders which, with various severities, result in defective development of lacrimal and salivary tract, often accompanied by abnormalities of the face, ears, eyes, mouth, teeth, digits and genitourinary system. These syndromes are caused by heterozygous missense mutations within FGF10 and FGFR2 genes (Milunsky et al., 2006, Rohmann et al., 2006, Entesarian et al., 2007, Scheckenbach et al., 2008) (Fig. 4.5). Similar phenotypes were also described in Fgf10 or FgfR2 heterozygous mice (Min et al., 1998, Entesarian et al., 2005). Defects caused by the described mutations are attributed to an impaired FGF10-FGFR2 binding or reduced stability and folding of the mutant protein (Shams et al., 2007). However, the molecular mechanism/s by which the Glycine (G) 138 to Glutamic Acid (E) substitution in NLS1 causes LADD syndrome is thus far unknown (Fig. 4.5).

Aims

The fact that mutation of hG138 (rG145) residue resulted in malfunction of the FGF10, signifies potentially it is one of the key residues within the protein sequence.

The peculiar position of this residue within NLS1 was analysed in the context of nuclear transport of the mutant FGF10 protein.

FGF10 mutations				
Mutation/ Deletion	**Amino acid change**	**Syndrome**	**Molecular consequence**	**Reference/s**
237G→A (exon 1)	W79X	ALSG	predicted truncated protein	Seymen et al. 2016
240A→C (exon 1)	R80S	ALSG	disruption of FGF10/ FGFR2-IIIb binding site	Entesarian et al. 2007; Chapman et al. 2009
317G→T (exon 1)	C106F*	LADD	protein unstable at physiological temperature	Rohmann et al. 2006; Shams et al. 2007
deletion (of exons 2 and 3)	not applicable	ALSG	potential lack of protein formation	Entesarian et al. 2005
409A→T (exon 2)	K137X*	ALSG & LADD	predicted truncated protein	Milunsky et al. 2006
413G→A (exon 2)	G138E*	ALSG/LADD	unknown	Entesarian et al. 2007
430G→A (intron 2)	not applicable	ALSG	truncated protein	Scheckenbach et al. 2008
467T→G (exon 2)	I156R	LADD	disruption of FGF10/ FGFR2-IIIb binding site	Milunsky et al. 2006; Shams et al. 2007
506G→A (exon 3)	W169X*	ALSG	predicted truncated protein	Milunsky et al. 2006
577C→T (exon 3)	R193X	ALSG	truncated protein; partial abolishment of FGF10/ FGFR2-IIIb binding	Entesarian et al. 2005
620A→C (exon 3)	H207P	Healthy phenotype	rare polymorphism	Entesarian et al. 2007
FGFR2 mutations				
Mutation/ Deletion	**Amino acid change**	**Syndrome**	**Molecular consequence**	**Reference/s**
1882G→A	A628T	LADD	positioned within ligand-binding domain, but affects tyrosine kinase catalytic activity	Rohmann et al. 2006; Shams et al 2007; Lew et al. 2007
1942G→A (exon 16)	A648T	LADD	affects ligand binding	Rohmann et al. 2006
Δ1947-AGA-1949 base depletion (exon 16)	R649S & ΔD650	LADD	affects ligand binding	Rohmann et al. 2006

Figure 4.5 Human heterozygous mutations of Fgf10 or FgfR2 result in ALSG or LADD syndromes, through characterised or predicted molecular mechanisms. However, a *de novo* arising G138E mutation generated phenotype characteristics between of those of ALSG and LADD syndromes through so far undescribed means. Star (*) indicates FGF10 mutations positioned outside its receptor binding site.

4.2.2 Glycine residing within FGF10-NLS1 is a well conserved residue

Through analysis of the FGF10 primary sequence it was revealed that the Glycine residue (mutation of which resulted in LADD) was well conserved among all vertebrate species (Fig. 4.6A). Moreover, this Glycine residue was present within all members of the subfamily to which FGF10 belongs (Fig. 4.6B) and it was found to be conserved in representative FGFs from other FGF subfamilies (Fig. 4.6C). Such extreme conservation suggests that human G138 (rat G145) residue may play an important role within FGF molecules as a whole.

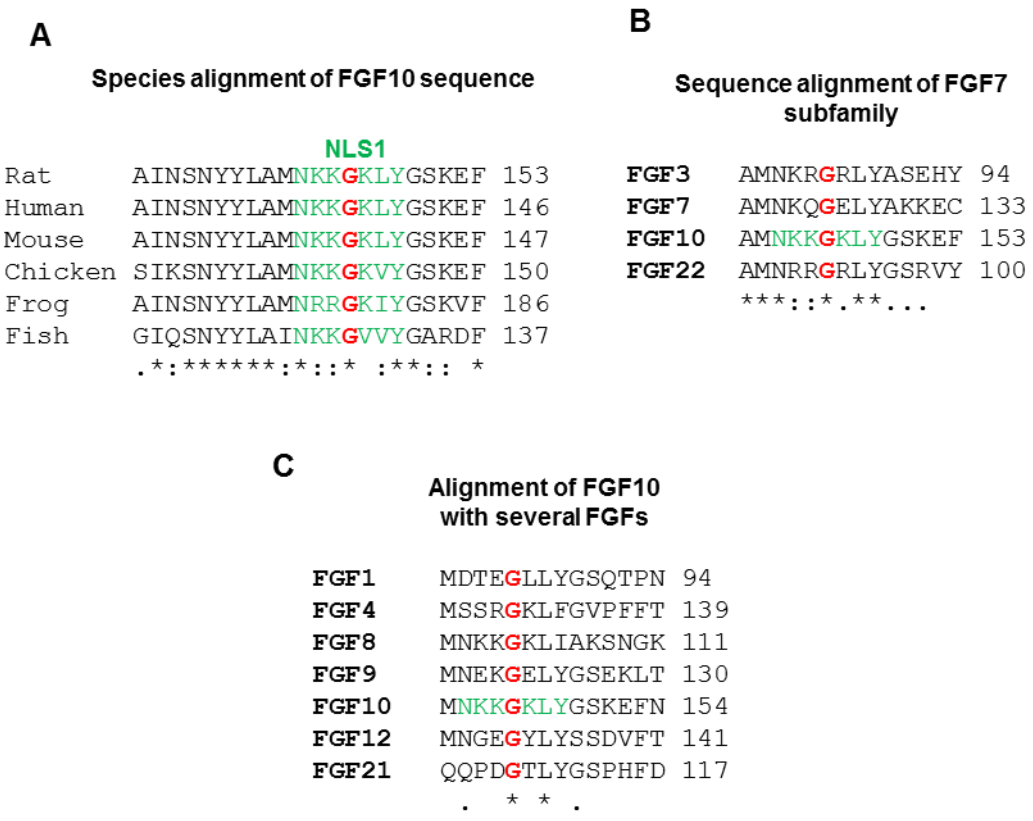

Figure 4.6 Extreme conservation of rFGF10's Glycine 145 (G145) residue across vertebrate species (A) as well as all other FGF molecules (B&C) signifies its functional importance within the protein.

4.2.3 Glycine 145 to Glutamic Acid residue substitution impairs intracellular distribution of FGF10 protein

To investigate the molecular importance of the Glycine 145 residue, an LADD-like mutation to Glutamic Acid/E was introduced into the rFGF10HA construct through site-directed mutagenesis (see Chapter 2). Correct incorporation of the mutation was determined by Sanger sequencing (Fig. 4.7A) and confirmed by alignment of DNA sequences with the WT rFgf10-HA (Fig. 4.7B).

Intra-cellular localisation of transiently transfected G145E-HA (here on called G145E) into ARPE cells was scrutinised by high resolution confocal microscopy. Interestingly, unlike non-mutated FGF10, the G145E mutant was completely absent from the cell nucleus, and concentrated in a high abundance within the cell cytoplasm (Fig. 4.7C). Therefore, the G145E residue substitution seemed to perturb the nuclear import of the FGF10 protein.

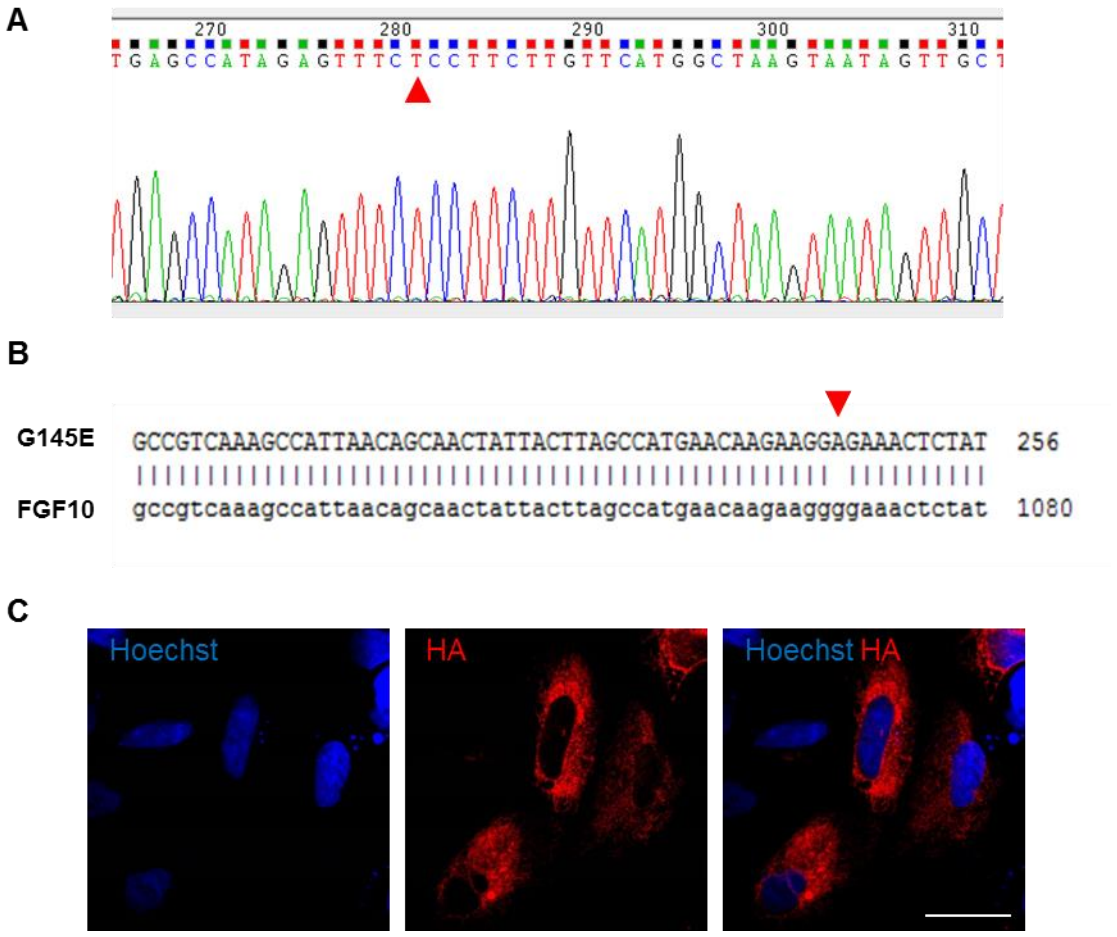

Figure 4.7 Successful generation of G145E mutation by single base substitution. (A) Incorporation of the mutation was confirmed by Sanger Sequencing. (B) Sequence alignment of rFGF10HA (lowercase) and G145E (uppercase) shows the single base change resulting in G to E substitution. (C) Confocal microscopy image reveal G145E nuclear exclusion within the ARPE cell culture; Scale bar 20µm.

Moreover, similar results were obtained regardless of the type of the transfected cells, as G145E was absent from the nucleus in epithelial (ARPE), mesenchymal (ATDC5) (Fig. 4.8) and neural (primary neural culture derived from hypothalamus) cells (see Chapter 6). Irrespective of cell type, rFGF10HA was found in the cell nucleus of at least 25% of total transfected cells, whereas G145E was invariably seen only in the cytoplasm (Fig. 4.8).

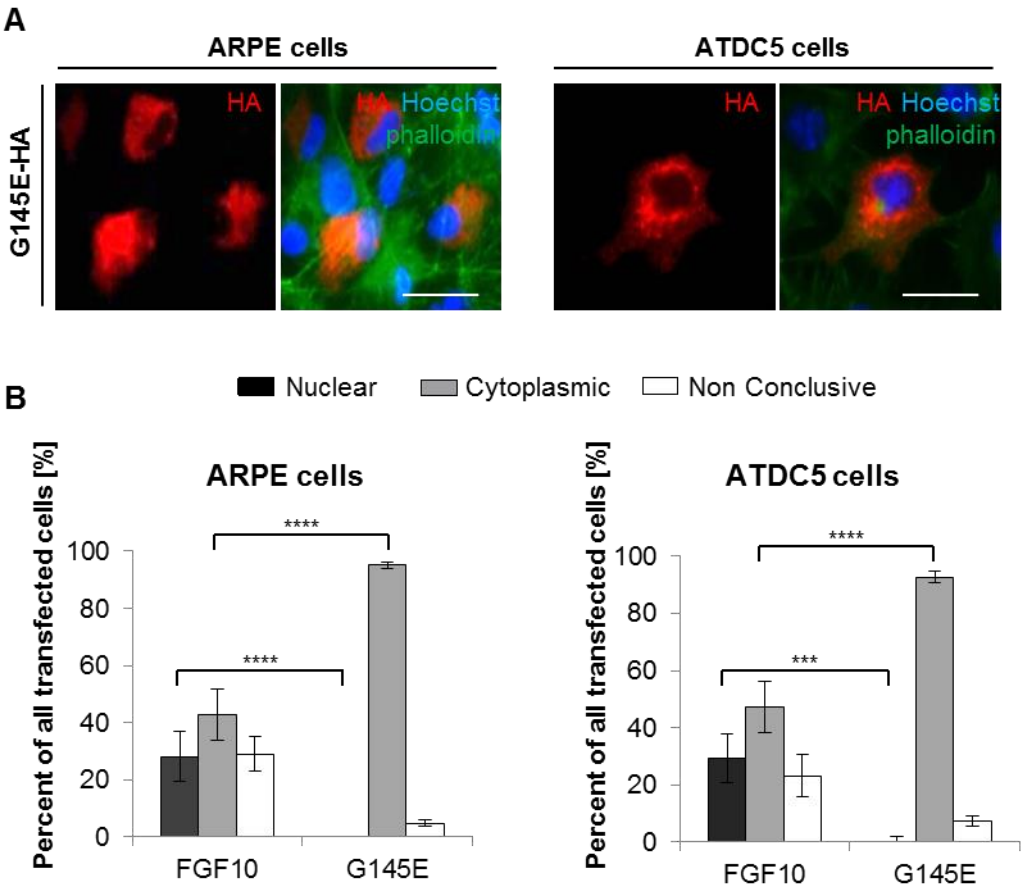

Figure 4.8 Analysis of the G145E mutant. (A) Nuclear exclusion was not specific to a particular cell type and similar results are obtained by detecting the florescent HA staining in ARPE and ATDC5 cell culture; Scale bar 40µm. (B) Quantification of the intracellular distribution of G145E in regards to non-mutated FGF10HA shows similar results in epithelial (ARPE) and mesenchymal (ATDC5) cell lines (Student T-test $p \leq 0.001$, n=3, error bar = SE).

4.2.4 A Glycine residue *per se* at position 145 is essential for the nuclear import of FGF10

It is conceivable that the LADD causing substitution of small neutral Glycine residue into a big and acidic Glutamate could result in disruption to FGF10 interaction with Importins (Fig. 4.9A). This hypothesis was tested through mutation of Glycine to a smaller and neutral residue, which theoretically should restore the protein's interaction with nuclear transport chaperones and yield similar intracellular distribution pattern as the non-mutated FGF10. Surprisingly, mutations of Glycine 145 to Valine/V (G145V) or Alanine/A (G145A) also resulted in complete nuclear exclusion of the protein (Fig. 4.9). Valine, in comparison to Glutamate is a small and non-polar residue, although its short side-chain is branched (Fig. 4.9), potentially causing steric repulsion that could explain still existing interruption to FGF10-Importin binding site. Alanine, by contrast, is the second (after Glycine) smallest residue, with a non-reactive methyl group on its short side-chain (Fig. 4.9), which should not prevent the whole region from binding to another molecule. Therefore it seems that the Glycine 145 *per se* is important for the intracellular distribution of FGF10 and any mutation of this particular residue leads to nuclear exclusion of the protein.

Bioinformatics analysis of the 3D structure of the FGF10 molecule revealed that the G145 residue within NLS1 generates a direct H-bond with a Glycine 196 within NLS2 sequence (Fig. 4.9 and Chapter 3). It was therefore investigated if this bond between the two NLS sites is crucial for the nuclear import of the protein, and becomes disrupted during the G145E residue substitution. However, mutation of the Glycine 196 to Glutamic Acid does not cause nuclear exclusion of the protein and the intra-cellular localisation of G196E is similar to the non-mutated FGF10 (Fig. 4.9).

These results show that the Glycine 145 *per se* is somehow important for the nuclear translocation of the FGF10 protein.

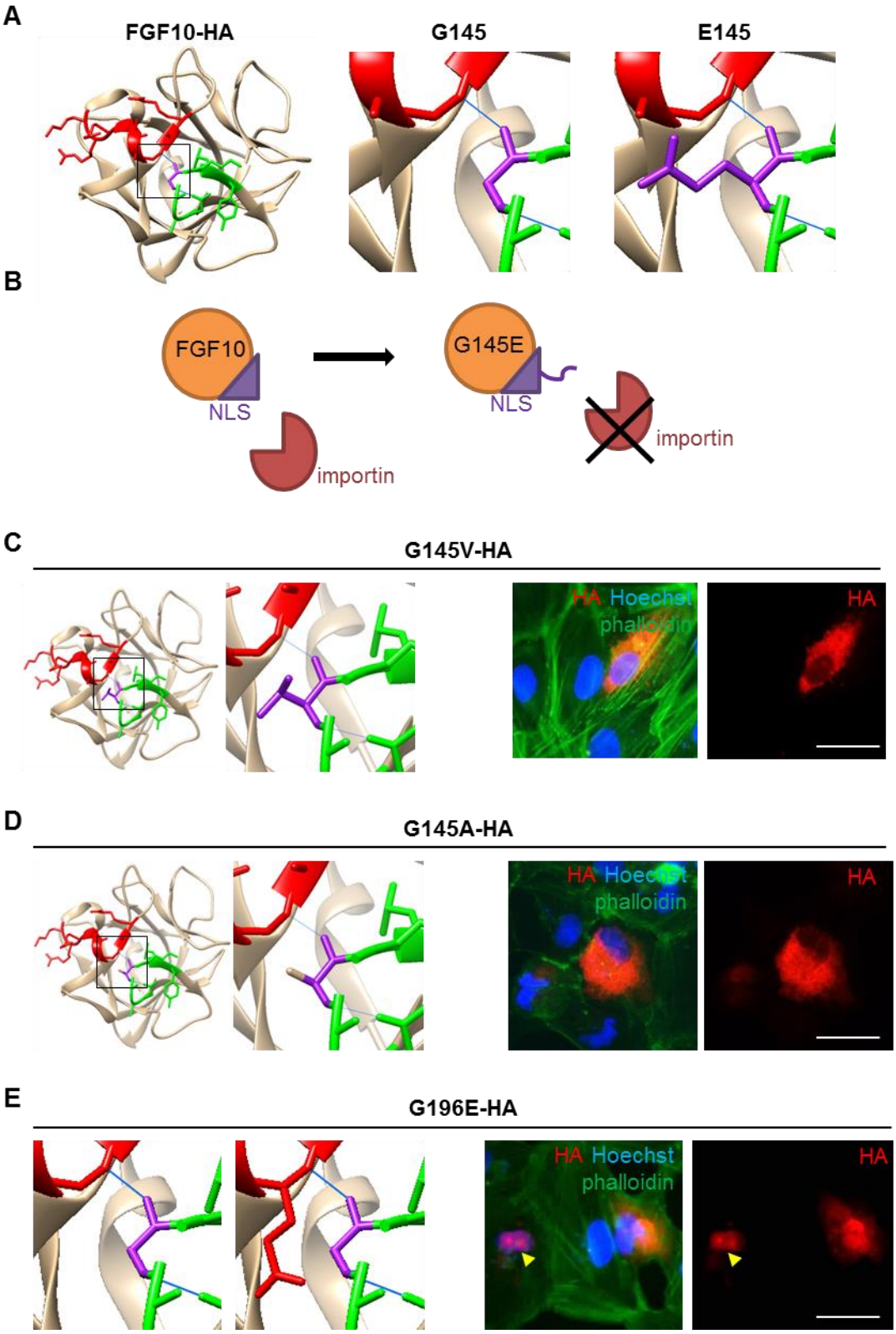

Figure 4.9 Structural analysis of Glycine at position 145. (A&B) In comparison to Glycine/G, the Glutamate/E residue contains big and acidic side chain that could affect binding to nuclear chaperone protein. (C) Substitution to smaller Valine (G145V-HA) and (D) Alanine (G145A-HA) was nuclearly excluded resembling G145E. (D) Glycine/G 196 (G196) residue forms a direct H-bond (blue line) with G145 but G196E mutant is not nuclearly excluded (yellow arrowhead); Scale bar 40µm.

4.2.5 Conclusion

Although the basic residues within NLS1 do not appear to have a major role in the intracellular distribution of the FGF10 (Kosman et al., 2007), the G145 residue within the sequence was shown to be crucial for the nuclear import of the protein. The G145E most likely indirectly impaired the FGF10-importin binding and the effect of mutation could not be rescued by substitution with other small residues, such as Valine and Alanine. Moreover, the H-bond generated between the NLS1 and NLS2 through the G145 is unlikely to be affected by the mutation to Glutamic Acid as mirroring of the G145E mutation by the G196E within the NLS2, did not perturb the nuclear import of the protein.

The subsequent investigations asked whether Glycine at position 145 is the only residue implicated in the nuclear translocation, or whether NLS2 also plays a role in FGF10's nuclear trafficking.

Part 4.3 Perturbation of NLS2 impairs nuclear import of FGF10 protein.

The basic amino acids within a NLS can attract and bind to Importins (see Chapter 3). Therefore mutations of these residues would disrupt this protein-protein interaction, preventing FGF10 from entering the cell nucleus. It was proposed that, due to their positioning within the protein tertiary structure, NLS1 and NLS2 act collectively to generate a stronger signal targeting FGF10 to the nucleus.

Aims

The aim of this section was to determine whether abrogation of NLS2 motif alone affects localisation of the FGF10 within a cell.

4.3.1 Impact of NLS2 mutations on the intracellular distribution of FGF10

The side chains of Arginine and Lysine residues have long positively-charged side chains that fit into the acidic grooves on Importin proteins. The NLS2 sequence, 194 RRGQKTRRK 202, harbours six basic residues. To investigate the contribution of each residue, each was substituted to much smaller and electrically neutral Threonines, which are unlikely to generate strong interactions with the Importin sites (Fig. 4.10A). The rFGF10HA vector was used as a template for all of the mutagenesis constructs, so that all proteins could be detected with the HA antibody. All generated mutation-bearing constructs were screened and validated by Sanger sequencing, as for G145E (Appendix 3).

All six basic residues within NLS2 were sequentially mutated using site-directed mutagenesis (see Chapter 2) (Fig 4.10B) in order to identify a potential key residue mediating the nuclear or nucleolar import of FGF10. For example, mutation of specific residues within NLS of FGF2 had a significant impact on protein nuclear and nucleolar localisation (Sheng, 2004). All FGF10 mutant variants were assessed in a similar fashion to the earlier described rFGF10HA for their intra-cellular localisation (see section 4.1.2). HA staining found exclusively or predominantly in the nucleus was classified as ‘nuclear’ and similarly, HA staining found exclusively or predominantly in the cytoplasm was classified as ‘cytoplasmic’. Statistically there was no significant difference between the nuclear or cytoplasmic protein localisation of FGF10HA protein in these assays (ANOVA $p>0.05$, $F=15.482$ & $F=41.366$), suggesting that individually none of the basic residues within NLS2 mediate nuclear import of FGF10 (Fig. 4.10C&D). Moreover, none of the single mutants affected the localisation of the protein

within cell nucleolus. Therefore, single mutations appeared not to perturb intra-cellular distribution of the FGF10 protein (Fig. 4.10E).

However, when double mutations at the N-terminal and C-terminal sections of the sequence were generated, i.e. the R194T/R195T, R200T/R201T and R200T/K202T (Fig. 4.10B), in comparison to the non-mutated FGF10 a higher proportion of cells displayed HA localising within the cytoplasm (ANOVA $p<0.0001$, $F=15.482$) (Fig. 4.10C&D). Moreover, perturbation of the N-terminal section of the NLS2, the R194T&R195T double mutant was significantly less likely to enter the nucleus than FGF10HA (ANOVA $p<0.0001$, $F=15.366$) (Fig. 4.10C&D). None of the double mutants seemed to affect the nucleolar entry of the protein. By contrast, mutation of four residues within the NLS2, the R194T/R195T/R200T/K202T (here called 4T-NLS2) caused 98% of the protein to be found in the cytoplasm, significantly limiting the nuclear import of FGF10 (ANOVA $p<0.0001$, $F=15.482$) (Fig. 4.10C&D).

Mutation of NLS2 caused impairment in the nuclear transport of the FGF10 protein, meaning that NLS2 is essential for nuclear entry of FGF10.

4.3.2 Conclusion

Single mutations with the NLS2 sequence appeared not to perturb the intracellular distribution of FGF10, unlike a single G145E mutation within the NLS1. However, combination of mutations of the basic residues resulted in significant impairment of the nuclear import, suggesting therefore that NLS2 potentially attracts and binds to importins.

Non-mutated FGF10 localised to the nucleolus. The nucleolar targeting signals can overlap with their nuclear localization signals. For example Lysine128 residing within NLS of FGF2, alone controls its nucleolar (but not nuclear) localization of the protein (Sheng, 2004). None of the mutants within C-terminal NLS of FGF2 appeared to interfere with nucleolar localisation of the protein, even after translocation into the nucleus. Therefore nuclear and nucleolar targeting of the FGF10 is likely to occur via different motifs and mechanisms.

Both, the G145E (within NLS1) and the 4T-NLS2 mutants resulted in the nuclear exclusion of FGF10. However, the observed cytoplasmic retention of the mutants is thought to be generated through different means. Therefore, the putative molecular mechanisms driving the nuclear exclusion caused by these mutants will be explored further and addressed in a context of FGF10's nuclear function.

Figure 4.10 Analysis of NLS2 (A) Schematic representation of putative replacement of basic (K&L) residues with neutral (T) within NLS impairs binding to importin protein and abrogates nuclear import of the protein. (B) Table of mutations made within NLS2. (C&D) Quantification of the percent of protein found in cell nucleus or in the cytoplasm, 24h post transient transfection into the ARPE cell line (ANOVA, n=4). (E) Fluorescent images of the representative protein distribution within a cell; Scale bar 20µm.

A

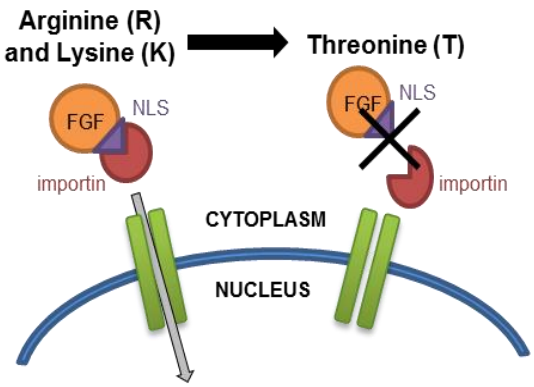

B

WT and mutant NLSs	sequence
WT NLS	194 RRGQKTRRK 202
R194T	194 T_____ 202
R195T	194 __T_____ 202
K198T	194 _____T_____ 202
R200T	194 _____T__ 202
R201T	194 _____T_ 202
K202T	194 _____T 202
R194T/R195T	194 TT_____ 202
R200T/R201T	194 _____TT_ 202
R200T/K202T	194 _____T_T 202
R194T/R195T/ R200T/K202T (4T-NLS2)	194 TT_____T_T 202

C

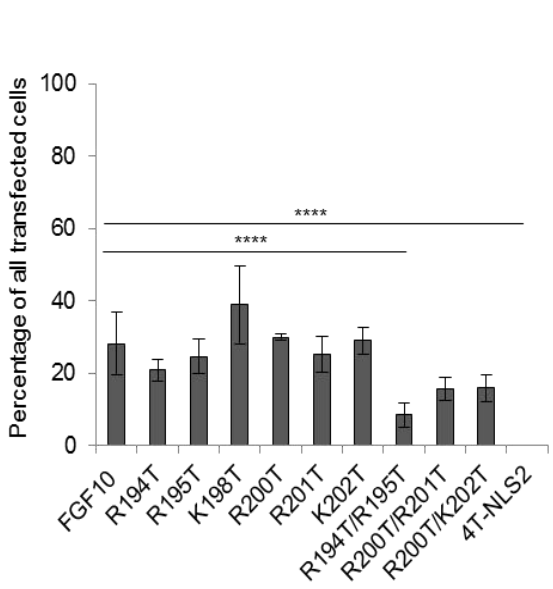

D

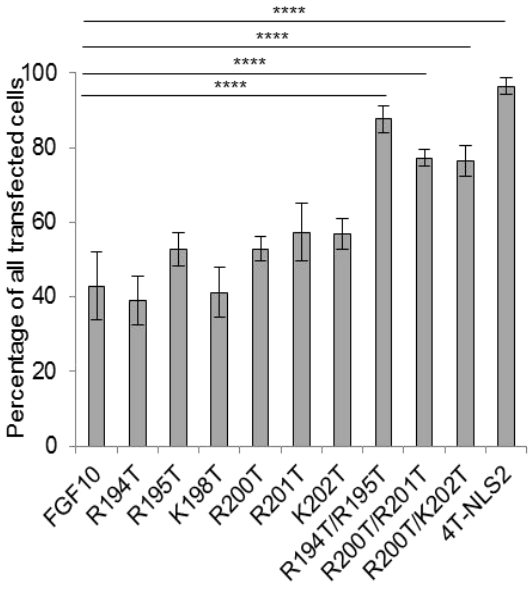

E

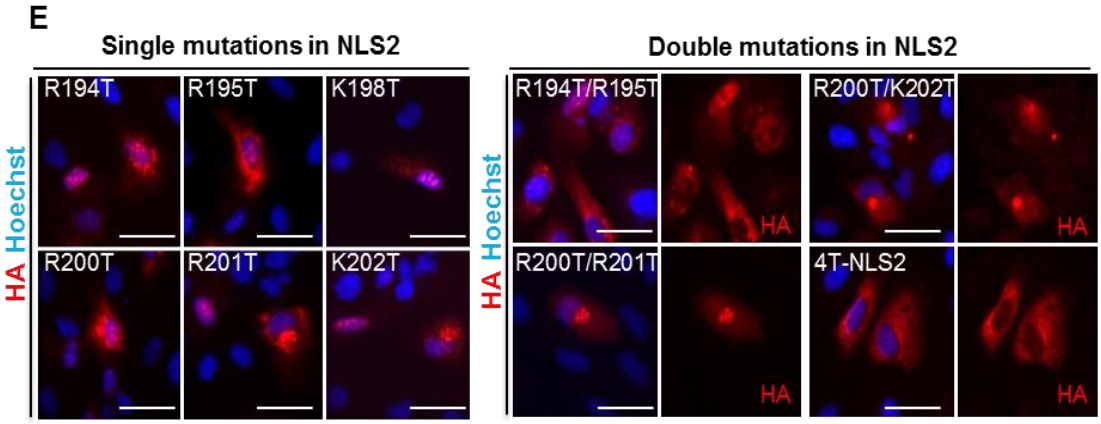

Part 4.4 Mutations within NLS1 and NLS2 trigger different nuclear exclusion mechanisms

The NLS1 and NLS2 motifs are positioned in close proximity to each other within the FGF10 tertiary structure (see Chapter 3). It was proposed that they may act in combination to generate a strong signal driving protein to the cell nucleus. However the G145E mutation alone seemed to result in a nuclear exclusion of FGF10 that is thought independent of the binding to importin.

Aims

The aim of this part of the chapter is to analyse the putative molecular mechanisms driving the nuclear exclusion of G145E and 4T-NLS2 mutants. Moreover, through analysis of the mutants investigate whether the NLS1 and NLS2 possibly cooperate or work independently of each other to generate nuclear import of FGF10.

4.4.1 Intra-cellular distribution of FGF10 and its mutants over time period

Multiple proteins are known to undergo nucleocytoplasmic shuttling, examples including ERK (Michailovici et al., 2014), galectin3 (Arnoys et al., 2015), Rac1 (Navarro-Lerida et al., 2015) and mammalian target of rapamycin (mTOR) (Rosner and Hengstschlager, 2012) as well as signal transducers and activators of transcription (STATs) (Xu and Massague, 2004). Therefore, proteins that enter the nucleus are often also transported out depending on the stage of cell cycle, function that they serve and interactions with other molecules, as protein binding could cause either nuclear or cytoplasmic sequestration. The transient transfection of FGF10 could potentially result in an initial and temporary accumulation of the protein within a cell nucleus, subsequently leading to its nuclear export at the later stages of cell cycle. Similarly, the nuclear exclusion of the G145E mutation may also be a temporary result.

To determine whether the wild type (WT) and mutant FGF10 proteins undergo nucleocytoplasmic shuttling and display differential intracellular distribution patterns over time, they were transiently transfected into a culture of epithelial ARPE cells (see Chapter 2) and analysed after 24, 48 and 72h post transfection, detecting HA epitope through fluorescent immunohistochemistry. Two single mutations within NLS2 (R194T and K198T) were also chosen as additional controls. After 24h, the mutants did not differ significantly from FGF10HA in terms of their nuclear and cytoplasmic distribution (see Chapter 4, page17-19 (above)). However, the single residue changes showed that

the nuclear exclusion is peculiar to G145E and not any other potential single mutation within the FGF10 sequence.

At each investigated time point, 24, 48 or 72h post transfection, at least 20% of the transfected cells with FGF10HA showed presence of the protein in the nucleus (Fig. 4.11), demonstrating that the nuclear import of FGF10 was not a temporary effect. Moreover, comparable proportion of transfected cells displayed protein present in the cell nucleus at 72h as 24h post transfection, suggesting that HA tagged FGF10 was not accumulating in the nucleus over time and therefore it was unlikely to undergo nuclear retention or nucleolar sequestration. The data rather suggest that FGF10HA shuttles freely in and out of the nucleus. The controls corresponding to single mutants within NLS2 showed similar intra-cellular distribution to the non-mutated FGF10, as expected (Fig. 4.11).

At the same time, at least 90% the G145E is detected only in the cytoplasm, with the remaining 10% corresponded to the “unclassified” category (obscured protein distribution), which suggests that the G145E mutant did not enter cell nucleus, even after a longer (72h) period of time and that the mutation fully abolished the nucleocytoplasmic shuttling of the protein.

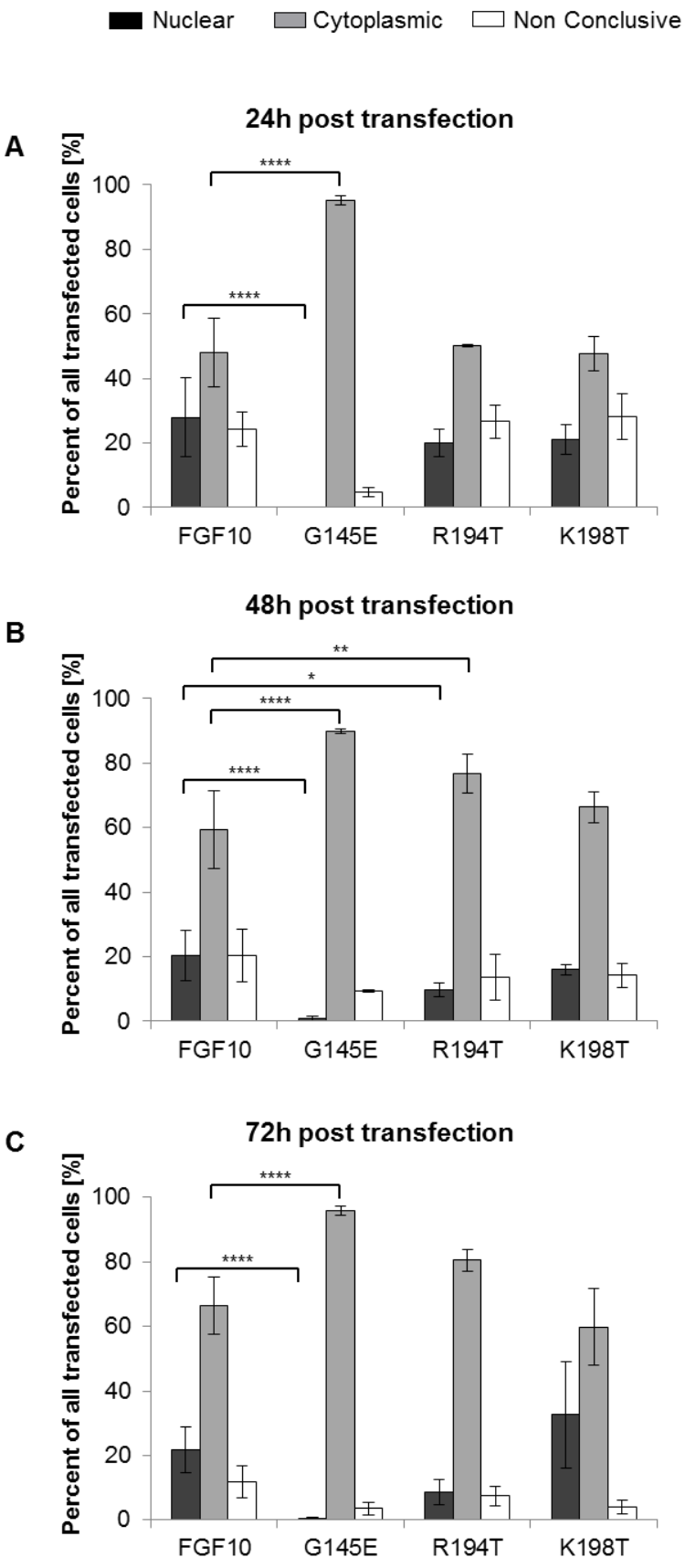

Figure 4.11 Intra-cellular distribution of FGF10HA and its mutants show little variation at (A) 24h, (B) 48h and (C) 72h post transfection (ANOVA, n=3).

4.4.2 Mutant proteins display different molecular properties than FGF10HA

To assure that the results of fluorescent immunohistochemistry are a genuine reflection of FGF10HA's intracellular distribution, FGF10HA and its mutants were further investigated by Western Blot analysis, specifically within cell's nuclear and cytoplasmic fractions. For this, HEK 293T cells were used because these cells were previously shown to express a proportion of a FGF10-HA protein in the cell nucleus (Fig. 4.4); are easily cultured and transfected with DNA, but additionally undergo subcellular fractionation more easily than ARPE cell type. Therefore, HEK 293Ts were chosen for this analysis and used interchangeably with the ARPE cells in further experiments. Thus cultures of HEK 293T cells were transfected with the FGF10HA, G145E and 4T-NLS2 mutants or mCherry positive control that was shown to be ubiquitously expressed within the cell (Fritz et al., 2008). Cells were harvested 24h post transfection, and their cytoplasmic and nuclear fractions separated using protocols described by Dimauro and colleagues (Dimauro et al., 2012). Firstly the cytoplasmic protein fraction was separated and purified through centrifugation in a sugar based buffer, subsequently followed by isolation and purification of nuclear fraction in salt based buffer (see Chapter 2). The fractions were then analysed on a SDS-polyacrylamide gel in a semi-quantitative fashion (see Chapter 2).

All HA tagged proteins and the control mCherry were found in the cytoplasm. Interestingly, the FGF10HA, G145E and 4T-NLS2 displayed different molecular weight protein isoforms within the cytoplasmic fraction (Fig. 4.12). The molecular weight of non-mature (full length) and mature (lacking signal peptide) rat FGF10HA corresponded respectively to 25kDa and 21kDa. Whilst, within the cytoplasmic fraction mature and non-mature FGF10HA protein was detected, the smaller (secreted) protein was more abundant than the non-mature FGF10. This may suggest that either, the newly generated protein was rapidly processed to maturation or, that the transient transfection generates limited transcript levels and restricts the protein production. Interestingly, high abundance of the mature protein was present within the nuclear fraction whereas the non-mature protein could not be detected in the nuclear fraction (Fig. 4.12).

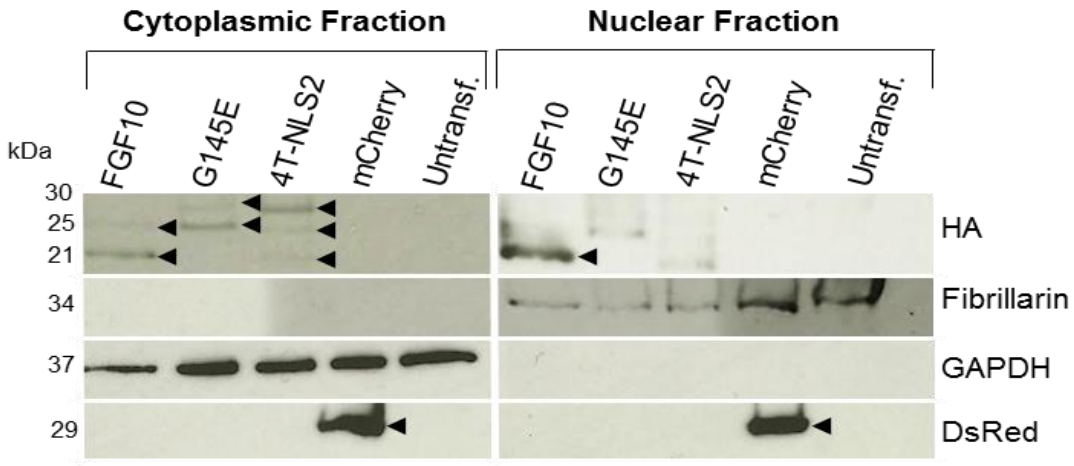

Figure 4.12 FGF10HA was found in both, cytoplasmic and nuclear fractions of the HEK 293T cells, whereas the mutant proteins G145E and 4T-NLS2 were detected only in the cytoplasmic fraction of the cell. Representative of n=3.

The cytoplasmic fraction also contained both of the mutant proteins, the G145E and 4T-NLS2. The 4T-NLS2, similarly to the non-mutated FGF10HA, was present in the non-mature and mature version of the protein (25 and 21kDa), but the mutant protein of 21kDa was not as abundant as the wild type FGF10. Interestingly, the G145E mutant could only be detected as the non-mature protein (25kDa). Surprisingly, another isoform of mutated proteins was detected within the cytoplasmic fraction, which corresponded to about 30kDa. This protein isoform was not detected within the cytoplasmic fraction of the non-mutated FGF10HA (Fig. 4.12). Importantly, in concordance with the fluorescent immunohistochemistry, the G145E and 4T-NLS2 mutants were virtually absent from the nuclear fraction (Fig. 4.12).

One possibility was that an introduction of any mutation within FGF10 would cause the appearance of the different protein isoform of about 30kDa. Further analysis of a whole cell lysate revealed that the higher molecular weight band of 30kDa was not detected in protein samples of single mutation within the NLS2 – the K198T and the R194T (Fig. 4.13). However, the cell lysate samples of mutants that impair nuclear translocation, the G145E, G145V, R200T&K202T and 4T-NLS2, all contained the additional protein isoforms of 30kDa, which will be further investigated in a section 4.3.3.

Importantly, only samples containing mutants of the G145 residue did not contain the 21kDa secreted version of the mature FGF10 (Fig. 4.13), suggesting that these proteins did not undergo maturation.

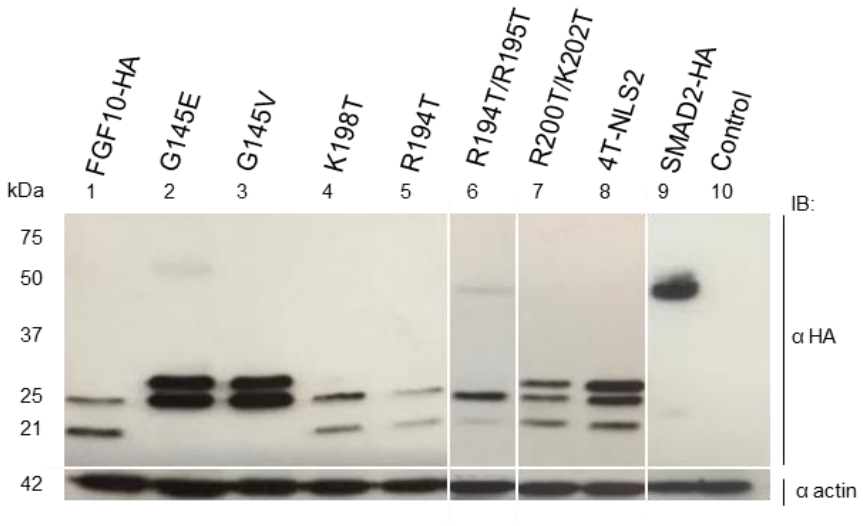

Figure 4.13 Analysis of the whole ARPE cell lysate revealed that mutants impairing the nuclear import of FGF10 (lanes 2,3,7,8) existed in 30kDa isoform of the protein that was absent in the non-mutated FGF10. Moreover, mutation of G145 residue (lanes 2,3) results in lack of the detection of the mature 21kDa protein. SMAD2-HA (kind gift of Dr A. Chantry) and lysate of non-transfected cells serve as positive and negative control respectively, controlling for antibody specificity towards HA. Representative of n=10.

4.4.3 Nuclear-excluded FGF10 mutants undergo hyper-glycosylation

Interestingly, cell lysate samples of FGF10HA mutants showing nuclear exclusion contained the additional 30kDa protein isoform, which was absent in non-mutated FGF10HA. Based on its size and the reduced conditions of SDS page, the 30kDa product was an unlikely product of intracellular FGF10 homo-dimerization (>50 kDa) or FGF10-FGFR2IIIb complex formation (>110 kDa). Therefore, likely it represented a form of a post-translational modification, putatively affecting the nucleocytoplasmic shuttling of the protein.

As a secreted protein, FGF10 undergoes glycosylation and was predicted to carry at least 26 glycosylation sites (see Chapter 3). Therefore, the possibility that 30kDa protein represents a hyper-glycosylated form of FGF10 was investigated. Cell lysates containing FGF10HA, G145E, 4T-NLS2 and a selection of single and double mutants were deglycosylated with PNGase F (‘N’ deglycosylation) or a cocktail of ‘O and N’ deglycosylating enzymes (using Protein Deglycosylation Mix) (see Chapter 2).

Interestingly, within all samples *N*-deglycosylation alone was sufficient to reduce 30kDa protein product to a single 25kDa (Fig. 4.14). Surprisingly, the 21kDa secretory product was also abolished in these assays, which could be due to low

stability of a mature version of a protein and susceptibility to degradation (Buchtova et al., 2015), not being able to withstand the enzymatic treatments. Nonetheless, the reduction of the 30kDa protein size to 25kDa suggests that the higher isoform of the protein resulted from hyper-glycosylation.

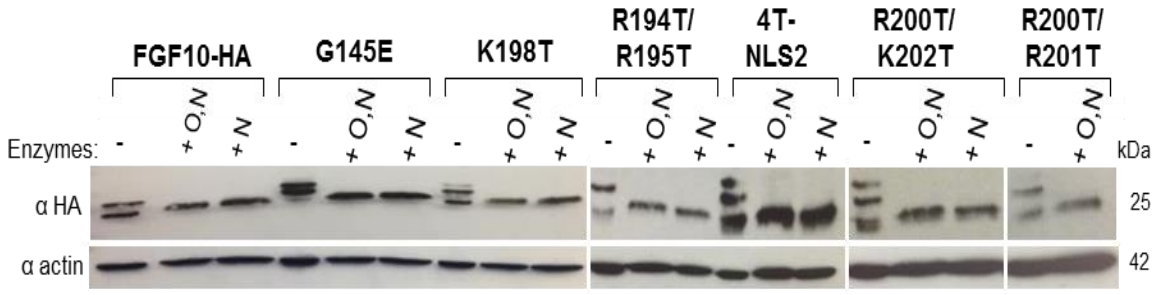

Figure 4.14 Treatment of HA tagged proteins with deglycosylation enzymes revealed that high molecular weight isoform (approximately 30kDa) of the mutant proteins was caused by *N*-linked hyper-glycosylation. ARPE whole cell lysate samples were treated with two types of De-glycosylation enzymes: commercial Protein Deglycosylation Mix (+O,N) removing all types of glycosylation and PNGase F (+N) removing *N*- linked glycosylation alone; (-) signifies sample not treated with enzymes. Representative of n=3.

4.4.4 LADD-like mutation disrupts secretion of the protein

A proportion of the mutant FGF10 produced is hyper-glycosylated with the *N*-linked type of glycosylation (Fig. 4.14). Biosynthesis of all *N*-linked oligosaccharides (glycans) is a multi-step process that begins in the rough ER, followed by entry into the Golgi complex with protein bearing one or more oligosaccharide chains. However, abnormal glycosylation patterns can obscure the folding of the protein and its progression through the secretory pathway. Therefore, in order to determine whether the secretion of the mutant proteins was potentially affected by the hyper-glycosylation status and differed from that of non-mutated FGF10HA, the wild type and mutant proteins secretion was investigated.

To compare the extent of secretion of the non-mutated FGF10HA to the mutant G145E and 4T-NLS2 culture media was collected 24 and 48h post transfection of the epithelial ARPE cells with the HA tagged constructs. Subsequently a total protein precipitation from the media was performed and the samples were analysed on a SDS-

polyacrylamide gel (see Chapter 2). Unfortunately, low transfection levels did not permit isolation of sufficient amount of secreted protein to achieve detectable levels of either WT or mutant proteins, preventing comparison of the secretory potential of WT and mutant FGF10. Moreover, addition of heparin to the media, used normally to stabilise any secreted FGF protein and allow its release into cell media from the cell surface, did not provide any detectable levels of the HA tagged protein. Similar problems with isolation of a secreted mouse FGF10 protein from cell media have been reported previously in literature (Beer et al., 1997). Therefore, to determine whether hyper-glycosylated proteins that are absent from the cell nucleus retain their secretory properties, the progression of FGF10HA, the G145E and the 4T-NLS2 along the secretory pathway was compared using markers that delineate the intermediate steps of the secretory pathway (Fig. 4.15). For this, transfected cells were co-immunolabelled with antibodies against –HA in combination with anti-ERp60 (an early secretory pathway marker within ER), anti-βCOP (a marker of transport between ER and Golgi) and anti-TGN46 (demarcating Golgi and vehicle transport stages) (Fig. 4.15A). Ten random cells was selected and co-localisation of the markers measured with specific computer software tool, basing on their fluorescent exposure (see Chapter 2). Whilst FGF10HA and 4T-NLS2 co-localised with all three markers (Fig. 4.15B,C,E,F,H,I,K), expression of G145E was restricted to the ERp60-positive compartment (Fig. 4.15B,D,G,J).

The results showed that the 4T-NLS2 mutant, although hyper-glycosylated, progressed through the secretory pathway in similar fashion to FGF10. However, the G145E mutant protein failed to progress through this pathway. Moreover high level of co-localisation with the ERp60 protein (Fig. 4.15B,D) suggests that instead, it has become largely trapped within the ER.

Figure 4.15 Tracking of proteins' progression through the secretory pathway. (A) Schematic of secretory pathway and its stage-specific markers: ERp60 (early ER stage); βCOP and TGN46 (late ER stages). (B) Quantification of fluorescence co-localisation between secretory pathway markers and HA-tagged proteins; FGF10HA and 4T-NLS2 show values above 0.5 Pearson's Correlation coefficient, indicative of co-localisation with all markers, whereas G145E co-localises only with the ERp60. (C-K) ARPE cells transfected with (C,F,I) FGF10-HA, (D,G,J) G145E and (E,H,K) 4T-NLS2 and probed with the secretion pathway markers, showing that unlike the WT and 4T-NLS2 proteins, (which were processed through the pathway), the mutant G145E was sequestered at the ER stage. Scale bars: 20 μm in all panels.

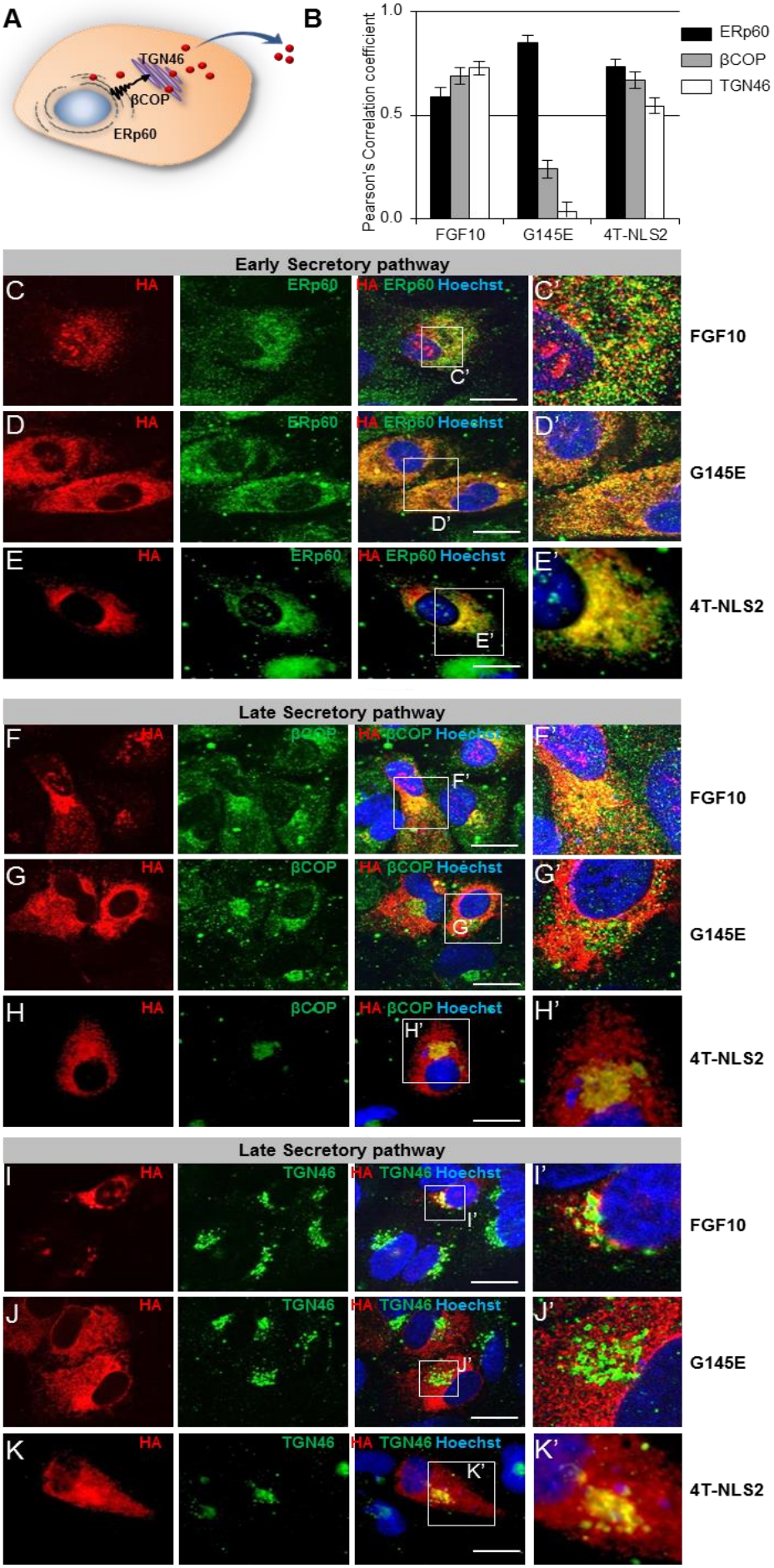
A
TGN46
βCOP
ERp60
B
Pearson's Correlation coefficient
1.0
0.5
0.0
ERp60
βCOP
TGN46
FGF10
G145E
4T-NLS2
Early Secretory pathway
C
HA
ERp60
HA ERp60 Hoechst
C'
FGF10
D
HA
ERp60
HA ERp60 Hoechst
D'
G145E
E
HA
ERp60
HA ERp60 Hoechst
E'
4T-NLS2
Late Secretory pathway
F
HA
βCOP
HA βCOP Hoechst
F'
FGF10
G
HA
βCOP
HA βCOP Hoechst
G'
G145E
H
HA
βCOP
HA βCOP Hoechst
H'
4T-NLS2
Late Secretory pathway
I
HA
TGN46
HA TGN46 Hoechst
I'
FGF10
J
HA
TGN46
HA TGN46 Hoechst
J'
G145E
K
HA
TGN46
HA TGN46 Hoechst
K'
4T-NLS2

4.4.5 Conclusion

The aim of this part of the chapter was to determine whether the nuclear exclusion caused by mutations within NLS1 and NLS2 is driven by similar molecular mechanisms. It was found that both the G145E and 4T-NLS2 mutants were detected only within the cell cytoplasm, as shown by compartmentalisation of HEK cells and immunofluorescence labelling of HA tagged proteins (Fig. 4.12). Furthermore, both mutants were shown to undergo hyper-*N*-glycosylation, although only the 4T-NLS2 mutant progressed through the classical protein secretory pathway (Fig. 4.15).

In regards to the cell fractionation, it may appear that more FGF10 protein concentrated within cell nucleus than in the cytoplasm. However, the protein concentration between cytoplasmic and nuclear fractions cannot be directly compared, despite the fact they were derived from the same pool of cells. The concentration of protein was aimed to maintain constant across cytoplasmic and nuclear fractions, as shown by the Glyceraldehyde 3-phosphate dehydrogenase (GAPDH) and Fibrillarin controls (Fig. 4.12). However, the total content of cytoplasmic proteins was different to total content of nuclear protein. HA tagged constructs would require purification (e.g. through protein immunoprecipitation) from the fractions prior to WB analysis in order to allow for reliable direct protein concentration comparison.

Importantly, hyper-*N*-glycosylation was also observed by Beer and colleagues in the mouse HA tagged FGF10. Prevention of this hyper-glycosylation was achieved through treatment of the HEK cells with glycosylation inhibitor, Tunicamycin (Beer et al., 1997). Tunicamycin is a mixture of homologous nucleoside antibiotics that block enzymes catalysing the *N*-linked glycosylation and therefore causes cell cycle arrest in G1 phase. Moreover, inhibition of glycosylation resulted in increased levels of 25kDa form of the protein (Beer et al., 1997), similarly to results presented here (Fig. 4.14). Each protein possesses its individual glycosylation pattern and correct glycosylation is crucial to protein biosynthesis and function. Whilst the *O*-linked sugars are added one at a time, the *N*-linked glycosylation begins with an addition of a large oligosaccharide, containing 14 sugar residues. Normally, certain sugar residues are subsequently removed, whilst others are added until correct arrangement is achieved for each protein. Failure of this system prevents the protein to progress further from the ER into other stages of the pathway, that most likely takes place in case of the hyper-glycosylated proteins (Nicolaou et al., 2012, Dersh et al., 2014, Tannous et al., 2015).

Further investigations could include blocking of the glycosylation *in situ* within the cell culture with the Tunicamycin in similar fashion to previous studies, which could reveal whether the mutant G145E can progress through the entire secretory pathway.

Part 4.5 Analysis of potential biological role of nuclear FGF10

Secreted FGF10 acts in a dose dependent manner by binding to FGFR2IIIb and any deviations result in developmental malformations, as demonstrated during teeth formation, where insufficient FGF10 signalling during molar development resulted in undeveloped tooth crown, whilst overexpression causes expansion of the crown epithelium of the tooth (Yokohama-Tamaki et al., 2006) (see Chapter 1). Therefore, a nuclear retention and immobilisation of the FGF10 protein could provide another level of post translational control of the amount of protein undergoing secretion. On the contrary, FGF10HA did not appear to over-accumulate within the nucleus over period of 72h, meaning that nuclear protein observed did not appear more abundant than 24h post transfection. This suggests FGF10 is more likely to undergo nucleocytoplasmic shuttling, rather than nuclear sequestration (Fig. 4.11). Nuclear entry of the protein at specific stage of the cell cycle could suggest protein's role in a control of cell proliferation and/or cell growth. In order to assess the stage of cell cycle when FGF10 enters the cell nucleus, transiently transfected with FGF10HA culture of ARPE cells was paused at G1 and G2 growth phases, through chemical treatment and by serum starvation (see Chapter 2).

To inhibit the cell cycle, the growth of ARPE cells was constrained by serum removal from the cell culture. Serum starvation causes cell growth restriction at G0/G1 phase, induces quiescence and prevents cell proliferation. Interestingly, FGF10 was found to translocate into cell nucleus even in quiescent ARPE cells, concluding from which that the nuclear import of FGF10 was independent of cell division (Fig. 4.16A).
During the cell division (mitosis), the nuclear envelope breaks down removing a physical barrier between the nuclear and cytoplasmic proteins. Since the FGF10HA was transiently transfected into already quiescent culture of cells, the results demonstrate that the breakdown of nuclear envelope is not necessary for the protein's nuclear translocation. Furthermore, mitosis is preceded by G2 phase of rapid cell growth and protein synthesis. Importantly, nuclear import of proteins (e.g. complex of cyclin B1/CDK1 (Porter and Donoghue, 2003) at this stage of cell cycle is strictly regulated for two reasons: firstly G2 serves as a DNA damage checkpoint, and secondly it exhibits control of the mitotic entry (Fig. 4.16B). Transiently transfected FGF10HA was detected in a nucleus of ARPEs treated with the nocodazole drug. Nocodazole is a known inhibitor of G2/M phase transition as it interferes with the polymerization of microtubules, and prevents formation of metaphase spindles. The results therefore demonstrate that FGF10 translocated into the nucleus before and after the proliferative stage of DNA replication and synthesis (S phase).

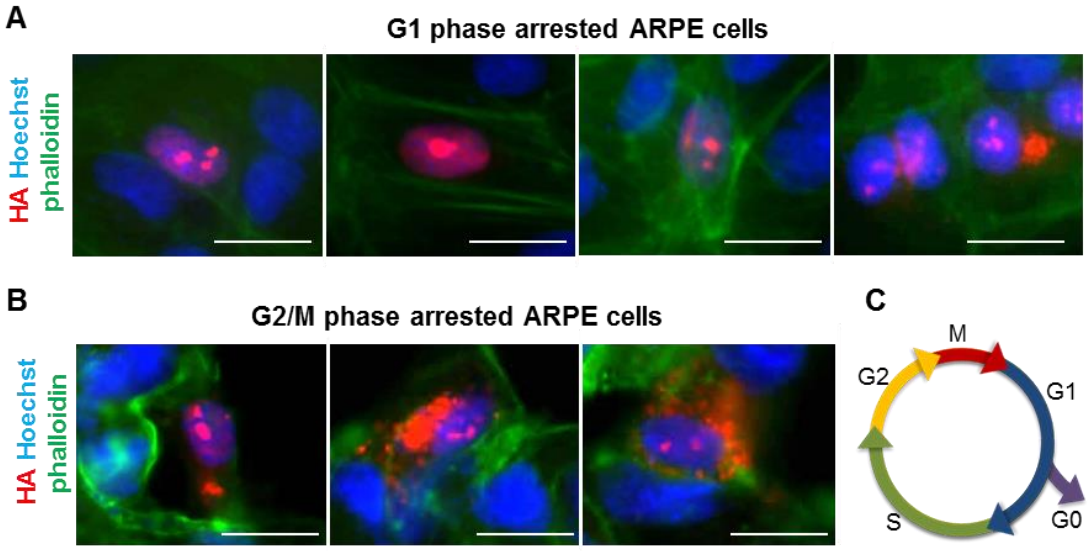

Figure 4.16 Cell cycle stage specific nuclear import of FGF10. (A) FGF10HA was transported into the cell nucleus in a quiescent (serum starved) culture of ARPE cells. (B) FGF10HA was found in the cell nucleus in ARPE culture arrested at G2/M phase through treatment with nocodazole drug. (C) Schematic diagram of the cell cycle, showing that nuclear FGF10 is found at growth phase 1 (G1), growth phase 2 (G2), that follows synthesis (S) phase and precedes mitosis (M). Scale bar 20µm.

During the S phase proteins involved in DNA replication, as well as detecting DNA damage and repair, such as ataxia telangiectasia and Rad3-related protein (ATR) (Marechal and Zou, 2013) are transported into the nucleus. The serum starvation data shows that FGF10 was present in a nucleus at a G1 phase just preceding DNA replication (Fig. 4.16A), and therefore it is essential to determine whether it affects cell proliferation itself. To test whether FGF10 is present in a nucleus of replicating cells, sister cultures of mesenchymal ATDC5 cells were transfected with the HA-tagged constructs encoding FGF10, as well as G145E or 4T-NLS2-bearing mutations, which were shown not to enter the cell nucleus, or mCherry as control. The ATDC5 cultures were chosen to analyse the cell proliferation effect, because *in vivo* FGF10 usually is generated within the mesenchyme, therefore may be likely to translocate endogenously into the nucleus within mesenchymal cells. The transfected cultures were pulsed for 4 hours with BrdU, which typically becomes incorporated into the cell nucleus during the S phase of a cell cycle. Co-expression of BrdU with HA or mCherry indicated actively proliferating cells (Fig. 4.17A). Interestingly, in comparison to mCherry-transfected cells, all FGF10-bearing constructs showed a significant reduction in cell proliferation

(ANOVA, post-hoc Tukey p=0.004, n=5). Only a small proportion of cells expressing FGF10 (~10%) showed incorporation of BrdU marker (Fig. 4.17B). Intriguingly, none of those cells that incorporated BrdU also showed nuclear presence of HA (Fig. 4.17A). Therefore FGF10HA was either not translocated into the nucleus in actively proliferating cells, or FGF10 functioned in the cell nucleus to abrogate cell replication.

Interestingly, in comparison to the mCherry control, the G145E and 4T-NLS2 transfections also resulted in the reduction of the cell proliferation (ANOVA, post-hoc Tukey p=0.015 and 0.026 respectively, n=5), in similar fashion to the non-mutated FGF10HA (ANOVA, post-hoc Tukey p>0.05, n=5) (Fig. 4.17B). Importantly these proliferating cells co-expressing HA and BrdU markers, did incorporate the HA-tagged protein into cell nucleus. There is a possibility that this reduction of cell proliferation observed in the mutation-bearing constructs could be a process independent of the one observed in FGF10HA. To determine whether intrinsic factors can interfere with conclusive results of this study, the culture of ATDC5 cells was assessed for expression (in a semi-quantitative manner) of FGF7-subfamily ligands and all FGF Receptors' isoforms (see Chapter 5). The RT-PCR profiling for ligands and receptors revealed that ATDC5 cells express transcripts for FGF10 itself and at lower levels its receptor, the FGFR2IIIb (Fig. 5.3). Consequently, it is possible that endogenously generated FGF10 was able to compensate for the effects of the mutant constructs, perhaps through cell autonomous mechanisms. However, this study would require further investigation to fully determine the mechanisms driving the observed reduction of cell proliferation.

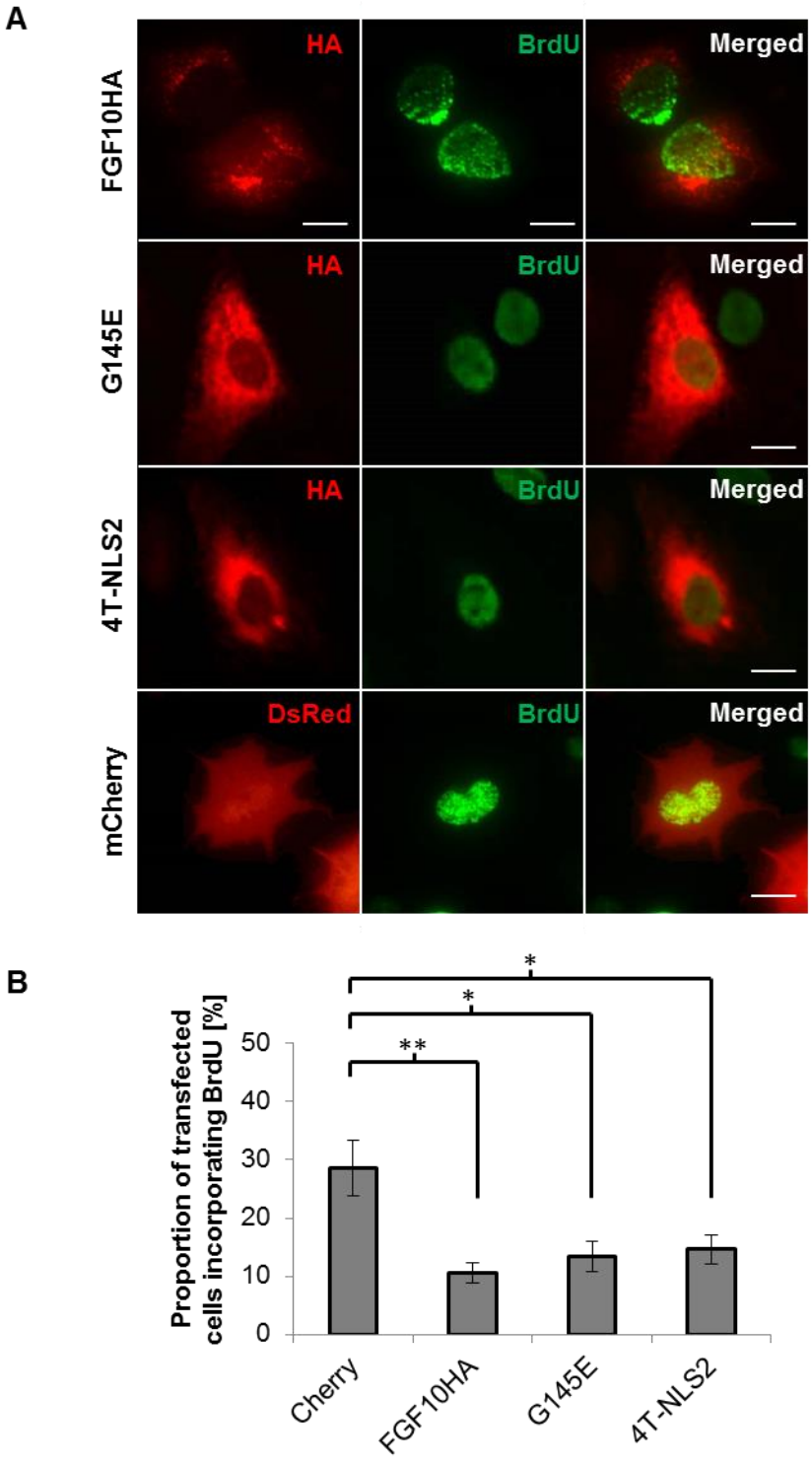

Figure 4.17 Transient expression of FGF10HA and its mutants affects the proliferation potential of ATDC5 cells. (A) Representative immunofluorescent images of co-localisation of BrdU marker of cell proliferation and HA staining; note lack of nuclear FGF10HA expression; scale bar 20µm. (B) Quantification of proliferating cells expressing the HA-tagged constructs or mCherry protein (ANOVA, $F=6.77$, $p<0.01$, $n=5$).

Part 4.6 Discussion

FGF10 is a secreted protein that upon release from the mesenchymal cells binds to receptor FGFR2IIIb on adjacent epithelium, stimulating downstream molecular pathways to drive cell proliferation and differentiation. However, transiently transfected FGF10, fused to a small HA tag, was detected in the nucleus of multiple cell types even 72h post transfection. Furthermore, the nuclear import of FGF10 depended on the G145 residue (within NLS1) and NLS2 sequence, which is presumed to interact with Importin chaperones. Nuclear FGF10 localised to the nucleolus where it may be involved in regulation of the cell proliferation. Moreover, nuclear exclusion of FGF10 through mutation within NLS1 (G145E) and NLS2 (4T-NLS2) appeared to occur independently, through two different mechanisms.

Analysis of the tertiary structure of the FGF10 revealed close positioning of NLS1 and NLS2 as well as a capacity for direct interaction through an H-bond (see Chapter 3). Therefore, it was investigated whether the two weak motifs provide one stronger signal driving FGF10 into the cell nucleus. The results showed that a single mutation in NLS1, G145E, which causes LADD syndrome in humans (G138E), prevented the nuclear import of FGF10 in similar manner to a combination of 4 mutations within NLS2 (4T-NLS2). The ablation of the nuclear import of FGF10 molecule could be an underlying cause for the symptoms of the LADD syndrome caused by the human G138E mutation, which has not been described before.

Further investigation revealed however that the G145E was also unlikely to be secreted out of the cells thereby indirectly impairing FGF-receptor signalling pathway. Several lines of evidence suggested that the G145E most likely encountered folding problems and therefore did not undergo further normal processing. The mutant accumulated at high levels at the ER, where it was associated with the ERp60 protein (Fig. 4.15). The ERp60 is known to play a role in folding of the newly synthesised protein and shows association with other molecular chaperones specific for the *N*-glycosylation of proteins (Koivunen et al., 1996). Since the mutant showed hyper-*N*-glycosylation (Fig. 4.14), it is therefore possible that the G145E was misfolded causing its greater association with the ERp60 and the glycosylation chaperones. This interaction potentially prevented the protein's further functional roles. The HA-tagged construct was detected within the cell cytoplasm even after 72h, suggesting that regardless of misfolding, the protein did not undergo degradation, although further studies are required to confirm this hypothesis. Misfolded proteins are likely to become substrates of the ER-associated protein degradation (ERAD), a multi-step 'quality control' mechanism involving an assortment of enzymes acting to prevent accumulation of misfolded proteins in the lumen and membrane of the ER (Ruggiano et al., 2014).

Therefore, to fully determine whether G145E mutation caused ER stress or was degraded, the mutant could be, for example, analysed in the context of ERAD pathway.

Moreover, the substitution of the Glycine (G) to other small residues, like Valine or even Alanine (the second smallest amino acid) also resulted in nuclear exclusion of the protein (Fig. 4.9). Biochemical studies have shown that Glycine at key positions within a protein molecule allows high flexibility of torsion angles in the polypeptide chain that otherwise are prevented by other residues (Zhao et al., 2012, Chen et al., 2011). Therefore, disruption of this particular residue can lead into protein misfolding and structural issues, rather than interfering with binding to Importins. Moreover the G145 residue is located on a protein structure within one of the loops (Fig. 4.9). Loops often serve functional roles, also in protein folding, and mutations can negatively affect the protein's structure. In conclusion, the mutation of the G145E residue, may lead to protein structural defects, causing its ER retention and consequently loss of FGF10-function.

On the other hand, the 4T-NLS2 mutant showed nuclear exclusion by potentially impairing the site of binding to Importin chaperone. The introduced mutations could cause a pool of generated protein molecules to encounter folding defects, and therefore, similarly to G145E undergo hyper-*N*-glycosylation at the ER. Nonetheless, the protein was able to follow the normal secretory pathway, similarly to the non-mutated FGF10HA (Fig. 4.15), showing therefore that a proportion of the protein folded and functioned normally. Moreover, even a minor perturbation of the NLS2 motif, such as mutation of couple of basic residues, limited the nuclear import of FGF10 molecule (Fig. 4.10). Major disruptions to the NLS2 resulted in nuclear exclusion of the protein altogether implying that this sequence was absolutely crucial for the nuclear import of the FGF10. To conclusively determine whether NLS2 alone is sufficient to target a protein to the nucleus, it would be possible to integrate the motif into a fluorescent protein of similar size to FGF10, and measure accumulation of the resulting complex in the cell nucleus.

Proteins found within cell nucleus serve several functions, for example multiple nuclear proteins are required to regulate transcription machinery, and transcription factors binding to DNA further modulate gene expression. Moreover some proteins are involved in DNA packaging into chromosomes and others determine DNA protection against mutation and degradation. In addition, a range of proteins play differential roles within the cell nucleolus, an organelle known as a site for assembly of ribosomal subunits. Transiently transfected nuclear FGF10 localised within the nucleolus (Fig. 4.2) where it could possibly interact with ribosomes. However, recent studies show that many non-ribosomal proteins accumulate in the nucleolus, for yet undetermined reasons (Lin et al., 2008, Catez et al., 2002). Moreover, there is evidence that the

nucleolus also plays a role in sequestering regulatory molecules, in response to specific environmental cues. Capturing and immobilization of proteins, also known as nuclear detention is believed to be a part of post translational regulatory mechanisms, to prevent proteins at certain conditions to interact with their binding partners. Examples of those include DNMT1, Hsp70, POLD1, and VHL, which bind to the nucleolar detention sequence (NoDS), characterised by arginine-rich repeats (Audas et al., 2012). It is therefore possible that nucleolar accumulation of FGF10 allows for nuclear detention and regulation of the amount of protein available for the secretory pathway and hence receptor stimulation. Since FGF10's receptor stimulation generates downstream signals in a FGF10-dose dependent manner (see Chapter1), the process of nucleolar detention could provide further regulation of the FGF10-FGFR2IIIb signalling.

However, analysis of protein intracellular distribution over period of a 72h showed that accumulation of FGF10 in the nucleus did not change significantly over a period of time (Fig. 4.11), suggesting that FGF10 most likely did not undergo nucleolar sequestration. Presumably FGF10 shuttles in and out of the nucleus, which requires future experimental investigation, for example through 'molecular tracking' - by observing and measuring the distribution of fluorescently tagged FGF10 in live cultures over a set period of time. Bioinformatics analysis did not show any classical nuclear export signals (NES) within FGF10 sequence and therefore, if FGF10 is transported out of the nucleus, it would most likely take place in a non-conventional manner (see Chapter 3). Although FGF10 having molecular weight of 21-25kDa is a small enough molecule to freely diffuse in and out of the nuclear pores, experiments performed in literature show that practically all proteins are actively chaperoned into the nucleus (Christie et al., 2015) (see Chapter 1).

Some proteins within nucleolus are responsible for modifying small RNAs, assembling ribonucleoprotein and contributing indirectly to regulating aging processes (Oh et al., 2007, Olson et al., 2000, Pederson, 2011). Interestingly, FGF2 and FGF3 have also been found within the nucleolus. Nucleolar FGF2 directly regulates synthesis of ribosomal RNA and stimulates Polymerase I transcription through binding to UBF transcription factor (Sheng, 2004, Sheng et al., 2005). Nucleolar FGF3 has been postulated to play a role in control of cell cycle and inhibition of cell proliferation through binding to NoBP protein (Reimers et al., 2001). Future studies will show if nucleolar FGF10 is able to interact with other nuclear proteins in a similar fashion to FGF2 and FGF3.

Secretory FGF10 is known to be involved in proliferation of pancreatic epithelial cells (Hart et al., 2003), epithelium of glandular stomach (Shin et al., 2006), and white adipose tissue (Konishi et al., 2006). In the absence of FGF10 signalling, pancreatic

and heptoblasts progenitor cells fail to proliferate (Norgaard et al., 2003, Berg et al., 2007). However, the nuclear form of FGF10 within ARPE and ATDC5 cells (Fig. 4.16 and 4.17) as well as in urothelial cells (Kosman et al., 2007) was associated with cells in a quiescent phase, and nuclear FGF10 may potentially be involved in negatively regulating cell proliferation. The putative nucleolar retention of FGF10 may possibly prevent the protein from entering its secretory pathway and therefore limiting indirectly the FGF10's proliferative effect, in either a paracrine or autocrine manner achieved through receptor stimulation. This suggests that nuclear FGF10, either through endogenous or restriction of exogenous pathway, counteracts the function of the secreted protein. Both FGF2 and FGF3 proteins are also known to display similar properties.

Nuclear FGF3 inhibits DNA synthesis and reduces cell growth (Kiefer and Dickson, 1995a) acting in an opposite way to its receptor-signalling role, where it functions as an oncogene (Muller et al., 1990). *In vitro* FGF3 and FGF10 have been shown to be mutually redundant, and can compensate for the lack of the other protein during induction and formation of the otic placode and inner ear (Wright and Mansour, 2003, Alvarez et al., 2003). Therefore, it is likely that FGF10 exhibits similar functional properties to the FGF3 molecule.

FGF2 exists as different isoforms with varying protein size, i.e. four high molecular weight (HMW) FGF2s have been described, which mostly confine to the cell nucleus (Quarto et al., 1991) and one low molecular weight (LMW) which is released from the cell and acts through the receptor signalling pathway. Furthermore, the LMW FGF2 has also been found within the cell nucleus, often in a complex with its cognate receptor (Clarke et al., 2001, Bossard et al., 2003). Although both HMW and LMW FGF2 are found in a cell nucleus, they localise to different loci which is reflected in the function they serve. LMW FGF2 was found to localise in nucleoli and Cajal bodies whereas HMW FGF2 shows a punctate pattern in the nucleoplasm and periphery of nucleoli (Claus et al., 2003, Dini et al., 2002). Both LMW and HMW can stimulate cell proliferation, but only LMW FGF2 increases cell migration and promotes tumour invasion, where HMW has an inhibitory effect (Dini et al., 2002). Moreover the HMW, but not LMW, FGF2 variant is necessary for promoting estradiol dependent endothelial cell migration and proliferation linked to angiogenesis (Garmy-Susini et al., 2004) meaning that the effect of the protein is tissue specific. Interestingly, FGF10 was noted to exist in a LMW isoform as it possesses a second translational site at Met position 42 (of the rat sequence) generating a protein of 19.2kDa (Lu, 1999) (Hajihosseini's unpublished data), but the potential function of this isoform has not been described yet. This LMW isoform was not detected in this study, although it is possible that translation

from additional Met sites occurs in a spatio-temporal manner, controlled by specific activators and therefore require future studies.

Regardless of its molecular weight, it is possible that a typically known as a paracrine molecule FGF10 serves an intra-cellular role, stimulating different pathways to the ones achieved via a recipient cell, through receptor activation. This intracellular function of FGF10 is most likely controlled in a cell and tissue specific manner. Therefore role of FGF10 in organogenesis and within adult tissue might require re-evaluation in all of the currently known systems.

Chapter 5

Putative functions of intracellular FGF10 during differentiation of mesenchymal progenitor cells (ATDC5s)

Part 5.1 FGF10 signalling is implicated during chondrogenesis and cartilage formation

FGF10 is typically produced and secreted by mesenchymal cells, acting on FGFR2-IIIb receptor present on adjacent epithelium to drive cell proliferation and differentiation. During development mesenchyme is derived from the mesoderm and is defined as embryonic connective tissue, however mesenchymal stem cells (MSCs) can also be found in the adult organism (Ullah et al., 2015). MSCs were first identified and isolated from bone marrow (Friedenstein et al., 1970). They are multipotent stromal cells that lack polarity and are able to differentiate, *in vivo* and *in vitro*, into osteoblasts (bone cells), myocytes (muscle cells), adipocytes (fat cells) and chondrocytes (cartilage cells), overall forming a connective tissue (Huang et al., 2015). Chondrocytes form cartilage tissue in the process of chondrogenesis, which is regulated by a series of cytokine and transcription factor interactions, including TGFβ, FGFs, and insulin-like growth factor1 (IGF1) (Lin et al., 2006). The process of chondrogenesis *in vitro* is induced in the presence of dexamethasone, β-glycerol phosphate as well as ascorbic acid, and differentiated cells express alkaline phosphatase. At the moment, there are several different models utilised *in vitro*, studying the processes of chondrogenesis, with the most prominent involving a so called 'micromass culture' derived from embryonic limb mesenchymal cells. During embryonic development, MSCs losing their pluripotency typically proliferate rapidly, crowding together and forming dense aggregates of chondrogenic cells, which often display properties of cartilage. The 'micromass culture' involves differentiation of MSCs into such cartilage aggregates, termed 'nodules', thus mimicking the processes taking place *in vivo* (DeLise et al., 2000). Moreover, chondrocytes show osteogenic properties through accumulation of calcium during differentiation, which eventually forms a mineralized extracellular matrix (ECM). Subsequently, *in vivo*, the differentiated cells begin secreting type II collagen, aggrecan, and anionic proteoglycans, found for example in articular cartilage, which covers the ends of the bones (Williams and Hare, 2011).

The process of chondrogenesis is an indispensable part of skeleton patterning in vertebrates. During limb formation, following condensation of mesenchymal cells, the proliferating chondrocytes form cellular columns. These are oriented along the longitudinal axis of the developing bone, midway along which these mitotically active cells differentiate into non-proliferative prehypertrophic chondrocytes. Chondrocyte hypertrophy is a tightly regulated process with key players being Sox9, Runt-related transcription factor2 (Runx2) and Runx3, Indian Hedgehog (IHH), BMP, Wnt and FGFs, that leads eventually to bone elongation. Hypertrophic chondrocytes can also begin to

mineralize their extracellular matrix and have the capacity to differentiate into osteoblasts (reviewed by (Ornitz and Marie, 2015)).

Fibroblast growth factors (including FGF10), together with other signalling factors (e.g. Wnts) (Danopoulos et al., 2013), are known to play a role in bone and cartilage formation, an example of which includes maintenance of the limb bud outgrowth. FGF10 generates a primary signal to coelomic epithelium that causes induction of an epithelial-to-mesenchymal cell transition, forming eventually a mesenchymal bulge. Further FGF10 signals emerging from the mesenchyme induce the formation of ectopic ectodermal ridge (AER), which subsequently secretes primarily FGF8 and then also FGF4, FGF9 and FGF17 (Sun et al., 2000). These FGFs generate reciprocal signals back to the mesenchymal cells, further maintaining the expression of Fgf10 resulting finally in proper growth and patterning of the limb bud along three axes – dorsoventral, proximodistal and anterio-posterior (Sekine et al., 1999). These FGF reciprocal signals ensure the viability of chondrogenic precursors that eventually form the cartilage templates of the limb (ten Berge et al., 2008).

Although the main known players of cartilage formation within the FGF family are FGF2, FGF8, FGF9 and FGF18 (Ellman et al., 2013, Ornitz and Marie, 2015), FGF10 was also shown to be involved during chondrogenesis. For example, FGF10 is responsible for the formation of a uniform cartilaginous sleeve during the development of a trachea. In humans suffering from the Apert Syndrome, FGF10's cognate receptor FGFR2IIIb, is ectopically expressed in the mesenchyme and this leads to increased proliferation of mesenchymal cells stimulated by atypical autocrine FGF10 signalling and results in tracheal stenosis, i.e. formation of a uniform tracheal cartilaginous sleeve (Tiozzo et al., 2009). On the other hand, overexpression of Fgf10 results in totally disorganized cartilage rings because of reduced cartilage formation. Furthermore, inactivation of FGF10 production results in shortened trachea with severe defects in patterning of the cartilage rings. FGF10 therefore is not required for the induction of cartilage differentiation, but it is involved in the proper patterning of trachea during mesenchymal differentiation (Sala et al., 2011).

FGF10 is also indirectly implicated in cartilage differentiation during lacrimal gland development. During chondrogenesis, the expression of collagens II and IX contributes to the formation and elongation of the lacrimal bud, and is controlled by Sox9 transcription factor. FGF10 regulates Sox9 function in the lacrimal buds, which leads to generation of a feed-forward signalling loop, where genes activated by Sox9 act to maintain FGF10 signalling (Chen et al., 2014, Makarenkova et al., 2000). A similar Sox9-FGF10 signalling loop maintains the mesenchymal tissue, regulating pancreatic progenitor cells (Seymour et al., 2012).

Terao and colleagues show that the role of FGF10 signalling extends beyond the epithelial stimulation and FGF10 regulates the size and shape of Meckel's cartilage during mandibular morphogenesis (Terao et al., 2011). Endogenous overexpression of Fgf10 induces the elongation of Meckel's cartilage by influencing chondrocyte differentiation, but not increased cell proliferation. Moreover overexpression of Fgf10 in mandibular mesenchyme leads to expression of chondrogenic marker genes.

FGF10 is also involved in craniosynostosis and other pathologies associated with bone and cartilage formation that have been generated through abnormal or elevated levels of the FGFR2. Knocking down levels of FGF10 in mice harbouring an Apert syndrome-type gain-of-FGFR2 mutation, can restore normal skeletal development (Hajihosseini et al., 2009).

Collectively, these studies show that paracrine FGF10 signalling is an integral part of mesenchymal cells maintenance, differentiation and patterning, particularly that of its cartilaginous derivatives (Sala et al., 2011).

5.1.1 Aims

Paracrine FGF10 signalling affects mesenchymal differentiation and chondrogenesis. However, FGF10 can also translocate into the nucleus of mesenchymal cells (Chapter 4, Fig. 4.4). The aim of this study was therefore to investigate whether nuclear FGF10 affects the proliferation or differentiation of cultured chondrocyte progenitors.

Part 5.2 Mesenchymal ATDC5 cells as a model to study chondrogenesis

ATDC5 cells were first described by Atsumi and colleagues in 1990, who isolated mouse teratocarcinoma fibroblastic cells and noticed their chondrogenic potential, by comparing it to other established cell lines, including C3H10T1/2 and RJC3.1 (Atsumi et al., 1990). Successive studies have shown that ATDC5 cells undergo a process of cellular condensation leading to sequential progressions analogous to chondrogenic differentiation. Culture of differentiated ATDC5s forms nodules with chondrocytic characteristics, i.e. elevated type X collagen expression, secretion of type II collagen, aggrecan and other extracellular matrix (ECM) molecules and matrix mineralization (Shukunami et al., 1996, Shukunami et al., 1997, Shukunami et al., 1998). Other advantages of using the ATDC5 culture system to study chondrogenesis, is that cells proliferate easily and can be maintained in their undifferentiated state. Therefore ATDC5 cells are widely used to investigate the intermediate steps of the mesenchymal differentiation as well as endochondral bone formation (Yao and Wang, 2013).

At a sub-confluent stage, undifferentiated ATDC5 cells were described as culture of cells with elongated and fibroblast-like morphology, able to proliferate until cells formed a confluent monolayer (Shukunami et al., 1996). Differentiation of ATDC5s is a multistep process, similar to those taking place *in vivo*, and initiated *in vitro* by supplementation of cultures with insulin and ascorbic acid (Temu et al., 2010).

In this work, the morphology and stage of confluency of ATDC5 culture was monitored daily under phase-contrast light microscope. Undifferentiated cells were seeded on glass coverslips in 24-well plate, cultured for 2 days to reach full confluency (Fig. 5.1A) and then induced to differentiate, alongside non-induced control sister cultures. During the early differentiation stages, which takes about 7 days (Fig. 5.1A), cells of a spindle-like morphology condensed and became polarised. Later, the cells grouped together into circular assemblies, discarded their monolayer behaviour, and slowly formed 3D structures. Once the nodules had started to form, the cells displayed a round morphology and began to express chondrogenic markers, such as glycosaminoglycans and deposition of calcific compounds similarly to that observed by other researchers (Shukunami et al., 1996, Atsumi et al., 1990). After 14 days of culture, treatment of ATDC5s cells with Alcian Blue (indicating cartilage formation) or Alizarin Red (a marker for matrix synthesis) revealed blue or red stained nodules, characteristic markers of chondrogenic and bone differentiation, respectively (Fig. 5.1B).

After initial experiments determining the timescale of normal differentiation, culture of ATDC5 cells was used to determine the role of FGF10 within mesenchymal cells.

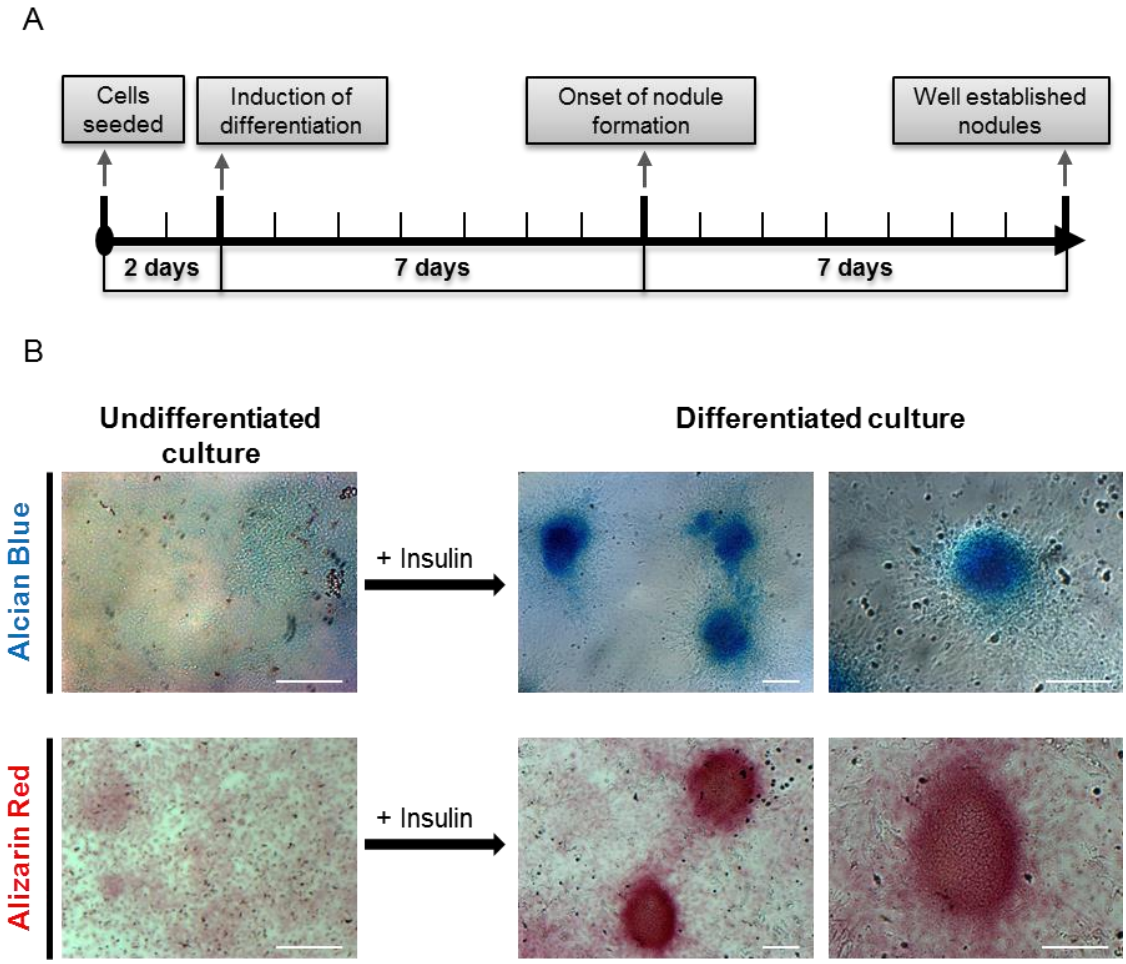

Figure 5.1 Differentiation of ATDC5s into chondrocytic nodules is a multistep process. (A) Schematic representation of a time scale of ATDC5 cells' differentiation shows that after 7 days of induction cells begin to form nodules, that are fully differentiated and shaped after 14 days. (B) After 14 days, the well-established nodules show cartilage formation (stained with Alcian Blue) and calcific deposition (stained with Alizarin Red), characteristic of mesenchymal differentiation; scale bar 200µm.

Part 5.3 Exogenous FGF10 treatment enhances differentiation of ATDC5 cells

FGF10 was shown to stimulate the mesenchymal differentiation through activation of its cognate receptor, during mandibular morphogenesis (Terao et al., 2011). However, at the moment little is known about the effect of FGF10 signalling specifically within the ATDC5 chondrogenic progenitors. To determine whether FGF10 applied exogenously can affect the proliferation or differentiation of the cell culture, ATDC5s were seeded in 24-well plate and either stimulated to differentiate or were maintained in their undifferentiated state. Confluent cultures were treated with recombinant human FGF10 at 1ng, 10ng or 100ng/ml and compared to untreated controls (Fig. 5.2A).

A series of images taken on a days 3, 5 and 7 of FGF10-treated cultures (Fig. 5.2A) allowed a monitoring of the effects of FGF10 on cell growth and differentiation. In the absence of insulin and ascorbic acid, exogenous FGF10 treatment alone could not elicit ATDC5 differentiation, whether used at low or high concentrations. Over time the differentiating cells became denser and changed shape from elongated to more compact, with a smaller cell body. However, the same changes were observed in the non-treated control as in the samples stimulated with FGF10. Moreover, when the cells formed a uniform monolayer of densely packed cells, they responded to contact inhibition and stopped proliferating, i.e. there was no observable difference between cultures at day 5 and day 7 of the FGF10 treatment, as well as the non-treated control. These results suggested that externally applied FGF10 did not trigger differentiation in a culture of undifferentiated ATDC5 cells; but neither did it inhibit cell proliferation to delay confluency (Fig. 5.2B).

On the contrary, FGF10 accentuated the differentiation of ATDC5s once they were induced with insulin and ascorbic acid. On the third day of differentiation the cells within all FGF10 treatment assays and including non-treated control, displayed a compact and polarised morphology. After 5 days, a great amount of cell death was evident and observed as floating cell debris, typical for this stage of differentiation as established by earlier pilot experiments. At day 7 of differentiation, the non-treated controls began to display small structures of densely packed cells which started to overlay each other forming 3D nodule-like structures. Treatment of the cultures with 1ng/ml of FGF10 showed comparable levels of differentiation to the control, as judged by the size and number of nodule-like progenitors formed within both cultures. Importantly, cultures treated with 10ng/ml of FGF10 had already displayed several, fully formed nodules, characteristic of fully differentiated cells (Fig. 5.2B). Subsequently, these nodules grew very rapidly over the period of next two days and resulted in massively overgrown culture (data not shown). Treatment of cultures with 100ng/ml of

FGF10 led to increased cell death and failure of cells to differentiate even if maintained for 21 days (Fig. 5.2B and data not shown).

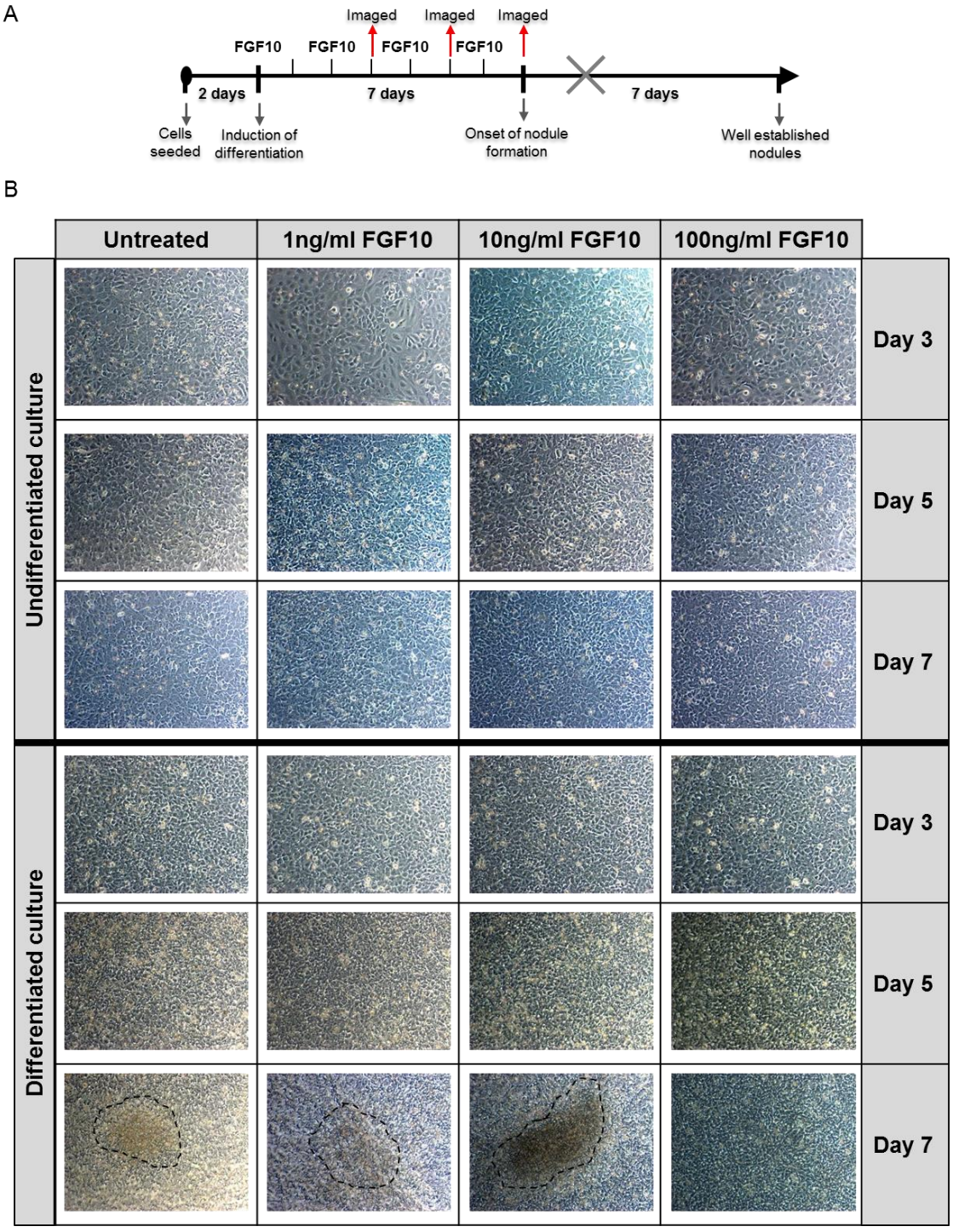

Figure 5.2 Exogenous FGF10 promotes differentiation of ATDC5. (A) Schematic representation of the experimental time scale, where FGF10 was applied on days: 0, 2 and 4 of differentiation, and the cultures were imaged on days: 3. 5 and 7; culture was fixed before completing full 14 days of differentiation. (B) A series of representative images showing that the treatment of FGF10 did not affect undifferentiated cells however, at a concentration of 10ng/ml enhanced the potential of already differentiating culture.

Mesenchymal cells typically express Fgf10 and further studies of the ATDC5 culture revealed endogenous expression of Fgf10 in undifferentiated state of the culture, which is maintained during cell differentiation (Fig. 5.3). Semi-quantitative RT-PCR profiling for the ligands that belong to the same subfamily as FGF10 showed that Fgf7 is also expressed by the culture of undifferentiated and differentiated ATDC5s, although not as prominently as Fgf10 (Fig. 5.3). As expected the receptor FGFR2IIIc was detected, and at a lesser lever the IIIb isoform as well. This intriguing expression of both receptor isoforms can be an effect of culture heterogeneity. Alternatively, as a transformed cell line, the strict splicing of receptor IIIc and IIIb isoforms may have become disrupted but nonetheless, provides a model to test exogenous effects of FGF10. Interestingly MSCs have been found to exist as heterogeneous population of cells *in vivo* and *in vitro*. They often express diverse surface markers, and even vary in morphology and differentiation capabilities (Williams and Hare, 2011). Therefore ATDC5s, as one of the types of MSCs, may also exist as a heterogeneous cell population. Heterogeneous culture could mean that cells potentially vary in their differentiation properties and Fgf10 might not be expressed uniformly across all cells in the culture. Use of a uniform culture would be important through implementing clonal selection in order to re-establish pure ATDC5 cells, which is beyond the scope of this project. Nonetheless, the ATDC5 culture remains a valuable system showing effects of external application of FGF10 on differentiation of chondrocytes.

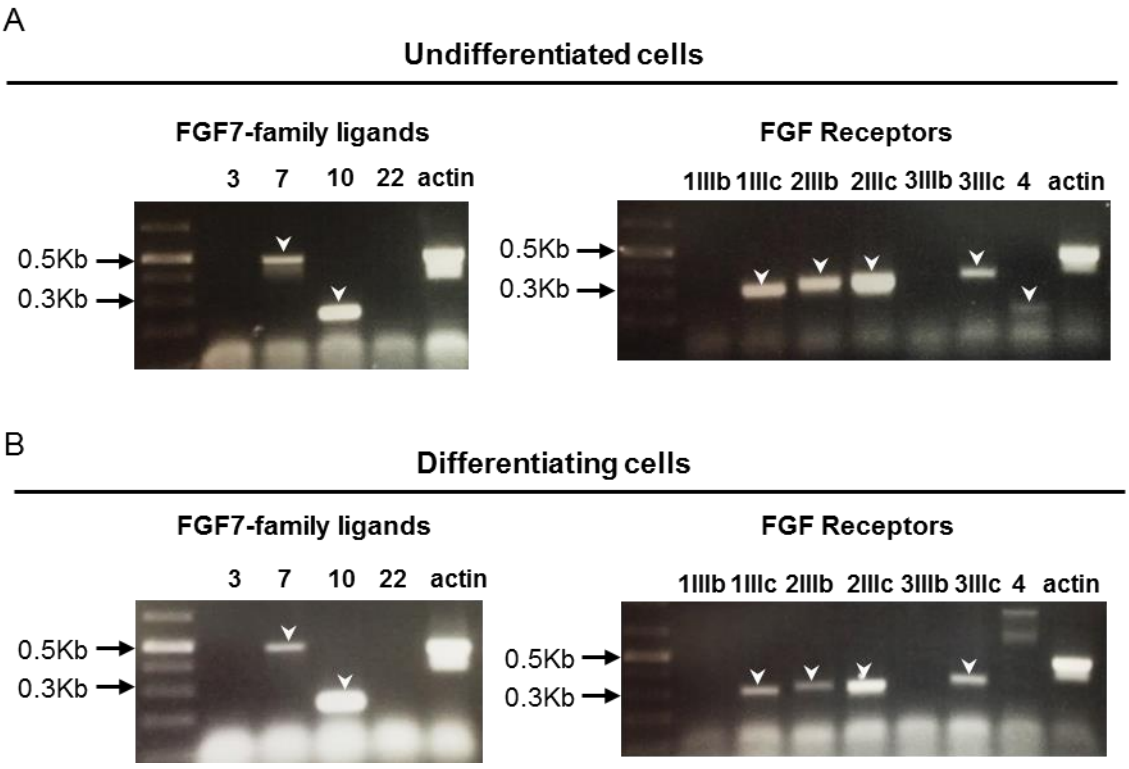

Figure 5.3 Semi-quantitative RT-PCR profiling for FGF7-subfamily ligands and FGF Receptors' isoforms in a culture of undifferentiated and induced to differentiate ATDC5 cell culture; note the heterogeneity of the culture, expressing both isoforms of the FGFR2 receptor.

Part 5.4 Endogenous overexpression of FGF10 inhibits differentiation of ATDC5 cell culture

Since exogenously applied FGF10 enhanced differentiation of ATDC5 cell, it was important to determine whether overexpression of the protein endogenously in the culture will have similar effect. As before, cultures of ATDC5s were set up and induced to differentiate with insulin and ascorbic acid. Sister cultures were then transiently transfected with either FGF10HA or G145E and 4T-NLS2 mutation-bearing constructs (see Chapter 4) primarily on the day of differentiation induction and then on two other occasions, therefore three times in total in order to maximize the overexpression of FGF10 within the differentiating culture (Fig. 5.4A). Cultures serving as negative controls were treated with transfection reagents alone and positive controls were transfected with mCherry fluorescent protein DNA, to demonstrate that transfection procedure itself does not disrupt the culture differentiation potential. At the end of the differentiation stage, the cultures were stained with Alcian Blue to determine the levels of cartilage formation.

Interestingly, overexpression of FGF10HA within the culture of ATDC5s caused reduction in cell differentiation, even after treatment with insulin and ascorbic acid. After 7-10 days of differentiation the control cells were dense, compact and small, began to overlay each other and form small nodules, with characteristic darker brown colour (Fig. 5.4B). Cells transfected with FGF10HA or with mutant-bearing constructs (G145E and 4T-NLS2) formed a uniform monolayer of cells that displayed elongated, spindle-like morphology, characteristic of undifferentiated cells, even on the 12th day of differentiation (Fig. 5.4B). Moreover extensive cell death was noted, in the samples transfected with G145E mutant when compared to the other assays. However, overall cell number did not seem to be affected. This observation requires further investigation, using specific markers of cell death and counts of cell numbers to fully assess the significance of this observation.

After 14 days of stimulation, the control assays, here termed as 'negative' meaning not-transfected as well as 'positive', meaning transfected with mCherry, both have showed full (i.e. normal) differentiation of the culture with multiple nodules that stained readily with Alcian Blue (Fig. 5.4B,C). By contrast, cultures transfected with FGF10HA showed only a few and very small 'patches' or 'micro-nodules' that were generated by a small group of condensed cells and have stained with Alcian Blue but failed to display a proper 3D nodule-like structure (Fig. 5.4B). The number of these micro-nodules was also significantly reduced in comparison to mCherry and not-transfected controls (Student T-test $p \leq 0.01$, $n=5$). Interestingly, transfection of mutant proteins also inhibited ATDC5 cell differentiation, comparable to FGF10HA (Fig. 5.4B).

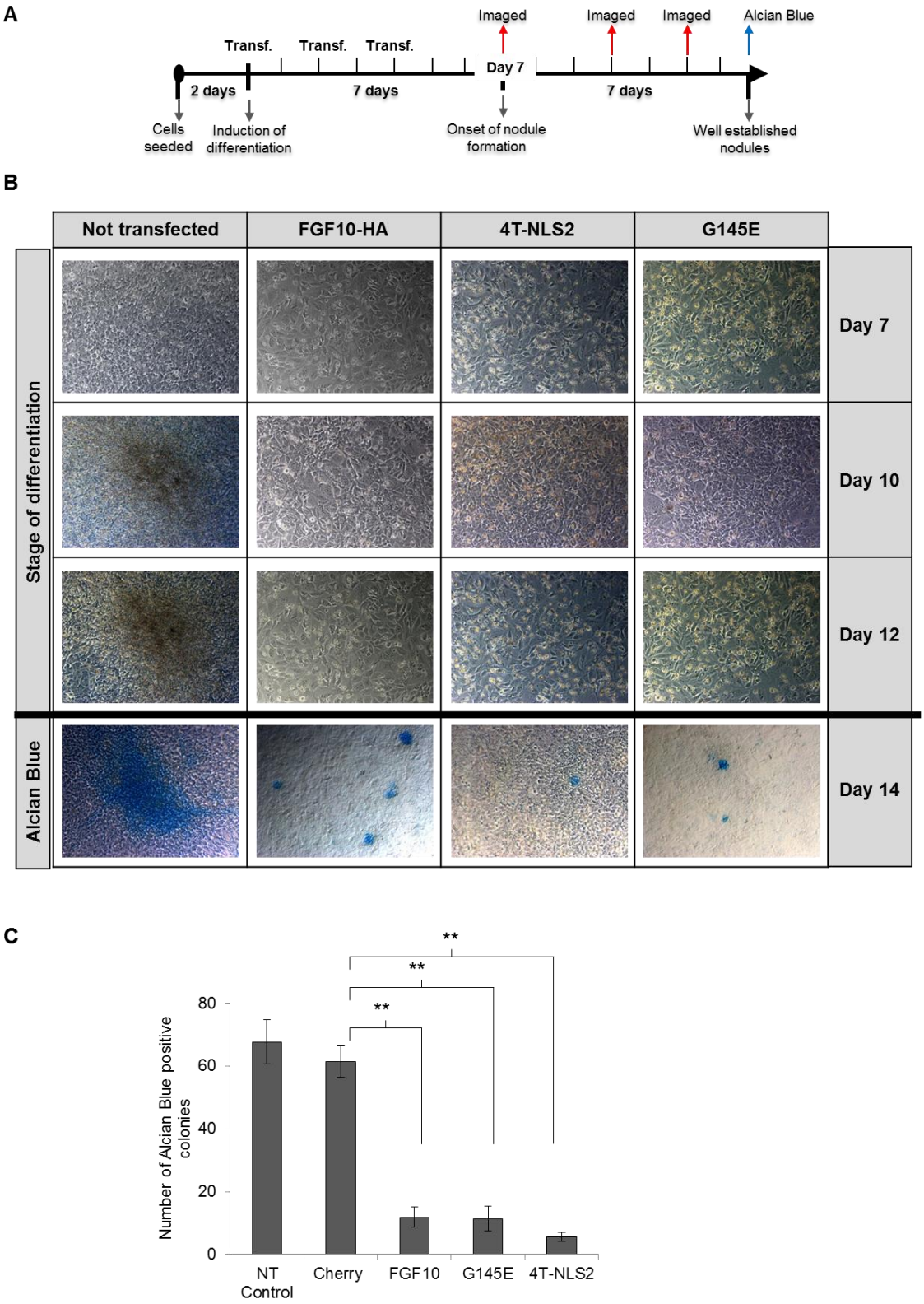

Figure 5.4 Overexpression of FGF10 limits the differentiation potential of the ATDC5 culture. (A) Schematic representation of the experimental set up; (B) Representative images of cultures imaged during later stages of differentiation and stained with Alcian Blue. (C) Nodules and micro-nodules (blue regions visible in the culture) were counted and compared to controls of not-transfected (NT) cells and cells expressing fluorescent mCherry protein (Student T-test $p \leq 0.01$, n=5).

Part 5.5 Discussion

Through these primary experiments it was shown that at specific concentrations an excess of exogenously applied FGF10 enhances the differentiation of ATDC5 culture (Fig. 5.2) whilst overexpression of endogenous Fgf10 causes significant cell perturbation to the differentiation (Fig. 5.4).

Although experiments performed here are primary, requiring further and more detailed studies, it was established that FGF10 alone was unable to trigger differentiation of ATDC5 chondrogenic progenitors, regardless whether supplied exogenously or overexpressed endogenously (Fig. 5.2 and data not shown). The same results have been observed *in vivo* where Fgf10-null mice display normal differentiation of mesenchymal cells during development of trachea (Sala et al., 2011). However, Fgf10-null mice display a significant decrease in proliferation of mesenchymal cells, resulting in abnormal cartilage patterning of trachea (Sala et al., 2011).

Externally applied FGF10 at 10^{-8}M, which is a concentration that is more than twice as high as concentration of 100ng/ml used in this study, was shown not to affect proliferation of either osteoblastic culture of mouse MC3T3-E1 cells, primary osteoblasts and ATDC5s (Shimoaka et al., 2002). Similarly, no increase in cell proliferation was observed during *in vitro* treatment of monolayered mandibular cells (Terao et al., 2011). In accordance with those results, no significant reduction in cell numbers was observed during the treatment with FGF10, either of undifferentiated or differentiated cultures of ATDC5s, at any of the FGF10 concentrations tested. Although, at the end of the experiment application of high concentrations of FGF10 (100ng/ml) lead to high levels of cell death, which may have been triggered by an altered differentiation processes resulting eventually in apoptosis, as undifferentiated culture remains unaffected (Fig. 5.2). To fully establish the effect of FGF10 on cell proliferation and cell death in this culture system more detailed studies succeeding the gross examination are required with a use of specific markers of cell death, proliferation and differentiation, which would provide detailed counts and nodule measurements and allow concrete conclusions to be drawn.

Unlike FGF18 and FGF2, but in accordance with the results shown here (Fig. 5.2), 10^{-8}M of FGF10 did not block the differentiation of osteoblastic MC3T3-E1 cell culture (Shimoaka et al., 2002). However results shown here indicate that, at a lower concentration, FGF10 can actually promote differentiation (Fig. 5.2). Supporting this observation, recombinant FGF10 added to a culture of explants (at 5ng/ml) was able to promote the formation of cartilage from the lateral mandibular cells (Terao et al., 2011). Therefore the effect of FGF10 on chondrocytic differentiation seems to be strictly dose dependent.

On the other hand, overexpression of FGF10 resulted in a significant abrogation of cell differentiation. The result is an unlikely effect of excessive protein accumulation as overexpression of mCherry construct did not limit the differentiation potential of ATDC5 cells (Fig. 5.4). Moreover, by its nature, transient transfection normally results in temporary protein production, which was unlikely to accumulate inside the cell over longer period of time. Moreover, FGFs were shown to be unstable and quickly degradable proteins in general (Buchtova et al., 2015), therefore further showing that protein over-accumulation is an unlikely event. However, the combinatory effect of transient transfections was sufficient to affect significantly the early differentiation of the culture, impacting subsequently the later stages. Interestingly, enhanced levels of endogenous FGF10 seem to have an opposite effect to the external treatment. Similar effect has been noticed regarding FGF3, a member of the same subfamily as FGF10. Nuclear FGF3 inhibits DNA synthesis and reduces cell growth (Kiefer and Dickson, 1995a) acting in an opposite fashion to its receptor-signalling role, where it functions as an oncogene, promoting cell proliferation (Muller et al., 1990).

During corticogenesis, FGF10 was shown to control differentiation of the stem/progenitor cells, and loss of FGF10 delayed but did not fully block neural cell differentiation. Moreover, FGF10 had no effect on cell proliferation (Sahara and O'Leary, 2009). Similarly, in ATDC5 culture FGF10 controlled differentiation, but with no discernible effects on cell proliferation or initiation of differentiation (Fig. 5.2).

These experiments provide interesting preliminary results of FGF10 function and leave room for further investigations. There are several caveats associated with this study that need to be addressed in the future. First of all, the experimental design did not control for the secretion of FGF10 and it is unknown therefore how much of the overexpression effect seen was caused by the activation of the FGFR2IIIb. However, previous experiments have shown that secreted from of FGF10 is undetectable in the overexpressed culture system (see Chapter 4), therefore it is unlikely that the protein was secreted at equally high levels as 5-10ng/ml and therefore its external signalling (promoting differentiation) might have not been as prominent as the internal signals (inhibiting differentiation).

Nonetheless, it would be required to silence the endogenous Fgf10 expression in the culture prior to future experiments, potentially through use of genetic manipulation tools. That would facilitate determination of whether endogenous FGF10 is essential for the cell differentiation in first place. Then stimulating the cells with external FGF10 would allow comparison with already obtained results. Moreover, overexpression of FGF10 protein lacking signal peptide, that currently directs it to the secretory pathway, would allow monitoring of the endogenous effect of FGF10 on the chondrocytic differentiation.

The G145E and 4T-NLS2 mutants proteins, that were shown to be excluded from the cell nucleus (Fig. 4.8 & 4.10), appeared to inhibit the cell differentiation in a similar manner to non-mutated FGF10 (Fig. 5.4). It is therefore possible that FGF10 affected the differentiation of ATDC5 cells via a cytoplasmic mechanism. Moreover, results presented here could be compromised by the endogenous production of the protein. Therefore a more controlled experimental set up would allow drawing clearer and more concrete conclusion.

The remaining matter is that ATDC5s, as one of the types of MSCs, may exist as a heterogeneous cell population, displaying two different isoforms of receptor FGFR2 (Fig. 5.3). Therefore, as part of the future projects a full characterisation of the culture would be required and ideally the cells expressing different types of receptor should be separated from each other, rendering pure cell populations. Interestingly, population of ATDC5 expressing different receptor isoforms may respond differently to FGF10 treatments. Furthermore, it would be crucial to determine whether the effect of FGF10 varies from data presented here, in different types of mesenchymal cells, e.g. through external treatments with recombinant protein or endogenous overexpression of the FGF10HA constructs within the lung mesenchyme or precursors of ocular glands. Currently, the commercially available mesenchymal cell lines are mostly limited to human and rodent MSC isolated from the bone marrow and adipose tissue, such as GIBCO® Mouse (C57BL/6) Mesenchymal Stem Cells, Human Marrow-Derived Mesenchymal Stem Cells (ATCC® PCS-500-012™) and STEMPRO® Human Adipose-Derived Stem Cell, which would provide a system very similar to presented here ATDC5 culture. Therefore, future studies might consider generating a primary culture of for example, lung mesenchyme, mimicking the *in vivo* processes where FGF10 seems to have one of its most prominent functions.

Chapter 6

Establishment and characterisation of primary hypothalamic cultures as an *in vitro* tool to determine FGF10 function in tanycytes

Part 6.1 Introduction to FGF10 in a culture of hypothalamic stem cells

Fgf10 is expressed in multiple but discrete regions of the postnatal and adult brain in a manner that is suggestive of a role in neurogenesis (Hajihosseini et al., 2008, Haan and Hajihosseini, 2009). Importantly, expression of the FGFR2IIIb receptor is virtually absent (Hajihosseini et al., 2008) suggesting an alternative mode of function of FGF10. In previous chapters (see Chapter 4 & 5) it was shown that FGF10 can translocate into cell nucleus. In hypothalamus, expression of Fgf10 is limited to a cell population called tanycytes, which have now been shown to act as neural stem/progenitors (see Chapter 1), but the function of FGF10 in these cells is currently unclear. Therefore, this system may be used as a great tool to study non-paracrine function of FGF10. Investigations *in vivo* are often difficult and require prolonged and costly studies (Rodriguez et al., 2005, Bolborea and Dale, 2013, Rojczyk-Golebiewska et al., 2014, Goodman and Hajihosseini, 2015). This can be aided by cell culture assays but currently protocols for studies of neurogenic tanycytes in vitro are lacking. An *in vitro* system allows for easier genetic and chemical manipulation of cells. Currently, culture of 'neurospheres' is the most commonly used tool to study properties of neural stem cells *in vitro*.

6.1.1 Overview of neurosphere forming assay

Stem cells display two cardinal properties, which are the ability to undergo self-renewal and the ability to differentiate into multiple tissue specific cell types. Therefore, adult stem cells serve crucial roles in maintaining tissue homeostasis and repair post injury. The discovery of adult neurogenesis, which is generation of new neurons in a postnatal brain (see Chapter 1), was shortly followed by *in vitro* studies of adult neural stem cells. The two well established niches of adult neurogenesis are sub-ventricular zone (SVZ) and sub-granular zone (SGZ). These are known to harbour stem cells shown to retain the capacity to self-renew over an extended period of time, proliferate and differentiate into three primary neural cell types, which are neurons, astrocytes, and oligodendrocytes (see Chapter 1). These neural stem cells (NSCs) were first cultured from an adult SVZ as cell suspension in non-adherent conditions, developed into a free-floating spheres, hence called 'neurospheres' (Reynolds and Weiss, 1992).

Since these early studies the 'neurosphere assay' has evolved and became more refined and the culture was shown to possess all of the properties of neural stem cells, such as proliferation potential and ability to undergo multiple passages as well as multipotency defined by differentiation into the three neural cell types (Bez et al., 2003). Furthermore, neurospheres were shown to express Nestin, Musashi and Sox2 which

are markers of neural stem cells (Reynolds and Weiss, 1992, Singec et al., 2006, Sousa-Ferreira et al., 2011).

6.1.2 Properties of neurospheres

A neurosphere is presumed to arise from a single cell, which is derived from enzymatically dissociated embryonic or adult mammalian CNS tissue. Dissected and dissociated single cell suspension is seeded in a non-adherent container, in serum-free medium and supplemented with EGF and FGF2 growth factors, maintaining their stem cell-like properties and facilitate proliferation (Chaichana et al., 2006). These single cells then are presumed to proliferate and give rise to clonal spherically shaped clusters of cells. As the cells continue to proliferate the sphere becomes larger and with greater diameter, that can be used to measure the growth rate of the culture (Ladiwala et al., 2012, Mori et al., 2006). However, the spheres do not form any nutrient transport network and as the sphere increases with diameter beyond 300-400μm the cells within the centre loose contact with the nutrients available from the media and die (Xiong et al., 2011). This can be observed under light microscope as dark brown colour at the centre of the sphere is typically an indication of necrotic cells, whilst healthy cells display more translucent (Bez et al., 2003). Before they reach their overgrown stage, the neurospheres can be dissociated into single cell suspension and reseeded, which is referred to as a passage. Dissociated single cells will proliferate to form secondary neurospheres, and the number of times this event can be performed (i.e. the number of subsequent passages) is a reflection of propagation potential of the neurosphere culture (Xiong et al., 2011).

Interestingly, it is typical that neurospheres derived from cells plated at the same time and under the same culture conditions differ in size and morphology, some showing regular and some irregular shapes. Moreover, cells present on the external layers of a neurosphere may occasionally display cytoplasmic processes resembling cilia or pseudopodia (Bez et al., 2003), which are used by the sphere to propel spontaneous locomotion and movement. Neurospheres have a tendency to aggregate together in a culture dish and adhere with each other in filopodia-mediated fashion (Ladiwala et al., 2012, Wang et al., 2006), showing that the culture is truly dynamic.

The neurosphere culture system was shown sensitive to the culturing method used. The main variable presents cell density which affects culture proliferation, differentiation as well as sphere clonality properties. High density cultures due to secretion into the culture media intrinsic factors were shown to promote cell survival and maintaining proliferation. However, higher culture density results in higher levels of sphere aggregation and was shown to reduce sphere clonality (Wang et al., 2006,

Coles-Takabe et al., 2008). On the contrary, low cell density levels although promote clonality of the culture, reduces the cell survival rate. Variations in cell density were shown to alter the microenvironment of the culture, affecting the cell proliferation capacity and differentiation potential (Jensen and Parmar, 2006), therefore it is essential to culture the neurosphere assay at a constant density.

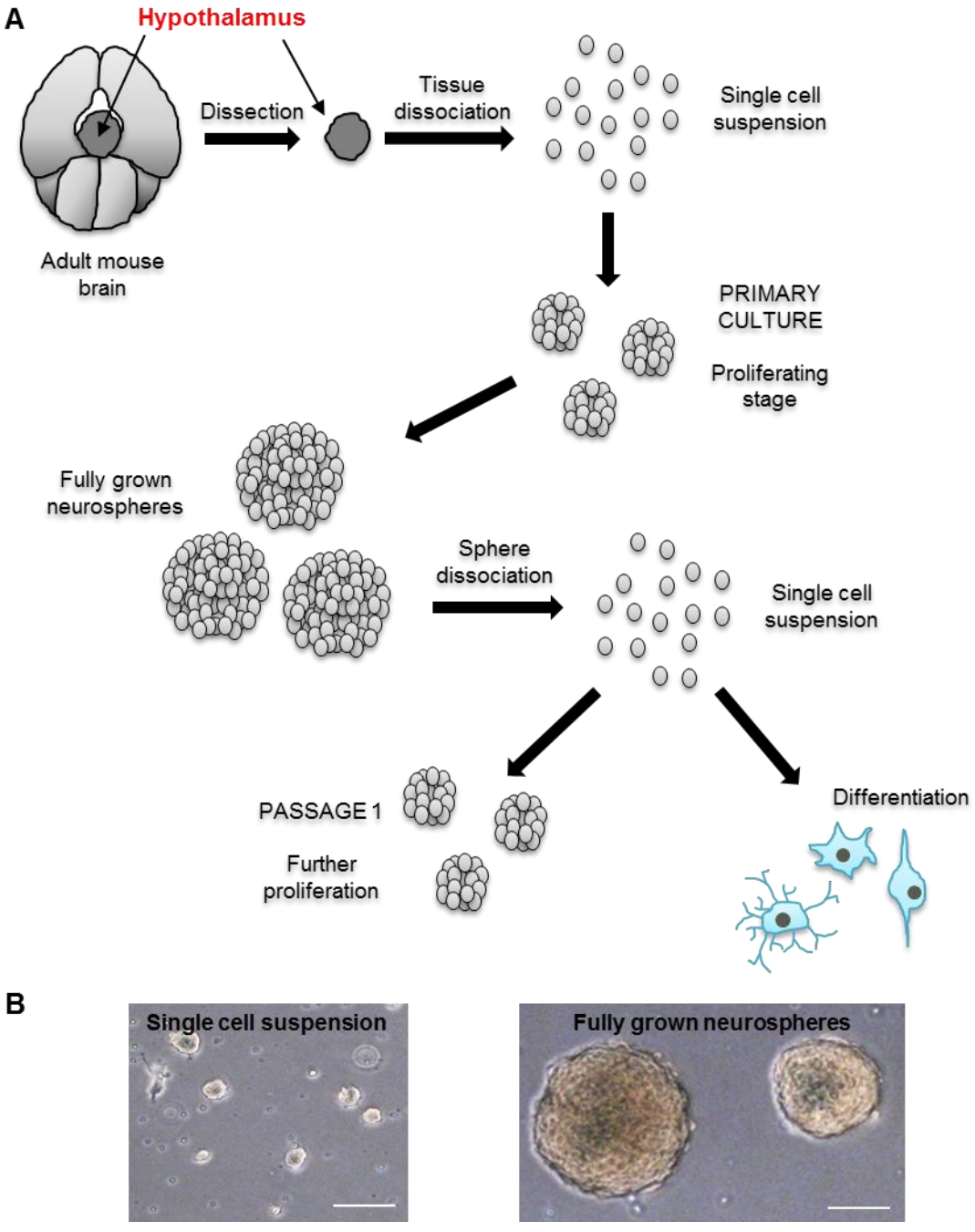

Figure 6.1 Culture of neurospheres (A) Schematic to show the subsequent stages of the neurosphere assay derived from tissue dissected from central nervous system, such as adult mouse hypothalamus (B) Representative images of culture of neurospheres at the stage of single cell suspension and mature spheres of diameter ~300µm; Scale bar 100µm.

6.1.3 Alternative systems of neural stem cell culture

The neurosphere culture was the first to *in vitro* system to culture stem cells derived from CNS. However, subsequent studies have generated alternative methods, which include simple adherent monolayers as well as three-dimensional Matrigel cultures. All hold their advantages and disadvantages, for example that monolayer culture allows ease of morphological and molecular characterization as well as analysis of lineage dynamics of individual cells, difficult to perform using the neurosphere assay (Babu et al., 2011, de Seranno et al., 2010). The Matrigel system, although expensive, is thought to provide powerful tool generating a proper microenvironment, mimicking the *in vivo* extracellular matrix structure (Pastrana et al., 2011). Yet, the neurosphere assay still remains the most commonly used tool to unequivocally demonstrate the presence of stem cells in the adult brain, allowing analysis of proliferation, self-renewal capacity, and multipotency of neural stem and progenitor cells.

6.1.4 Aims

Although neurogenesis is now known to take place in the hypothalamus (Gould, 2007), and NSC derived from the hypothalamus have been successfully grown *in vitro* as neurospheres, little is known of the exact location of these stems cells within hypothalamus (Xu et al., 2005). There seem to be three opposing theories of the origin and positioning of the hypothalamic stem cells: one is that the NCS are located in a parenchyma; second theory relates the α-tanycytes as the putative stem cells, which then give rise to population of cells migrating to the median eminence (Robins et al., 2013); thirdly, it is thought that the β-tanycytes are the true neural progenitors, which express Fgf10 and give rise to precursors that migrate up to the other parts of the hypothalamus (Hajihosseini et al., 2008, Haan et al., 2013).

The purpose of this study is to attempt to decrypt the function of FGF10 in the hypothalamic cells and the neurogenic niche through *in vitro* systems:

- Use of the well-established neurosphere assay system, to determine whether the Fgf10 expressing cells (and therefore β-tanycytes) show characteristics of stem cells
- Compare the characteristics of Fgf10-expressing to the Fgf10-not expressing cells, indicating the function of FGF10
- Establish and characterise a monolayer assay of hypothalamic primary cells as an additional tool to study the biology of Fgf10 expressing cells

Part 6.2 Neurospheres as a system to study Fgf10-expressing neural cells

Neurospheres assay is an *in vitro* system, commonly used to study existence of NSC in particular areas of developing or adult mammalian central nervous system (CNS) (Ladiwala et al., 2012, Gil-Perotin et al., 2013). Neurospheres are generated from mitotically active cells, which form spheroid clusters when cultured as a suspension in a serum-free medium on a non-adhesive substrate and in the presence of EGF and FGF2.

6.2.1 Fgf10-expressing hypothalamic cells can form neurospheres *in vitro*

Neurosphere assays were cultured with a purpose to determine the stem cell-like properties of hypothalamic tanycytes expressing Fgf10, in an *in vitro* cell culture system. The hypothalamus was micro-dissected from four wild type (WT) control and four Fgf10 reporter, the Fgf10$^{+/CreERT2}$ ROSA^{tomato} transgenic mice (herein referred to as Fgf10-tomato) at postnatal day 10 (see Chapter 2). Prior to dissection, the tomato-reporter system was conditionally activated by treatment of mice at postnatal day 4 and 5 (P4-5) with tamoxifen (txn). Thus tomato would become constitutively activated in Fgf10-expressing and their descendants (see Chapter 2 and Fig. 6.11A,B). After dissection, cells were dissociated and cultured in non-adhesive conditions, with the supplementation of growth factors. Cells were also isolated from the SVZ region, a well-established neurogenic niche but lacking Fgf10 expression (Gil-Perotin et al., 2013, Hajihosseini et al., 2008), was used as a control for culture conditions enabling neurosphere growth.

Under the culturing conditions (see Chapter 2) cells derived from the two dissected brain regions (the SVZ and the hypothalamus) formed neurospheres, regardless of the mouse genotype, either WT or Fgf10-tomato reporter (Fig. 6.2A,B). The presence of the tomato reporter was monitored regularly in the live cultures under a fluorescent microscope, where the red fluorescence was absent from the control groups corresponding to any cells derived from WT mice or Fgf10-tomato SVZ region. However, red fluorescence was seen in neurospheres originating from hypothalamus of Fgf10-tomato mice (Fig. 6.2A,B).

Detection of the tomato reporter signifies the expression from the Fgf10 locus, meaning that fluorescently labelled hypothalamic neurospheres arose from the Fgf10 lineage of the β-tanycytes (Haan et al., 2013, Hajihosseini et al., 2008), as post-mitotic neurons do not proliferate, therefore do not generate neurospheres. Absence of the fluorescence in the SVZ cultures showed that the expression of Fgf10 or its reporter was unlikely to occur spontaneously *in vitro*, after the dissection.

The neurosphere cultures were monitored daily through microscopic observations for their physical properties. Within a culture of neurospheres, colour of the sphere is an indicator of cell survival/ cell death, as a dark brown colour of the spheres signifies the cell death, whilst more translucent colour represents healthy cells (Bez et al., 2003). Morphologically no difference was observed between the Fgf10-tomato hypothalamic neurospheres and the control neurospheres. Specifically, no difference was noticed in the shape of the spheres or their colour, and cultured neurospheres in all assays appeared mostly round, with clearly defined edges with light brown/translucent colour, turning darker in the middle as the spheres grew (Fig. 6.2). Moreover, a minor proportion of neurospheres, occurring within each assays at comparable levels, underwent spontaneous differentiation through attaching to the bottom of the culture dish. Therefore, regardless of their origin, the neurospheres were maintaining at similar levels their stem cell-like characteristics in the *in vitro* culture. Interestingly, the Fgf10-tomato neurospheres on average were smaller in size, than neurospheres in the other assays (Fig. 6.2A), which was explored further in section 6.2.2.

Neurospheres, showed expression of neural stem cell markers, and importantly the Fgf10-tomato positive neurospheres expressed the Sox2 and Nestin markers (Fig. 6.2C), providing further evidence that the Fgf10-expressing cells *in vitro* displayed the stem/progenitor cells characteristics.

Interestingly, only approximately 20-30% of all neurospheres cultured from a Fgf10-tomato mouse hypothalamus were displaying tomato reporter, which was absent in the other spheres present within the same culture dish. This could be interpreted in two ways: (1) hypothalamus contains a mixed population of stem cells; or (2) a subset of cells turn off the expression of Fgf10/tomato *in vitro*. This issue was addressed further in the section 6.3.

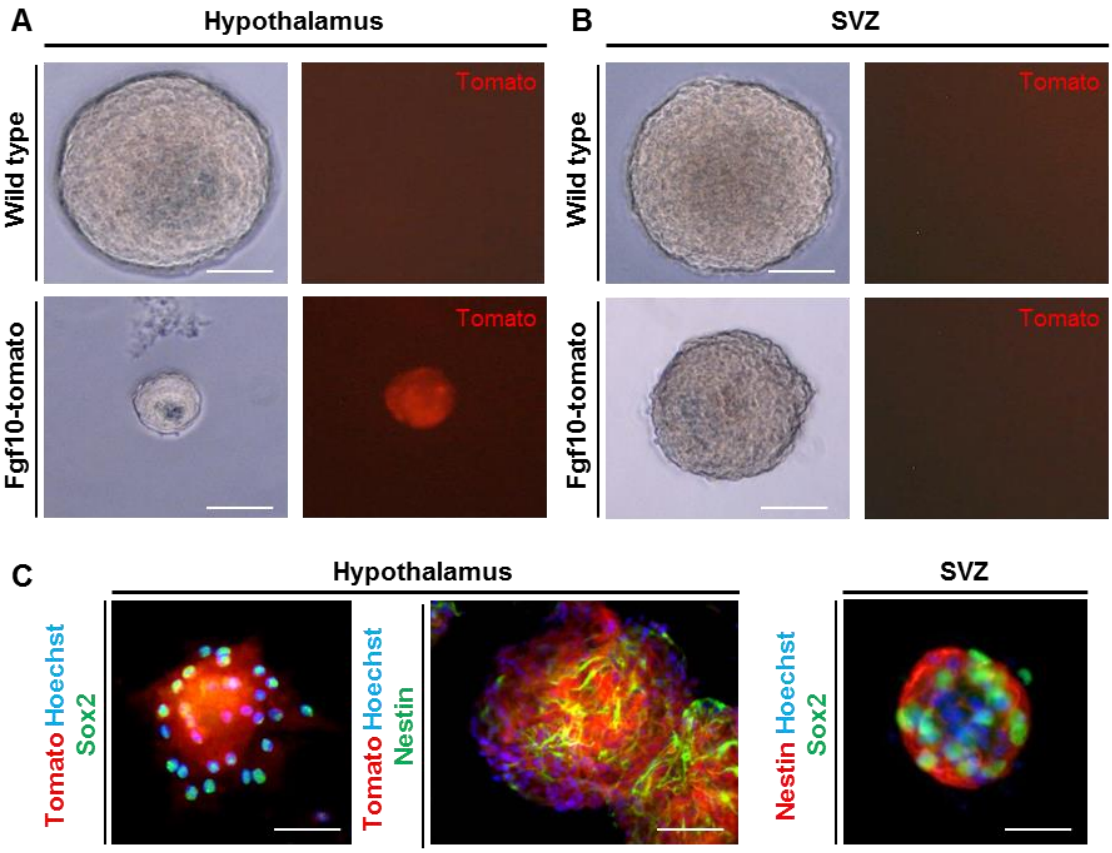

Figure 6.2 Neurosphere assay shows hypothalamic Fgf10-reporter expressing cells show neurogenic potential. (A) Primary hypothalamic neurospheres derived from Fgf10-tomato mouse showed expression of the tomato fluorescence in contrast to tomato negative control spheres derived from wild type (WT) mouse; note that regardless equal time in culture the WT and SVZ neurospheres are larger in size than the hypothalamic Fgf10-tomato neurospheres; Scale bar 100µm. (B) The control spheres derived from SVZ did not express tomato fluorescence, regardless whether derived from WT or Fgf10-tomato mouse. (C) The tomato expressing neurospheres express also Sox2 – a marker of stem cells; Scale bar 100µm.

6.2.2 Analysis of growth rate discrepancies of the hypothalamic neurospheres derived from the Fgf10-tomato and WT mice

A defining characteristic of neural stem cells is their ability to self-propagate. Accordingly, neurospheres can be passaged with cells still retaining their molecular characteristics and multipotency after each passage. Hypothalamic neurospheres have been previously shown to retain all of the properties of the stem cells, including their propagation potential, in a similar fashion to the neurospheres derived from SVZ (Sousa-Ferreira et al., 2011, Cortes-Campos et al., 2015, Haan and Hajihosseini, 2009). However, the stem cell properties of neurospheres are known to decline with the number of passages, and their propagation potential is limited (Jensen and Parmar, 2006, Xiong et al., 2011). Propagation potential of neurospheres was shown to be directly proportional to the seeding cell density and higher seeding densities provide better propagation sustainability. On the contrary, lower seeding densities prevent spheres from merging (see Fig. 6.6 and section 6.2.4) allowing “clonal cluster” studies (Jensen and Parmar, 2006, Bez et al., 2003).

To determine whether Fgf10-expressing neurospheres have different passage potential from non-Fgf10-expressing neurospheres, the Fgf10-tomato positive neurospheres as well as the control assays, were taken through several passages. Moreover, the spheres’ growth rate was measured and compared. Briefly, once the spheroid cultures reached their maximum size of ~300μm in diameter, they were dissociated into single cells, that gave rise to new neurospheres. Seeding these single cells at a low density (of $5x10^2$ cells/ml), in new culture dish was defined as a passage (see Chapter 2).

Neurospheres, derived from WT and Fgf10-tomato mice, from SVZ and hypothalamus, were passaged a maximum of 3 – 5 times before their propagation potential was exhausted and cells stopped proliferating (Fig. 6.3). The passaged neurospheres did not vary in their morphology, regardless of their origin and number of passages. On average, the spheres were darker in colour in the centre and the outer portion was bright and translucent with light, with easy to distinguish round healthy cells.

To determine whether hypothalamic Fgf10-tomato expressing neurospheres differ in their propagation potential from the controls, the neurosphere growth rate was measured during each passage and calculated as percent of the sphere growth per day. The growth rate was calculated by measuring per day an increase in sphere diameter and therefore overall sphere size, generated from increase of cell number (see Chapter 2). The primary (i.e. post seeding) WT hypothalamic neurospheres had a very fast growth rate of 58% increase in size/day, which was approximately three

times faster than neurospheres derived from hypothalamus Fgf10-tomato mice, which showed only 21% increase/day; and twice as fast as the neurospheres derived from SVZ region with 31% increase/day (Fig. 6.3). Nonetheless, this difference in growth rate was not observed after subsequent passages and further investigation would be required to determine the significance of this observation. In general, there was little variation in the percent of growth rate of the control neurospheres: derived from WT hypothalamus, WT SVZ as well as Fgf10-tomato SVZ (Fig. 6.3). However, the neurospheres obtained from the hypothalamus of the Fgf10-tomato mice on average, after each passage, showed slower growth rate in comparison to control neurospheres (Fig. 6.3), suggesting that hypothalamic Fgf10-tomato positive cell did not proliferate at the same rate as cells derived from control assays. Moreover neurospheres derived from the Fgf10-tomato mice could not be passaged to the same extent (number of passages) as the neurospheres obtained from WT mice (Fig. 6.3 and observation from pilot experiments).

As a knock-in creERT2 allele, the Fgf10-tomato reporter mouse is technically heterozygous for Fgf10, which generates reduced levels of FGF10 comparing to WT (see Chapter 2) (El Agha et al., 2012). This could have caused developmental problems with associated knock-off effects present later in the adult, and therefore could have resulted in the observed reduction of neurosphere proliferation potential. This experiment would require several repetition and statistical validation, although it has clearly demonstrated that primary hypothalamic neurospheres derived from Fgf10-expressing cells can be passaged successfully, displaying self-propagation potential.

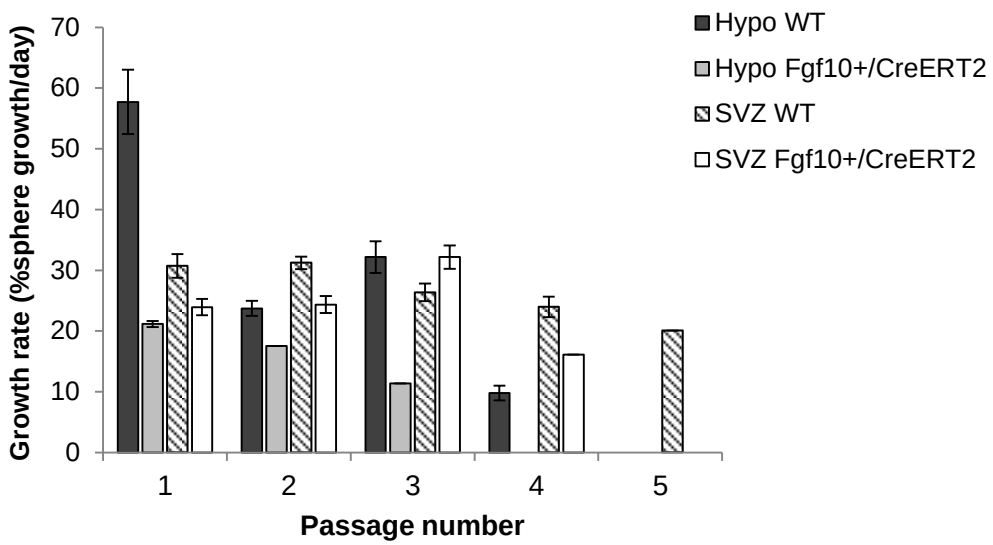

Figure 6.3 Propagation potential of neurosphere assays, determined by the number of passages each assay was able to sustain and growth rate of the neurospheres measured between the passages, shows that hypothalamic neurospheres expressing tomato reporter had a lower propagation potential than the control spheres. Error bars – SE.

6.2.3 Analysis of the multipotency of the Fgf10-expressing hypothalamic neurospheres

Adult NSC, *in vivo* and *in vitro* are able to give rise to differentiated cells of all three neural cell types (neurons, astrocytes and oligodendrocytes), which is defined as multipotency (Cortés-Campos et al., 2015). However, it is unclear whether expression of Fgf10 affects the differentiation potential of hypothalamic neurospheres *in vitro*, therefore tomato-expressing neurospheres, alongside with the controls, were induced to differentiate. Neurospheres derived from WT and Fgf10-tomato mice, from SVZ and hypothalamus, were dissociated and seeded on PDL coated glass coverslips, which provided an adhesive substrate promoting differentiation. Differentiating cultures were further stimulated by a withdrawal of growth factors and addition of serum to the culture media, as described in literature (Sousa-Ferreira et al., 2011) (see Chapter 2).

Under these culture conditions, the control SVZ and the hypothalamic neurospheres differentiated into all three neural cell types, regardless of their genotype of origin - WT or Fgf10-tomato. Cell type composition of differentiated neurospheres was revealed using a combination of neural cell-type-specific antibodies. The differentiated cells showed expression of the neuronal class III β-tubulin (Tuj1) protein, which marked differentiating neurons, the glial fibrillary acidic protein (GFAP) – the

marker of astrocytes, and the oligodendrocyte transcription factor (Olig2) protein, marker of oligodendrocytes (Fig. 6.4A,B). Furthermore, the neurospheres still retained their potential to differentiate after 3 to 4 passages, which corresponds to the findings presented in literature (Sousa-Ferreira et al., 2011, Cortes-Campos et al., 2015).

Importantly, the cells derived specifically from Fgf10-tomato hypothalamus (and expressing the tomato reporter) differentiated into neurons, astrocytes and oligodendrocytes, co-labelling with the lineage specific markers Tuj1, GFAP and Olig2 respectively (Fig. 6.4C). Therefore, these results show that hypothalamus derived cells marked by Fgf10 expression were multipotent neural stem cells, displaying similar potential to differentiate as neurospheres derived from the SVZ.

.

Figure 6.4 Neurosphere assays demonstrate multipotency by differentiating into neurons (Tuj1), astrocytes (GFAP) and oligodendrocytes (Olig2). (A) Differentiated neurospheres derived from hypothalamus of WT and Fgf10-tomato mice. (B) All three neural cell types differentiate from SVZ of WT and Fgf10-tomato mice. (C) The Fgf10-tomato hypothalamic cells expressing tomato differentiate into all three types of neural stem cells. Scale bar 50µm, (C) bottom panels 20µm; representative images of cells differentiated after passage 1 and 2.

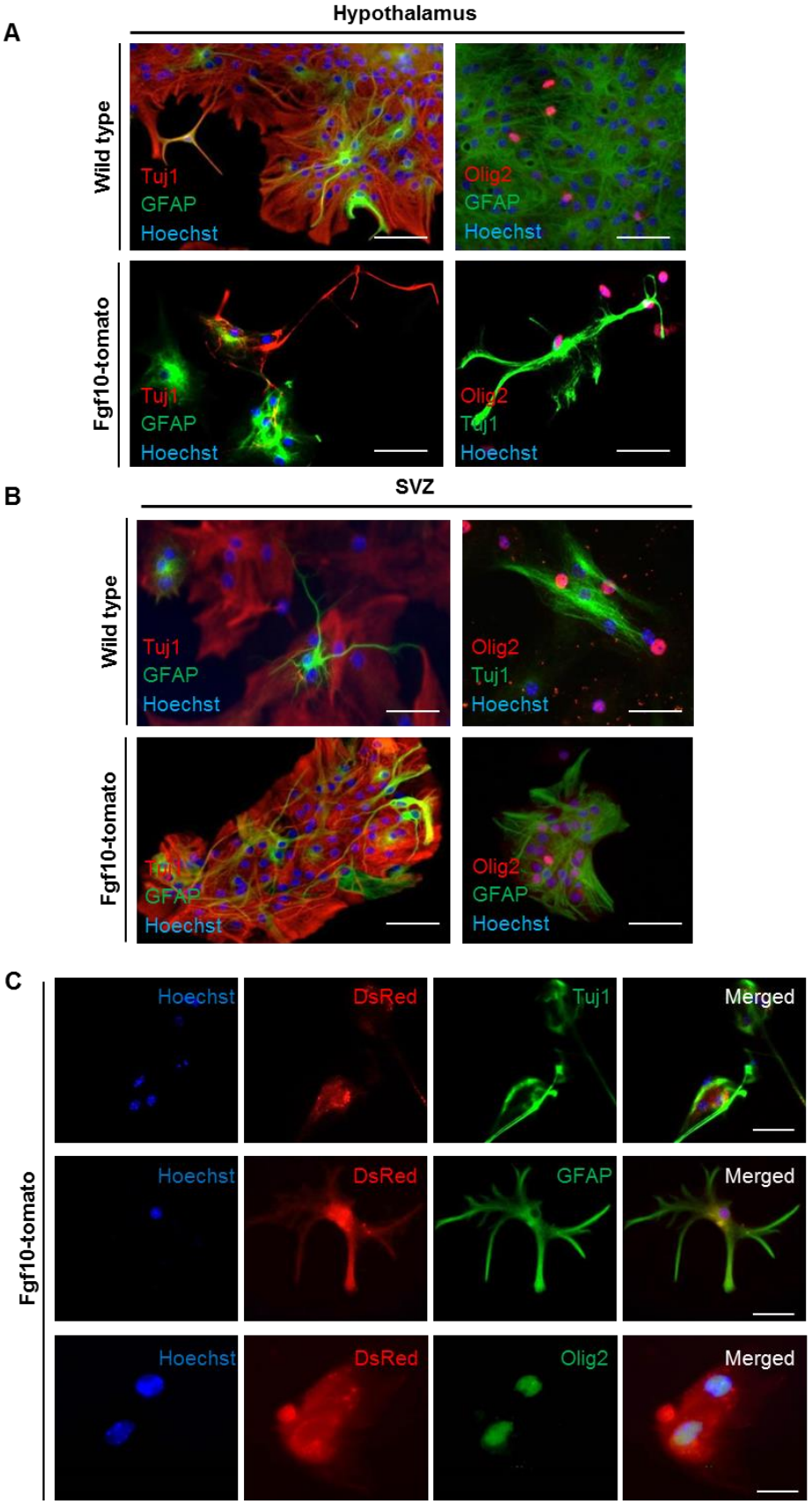
A
Hypothalamus
Wild type
Tuj1
GFAP
Hoechst
Olig2
GFAP
Hoechst
Fgf10-tomato
Tuj1
GFAP
Hoechst
Olig2
Tuj1
Hoechst
B
SVZ
Wild type
Tuj1
GFAP
Hoechst
Olig2
Tuj1
Hoechst
Fgf10-tomato
Tuj1
GFAP
Hoechst
Olig2
GFAP
Hoechst
C
Fgf10-tomato
Hoechst
DsRed
Tuj1
Merged
Hoechst
DsRed
GFAP
Merged
Hoechst
DsRed
Olig2
Merged

6.2.4 General caveats and limitations of the neurosphere assays

The neurosphere assay is commonly used as a litmus test for existence of neural stem cells in the tissue/brain region from which the cells were derived (Bez et al., 2003, Jensen and Parmar, 2006, Chaichana et al., 2006, Desai et al., 2011). However, this assay has several limitations that make it unsuitable for progressive characterisation and studies of the role of FGF10 in hypothalamic stem cells.

A culture of hypothalamic neurospheres derived from Fgf10-tomato reporter mice results in a heterogeneous population of tomato expressing and tomato negative spheres. The cell clusters can migrate around in the cell suspension and when encounter another neurosphere they show tendency to merge together (Fig. 6.6A) – a phenomenon that is already described in literature (Coles-Takabe et al., 2008, Ladiwala et al., 2012, Singec et al., 2006). Merging of the neurospheres is directly proportional to the cell culture density, and the higher the cell density the higher number of merging events takes place. On the contrary, the low cell density is linked to low cell survival rate (Reynolds and Weiss, 1996b, Coles-Takabe et al., 2008, Pastrana et al., 2011), resulting in a trade-off between maintaining cell survival and reducing merging events. Although, assays presented here were cultured under low/ semi-clonal cell density, merging of the spheres was unavoidable (Fig. 6.6A). Merging of tomato positive neurospheres with the tomato negative as well as decreasing the cell survival rate at low cell density, was thought to prevent reliable *in vitro* studies of FGF10 function in hypothalamic stem cells.

To circumvent the problem of heterogeneity in hypothalamic reporter negative and positive neurospheres, attempts were made to isolate tomato expressing from the tomato negative cells, through fluorescence-activated cell sorting (FACS). However, for several reasons, this proved unsuccessful: (i) very low number of cells expressed the tomato reporter (1.49% of total) vs the non-fluorescent cells (remaining 98.51%) (Fig. 6.5B), resulting in a very high noise-to-signal ratio (Donnenberg and Donnenberg, 2007); and (ii) poor survival rate of sorted cells, due to low final density of the tomato positive cells. The FACS has been attempted on 3 separate occasions (performed with consultations of experienced scientists) each time providing the same results. Non-pure population of Fgf10-tomato expressing culture, merging together made the neurosphere assay unsuitable for further studies.

A

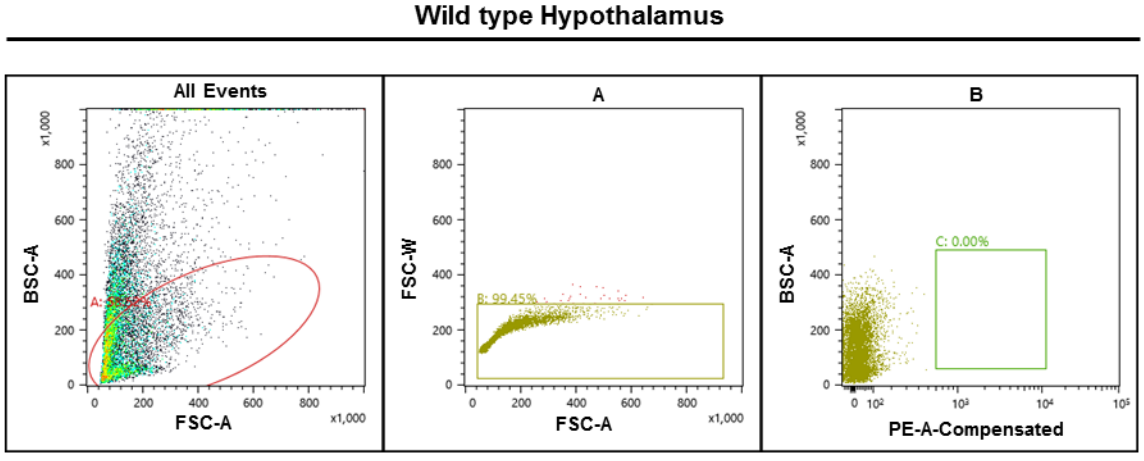

Gates and Statistics

Name	Events	%Parent	%Total
All Events	10,527	0.00%	100.00%
A	6,160	58.52%	58.52%
B	6,126	99.45%	58.19%
C	0	0.00%	0.00%

B

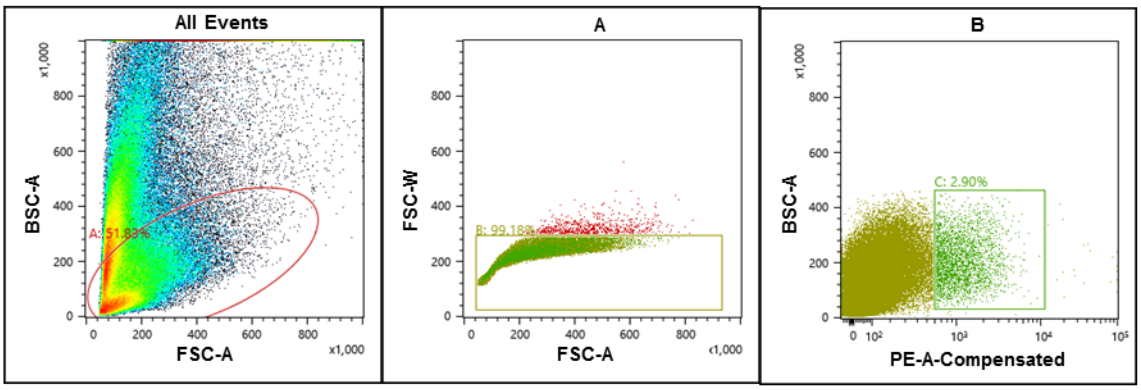

Gates and Statistics

Name	Events	%Parent	%Total
All Events	192,104	0.00%	100.00%
A	99,568	51.83%	51.83%
B	98,749	99.18%	51.40%
C	2,866	2.90%	1.49%

Figure 6.5 Representative data of identification and separation by FACS tomato fluorescence expressing hypothalamic cells. (A) Control hypothalamic cells not expressing tomato contained healthy cells of appropriate size ('A' and 'B' channels) but showed no detection ('C' channel) of 'tomato' sorted cells, as determined by the Forward (FSC) and Back (BSC) scatters and channel selecting for red Phycoerythrin (PE) fluorescence. (B) Tomato expressing cells were successfully detected and sorted from the Fgf10-tomato hypothalamic extract, but the sorted number of cells was too low for them to survive subsequent culturing.

Neurospheres in general, are also prone to attaching to the bottom of the culture dish, which leads to their spontaneous differentiation and cell-migration, even when cultured in non-adhesive containers in stem-cell promoting conditions. This spontaneous differentiation is thought to be directly related to cell culture density and therefore, the higher the cell density the greater the levels of spontaneous differentiation observed (Viktorov et al., 2007, Pastrana et al., 2011). In the studies performed here, through daily observations of the culture container under a light microscope, the differentiation was noticed in a similar proportion in all of the tested assays – regardless of the mouse genotype (transgenic or WT) or origin of derived cells (hypothalamus or SVZ) (Fig. 6.6A). Nonetheless, spontaneous differentiation of tomato positive cells, that in their natural *in vivo* conditions would retain their stem-cell potential, might affect the readout of the *in vitro* obtained results (Fig. 6.6B).

Although neurospheres are commonly used to study the NSC *in* vitro, the numerous limitations of this cell culture collectively have made it unsuitable for the studies of FGF10 function within hypothalamic stem cells. Nonetheless, data shown here confirms that hypothalamic tomato positive cells can be cultured as neurospheres *in vitro* confirming their putative neural stem-cellness.

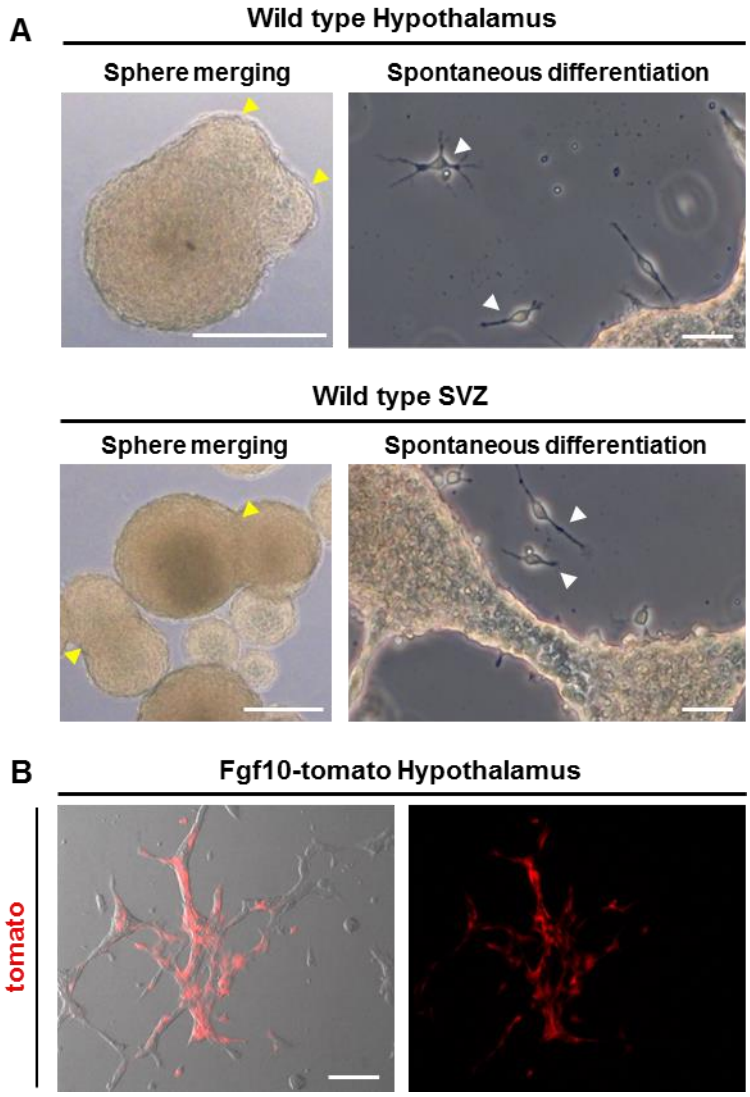

Figure 6.6 Examples of come neurosphere culture limitations. (A) Cultured neurospheres can spontaneously merge together and differentiate by attaching to the bottom of a culture dish. (B) Tomato expressing cells have been found attached to the culture dish, which could either undergo differentiation or be lost during passaging of the culture, not representing ideal experimental conditions. Scale bar 100µm.

Part 6.3 *In vitro* characterisation of the hypothalamic Fgf10 expressing cells cultured as a monolayer

The neurosphere assay was the first *in vitro* system to culture the NSC and is still commonly used to study processes taking place during neurogenesis, for example to study the effects of Zika virus infection on brain development (Garcez et al., 2016), or analysis of effects of magnesium on NSC proliferation (Jia et al., 2016).

Due to the unsuitability of neurospheres for clonal analysis, studies switched to the establishment of a monolayer cultures system, which has the advantage of fully exposing cells to a controlled extracellular environment as well as clear assessment of the morphology of individual cells, used for example, to study functionality of mouse dentate gyrus granule cell-like newly generated neurons (Babu et al., 2007). Therefore, in order to study function of FGF10 in tanycytes, a monolayer culture of tanycytes has been generated. Moreover, attempts have been made to characterise the stem-cell properties of the Fgf10 expressing cells.

6.3.1 Fgf10-LacZ positive primary hypothalamic cells proliferate and propagate as a monolayer culture *in vitro*

The cultures of primary hypothalamic neurospheres (section 6.2) derived from Fgf10-tomato mice, displayed a mixed population of tomato expressing and tomato negative spheres. To determine whether the cells were derived from a heterogeneous population of stem cells within the hypothalamus, they were isolated from an adult 30-day old (P30) $Fgf10^{nLacZ/+}$ transgenic mice (herein called Fgf10-LacZ) and cultured as a monolayer. The Fgf10-LacZ reporter marks cells expressing Fgf10, due to incorporated LacZ gene 114kb upstream of Fgf10 translational start site, generating a nuclearly targeted β-galactosidase (β-gal) product (see Chapter 2).

Hypothalamic cells from Fgf10-LacZ reporter mice were obtained using similar protocols for establishment of neurospheres. Briefly, hypothalamic median eminence was micro-dissected, dissociated into single cells and seeded at semi-clonal density of approximately $5x10^2$ cells/ml on PDL coated dishes (providing the cells with an adhesive substrate). Proliferating cells were observed 2-3 days post seeding, which began forming ‘clonal patches’, i.e. groups of various numbers of cells propagating in a close proximity, as tight clusters (Fig. 6.7A). After 7 days cells were observed within patches ranging in size from two to hundreds of cells; individual cells were rarely observed.

Fgf10-LacZ reporter-positive colonies were revealed by incubation in X-gal solution, which generated a blue nuclear staining in cells expressing the LacZ gene

(see Chapter 2) (Fig. 6.7A). The β-gal shows high stability in mammalian cells and is not degraded easily (Lee et al., 2006) therefore, the presence of β-gal was not treated as a direct readout of the expression on Fgf10 in a culture.

Importantly, β-gal most likely marked any cells that have had either *in vitro* or *in vivo* expressed Fgf10, regardless whether the gene expression was turned off at later stages of the cell life (Fig. 6.11). Therefore, the observed LacZ+ cells represent Fgf10-expressing hypothalamic tanycytes and/or their descendants. As with neurosphere Fgf10-tomato cultures, the clonal patches of monolayer culture derived from Fgf10-LacZ reporter hypothalamus showed heterogeneity with respect to lacZ-staining (β-gal expression) (Fig. 6.7A). Absence of β-gal signifies that these cells have not expressed Fgf10 either *in vivo* or *in vitro.*

Importantly, looking at the number of cells derived from young adult mouse hypothalamus, on average the LacZ+ number contributed to 36% of total cultured cells, which was nearly half as many as LacZ negative numbers (61.3%) (ANOVA p=0.000; post hoc Tukey HSD p=0.000) (Fig. 6.7B). This observed difference in the number of LacZ+ and LacZ- cells, as well as the difference in the total number of patches, suggests that within the hypothalamus there potentially was a heterogeneous population of mitotically active cells – one expressing Fgf10 and one that did not express Fgf10. Within the monolayer cultures a very small proportion (2.7%) of total cell patches contained a mixture of β-gal positive and negative cells (Fig. 6.7B). Possibly, this arose from random seeding of two or more progenitor cells in close proximity of each other during the plating process.

From microscopic inspection of the cell shape and size it was concluded that morphologically there was no observable difference between the cells expressing the LacZ reporter or not. Interestingly, a close inspection under a microscope of the X-gal stained culture revealed that pairs of LacZ positive (LacZ+) as well as negative (LacZ-) cells were often observed indicating recent cell division (Fig. 6.7A), and demonstrating that the culture was mitotically active. Moreover, some cells appeared migratory, which is known characteristic of cultured NSCs *in vitro* (Heese et al., 2005) (Fig. 6.7A middle panel).

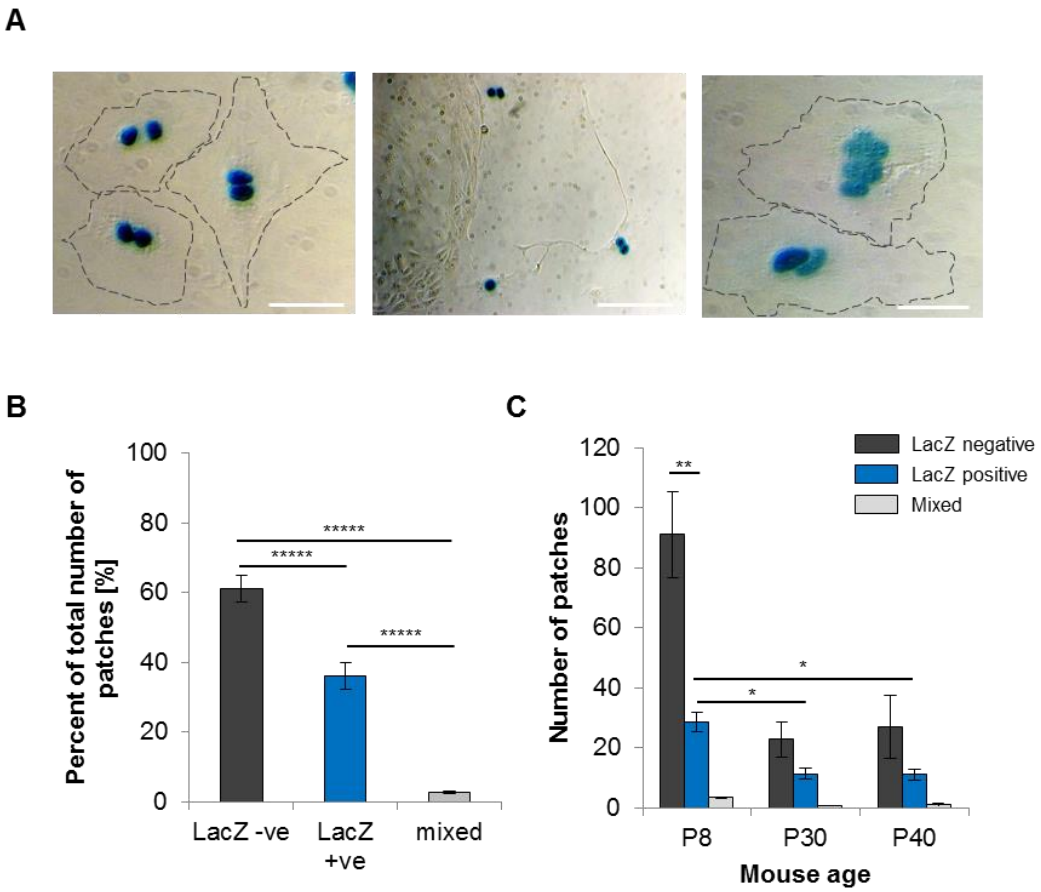

Figure 6.7 Hypothalamic cells were successfully cultured as proliferative monolayer of Fgf10-LacZ expressing and Fgf10-LacZ non-expressing cells. (A) Examples of pairs of LacZ-positive cells indicative of cell division generating cell clusters; note the presence of Fgf10-LacZ negative cells in the middle panel; scale bar 100µm. (B) Percent quantification of LacZ negative and LacZ positive number of patches of the total present within a culture suggests existence of a a heterogeneous population of proliferative cells (ANOVA p=0.000, n=22). (C) Number of cultured patches changes according to the age of a mouse, where the cells are originally derived from (T-test p≤0.01; Kruskal-Wallis, Chi-Square p<0.05). Error bars – SE.

The monolayer cultures yielded significantly less LacZ+ than LacZ- cell patches, which could possibly result from a lower number of LacZ+ cells present at seeding, meaning that *in vivo* there are less LacZ+ than LacZ- cells with a potential to proliferate. Alternatively expression of Fgf10 (as marked by the presence of the reporter) could have decreased the plating efficiency of the cells and/or reduced their survival rate. Another plausible explanation is that Fgf10 expression affects cell division and proliferation, detaining the cell cycle, or that Fgf10-expressing population

survival is reduced under these particular culture conditions. This observed difference between numbers of LacZ+ and LacZ- cell patches may possibly be linked to the function of FGF10 in the hypothalamic neurogenesis, which was explored further in subsequent sections.

6.3.2 Differential proliferation of hypothalamic cells in cultures of postnatal vs young adult mice

The process of neurogenesis continues postnatally in SVZ and hippocampus, but slowly declines with age (Kuhn et al., 1996, Urban and Guillemot, 2014, Abrous et al., 2005). Similarly, in the adult hypothalamus the number of proliferating and importantly, the number of Fgf10-expressing cells decreases with the age of a mouse (Haan et al., 2013). Therefore, it was investigated, whether primary hypothalamic cells derived from mice at early postnatal age (P8) have a different propagation potential (cultured *in vitro*) to cells derived from young adult mice (P30 and P40) and whether increasing age influences the number of Fgf10-expressing cells cultured *in vitro*.

For this, the median eminence from hypothalamus was micro-dissected from mice at age P8 (n=3), P30 (n=10) and P40 (n=9), dissociated, seeded and cultured on an adhesive substrate in the same fashion as previously described (also see Chapter 2). Number of assay repeats corresponded to number of mice and hypothalamic extracts dissected. Then cells obtained from a single hypothalamus were seeded across 3 wells of 24-well plate, cultured for 7 days, fixed and stained with X-gal as described above. Cells cultured from the P8 mouse gave rise to significantly greater total number of patches (both LacZ+ and LacZ-) than cells cultured from the young adult mice (either P30 or P40) (Fig. 6.7C). The number of LacZ negative patches was about three times greater at age P8 (91) comparing to P30 (23) or P40 (27) (Kruskal-Wallis, Chi-Square p=0.039, *post hoc* Mann-Whitney Test p=0.018; p=0.033). Moreover, the total number of LacZ positive patches at age P8 (29) was significantly higher comparing to age P30 (11) and P40 (11) (Kruskal-Wallis, Chi-Square p=0.023, *post hoc* Mann-Whitney p=0.011; p=0.012). However, there was no significant difference in the number of observed patches between the P30 and P40 (Fig. 6.7C). Therefore, the results suggest that *in vitro*, the proliferation potential of both Fgf10-expressing and Fgf10-non expressing cells, is greater at early postnatal stages (P8) than at the later mouse ages (P30 and P40), which corresponds to the observations made *in vivo* (Haan et al., 2013).

Interestingly, at P8 (but not at the later ages) there were significantly fewer patches of LacZ+ cells than LacZ- (Ttest p=0.0133) (Fig. 6.7C). This could suggest that at P8, LacZ- cells have either higher proliferation or survival potential than LacZ+

(Fgf10-expressing) cells, which is lost over time. This intriguing observation was further scrutinised in subsequent section.

6.3.3 Analysis of the age-related decline of Fgf10-expressing and not-expressing cells

Patches of hypothalamic cells, cultured from mice at age P8, P30 and P40 varied in size and hence were classified in three categories according to the number of cells present within the patch: small patch (1-5 cells), medium patch (6-50 cells) and large patch (51 and above) (Fig. 6.8). The cells were seeded at a semi-clonal density therefore, it was assumed that the individual patches resulted from clonal propagation of individual stem cells and were indication of stem cell proliferation rate, i.e. the larger the patch, the greater the proliferation potential of the cells within.

To determine differences between LacZ+ and LacZ- cell proliferation potential, the size variation of the patches was analysed individually within the different mouse age groups.

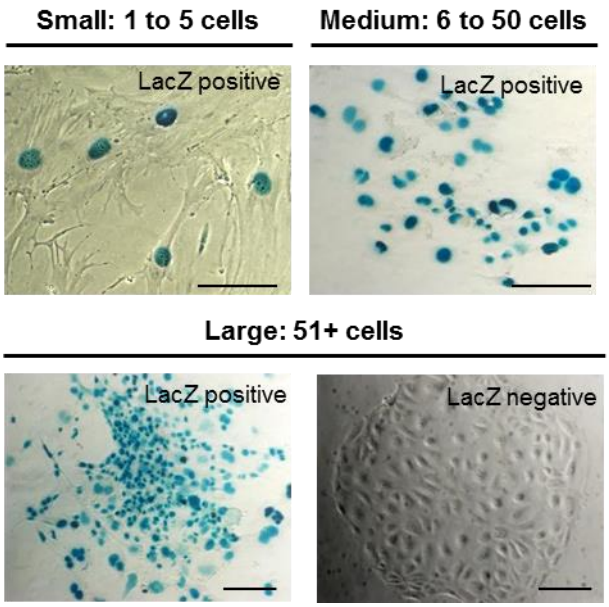

Figure 6.8 Representative images of small, medium and large patches formed by the clonal expansion of primary hypothalamic cells. Patches were either Fgf10-LacZ positive or Fgf10-LacZ negative.

In P8-derived cultures there was significantly greater number of small LacZ+ than LacZ- patches (T-test p=0.004) and there was no significant variation in the middle sized patches (T-test p=0.09), whereas there were excessively more large

LacZ- than LacZ+ patches (T-test p=0.007) (Fig. 6.9A). This suggests that the LacZ- cells proliferated very quickly and gave rise to a very high number of cells and very large patches. By contrast, the LacZ+ cells proliferated at much slower rate and did not give rise to the patches to the same extent as the LacZ- cells. Therefore, potentially P8-derived LacZ- cells proliferate more rapidly with greater propagation potential than LacZ+ cells. Alternatively the survival of the LacZ+ cells was compromised, perhaps due to expression and function of Fgf10.

The variation in number of small, medium and large patches was less prominent in cultures derived from mice age P30 and P40 (Fig. 6.9A). There was no significant difference in the number of small patches of the LacZ- and the LacZ+ cells (T-test p=0.55; 0.62). There was also little variation in the number of LacZ- and LacZ+ medium sized patches at the age of P30 (T-test p=0.01) but not at the age of P40 (T-test p=0.19). At both ages there were few large patches but there was no significant difference between the number of LacZ- and LacZ+ cells (T-test p=0.08; 0.13). It therefore appears that at the later mouse ages (P30 and P40) there was little difference between the proliferation potential of the LacZ negative and LacZ positive cells (Fig. 6.9A).

To determine whether the number of small, medium and large patches of the LacZ- and LacZ+ cells changes with the age of a mouse they were derived from, the data was compared across the three age groups – P8, P30 and P40. A small variation in the number of small LacZ negative patches was observed (Kruskal-Wallis, Chi-Square p=0.034, *post hoc* Mann-Whitney Test p=0.084; p=0.019), but no significant variation in the LacZ positive small patches was noted (Kruskal-Wallis, Chi-Square p=0.26) (Fig. 6.9B). Moreover, the number of medium sized patches found (both LacZ+ and LacZ-) decreased with the age of the mouse.

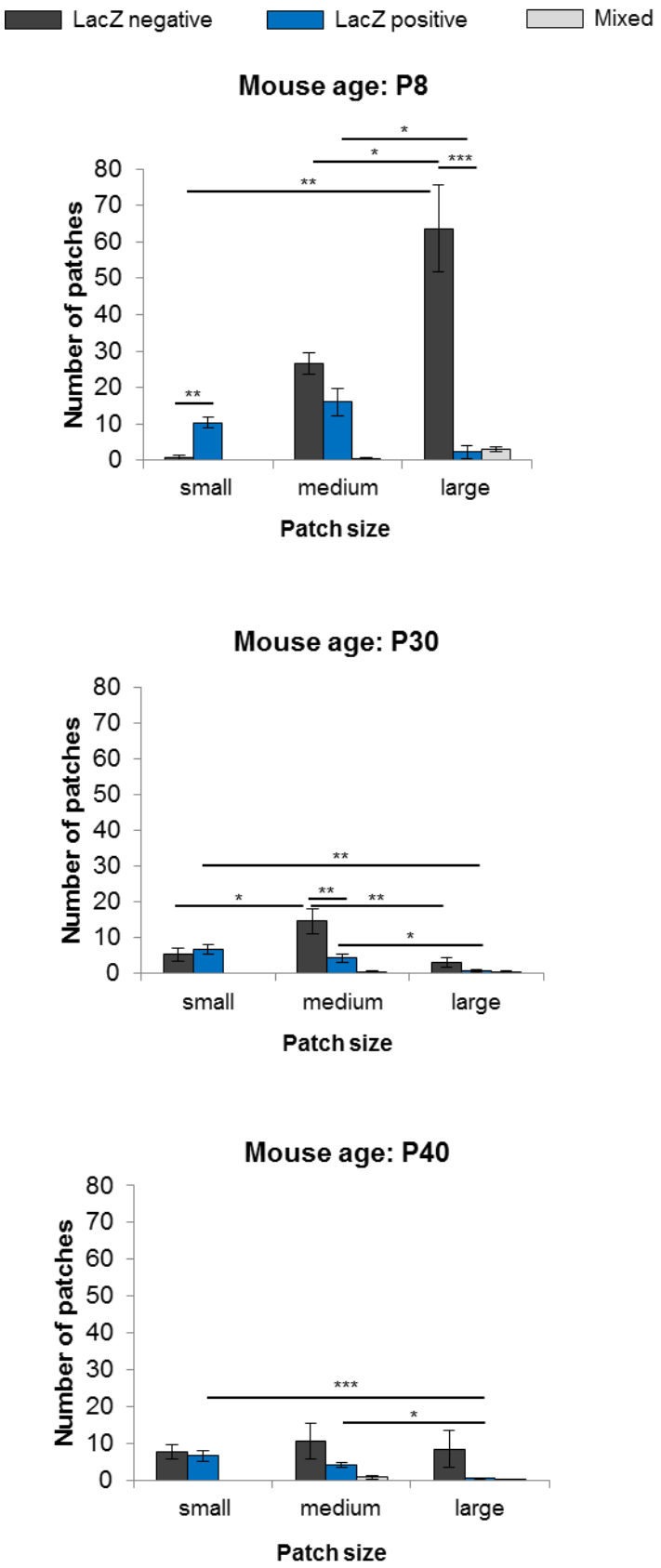

Figure 6.9A Primary hypothalamic cells show a different proliferative potential, depending on the age of a mouse that they are derived from – comparison of the patch sizes within each age group (T-test p≤0.05; Kruskal-Wallis, Chi-Square p≤0.05; P8 n=3, P30 n=10, P40 n=9). Error bars – SE.

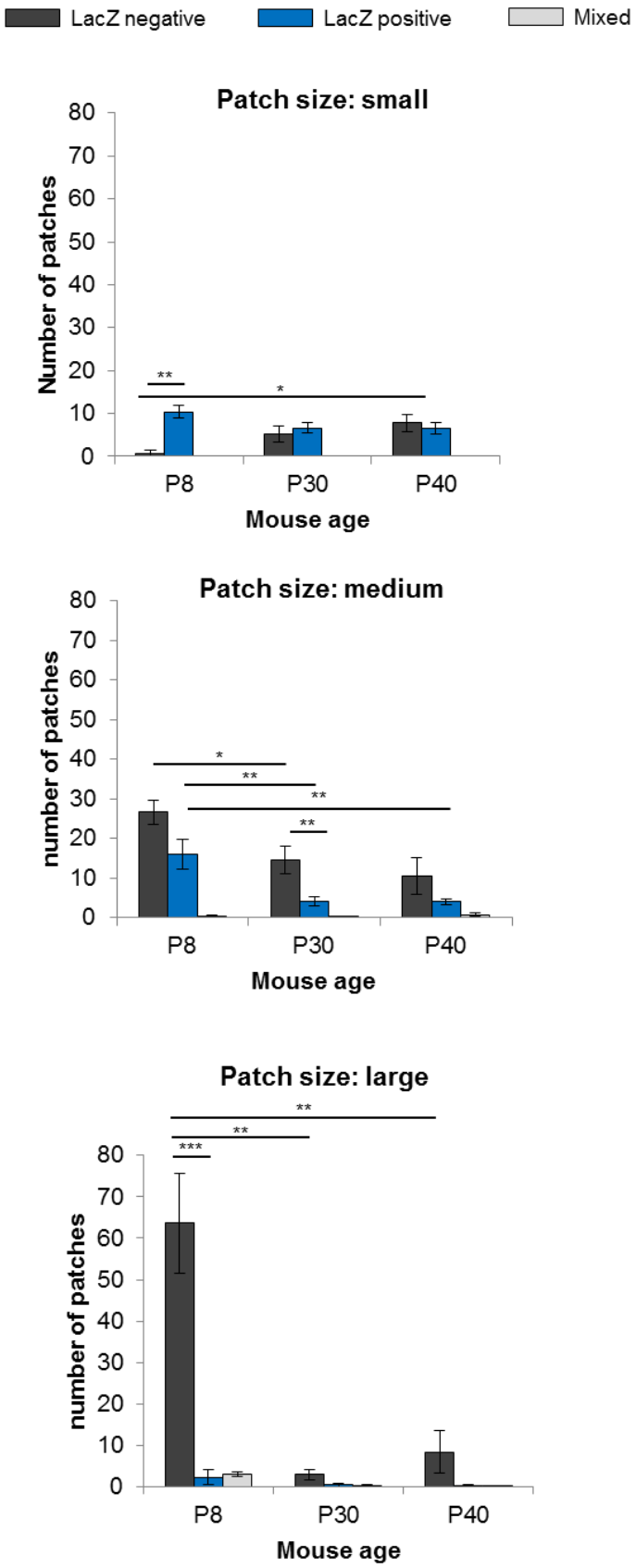

Figure 6.9B Primary hypothalamic cells show a different proliferative potential, depending on the age of a mouse that they are derived from, data reformatted to show comparison of patch sizes between different mouse ages (T-test p≤0.05; Kruskal-Wallis, Chi-Square p≤0.05; P8 n=3, P30 n=10, P40 n=9). Error bars – SE.

Interestingly, the most significant difference was seen regarding the large patches, showing a high reduction in the number of large LacZ- patches at the P8 comparing to P30 and P40 (Kruskal-Wallis, Chi-Square p=0.024, *post hoc* Mann-Whitney Test p=0.010; p=0.015). On the contrary, the number of large LacZ+ patches did not statistically vary between the different age groups (Kruskal-Wallis, Chi-Square p=0.284), however there were consistently fewer in number than the LacZ- (Fig. 6.9B). Together these results suggest that the proliferation potential of the LacZ- cells was significantly affected by the age of the mouse from which they were derived from, whereas, in comparison, the proliferation potential of the LacZ+ cells was not severely affected by the age of the mouse, although they did not at any point, proliferate at the same high rate as the LacZ- cells.

6.3.4 Analysis of cell division rate of hypothalamic monolayers

Generation of clonal cell patches is a likely result of a combination of rate and mode of cell division in relation to the survival of the precursor cells, as well as differentiation and survival of the progeny. Two possibilities of cell division can potentially take place: (i) cells divide symmetrically and are constantly adding two mitotic cells to the pool of precursors, if both daughters remain proliferative, or generate a pair of differentiated cells, such as neurons; or (ii) alternatively cells undergo asymmetric division and produce at each division one mitotically active precursor and one post-mitotic progeny, such as neuron. A combination of both can also occur within a culture. In a culture of primary hypothalamic monolayer there was a range of patch sizes, from small to large, indicative of not equal rate of cell division across the patches. The average mammalian cell cycle was estimated to last approximately 24h (Li et al., 2012b). However, some types of cells, such as crypt cells in the intestinal epithelium can proliferate as fast as every 9-10h (Al-Dewachi et al., 1979) and embryonic cells are known to divide in less than 2h, skipping the growth phases (Ciemerych et al., 1999).

Small patches observed that comprised of 1 to 5 cells, whether expressing Fgf10 or not, could have arisen through the death and subsequent loss of the siblings. Alternatively, slow dividing precursors, with putative cell cycle greater than 24h, undergoing an asymmetric division, over the period of 7 days would generate the maximum of seven cells. Another possibility is that the cells have divided symmetrically but gave rise to two differentiated and post mitotic daughter cells, which rarely were visible in the culture. Most likely, a combination of all of these events could have taken place to give rise to very small patches. Numbers of these small patches were comparable at all ages, regardless of the expression of Fgf10 (Fig. 6.9A,B),

therefore it might be assumed that typically 10% or less of the cultured cells displayed such a behaviour.

While not able to fully confirm asymmetric division of the small clones, it was assumed that clones larger than 50 cells were an evidence for symmetrical division. The propagation potential of the LacZ negative cells was greater than the LacZ positive, regardless of the mouse age (Fig. 6.9C). The numbers of cells within the large LacZ negative patches often considerably exceeded 51 cells and were frequently greater than several hundred, even at the age of P40. Potentially these cells have a very fast division rate of several hours, or alternatively have arisen from several patches proliferating in a close proximity generating one patch. Therefore the earlier described comparison of number of patches (see section 6.3.2 and 6.3.3), rather than number of cells within a patch was a good indicator of the proliferation potential of these cells.

On the contrary, large patches of the LacZ positive cells did not exceed 400cells/patch. Therefore in order to determine, whether the propagation potential of LacZ positive cells decreased with the age of a mouse, the growth rate of the LacZ positive cells derived from the three mouse ages – P8, P30 and P40 was estimated and compared. Due to seeding at semi-clonal densities it was assumed that each patch was a clonal expansion of a single cells, dividing symmetrically (as NSC) in an exponential fashion. Therefore, from each assay (post fixing and staining with X-gal) three biggest patches of LacZ positive cells per culture were selected, number of cells within was counted and averaged, in order to determine the maximum possible proliferation potential of the given culture measuring the exponential growth rate (%) (see Chapter 2). At the P8 (n=3, where ‘n’ is the number of mice used), the growth rate of 72% was the greatest (Kruskal-Wallis, Chi-Square p=0.021, *post hoc* Mann-Whitney Test p=0.018; p=0.079) whereas, at the age of P30 (n=10) and P40 (n=9) the growth rates of 41% and 53% respectively, were closely comparable to each other and statistically not significantly different (*post hoc* Mann-Whitney Test p=0.079) (Fig. 6.10). Therefore, the growth rate potential, which signifies the proliferation potential of the LacZ+ cells derived from young adult mouse (P30/40) is closely comparable to the early postnatal mouse (P8), suggesting that the age of the propagation potential of LacZ+ (Fgf10 expressing) cells correlates with the age of a mouse.

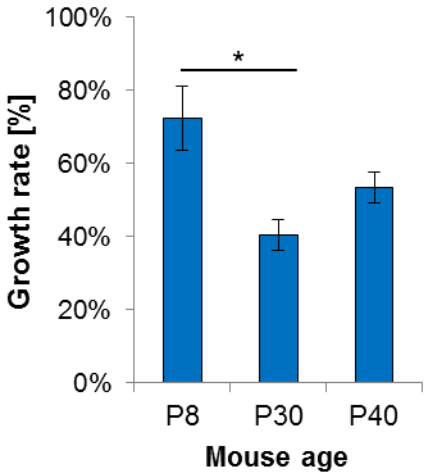

Figure 6.10 Growth rate of the LacZ-positive patches is closely comparable across young and older mouse ages. Note that there is no statistical difference between growth rate (proliferation potential) of LacZ-positive cell patches at age P8 and P40 (Kruskal-Wallis, Chi-Square p≤0.05; P8 n=3, P30 n=10, P40 n=9). Error bars – SE.

6.3.5 Examination of the Fgf10 expression of the hypothalamic cells cultured *in vitro*

Cultures of cells *in vitro* are used to reflect and study processes occurring *in vivo*, Cultures of cells *in vitro* are used to reflect and study processes occurring *in vivo*, but the primary cells may change in culture their molecular content and differentially regulate their gene expression (Ming and Song, 2005). The β-gal product of the Fgf10-LacZ reporter showed high stability in a culture of mammalian cells (Lee et al., 2006). Therefore, LacZ reporter marked indiscriminately cells that have either expressed Fg10 (*in vivo* or *in vitro)* or were derived from cells expressing Fgf10, but did not express it themselves (Fig. 6.11B).

In order to determine whether the cultured Fgf10-reporter expressing cells were in fact derived from the adult hypothalamic Fgf10 expressing β-tanycytes (Hajihosseini et al., 2008), $Fgf10^{CreERT2}/ROSA^{tomato}$ (Fgf10-tomato) (see section 6.2) reporter mice were induced with tamoxifen *in vivo* and cells were harvested from their hypothalamus a week later. This conditional reporter system allows time specific induction of the tomato reporter protein and therefore marked cells that expressed Fgf10 in the adult mouse hypothalamus (see Chapter 2) (Fig. 6.11A,B). Cells derived from Fgf10-tomato mice (age approximately P20-P30) were cultured in similar fashion to the earlier described Fgf10-LacZ cells (Fig. 6.11B). The tomato fluorescence expressing the reporter was detected in live cells under a fluorescent microscope and

the cultured cells were allowed to proliferate to confluency. Tomato-expressing cells were observed, proliferating in small patches, similarly to results obtained with Fgf10-LacZ reporter (Fig. 6.11C). Unfortunately these cultures presented survival problems and could not be seeded under semi-clonal densities, therefore the numbers of tomato-positive cells could not be directly compared to the Fgf10-LacZ data. The Fgf10-tomato reporter mouse is Fgf10 heterozygote (see Chapter 2) with reduced levels of Fgf10, that could affect the development of the hypothalamus and result in a poor survival rate of Fgf10-tomato cells *in vitro*. Nonetheless the results show that the cultured cells are derived from adult hypothalamic Fgf10-expressing cells.

Interestingly, the micrograph images revealed that only few cells within a patch were expressing tomato fluorescence (Fig. 6.11C). This suggests that the remaining cells within the patch were derived from the Fgf10-non expressing lineage, due to high seeding density. It is likely that a proportion of Fgf10-tomato expressing cells had lower survival rate than the Fgf10-tomato negative cells, due to either reduced level of Fgf10 expression or other (unknown) endogenous function of Fgf10. This could be measured in the future, by potential daily monitoring the cell death of cultured colonies.

The remaining issue was to determine whether Fgf10 continues to be expressed *in vitro* in culture derived from the hypothalamus or whether cells spontaneously turn off the gene expression post dissection (Fig. 6.11A,B). The hypothalamus was dissected out from tamoxifen non-induced Fgf10-tomato reporter mice (age P44), and its cells were seeded, allowed to adhere and proliferate for approximately 3 to 4 days. When medium sized patches had developed (~6 to 50 cells/patch), the cultures were pulsed with tamoxifen *in vitro* (see Chapter 2), to trigger the tomato expression and test for expression the Fgf10 reporter (Fig. 6.11A), generating a novel *in vitro*-inducible Fgf10-tomato reporter system. Subsequently, the cultures were allowed to proliferate to confluency and tomato fluorescence was detected in live cells under fluorescent microscope. Several small cell groups were observed to express the tomato reporter. This culture also presented cell survival issues and had to be cultured under high cell density conditions therefore the number of cells could not be directly compared to Fgf10-LacZ reporter data. Importantly, this *in vitro* inducible system provided an unique tool to study Fgf10 expressing cells and showed that a proportion of cells was maintaining the expression the Fgf10 under the given culture conditions.

Collectively the results show that cultured hypothalamic cells were derived from adult Fgf10-expressing β-tanycytes and that cultured cells were capable of maintaining the expression of Fgf10 *in vitro*.

Figure 6.11 Fgf10-reporters show Fgf10 *in vitro* and *in vivo*. (A) Schematic diagram of the inducible Fgf10-tomato system, where Cre-ERT2 produced in Fgf10 expressing cells is retained in cell cytoplasm until treatment with tamoxifen, that allows the nuclear incorporation of the complex, which binds to the loxP sites removing the STOP cassette and permits the tomato transcription. (B) Schematic of the time points at which specific Fgf10-reporters mark the Fgf10-expressing cells; note that Fgf10-tomato can be induced both *in vivo* and *in vitro*. (C) Primary hypothalamic cells expressing tomato fluorescence were cultured as monolayer *in vitro*; note that Fgf10-tomato system was induced *in vitro* demonstrating that cells do not turn off Fgf10-expression in the culture and are derived from hypothalamic β-tanycytes; Scale bar 100μm.

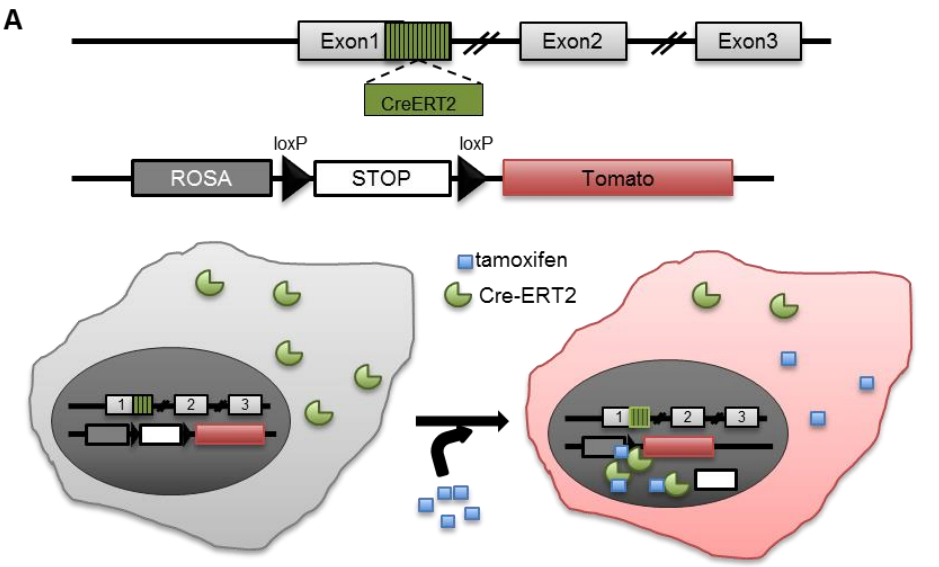
A
Exon1
Exon2
Exon3
CreERT2
loxP
loxP
ROSA
STOP
Tomato
tamoxifen
Cre-ERT2
1
2
3

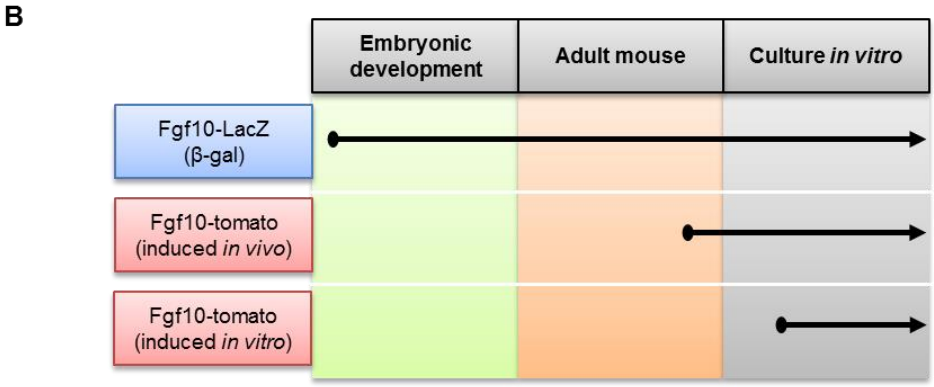
B
Embryonic development
Adult mouse
Culture in vitro
Fgf10-LacZ (β-gal)
Fgf10-tomato (induced in vivo)
Fgf10-tomato (induced in vitro)

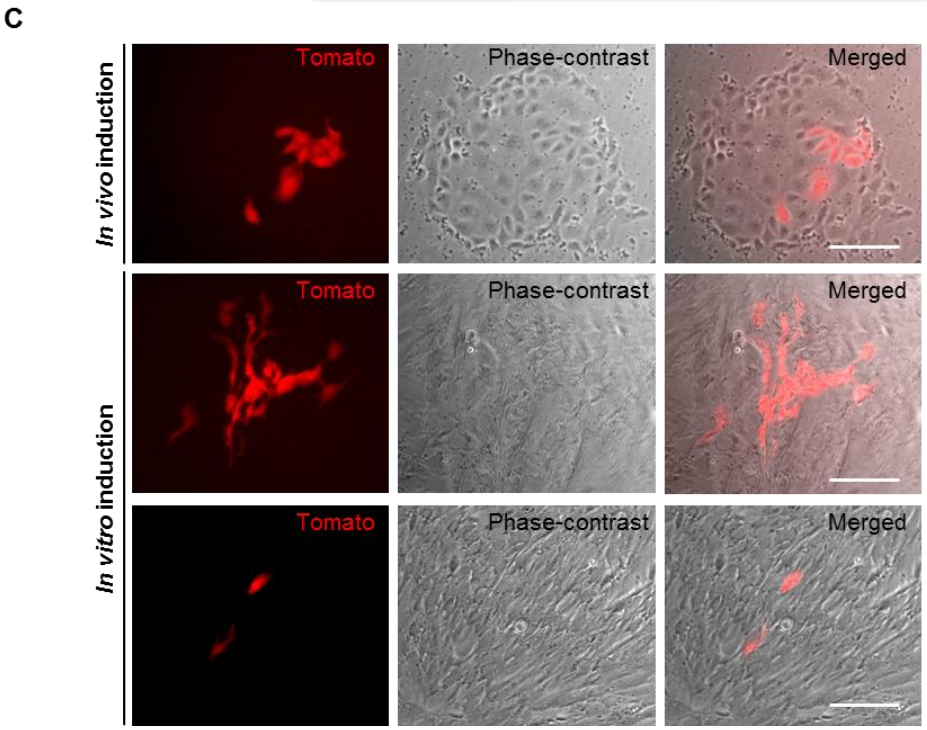
C
In vivo induction
In vitro induction
Tomato
Phase-contrast
Merged

6.3.6 Characterisation of expression of cell markers in monolayer cultures of hypothalamus

Primary hypothalamic cells cultured as monolayers propagate *in vitro,* regardless whether they express Fgf10 or not. Although self-propagation is one of the properties displayed by the stem cells, it is also a feature of trans-amplifying cell progenitors (see Chapter 1) (Fig. 1.12 & 1.13). In order to further define the characteristics of cultured hypothalamic cells, the semi-clonal patches derived from Fgf10-reporter adult mice, were assessed for expression of markers of stem cells Sox2 and Nestin, as well as marker of cell progenitors, NG2, and marker of radial glial cells, BLBP. Simultaneously, it was investigated whether the Fgf10-expressing and non-expressing cells differ in their expression of these markers.

The SRY (sex determining region Y)-box 2 (Sox2) is a transcription factor found in the cell nucleus. During embryonic neurogenesis, Sox2 is expressed throughout development of the neural tube and in proliferating CNS progenitors. It is essential for maintaining self-renewal and pluripotency of stem cells and it is downregulated during the process of cell differentiation (Graham et al., 2003b). Therefore, Sox2 is regarded as one of the markers of undifferentiated stem cells. A majority of cells within each of the Fgf10 reporter positive and negative patches expressed the Sox2 marker (Fig. 6.12A), regardless of the age of a mouse from which the cells originated (range from P8-P40).

Another well-known marker of NSC is the intermediate filament protein called Nestin (Fig. 1.12 & 1.13). It is present in dividing and undifferentiated neural cells and becomes downregulated during the process of differentiation (Michalczyk and Ziman, 2005). Nestin is known to mark mitotic neural cells and it is also involved in dynamic and highly proliferating cells. A subpopulation of Fgf10 reporter positive and negative cells showed expression of Nestin (Fig. 6.12B).

The Fgf10 expressing and non-expressing populations of hypothalamic cells cultured *in vitro* differed with respect to the brain lipid binding protein (BLBP). BLBP is considered a marker of radial glial cells (von Bohlen und Halbach, 2011), involved in the process of cell migration of immature neurons in developing central nervous system as well as signaling pathway that lead to differentiation of neurons (Schmid et al., 2006), neural precursors (Anthony et al., 2004) and immature neurons (Feng et al., 1994, Retrosi et al., 2011). Numerous Fgf10-tomato negative cells expressed BLBP, which was not detected in the tomato positive cells (Fig. 6.12E). This may indicate that a high proportion of the Fgf10 negative cells were cell-progenitors already dedicated to the differentiation pathway.

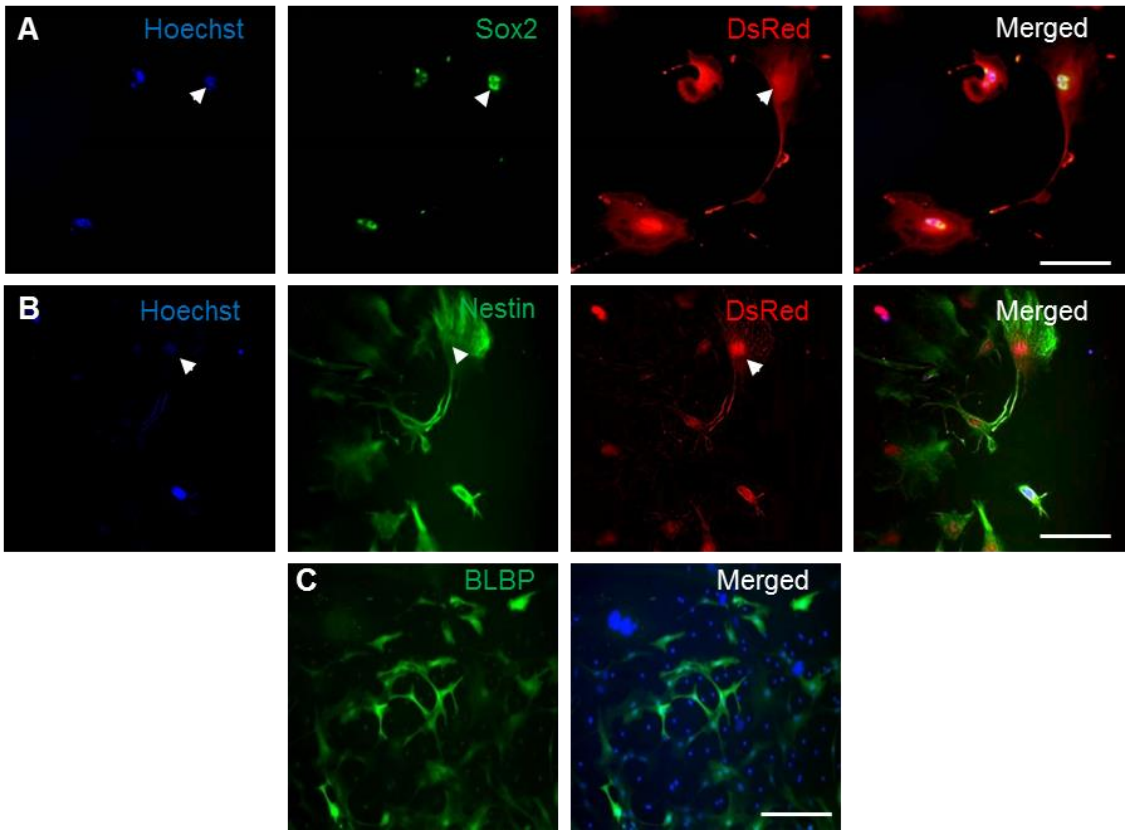

Figure 6.12 Characterisation of hypothalamic monolayer culture by detection of stem cell/progenitor markers. Expression of (A) Sox2 and (B) Nestin markers of NSC, was observed in Fgf10-tomato (DsRed) positive and Fgf-tomato negative cells; white arrowheads point to examples of tomato positive cells co-localising with specific marker. (C) Expression of BLBP marker of radial glial cells was observed only in cells not expressing the Fgf10-tomato reporter; Scale bar 100µm.

Furthermore, a subset of Fgf10-tomato positive and negative cells expressed the neural/glial antigen 2 (NG2). NG2 is a marker of proliferative glial cells (during development and in an adult) and neural cell progenitors, which in a majority give rise to oligodendrocytes (Levine et al., 2001), but can also differentiate into astrocytes and neurons (Trotter et al., 2010). Importantly, expression of NG2 protein is down-regulated upon maturation and differentiation of the cells (Nishiyama et al., 2009). Interestingly, in a culture of hypothalamic monolayers NG2 expression was observed within semi-confluent cultures at the periphery of the patches, where the cells from one patch came into contact with another patch (Fig. 6.13A,B). NG2 is a large transmembrane protein, shown to play a role in cell adhesion, cell-cell communication, as well as determination of cell polarity and migration (Biname, 2014). Potentially

contact with a different type of cell, from another patch stimulates cell-cell signaling resulting in molecular changes and expression of NG2 (Fig. 6.13C).

On the contrary, the peculiar expression of NG2 at the periphery of the patches could suggest that expression of NG2 is prevented in cells densely packed at the center of the patch. Potentially, the cells began to express NG2 and possibly endured other molecular changes, when they did not undergo contact-inhibition by other surrounding cells (Fig. 6.13D). This suggests that release from contact-inhibition could promote differentiation of the cultured cells.

Alternatively, cells at the center produced a currently unknown morphogen that at lower concentration promotes molecular changes resulting in expression of NG2. However, this would mean that the patches did not consist of clonal cell clusters but each cell within the patch possessed a different identity. The remaining possibility is that these NG2 expressing cells are derived from the pool of migratory cell progenitors residing within the hypothalamus, rather than true stem cells, and have migrated to different locations during period of culture.

Nonetheless, presence of these NG2 positive progenitor cells suggests that the culture has a potential to give rise to differentiated cells *in vitro*, which was subsequently explored further in section 6.3.8.

Figure 6.13 NG2 was found expressed in a culture of hypothalamic monolayer. (A) Fgf10-tomato (DsRed) positive cells showed expression of the NG2 marker; white arrowheads show examples of co-localising markers. (B) Stitched micrograph images showing cells, both tomato positive or negative, expressing NG2 at the periphery of the patches; scale bar 100µm. (C) Schematic representation of the theory that expression of NG2 within cells at the periphery of the patch, results from mutual interaction of cells from neighbouring patches. (D) A schematic to show that cells do not express NG2 when residing in close proximity to each other, however they do express NG2 when are no longer undergoing contact-inhibition.

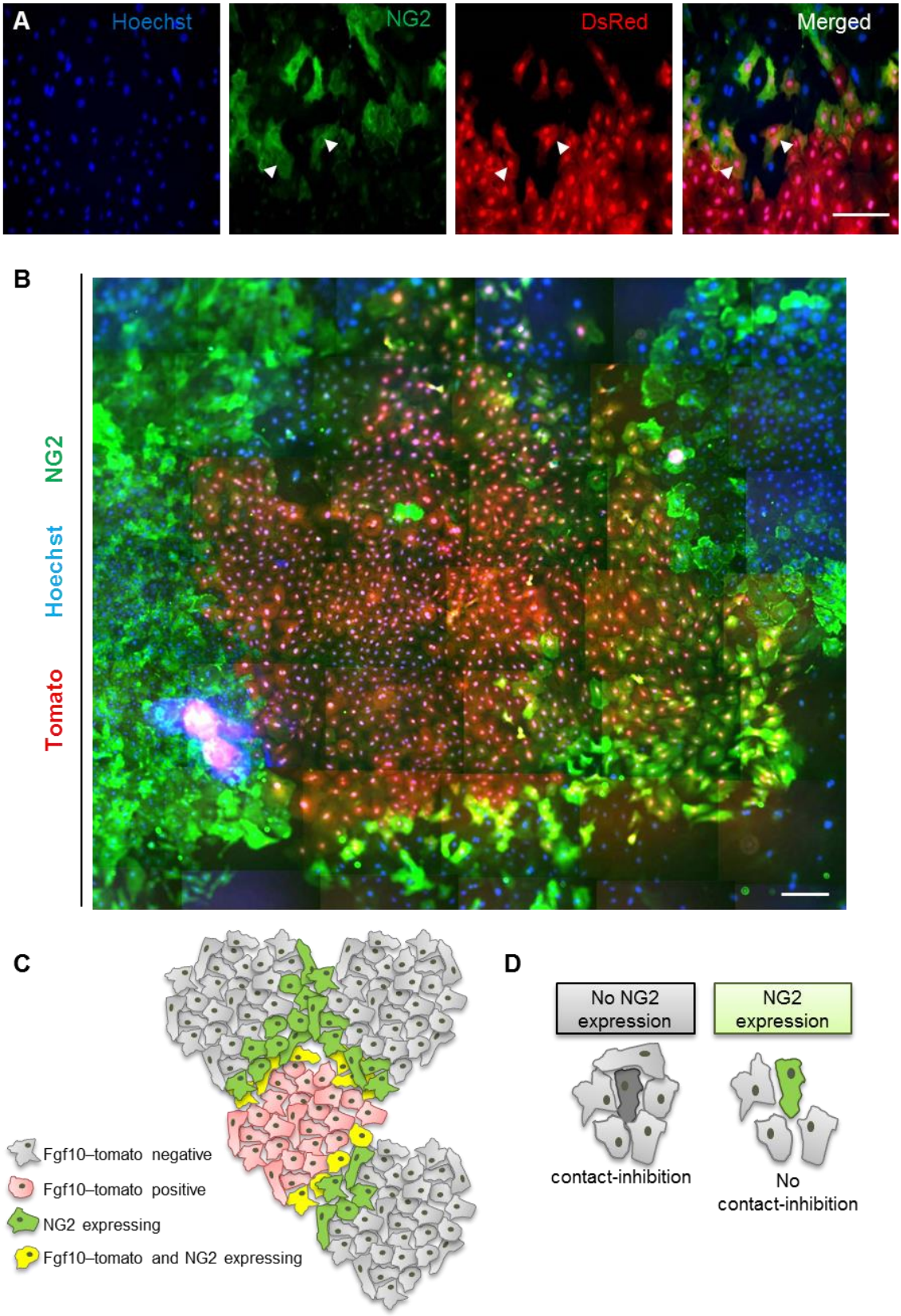
A
Hoechst
NG2
DsRed
Merged
B
NG2
Hoechst
Tomato
C
Fgf10–tomato negative
Fgf10–tomato positive
NG2 expressing
Fgf10–tomato and NG2 expressing
D
No NG2 expression
NG2 expression
contact-inhibition
No contact-inhibition

6.3.7 Sub-passaging capacity of cells in hypothalamic monolayer cultures

Stem cells are characterised by their ability to maintain self-propagation, therefore it is required, that when cultured *in vitro*, they are able to undergo passaging. It was observed previously that the hypothalamic monolayers self-propagate by forming specific clonal patches of Fgf10 expressing and Fgf10 non-expressing cells. However, as true NSC they should be able to sustain sub-passaging.

Therefore, in order to determine whether the hypothalamic monolayer cultures were able to withstand passaging, culture of cells derived from WT mice were taken through three to four passages. For this, cells were detached from semi-confluent (80%) culture dish and re-seeded onto fresh dishes at a 1 in 10 dilution, allowing further semi-clonal culture expansion. However, cells plated at (clonal) re-seeding density of $5x10^2$ cells/ml stopped proliferating. After passaging, cells formed a uniform monolayer without distinctive “cell patches” observed earlier at primary seeding. This could have arisen due to higher seeding density as well as more uniform dispersal across the culture dish due to low amount of debris comparing to the primary seeding.

Having established that the culture can be successfully passaged, it was important to determine and compare the sub-passaging capacity of Fgf10-ve versus Fgf10+ve cells. Passaged cultures derived from the Fgf10-LacZ reporter mouse (age P35) were stained with X-gal solution to determine the proportion of β-gal Fgf10-reporter expressing cells (see Chapter 2 and section 6.3.1). Within the primary culture at the point of passaging 71% of cells did not express LacZ reporter and 29% were LacZ positive (Fig. 6.14). After passaging, cells have formed a uniform monolayer of mixed LacZ+ and LacZ- cells, 80% of which consisted of the LacZ- and only 20% of the LacZ+ cells (Fig. 6.14). The proportions of LacZ+ and LacZ- cells appeared to be comparable before and after passaging, although further repeats would allow statistical comparison to validate conclusion drawn here.

As this is a novel system, further work would be essential to fully determine the character of the passaged cells. It is possible that re-seeding of a primary cell culture influences the molecular properties of the cells, affecting therefore their behaviour and mutual cell-cell interactions. Furthermore, the culture would require further investigations to determine the cell type composition (using stem cell markers) and differentiation potential after each subsequent passage, as well as expression of Fgf10-reporter. Therefore, to fully establish the effects of sub-passaging on a culture of hypothalamic monolayer this experiment requires subsequent repetition and further investigation, which was not undertaken in this study due to time limitation also linked to the number of mice available. Importantly, the results demonstrate the self-

propagation potential of the primary hypothalamic monolayer cells, including the cells derived from Fgf10-expressing tanycytes.

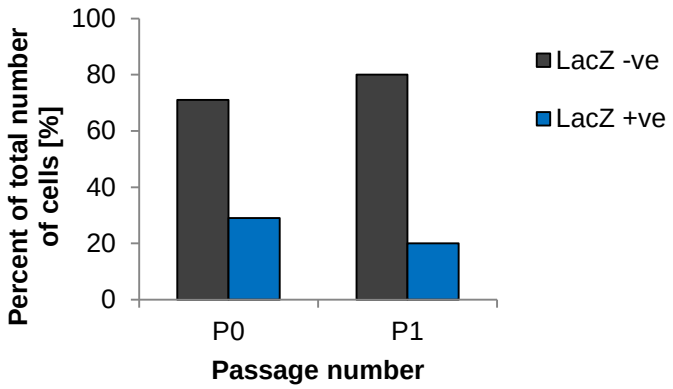

Figure 6.14 The primary hypothalamic cultures of Fgf10-LacZ positive and Fgf10-LacZ negative cells, were shown to be successfully passaged, demonstrating their propagation potential.

6.3.8 The hypothalamic primary monolayers display multipotency

The ability to differentiate and give rise to all three neural cell lineages - neurons, astrocytes and oligodendrocytes, known as multipotency is a key property of NSC. To determine their multipotent capability, the primary hypothalamic monolayer cultures derived from Fgf10-tomato mice (age P30 and induced *in vivo*) were stimulated to differentiate by seeding at high density and/or culturing for a prolonged period of time (see Chapter 2), until round or slightly elongated cells (some also with processes) began to emerge on the top of the monolayer (Fig. 6.15A), signifying differentiation. Cell type composition of the cultures was then subsequently revealed using combination of cell-type-specific immunofluorescent markers of differentiated cells.

The neuronal class III β-tubulin (Tuj1) protein is associated with microtubule stability and expressed almost exclusively by neurons and neuronal progenitors (von Bohlen und Halbach, 2011). Within the hypothalamic monolayer cultured for at least 30 days, several Fgf10-tomato positive cells was found to express the Tuj1 marker (Fig. 6.15B,C), showing their ability to differentiate into neurons. Differentiated neurons derived from the hypothalamus were selected against during seeding and therefore were not present within the clonal cultures maintained for short period of time (7 days),

as deducted from the lack of presence of the Tuj1 marker at the earlier culture stages (data not shown). Therefore, presence of neurons is an effect of cells differentiating in the culture and not direct seeding of already differentiated cells. Furthermore, majority of the tomato negative cells expressed the Tuj1 marker in the culture (Fig. 6.15B,C), suggesting that in a long term culture majority of Fgf10 reporter negative cells was unable to maintain the stem cell properties and committed to neuronal differentiation.

To detect astrocytes, the cultures were assessed for expression of glial fibrillary acidic protein (GFAP) (Fig. 6.15D). This intermediate filament (IF) protein is a commonly used as a marker of astrocytes *in vitro* and *in vivo* (Yang et al., 1994, von Bohlen und Halbach, 2011). In the cultures of the primary hypothalamic cells, GFAP protein was detected in numerous Fgf10-tomato negative cells as well as within several tomato positive cells (Fig. 6.15D). Similarly to neurons, the expression of GFAP was not detected in the early cultures, showing the capability of the Fgf10 tomato positive and negative cells to differentiate *in vitro* into astrocytic lineage.

The short term culture (7days) was earlier shown to express NG2 marker of cell progenitors that in majority give rise to oligodendrocytes (see section 6.3.6). To determine whether high density long term culture (>30days) provided cell differentiation into oligodendrocytes the culture was assessed for the presence of the oligodendrocyte transcription factor 2 (Olig2) protein. Olig2 specifically marks the cells dedicated to the oligodendrocytic and moto-neuron lineages (Takebayashi et al., 2000, Takebayashi et al., 2002) and it was detected within both Fgf10-tomato positive and negative cells (Fig. 6.15E). Again, the presence of the marker is only detectable in the high density long-term monolayers and therefore the presence of Olig2 was a result of differentiation of cultured cells rather than effect of seeding already differentiated cells.

Overall, it was found that Fgf10 expressing and some Fgf10 negative cells, originating from adult mouse hypothalamus, can give rise to all three types of differentiated cells, demonstrating their multipotency.

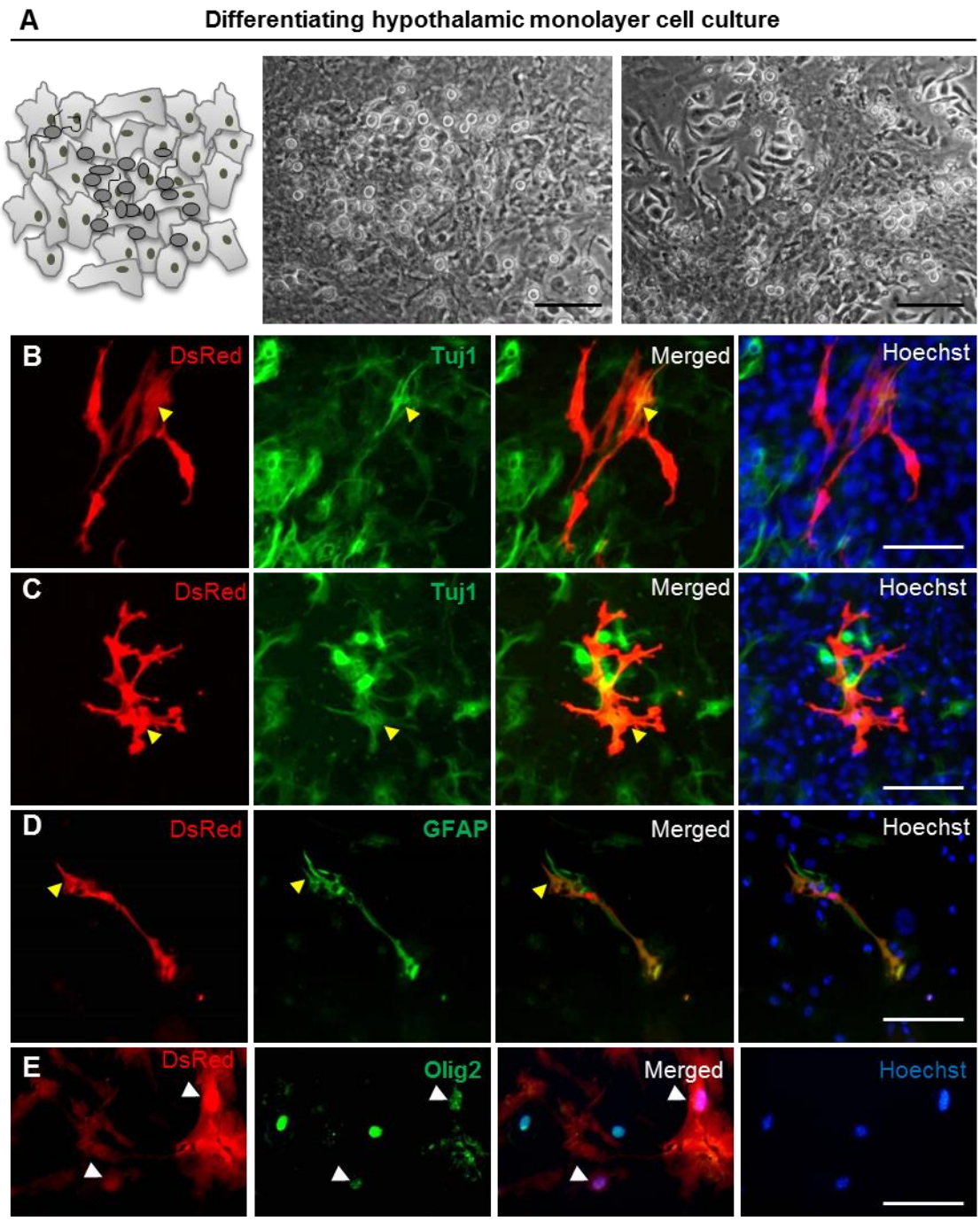

Figure 6.15 Differentiation potential of the primary hypothalamic Fgf10-tomato culture. (A) A schematic representation (left hand side) of phase contrast micrographs showing a differentiating hypothalamic culture, where cells at the top layer mostly correspond to neurons and oligodendrocytes and are sitting on a layer of astrocytes and remaining undifferentiated cells, which were further immunolabelled with fluorescent markers to confirm their identity; scale bar 100µm. (B&C) The tomato fluorescent cells express also the Tuj1 – a marker of differentiated neurons. (D) The tomato positive cells do not show expression of the GFAP marker of astrocytic lineage. (E) The tomato fluorescent cells express the Olig2 marker of oligodendrocytes; scale bar 100µm.

Part 6.4 Expression profile of Fgf ligands and Fgf Receptors in primary hypothalamic monolayers

Successful induction of the Fgf10-tomato reporter *in vitro* signifies that Fgf10 was expressed post dissection, in a culture of hypothalamic monolayers derived from adult Fgf10-tomato reporter mouse (Fig. 6.11). FGF10 is a signalling protein that through binding to FGFR2IIIb triggers multistage-downstream pathways leading to changes in cell proliferation, migration and gene expression. Moreover, on several occasions it was shown to work in a cooperative (and sometimes redundant) manner with other members of its subfamily, i.e. FGF7, FGF3 and FGF22 (see Chapter1). To determine whether the function of FGF10 in the monolayer of primary hypothalamic cells may be intertwined with other members of the FGF family it was therefore important to establish expression profiles of these proteins in the culture. Furthermore, the *in vitro* culture was generated with the purpose to reflect and study molecular processes occurring *in vivo*. However, cultured primary cells can potentially modify their molecular characteristics post dissection, changing their gene expression. Therefore it was important to determine any differences in protein profiles, between those expressed *in vivo* (Hajihosseini and Dickson, 1999, Hajihosseini and Heath, 2002) to those occurring *in vitro*.

The use of RT-PCR analysis of sub-confluent cultures, derived from WT mice of the age P30, allowed for the semi-quantitative comparison of the expressed mRNA levels of each protein. The results showed that Fgf10 was expressed at high levels in the *in vitro culture* (Fig. 6.16A), which agreed with the results of Fgf10-reporter culture studies where at least 20% of total number of cultured cells was found to express Fgf10 (see section 6.3 and Fig. 6.7). Moreover, strong expression of Fgf1, Fgf13 and Fgf21 was also noted. From Fgf10 subfamily members, only a weak expression of Fgf7 was detected and no expression of Fgf3 and Fgf22 was observed. Other ligands detected within the cultures were: Fgf2, Fgf9, Fgf12, Fgf16 and Fgf18. Some weak expression of Fgf5 and Fgf11 was seen as well (Fig. 6.16A).

There was some discrepancy between the *in vivo* and *in vitro* Fgf expression profiles. Fgf5 expression was found in the cell culture but not in the hypothalamic extract, and the Fgf14, 17 and 20 were found *in vivo* but not in the monolayers (Fig. 6.16B). However, expression of these ligands was found at very low levels in each case. Another notable difference was that Fgf13 was found expressed at high levels *in vitro* but at low levels *in vivo* (Fig. 6.16B). Other small differences in expression levels might be a result of sample variation or experimental issues.

Additionally to the ligands, the FGFR1IIIc and FGFR3IIIc receptors were expressed at high levels, the FGFR1IIIb expression was also faintly detected, whereas the FGFR3IIIb was not detected at all (Fig. 6.16A). The *in vivo* studies showed the absence of FgfR2IIIb expression from hypothalamus (Hajihosseini et al., 2008). Conversely, the RT-PCR profiling of the *in vitro* monolayer showed that the FgfR2IIIb was expressed at low level in the cell culture which was considered negligible when compared to the high levels of the FgfR2IIIc isoform expression (Fig. 6.16A). Alternative splicing mechanism commits cells to express either one or the other form of the receptor, but not both (Holzmann et al., 2012). Therefore, detection of both receptor isoforms suggests a mixed population of cells or residual contaminating cells, such as meningeal or blood vessels' cells.

.

A

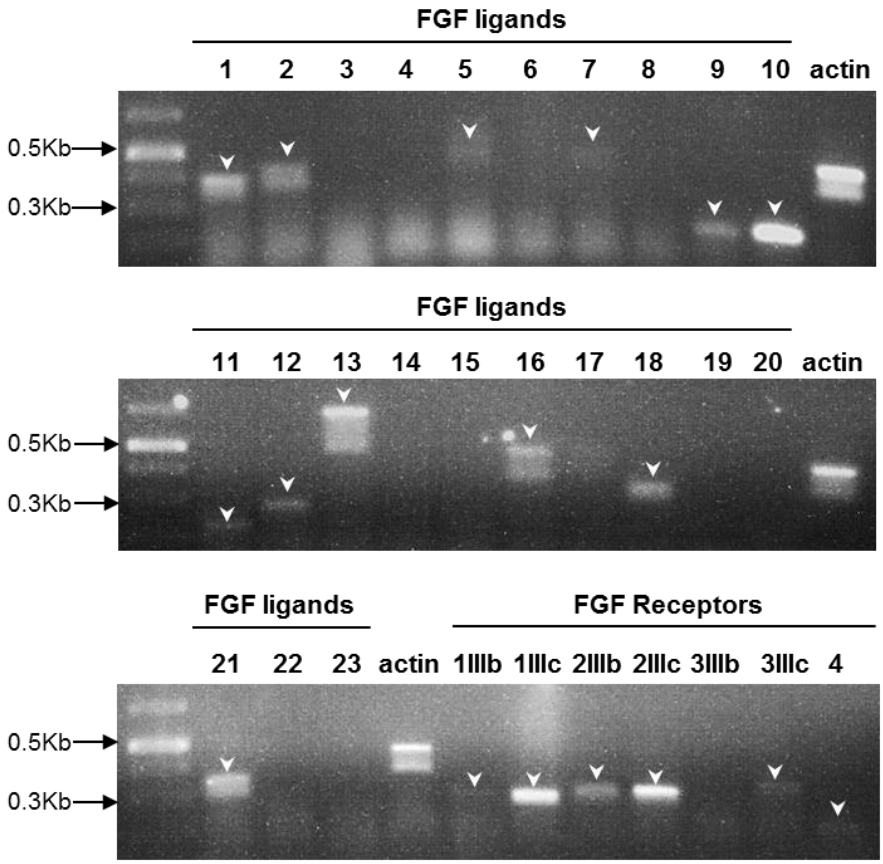

B

	FGF LIGANDS														
	1	2	5	7	9	10	11	12	13	14	16	17	18	20	21
in vitro	+++	++	+	+	++	+++	++	++	+++		++		++		++
in vivo	++	+		+	+	++	++	++	+	+		+	+++	+	

Figure 6.16 Characterisation of expression of Fgfs and FgfRs in a culture of hypothalamic monolayer. (A) Semi-quantitative RT-PCR profiling of Fgf ligands and receptors in the primary hypothalamic monolayer. (B) Table comparing the Fgf expression patterns *in vitro* to the ones found *in vivo*; note that the *in vivo* data was generated and provided by members of Dr Hajihosseini laboratory.

Part 6.5 Testing the transfection efficiency of cultured primary hypothalamic cells

The suspension culture of neurospheres is often difficult to transfect with plasmid DNA. Therefore establishment of the primary hypothalamic monolayers aimed to provide an alternative tool to study the biology of the Fgf10 expressing hypothalamic cells and investigate a role of FGF10 within tanycytes.

To investigate whether the monolayer of primary hypothalamic cells can undergo successful DNA transfection, cultures established from adult WT mice (age P28) were transiently transfected with mammalian vectors used in previous studies (see Chapter 4), i.e. FGF10 tagged to HA (rFGF10-HA) and its mutant version G145E (G145E-HA), as well as a control mCherry. Similarly to the previous studies, the mCherry protein was ubiquitously distributed around the cell (Fig. 6.17A), whereas FGF10HA was present in both, cell nucleus and cell cytoplasm to various degrees, depending on a cell (Fig. 6.17B). As with other cell types, the G145E mutant showed nuclear exclusion (Fig. 6.17C) (see Chapter 4).

Overall, these results showed that the primary hypothalamic monolayers can undergo successful cell transfection and could therefore be used in the future, in further molecular manipulation. Moreover, it was found that FGF10HA (but not its mutant version, G145E) was transported into the cell nucleus of this specific type of cells.

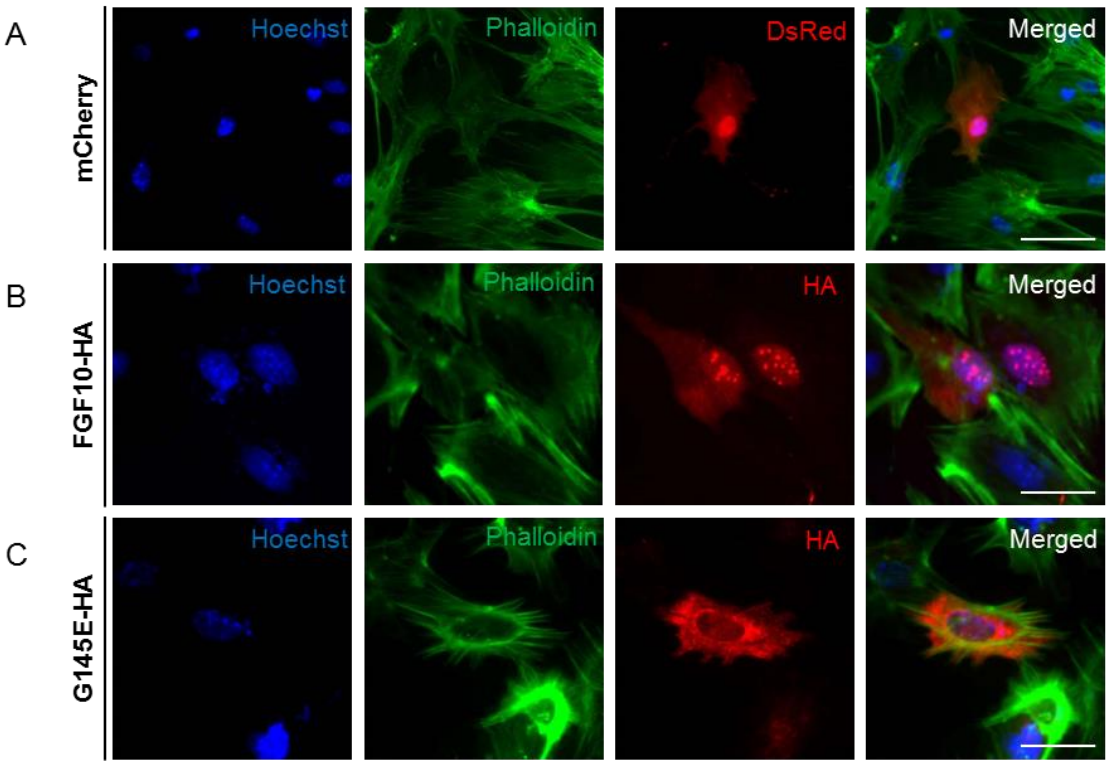

Figure 6.17 Successful transient transfection of the primary hypothalamic culture with DNA plasmids. (A) Transiently transfected mCherry is found ubiquitously present around the cell, detected by DsRed immunolabelling. (B) The HA immunofluorescence showed that FGF10 was found present in a cell nucleus of the hypothalamic cells. (C) Transiently transfected G145E is excluded from the nucleus and retained in a cell cytoplasm, determined by the HA immunofluorescence in the

Part 6.6 Discussion

With the use of the Fgf10-LacZ (Hajihosseini et al., 2008) and the Fgf10-tomato (El Agha et al., 2012, Haan et al., 2013) transgenic mice, it has been established that Fgf10 is expressed by hypothalamic cells called tanycytes, which display the characteristics of stem/progenitor cells.

Studies of the gene function *in vivo*, through conditional gene deletion, knock-out or overexpression are often very laborious, costly and require long time scale for analysis. Therefore *in vitro* systems mimicking the *in vivo* conditions, provide greater experimental flexibility, and generate strong predictions that can be subsequently related to the *in vivo* work. In this study, primary hypothalamic cells were cultured by two means – the commonly used NSC assay, known as 'the neurospheres', or as an adherent monolayer system. These cultures were derived from Fgf10-LacZ and Fgf10-tomato transgenic (reporter mice, previously used to study Fgf10 *in vivo*) and used to analyse whether Fgf10 expressing cells cultured *in vitro* show NSC characteristics, in similar fashion to the *in vivo* cells.

Since the 1990's, when the culture conditions for the stem cells derived from mammalian central nervous system (CNS) were first described (Reynolds and Weiss, 1992), the neurosphere assay has become a frequently adopted method to isolate, enrich and expand NSC *in vitro* (Gil-Perotin et al., 2013). Furthermore, neurospheres derived from adult mouse hypothalamus have been described in literature, where they were shown to retain all of the properties of the stem cells, i.e. multipotency, expression of stem cell markers, self-propagation and differentiation into functional neurons. However, the exact origin of these cells within hypothalamus itself was not defined (Cortes-Campos et al., 2015, Sousa-Ferreira et al., 2011). Here, it was demonstrated that neurospheres can be successfully cultured and expanded from hypothalamic (and SVZ) cells derived from adult Fgf10-tomato transgenic mouse. Importantly, the Fgf10-tomato expressing cells formed neurospheres, which possessed stem cell-like characteristics, including expression of stem cell markers Sox2 and Nestin, multipotency and self-renewal properties with the ability to undergo passaging. Therefore, these Fgf10-expressing neurospheres were most likely derived from Fgf10-expressing cell lineage within hypothalamus, i.e. the proliferative β tanycytes residing within median eminence, which were shown to possess similar properties *in vivo* (Haan et al., 2013).

Cultures of primary cells, unlike cell lines, have a restricted and predetermined number of cell divisions before entering senescence, therefore the number of times a primary cell culture can be passaged is limited (Jensen and Parmar, 2006). Analysis of neurosphere passaging revealed that cultures derived from the control WT SVZ, WT

hypothalamus and Fgf10-tomato SVZ showed very similar growth rate during subsequent passages. Conversely, cultures derived from the Fgf10-tomato positive hypothalamus showed delayed growth rate in comparison to the other assays and could not be passaged to the same extent as the control cultures derived from the WT hypothalamus. The knock-in allele of the Fgf10-creERT2 results in the reduction of the Fgf10 mRNA levels even up to 50% (El Agha et al., 2012). Hypomorphic Fgf10 mice and humans display defects within multiple organs and tissues (e.g. malformations of ocular glands, ears, teeth, kidney, respiratory system and genitalia) (see Chapter4, part 4.2) suggesting developmental problems. It is therefore possible that lower levels of FGF10 during embryogenesis had further implications on the normal development of the brain, affecting also the adult tissue. Therefore knock-down of FGF10 within neurosphere cultures, derived from Fgf10-tomato mouse, could putatively affect their stem cell properties of self-propagation. Alternatively, expression of Fgf10 could have decreased the survival rate of the seeded cells resulting in lower proliferation potential rather than affect the cell division. To investigate further the effect of FGF10 and validate results observed here, it would be necessary to generate a conditional FGF10-knock out neurospheres and investigate their propagation capacity, comparing to the WT.

Due to several limitations, the neurosphere assay is not an ideal system to study the role of FGF10 in the hypothalamic cells. Some of the spheres may not be clonal structures, but instead are chimeric in nature and composed of small number of stem cells and greater number of stem progenitors and differentiated cells (Bez et al., 2003), similarly to the neurogenic niches observed *in vivo*. The precursors, or "trans-amplifying" cells also can give rise to neurospheres in the culture, generating difficulties in depicting the true stem cells from the neurosphere population (Pastrana et al., 2011). Moreover, neurospheres (and NCS in general) are highly motile, dynamic structures and demonstrate a spontaneous locomotion, partly induced by beating cellular surface processes. Studies performed have observed the movement of neurospheres within cell suspension even when a culture was left untouched in an incubator, removing the factor of "induced motility" generated by movement of the culture dishes. Moreover, time-lapse imaging studies have shown that neurospheres migrate around, interact and generate aggregates even at low cell densities (Ladiwala et al., 2012). Neurospheres therefore frequently 'fuse' or 'merge' together (Fig. 6.6) producing an inherent error in the experimental assay in terms of clonality, size and growth rate (Mori et al., 2006, Coles-Takabe et al., 2008). To overcome these issues it would be important to purify the hypothalamic Fgf10 expressing cells from the remaining in the culture. However, attempts to use FACS sorting have proven unsuccessful, because conditionally induced reporter expression through *in vivo*

tamoxifen pulsing resulted in small number of Fgf10-tomato expressing hypothalamic cells in proportion to the reporter negative cells, generating very high noise-to-signal ratio (Fig. 6.5). Moreover any sorted cells struggled to survive due to very low cell plating density.

The encountered limitations of the neurosphere assay have led to generation of an adherent monolayer culture. Compared with neurospheres, the monolayer of cells may represent more homogenous population of undifferentiated cells, because of their uniform exposure to the growth factors and nutrients within the culture medium (Bez et al., 2003). Neurospheres display a population of the NCS at the periphery of the sphere (Bez et al., 2003, Babu et al., 2007), with differentiated cells present within the centre, which have limited contact with the growth factors and other nutrients, allowing differentiation to occur. Therefore, monolayer cultures are more likely to undergo symmetrical cell division and are less likely to undergo spontaneous differentiation (Conti et al., 2005).

Importantly, the monolayer culture is more accessible to any drug treatments and DNA transfections therefore serve as a great tool to study role of FGF10 in hypothalamic tanycytes. Although monolayer cultures of NSC have already been described, derived from denate gyrus (Babu et al., 2011), SVZ and olfactory bulb (Theus et al., 2012). However, the culture of hypothalamic tanycytes, cultured as stem cells, is unique to this study.

An age-related decline in neurogenesis has been confirmed *in vivo* in mice and rats (Bizon and Gallagher, 2003, McDonald and Wojtowicz, 2005, Jin et al., 2003), and therefore the neurogenic potential of the adult brain is the greatest in young animal and decreases with the age. However, the exact mechanisms that to lead to such a decline are yet unclear - perhaps the reduction in proliferative activity is a consequence of a lengthening of the cell cycle time or an inherent dwindling of the proliferative cell population (Abrous et al., 2005). Moreover, the decline in proliferative cells has been noted *in vivo* specifically in the murine hypothalamus (Haan et al., 2013).

The results presented here complement the *in vivo* studies and primary hypothalamic monolayer cell cultures established from the young mice of postnatal age of day 8 (P8) generated more and large colonies than cultures obtained from young adult mice of age around P30 and P40 (Fig. 6.7). Furthermore, in agreement with the neurosphere assays, the monolayer culture shows that there is a heterogeneous population of stem/progenitor cells in the postnatal hypothalamus, because two different populations of cells, expressing and not-expressing Fgf10, are able to self-propagate, are multipotent and express stem cell markers. Similar observations have been made *in vivo* and there is a dispute over where the exact

niche of stem cells resides within hypothalamus (Hajihosseini et al., 2008, Haan et al., 2013, Robins et al., 2013, Li et al., 2012a). It appears likely that the Fgf10-non expressing cells cultured *in vitro* originate from the population of proliferative parenchymal cells (Li et al., 2012a) or cells that are located more dorsally around the ventricle, called α tanycytes (Robins et al., 2013), as both of these cell niches do not express Fgf10, but have been shown to proliferate *in vivo*.

In order to assess the propagation potential of the cultured putative stem/progenitor cells, size of the generated Fgf10-expressing and non-expressing patches was compared. Cultures of Fgf10 reporter negative and positive cells were derived from the same mice, grown under identical conditions and were seeded simultaneously, therefore the cell growth rate can be compared directly. The size of the patch obtained is a balance between rate of the cell division, mode of the division (either symmetric or asymmetric), cell survival and differentiation of the progeny. Although small patches of either Fgf10-expressing or Fgf10-non expressing cells observed were speculated to have arisen through several means, such as asymmetric cell division, cell differentiation or cell death, the middle sized (6-50 cells) and bigger patches (51+) of cells were assumed an evidence of symmetrical division of cell progenitors. Number and size of these patches were putatively an indication of cell proliferation potential. The difference in this cell proliferation potential between the Fgf10-expressing and Fgf10 negative cells was most prominent at the cultures derived from the very young mice (P8) (Fig. 6.9). At this stage, the Fgf10-negative cells were very abundant and divided rapidly, whereas only small proportion of Fgf10-expressing cells was able to proliferate at similar rate and gave rise to big patches. The proliferative potential difference, between the two populations, was somehow lesser at the later ages of a mouse (P30-P40), where the propagation of the Fgf10-negative and Fgf10-positive cells is closely comparable (Fig. 6.9). This suggests that Fgf10-negative cells might not be able to sustain their proliferative potential with the age.

In general, the number of LacZ-positive cell patches was lower than the LacZ-negative regardless of the age of the mouse (Fig. 6.7B,C). It is possible that more LacZ-negative than LacZ-positive cells were present at seeding, suggesting that there might be more LacZ-negative mitotically active cells present in the hypothalamus *in vivo*. Alternatively, expression of Fgf10 marked by the LacZ reporter, could have decreased the plating efficiency of the cells by affecting their survival rate, even potentially inducing cell death. The remaining possibility is that expression of Fgf10 affects the cell cycle and controls the rate of cell division, therefore resulting in lower number and smaller patches.

Despite the fact that Fgf10-expressing cells do not give rise to big patches to the same extent that Fgf10 non-expressing cells do, there is little variation between

different ages of mice. Therefore, regardless of the age of the mouse, in comparison to Fgf10-negative cells the Fgf10-expressing cells proliferate at a slow but constant rate (Fig. 6.9). On the contrary, the Fgf10-non expressing cells proliferate very rapidly at early age of a mouse, but lose their proliferative potential as the mouse ages (Fig. 6.9). To further explore the proliferative capabilities of the two populations, an experiment could be performed culturing cells derived from mice older than P40 (ranging from young adults, mature, old to very old mice). The prediction would be that the differences in the proliferation potential of each culture would reduce with the age of the mouse. Moreover, assuming that Fgf10-non expressing cells decline in their propagation potential at a greater rate than the Fgf10-expressing cells (that remain relatively constant), potentially, at older mouse ages, the Fgf10-expressing cells could show greater proliferative potential than Fgf10-negative cells.

Adult stem cells *in vivo* are slow dividing, with a very long cell cycle and are sometimes considered even quiescent. However, when stimulated (chemically or through injury) they become rapidly activated and generate rapidly proliferating neural cell precursors (Seri et al., 2001, Kuo et al., 2006). Strict regulation of the cell cycle of stem cells prevents build-up of neurons, potentially resulting in tumours and cancer (Williams et al., 2015). Besides stem or progenitor cells, each neurogenic niche of an adult brain contains a population of fast amplifying precursors, displaying all the characteristics of stem cells, i.e. markers of stem-cellness, multipotency and self-renewal through cell division, however they also have limited life span and are more committed than stem cells (Abrous et al., 2005). The population of these trans-amplifying cell precursors is maintained by the stem/progenitor cells. Due to their slow (however constant) dividing character *in vitro*, the Fgf10-expressing cells potentially could be a population of the stem/progenitor cells, whereas the fast dividing Fgf10-non expressing cells could arise from the population of precursor cells - rapidly dividing at young age of the mouse but losing their proliferation potential with the age of the mouse. Furthermore, both cell populations within the culture were shown to undergo successful passaging (Fig. 6.14), which further demonstrates their proliferative potential. However, it would be important to determine whether the cultures derived from different ages display the same passaging potential. Additionally, the number of passages, that each of the populations (Fgf10 expressing and non-expressing) is able to sustain would also provide the information about self-renewal properties of the cells cultured, and could provide a more comprehensive view on the differences between populations.

To further determine the identity of cultured hypothalamic monolayers, the cells were assessed for expression of neural stem/progenitor cell markers. Both of the two populations, the Fgf10-positive and Fgf10-negative, showed expression of Sox2 and

Nestin (Fig. 6.12), which are common markers of stem cells (Feng et al., 1994) and corresponds to the *in vivo* studies of hypothalamic tanycytes (Haan et al., 2013). However, numerous Fgf10-negative cells expressed BLBP (Fig. 6.12), which is not detected in the Fgf10-positive cells. BLBP is a marker of radial glia cells, *in vivo* it is known to participate in a signaling pathway that is critical for differentiating neurons (Retrosi et al., 2011). Therefore, it is likely to be detected within the trans-amplifying cell precursors, further supporting the theory that the Fgf10-negative cell population constitutes a population of cell precursors.

Important aspect defying stem cells is multipotency and differentiation potential. In the provided culture conditions small proportion of the Fgf10-reporter positive and negative cells is able to differentiate into all three neural cell lineages: neurons, astrocytes and oligodendrocytes (Fig. 6.15). However, a difference was noted in the numbers of differentiated cells, where the majority of Fgf10-negative cells displayed the differentiation markers and Fgf10-positive cells showed minor levels of differentiation. In the given culture conditions, the Fgf10-expressing cells potentially are maintaining their stem-cell identity, while the Fgf10 negative cells as “progenitor cells” struggle to sustain their stem-cellness and therefore readily differentiate. Furthermore, the culture conditions and media composition have a significant impact not only on current state of the cell, but can also affect the differentiation potential of the culture (Reynolds and Weiss, 1996a). For example, culture media containing Brain-derived neurotrophic factor (BDNF) and Sonic Hedgehog (Shh) stimulate NSC to differentiate into neurons (Babu et al., 2007) and Platelet-derived growth factor (PDGF) promotes survival of oligodendrocytes and therefore stimulates their differentiation in the culture (Gogate et al., 1994). Furthermore it was shown that treatment of cortical precursors with FGF8b isoform stimulated the differentiation of astrocytic lineage of cells (Hajihosseini and Dickson, 1999). At the moment, the characterisation of the two different hypothalamic populations of cells (Fgf10-expressing and not expressing) is preliminary. Therefore, it is possible that these cells respond differently to culture composition and may show a varied differentiation potential if treated at a wide range of specific conditions, which would require further detailed investigation, beyond the scope of this project.

The hypothalamic monolayer culture system was set up to be used as a tool aiding *in vivo* studies decrypting the function of FGF10 in the hypothalamus. To gain a comprehensive view on the *in vitro* system and its resemblance to the *in vivo* processes, the culture was assessed for expression of all Fgf factors and their receptors in a sub-quantified manner using RT-PCR and related to the data obtained from acutely extracted hypothalamic tissue (Hajihosseini’s lab, unpublished data). Although the *in vitro* cultures are not the exact replica of the processes taking place *in*

vivo, and existing differences should not be disregarded, nonetheless the profiling results showed that expression of Fgf ligands and their receptors majorly corresponds *in vitro* and *in vivo*. Importantly, the members of the FGF10 subfamily, the FGF3 and FGF22 were fully absent *in vitro* and *in vivo*, and FGF7 was expressed at very low, barely detectable levels. Therefore, unlike in some other systems, e.g. ear (Wright and Mansour, 2003), teeth (Harada et al., 1999) and developing salivary and lacrimal buds (Govindarajan et al., 2000), FGF10's role in hypothalamus is not complemented by the members of its subfamily, highlighting its importance in this brain region. Interestingly, the expression of Fgf10 *in vitro* is the strongest of all of the FGFs, with similar pattern seen *in vivo*, that further highlights its importance in this brain region. However, this assay detects the transcript levels and does not provide information about amount of the protein actually generated. Ideally, the levels of each FGF protein would be measured, detecting the ligands with protein specific antibodies, which currently are majorly unavailable. Furthermore, it is possible that FGF10 acts in cooperation with other FGFs to maintain the neurogenic niche, for example FGF2 was shown to promote neural cell proliferation *in vivo* and *in vitro* (Woodbury and Ikezu, 2014). The exact roles of other FGFs and their receptors in the hypothalamic neurogenic niche are still yet to be discovered.

The exact function of FGF10 in hypothalamus, *in vivo* or *in vitro* is still not fully determined and unclear. From the transfection studies, with the FGF10HA construct, and basing on the evidence from the previous studies in different cell types (see Chapters 3, 4 & 5), it is possible that FGF10 serves an intracrine role, acting within the cell nucleus. Earlier, it was proposed that the nuclear FGF10 negatively regulated the cell cycle, maintained slow cell growth and lowered the cell proliferation rate within the epithelial and differentiating mesenchymal cells. This data potentially coincides with the results of the Fgf10-expressing population of hypothalamic cells, which show slow proliferation rate in respect to the Fgf10-non expressing cells.

Here it is shown that the monolayer culture can be transiently transfected, which provides a great potential for further experiments. It might be used to generate a FGF10 overexpression system to analyse the result of its function in the cultured cells. Moreover, if the FGF10 nuclear function involves binding to other molecules, the tagged FGF10 protein could be used in immunoprecipitation experiments to pull down FGF10's binding partners. This would provide a very useful indicative of its functioning pathway *in vivo*.

The transiently transfected FGF10HA was found to translocate into the cell nucleus within the hypothalamic culture, providing basis for assumption that a pool of endogenously made FGF10 is also able to enter cell nucleus of this specific cell type. Therefore, it is possible that the observed differences between the Fgf10-expressing

and Fgf10-non expressing populations of cell cultures result from the nuclear function of FGF10. Low levels of expression of the FgfR2IIIb *in vitro*, which could have resulted from residue contamination of epithelial meningeal cells, as well as negligible expression of the receptor *in vivo* (Hajihosseini et al., 2008) further could suggest an intracrine/nuclear function of FGF10 within this cell population. Alternatively, secreted FGF10 acts, through so far undescribed mechanisms, on the population of the Fgf10-non expressing cells promoting their proliferation or regulating differentiation. Possibly, these cells express the FgfR2IIIb (although at a very low levels), allowing the typical FGF10-FGFR2IIIb signalling pathway. Secreted FGF10 is known to stimulate proliferation of cardiomyocytes (Rochais et al., 2014), cochlear epithelium (Urness et al., 2015) as well as some endothelial and tumour cells (Sugimoto et al., 2014). However, the FGF10 signalling occurs in a dose dependent manner of receptor ligand levels, therefore judging by the negligible receptor transcript levels it is unlikely to generate a prominent effect through this pathway. Nonetheless, although implausible, until proven so, this theory cannot be discarded. To clarify the receptor presence, the two populations would require separation and individual profiling for the ligands and receptors, ideally with the determination of protein levels as well.

Furthermore, it is possible that FGF10 is generated by the tanycytes but functions away from the hypothalamus. Potentially, the β-tanycytes secrete FGF10 either: to the 3V cavity, where it is uptaken by other cells; and/or into the blood capillaries lying beneath hypothalamus, where FGF10 serves its function, for example in the pituitary gland, lying underneath hypothalamus. On the contrary mature and secreted FGF10 as a typical paracrine protein it is relatively unstable (Buchtova et al., 2015), therefore unlikely to sustain long-distance signalling. However, until tested it should not be discarded as an option.

Chapter 7

General Discussion

FGF10 deficient mice die shortly after birth demonstrating that this protein plays an essential part during normal mammalian development. It is essential for development and maintenance of multiple organs, including limbs, lungs, heart, liver, kidney, ocular and salivary glands, thymus, white adipose tissue, liver, inner ear, brain, teeth and the trachea (Itoh and Ohta, 2014). Furthermore, FGF10 is also expressed postnatally in vital adult tissues, such as brain (Hajihosseini et al., 2008), and is an important factor involved in the oncogenicity of pancreatic and breast cancer cells (Nomura et al., 2008, Theodorou et al., 2004) as well as in ameloblastoma and tumour formation (Nakao et al., 2013, Sugimoto et al., 2014). Importantly, mice phenotypes caused by the FGF10 knockout closely resemble those observed in FGFR2IIIb knockout mice, implying that FGF10-FGFR2IIIb signalling underlies much of Fgf10's effects during the normal mouse multi-organ development. A few discrepancies in the FGF10 and FGFR2IIIb knockout phenotypes have been noted, but this may be explained by ligand or receptor redundancy (Ornitz and Itoh, 2015).

In addition to their paracrine role, several FGFs are thought to function cell-autonomously through intracellular interactions with other molecules. For example, FGF1 binds to acidic FGF intracellular binding protein (FIBP) (Kolpakova et al., 1998) and mortalin (Mizukoshi et al., 1999) in the cytoplasm. Furthermore, FGFR1 and FGF2 have been found within cell nucleus where they function to promote pancreatic cancer cell invasion (Coleman et al., 2014). Therefore, it is possible that FGF10 also possesses cell-autonomous intracellular function/s.

This study investigated whether FGF10 translocates into the cell nucleus, and if so, what are the mechanisms that promote its nuclear transport. Furthermore, as a follow on question, it was explored whether nuclear FGF10 serves a functional role affecting cell proliferation or cell survival.

Part 7.1 Nuclear transport of FGF10

A previous study showed that, when applied exogeneously, recombinant-FGF10 can be taken up by urothelial cells and translocate into the cell nucleus (Bagai et al., 2002, Kosman et al., 2007). By contrast, the studies presented here mimicked the in vivo situation to show that FGF10 can enter the nucleus of cells in which it has been over-expressed. Often FGFs behave in a cell-specific manner but here it was shown that nuclear entry of FGF10 can occur in multiple cell types, including human epithelial (ARPEs), mesenchymal chondroprogenitors (ATDC5s), human embryonic kidney (HEK 293Ts) as well as primary astrocytes and tanycytes (Fig. 4.4). Therefore,

at the molecular level, nuclear translocation of FGF10 appears to be a universal process.

The most commonly observed nuclear import pathway involves the newly translated and fully folded protein being directly translocated into the nucleus (Fig. 7.1A), an example of which includes proteins involved in DNA damage response, such as Rif1 (Xu and Blackburn, 2004), or transcription factors, for instance GATA (Hunter et al., 2014). Moreover, both HMW and LMW isoforms of FGF2 translocate endogenously into the cell nucleus (Quarto et al., 1991, Dell'Era et al., 1991). Typically, secreted proteins possess an N-terminal signal peptide (SP) that targets the newly synthesised protein towards the secretory pathway. For this instance, a secretory FGF3 besides its SP also possess multiple weak NLS-like motifs, some of which are driving the nuclear translocation and others only facilitate the process in subsequent stages, therefore allow the competition between protein secretion and nuclear import (Kiefer and Dickson, 1995a). FGF3 and FGF10, as close relatives, share a lot of structural, biochemical and functional properties (see Chapter 1). Interestingly, one of the FGF10 NLSs characterised in this study (the NLS2) is homologous to one of the NLS-like motifs present in FGF3 (Fig. 3.3). It is therefore tempting to speculate that FGF10, in similar fashion to FGF3, is endogenously transported into the cell nucleus, distributing the pool of protein molecules between the nuclear and secretory pathway.

Alternatively, the protein becomes secreted from the cell and subsequently binds to the receptor present on the cell surface, which then causes its internalisation (endocytosis) back into cytoplasm, leading to nuclear import, which can take place with (Fig. 7.1C), or without the receptor (Fig. 7.1B). For example, the endocytosis of the FGF1 protein is stimulated only by binding to FGFR1 or FGFR4, and the protein-receptor internalisation is independent of the receptor's tyrosine kinase domain activity (Sorensen et al., 2006). Furthermore, FGF2 was shown to co-localise in the nucleus of pancreatic cancer cells together with FGFR1. The complex was specifically located at sites of RNA polymerase II mediated transcription, suggesting its role in regulation of gene transcription involved in cell proliferation (Coleman et al., 2014). Simultaneously, non-receptor bound FGF2 was found in the cell nucleolus, and it was speculated that FGF2, present within distinct regions of cell nuclei, potentially triggers distinct biological effects either with or without its receptor (Coleman et al., 2014), which adds another complexity to the system. Interestingly, externally applied to urothelial cells FGF10 was thought to co-localise in the nucleus with its cognate FGFR2IIIb receptor (Kosman et al., 2007), which does not discredit the fact the protein might also localise in the nucleus in a receptor-independent manner.

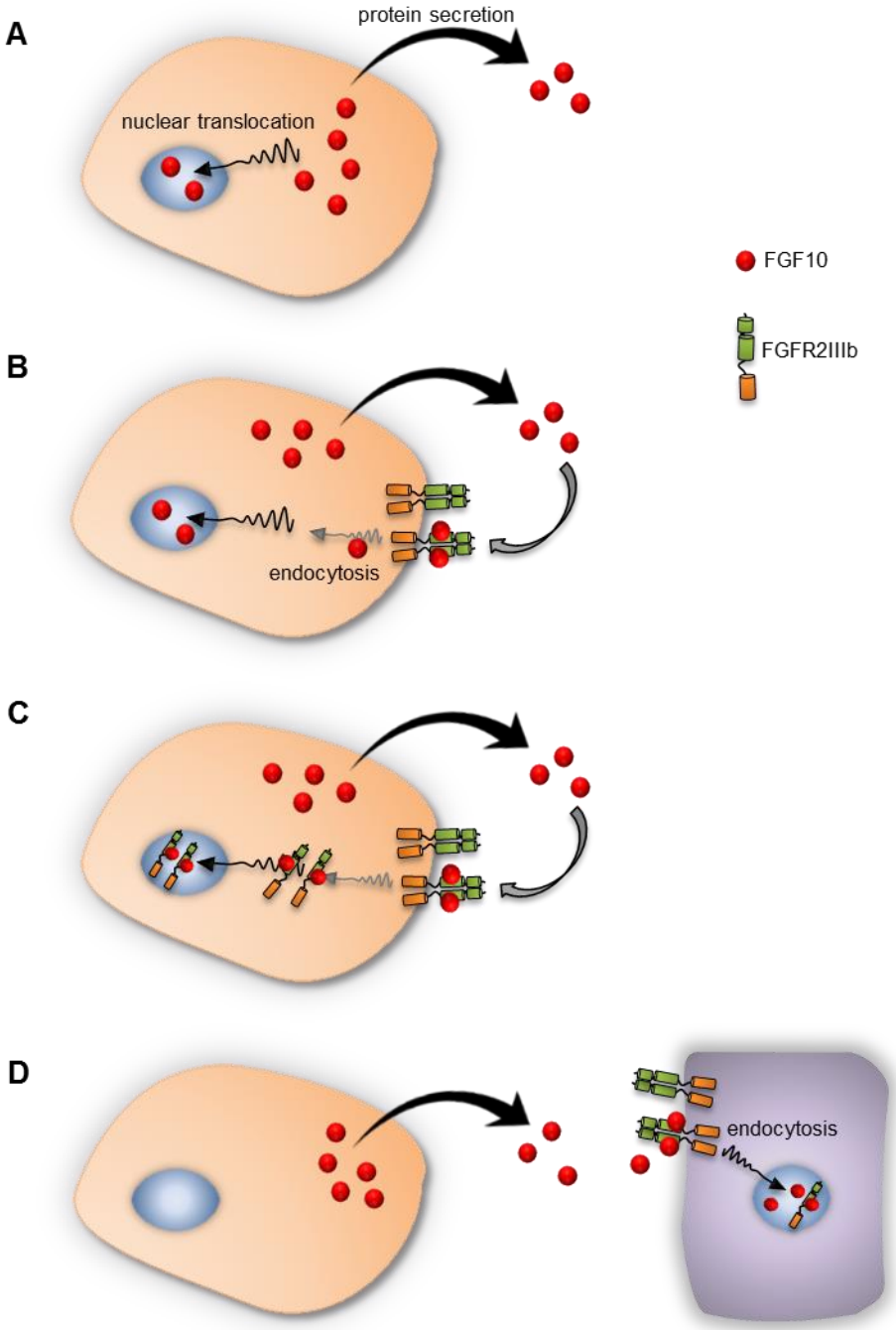

Figure 7.1 Models of potential pathways of nuclear transport regarding secreted proteins. (A) Paracrine and endocrine signalling signifies secretion of a ligand by one cell that then binds to a receptor present on a surface of a different cell, triggering downstream signalling events. (B) Autocrine signalling is generated by cells that bind through the receptors their own secreted ligands. The ligand then might undergo endocytosis and be transported to the cell nucleus (C) Upon binding of the ligand, the receptor might also undergo internalisation and be transported to the nucleus, potentially in a complex with the ligand. (D) Alternatively, a secreted protein can bind to adjacent cell, where it becomes endocytosed and potentially translocated into cell nucleus.

Additionally, secreted protein, binding to the receptor present on the adjacent cell, subsequently becomes endocytosed (with or without the receptor) and translocated into the nucleus (Fig. 7.1D). If this would be true for FGF10, it would result in FGF10's double effect on the epithelial cells – the classical activation of receptor TK phosphorylation at cell surface and then the intracellular, from the cell nucleus. Although this scenario is probable, and should be taken into consideration, it is tempting to speculate that nuclear FGF10 is more likely to act in a cell-autonomous manner (see Chapter 4).

7.1.1 Is the nuclear transport of FGF10 mediated by NLS1 and/or NLS2?

The classical nuclear import of proteins occurs via interactions with adapter proteins, known as karyopherins (or importins) (see Chapter 1) (Fig. 1.10). FGF1, FGF2 and FGF3 were all shown to possess more than one NLS (Wesche et al., 2005b, Sheng, 2004, Kiefer and Dickson, 1995a). FGF10 was proposed to contain a NLS (here named NLS1), which resembles, but is not homologous to NLS found in FGF1 (Kosman et al., 2007). In this study, through bioinformatics analysis, a second NLS was identified within FGF10's sequence (here named NLS2), positioned within its carboxyl terminus (Fig. 3.2). The two NLSs were found positioned in a close proximity in the protein's three dimensional structure, and directly interacting via an H-bond. H-bond represents one of the strongest molecular interactions shown crucial for protein folding and protein structure. Moreover, H-bonds have also been found to play a role in molecular recognition and interactions with other proteins (Nick Pace et al., 2014, Huang et al., 2014). On this premise, it was hypothesized whether FGF10's NLS1 and NLS2 cooperated to facilitate its interactions with importin molecules and consequently its nuclear import.

Kosman and colleagues found that mutation of basic residues within NLS1, which typically promote binding to importins, diminishes, but does not abrogate FGF10's nuclear localization (Kosman et al., 2007). By contrast, here it was recognised that human G138E mutation was positioned within the NLS1 (Fig. 4.5). This mutation is known to cause LADD syndrome in humans, but the molecular mechanisms responsible for this phenotype have been so far undescribed (Entesarian et al., 2007). Analysis of this mutation, modelled within the equivalent rat protein (G145E) *in vitro*, revealed that the mutation results in protein's nuclear exclusion. Although, the possibility that G145E encodes an unstable protein targeted for rapid degradation cannot be excluded, the results suggest that the mutation attenuates the process of FGF10 secretion and causes protein's retention at ER, which is subsequently coupled to abrogation of its novel nuclear trafficking role (see Chapter 4). On the contrary, each

ligand is known to interact with the D2 domain of a second receptor through a secondary receptor binding site (Ibrahimi et al., 2005). G145E may potentially fall within this site, reducing the receptor dimerization and signalling without affecting ligand–receptor binding. However, the results suggest rather that the mutation leads to FGF10's structural and folding complications, resulting in hyperglycosylation and cytoplasmic retention. Therefore, it is possible that the observed LADD phenotypes caused by G138E are a result of abrogation of two separate FGF10 functioning pathways, i.e. indirect attenuation of paracrine signalling in epithelial cells due to reduced FGF10 secretion and/or abolition of receptor dimerization, as well as diminished endogenous FGF10 function/s.

By comparison with NLS1, mutation of residues within the NLS2, especially the 4T-NLS2, also seem to abrogate the FGF10 nuclear localization, but most likely through disruption to the nuclear transport pathway mediated by importin/s (see Chapter 3 & 4). Mutation of two basic residues within this sequence already significantly diminishes the protein's nuclear import and further mutation results in complete nuclear exclusion. Regardless that NLS2 was predicted as a non-classical and weak NLS (see Chapter 3), the experimental results suggest this sequence acts via binding to the importins, but the direct protein interaction remains to be demonstrated. Similarly to mutation of NLS1, a possibility that the 4T-NLS2 affects protein structure and folding and therefore targets it for early degradation, cannot be disregarded. In similarity to G145E mutation, the 4T-NLS2 may also undergo hyperglycosylation (Fig. 4.14). However, the results also show that, unlike G145E, the 4T-NLS2 does follow the secretory pathway, therefore most likely retains its paracrine function (Fig. 4.15). Furthermore, it cannot be yet discarded that FGF10 might interact via NLS2 with a different nuclear-import chaperone, in an importin independent fashion. For example, a ribosomal protein called Rpl5 was found to translocate into the nucleus via an adaptor protein named symportin-1 (Syo1) and calmodulin was shown to act as a nuclear import chaperone, for several transcription factors, such as Non-histone chromosomal protein 6A (Nhp6Ap) (Hanover et al., 2007) and Sox9 (Argentaro et al., 2003). Nonetheless, mutations within the NLS2 demonstrate that integrity of this sequence is essential for the nuclear import of FGF10.

Although both G145E and 4T-NLS2 mutations result in nuclear protein exclusion, the results suggest it occurs via different molecular mechanisms. Moreover, it appears that NLS2 is essential to target the protein into the nucleus, but it is possible that the NLS1 facilitates and aids the process further (Fig. 7.2).

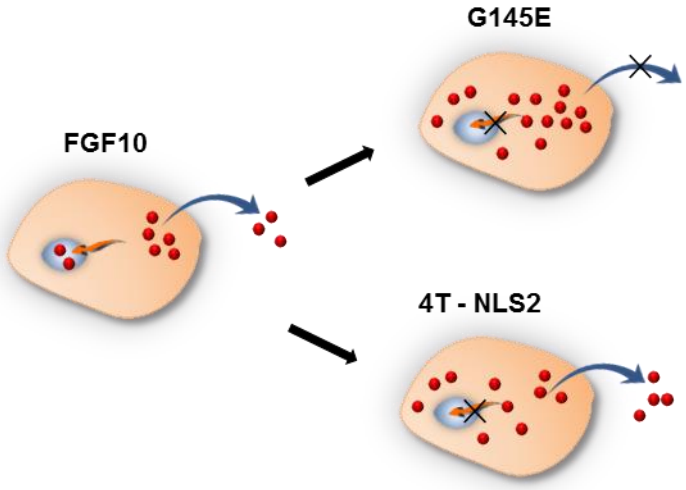

Figure 7.2 Representation of the effects caused by FGF10 mutations. FGF10 (represented as red dots) follows the secretory pathway and is released from the cell and it was found translocated into cell nucleus. The LADD-mimicking G145E mutant falling into the NLS1 sequence abolished the nuclear transport pathway and, moreover, was not found to progress through the secretory pathway, making the protein cytoplasmically retained and fully abolishing its secretory and nuclear role. On the contrary, the 4T-NLS2 mutation prevented the protein from entering the nucleus but did not disrupt its secretion, potentially allowing its receptor-mediated signalling.

7.1.2 Are there other factors potentially affecting nuclear transport of FGF10?

In addition to the NLS-karyopherins nuclear import pathway, there are other known factors that could influence protein intracellular distribution. A range of post-translational modifications (PTM) have been shown to either promote or prevent nuclear import of various proteins. These are known to fine tune the biochemical reactions taking place between protein cargo and its chaperone/s by up- or downregulating already occurring basal levels of nuclear transport. For example, methylation of specific arginine residues is essential for the nuclear accumulation of the HMW, but not the LMW isoform of FGF2. Inhibition of methylation resulted in reduction of HMW FGF2 nuclear accumulation (Pintucci et al., 1996).

Glycosylation is an important form of PTM, that was shown to influence protein's nuclear import in a process employing molecules called lectins (Monsigny et al., 2004). Modification of glycosylation status of bovine serum albumin (BSA) have shown that glycosylation alone can drive protein's nuclear import in a cell cycle specific manner (Rondanino et al., 2003). Moreover, certain glycosylation patterns, especially those located in close proximity to a NLS, can potentially diminish the nuclear transport, as demonstrated by glycosylation of Serine residue residing in a close

proximity to NLS of Jun protein (Schlummer et al., 2006). Bioinformatics presented in Chapter 3 predicted about 26 putative glycosylation sites within FGF10 (Fig. 3.8), but only experimental investigation can pinpoint the key sites which could affect FGF10's intracellular distribution. Interestingly, it has been found that mutated FGF10 showing nuclear exclusion (G145E or 4T-NLS2) undergoes hyperglycosylation (Fig. 4.14). Possibly the hyperglycosylation prevents the protein from entering the cell nucleus, or alternatively the ER retention results in the protein's hyperglycosylation. Although, the hyperglycosylation is associated with protein's nuclear exclusion, as demonstrated by G145E mutant, it is possible that glycosylation of specific non-mutated sites actually aids in nuclear transport of FGF10.

Bioinformatics analysis identified a putative SUMOylation site present within rat and human FGF10 sequences but absent from mouse protein (Fig. 3.6). SUMOylation is known to play key roles in directing the nuclear import and localisation of transcription factors, for example sumoylated version of promyelocytic leukemia (PML) protein was detected in either sub-nuclear oncogenic domains or nuclear bodies (Freiman and Tjian, 2003). Similarly, LEF1 protein, which is a downstream effector of the Wnt signalling pathway, undergoes sequestration into nuclear bodies, regulated by SUMOylation (Sachdev et al., 2001). Therefore, SUMOylation appears to regulate the activity and function of transcription factors, through targeting them to specific transcription sites (Freiman and Tjian, 2003). The fact that FGF10's SUMOylation site most likely is not conserved among species (Fig. 3.6) (although some non-classical SUMOylation cannot be excluded), suggests that even if it aids the FGF10's nuclear transport, it may not be the main driving factor. However, this could account for species specific differences, and nuclear FGF10 potentially serves more predominant roles in rats and humans than in mice.

There are also other forms of PTMs that could potentially impact FGF10's nuclear import, for example phosphorylation, that is commonly known to either promote or inactivate biological pathways. This seems to be a protein specific event as, for example, phosphorylation within the NLS site can either promote or reduce strength of importin binding, in a residue dependent manner, which was shown in Epstein-Barr virus (EBV) nuclear antigen 1 (EBNA-1) protein (Kitamura et al., 2006). Moreover, in specific cases, phosphorylation was shown to enhance docking of cargos to the NPC, positioned upstream of an NLS may enhance its recognition by importins, as well as mask NLS recognition and cause protein's cellular retention (Nardozzi et al., 2010). It might be likely, that specific phosphorylation patterns further control the FGF10's intracellular localisation.

Part 7.2 Putative nuclear function of FGF10

Regardless of the dynamics and molecular mechanisms driving FGF10's nuclear import, transiently transfected rFGF10HA was found to translocate into the nucleus of a variety of cell types (Fig. 4.4). Paracrine FGF10 serves diverse roles during development and postnatally, but these could be accompanied by so far overlooked intracellular/nuclear role of the protein. It is possible that, targeting of FGF10 to the nucleus could play a critical stoichiometric role in regulating the normal level of paracrine FGF10 signalling, meaning that the amount of secreted FGF10, available for paracrine signalling in epithelial cells, could be titrated down by nuclear-targeted protein retention. FGF10 is known to act in a dose dependent manner (see Chapter 1), and for example genetic knockdown of Fgf10 in a mouse model of Apert syndrome rescues much defects caused by hyperactive receptor mutation (Hajihosseini et al., 2009). However, Fgf10 is expressed in brain regions, such as hypothalamus, which lacks expression of its cognate receptor, the FGFR2IIIb (Hajihosseini et al., 2008), suggesting non-paracrine FGF10 function in these tissues.

Nuclearly transported proteins play a variety of functions, which are often interlinked with protein's nuclear distribution. Although it cannot be excluded that nuclear transported FGF10 subsequently undergoes degradation, it is considered an unlikely event, since protein degradation pathways are also present within the cell cytoplasm, therefore making the nuclear-import pathway redundant. Moreover, nuclear FGF10HA was found to localise to specific loci, and co-localise with Fibrillarin (Fig. 4.2), which is a protein located in the dense fibrillar component (DFC) of the nucleolus, suggesting FGF10 might play a nucleolar function.

7.2.1 Putative nucleolar function of FGF10

Within eukaryotic cells, the nucleolus is considered the largest structure in the nucleus and it is commonly known as the site of ribosome synthesis and their assembly. The nucleolus is a non-membranous organelle, that is mainly composed of proteins and RNA molecules. Nucleolar accumulation of FGF10 (Fig. 4.2) could take place by interaction with another nucleolar protein causing indirectly its nucleolar retention. Alternatively FGF10 serves a particular nucleolar function. Since, the nucleolus is considered as the "ribosome factory", it is possible, that FGF10 serves a function affecting ribosomal biogenesis. Moreover, due to nucleolar sequestration processes of regulatory molecules, in response to specific environmental cues, many non-ribosomal proteins are captured and immobilized. Nuclear detention prevents proteins from interacting with their binding partners, potentially presenting a further post

translational regulatory mechanism (Lam and Trinkle-Mulcahy, 2015). Potentially FGF10 is also subject to this regulation. Additionally, recent studies showed that nucleolus plays also significant part in modifications of small RNA, RNA editing, telomerase maturation and well as sensing stress and control of cell cycle (Lo et al., 2006).

Interestingly, other nuclear FGFs, such as FGF2 and FGF3, have been found localising within the cell nucleolus. Nucleolar FGF2 directly regulates synthesis of ribosomal RNA and stimulates Polymerase I transcription through binding to UBF transcription factor (Sheng, 2004, Sheng et al., 2005), and was speculated to drive cell proliferation. Moreover, nucleolar function of FGF2 may be associated with pancreatic cancer (Coleman et al., 2014). Nucleolar FGF3 has been postulated to play a role in control of cell cycle and inhibition of cell proliferation through binding to NoBP protein (Reimers et al., 2001). It is therefore tempting to speculate that the nucleolar role of FGF10 is also associated with cell proliferation and control of cell cycle, however further investigations are necessary before any conclusion can be drawn.

7.2.2 Potential regulation of cell cycle and cell proliferation by FGF10

Several lines of evidence suggest that nuclear accumulation and function of FGF10 might be linked to cell cycle and/or cell proliferation control. First, it was demonstrated that FGF10 undergoes nuclear translocation in cultured quiescent cells (Fig. 4.16). Moreover, nuclear FGF10 was absent in actively proliferating cells as judged by segregation of BrdU label and nuclear FGF10-HA in transfected cells (Fig. 4.17). Therefore, a conclusion can be drawn that either, FGF10 is not translocated into the nucleus in actively proliferating cells or nuclear FGF10 obstructs the cell proliferation. Nuclear accumulation of over-expressed protein could potentially affect the normal cell division rate, which is not directly related to FGF10's function. However, nuclear accumulation of the control mCherry protein did not cause such cell proliferation inhibitory effect. Therefore, it is unlikely to take place with regards to accumulation of FGF10.

Interestingly, in a culture of mesenchymal progenitors (ATDC5 cells), transiently transfected FGF10HA negatively affected the rate of cell proliferation, which subsequently caused knock-on effects on cell differentiation potential (Fig. 5.3). A small proportion of cells demonstrated differentiation properties, displaying a small number of 'micro-nodules' indicative of cartilage formation (Fig. 5.3). Nonetheless, the culture has retained small degree of differentiation potential, therefore over-expression of FGF10-HA most likely did not disturb the differentiation processes *per se*. However, the normal processes of initial proliferation of differentiating culture of ATDC5s were disturbed in

case of FGF10-HA over-expression (Fig. 5.3). Intriguingly, exogenously applied FGF10 seemed to promote cell differentiation, suggesting the at least in ATDC5s, paracrine and intracrine FGF10 might function in opposite fashion (see Chapter 5). FGF3 was earlier shown to present similar properties (Kiefer and Dickson, 1995a).

Concluding therefore from the results, a model can be proposed where FGF10 shows dual function: (1) the paracrine stimulation of the receptor present on the epithelial cells to stimulate their proliferation and (2) nuclear and inhibitory role of proliferation of the mesenchymal cells (Fig. 7.3). There might be a possibility that intracrine FGF10 triggers cell death, functioning to induce apoptosis. Observations of the FGF10-HA transfected cultures did not suggest greater cell death than the controls (see Chapter 4 & 5), but exact measurements are needed to exclude this possibility.

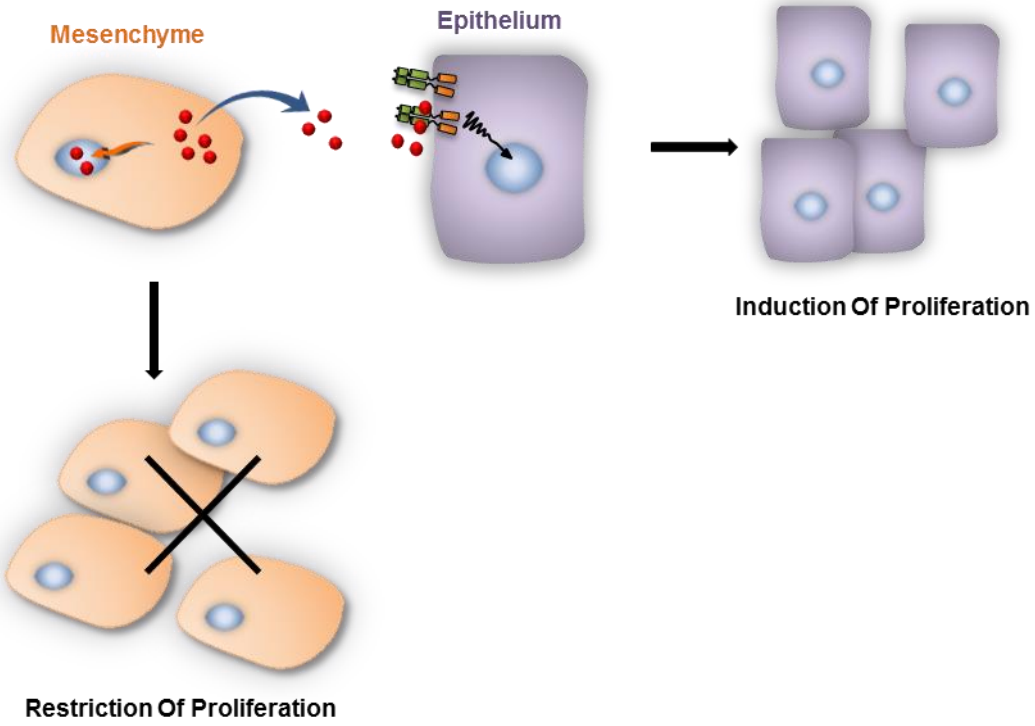

Figure 7.3 Putative model of FGF10's function. FGF10 (represented as red dots) has a well-established receptor-mediated function of resulting in induction of epithelial cell proliferation. However, results presented here suggest that FGF10 translocated into nucleus of mesenchymal cells might act to restrict cell proliferation.

Investigation into Fgf10 expression in a culture of hypothalamic tanycytes (see Chapter 6) seems to further support the proposed model of nuclear function restricting cell proliferation. *In vivo* it has been demonstrated that Fgf10 expression demarcates a

niche of proliferative stem cells of the hypothalamus (Hajihosseini et al., 2008, Haan et al., 2013), in a tissue that lacks expression of FGFR2IIIb. An *in vitro* culture of hypothalamic cells shows that Fgf10 expressing cells have a potential to proliferate and sustain their self-propagation properties over long period of time, yet their division rate is slower than Fgf10 non-expressing culture counterpart cells. The results suggest that Fgf10 expressing cells correspond to the population of slow dividing true stem/progenitor cells in contrast to Fgf10-non expressing fast dividing trans-amplifying cell progenitors (see Chapter 6). Again, the possibility that Fgf10 expression triggers cell death or limits cell survival cannot be excluded. However, the results rather indicate that FGF10 might function intracellularly, in the culture of hypothalamic tanycytes to control the division rate of true stem cells.

FGF10 might not be the main player determining the cell progression thought the cell cycle, however it might affect other factors controlling cell division checkpoints. Furthermore, it seems that the receptor-mediated paracrine function of FGF10 generates stronger signals that can override the intracellular/nuclear function of the protein. For example, in cardiomyocytes FGF10-FGFR2IIIb cell-autonomous signalling results in promotion of cell proliferation (Rochais et al., 2014) therefore, the putative endogenous FGF10 inhibitory signals would have been superseded by the inducible signals from the conventional receptor phosphorylation pathway. In a more likely scenario, nuclear FGF10 acts as additional restriction/control system, potentially through binding to key factors of cell transcription machinery, or other cell cycle check-points determinants, to affect their function. These processes could be tissue, time and species specific.

Control of cell division might be important from several aspects. For example, during development FGF10 is expressed in mesenchymal cells and promotes proliferation of epithelium. Therefore, it seems logical that a cell-autonomous mechanism should restrict mesenchymal cell proliferation, allowing epithelial cells to proliferate. Moreover, adult neural stem cells are characterised by slow cell division to prevent accumulation of new neurons in the brain, which could lead to brain tumours and other complications. FGF10 has already been implicated in cancer formation. For example, externally applied FGF10 stimulated the proliferation and cancer formation of ameloblastoma in a dose dependent manner, through stimulation of the MAPK pathway (Nakao et al., 2013). Furthermore, FGF10-FGFR2IIIb signalling was shown to induce migration and invasion of pancreatic cancer cells, where FGF10 is actually expressed in stromal cells surrounding pancreatic cancer cells (Nomura et al., 2008). Moreover, high levels of Fgf10 expression were shown to promote sarcoma (non-epithelial type of tumour) formation, whereas expression of Fgf10 did not stimulate the fibrosarcoma (mesenchymal tumour) formation (Sugimoto et al., 2014), although both

types of tissue were shown to express the Fgfr2IIIb. This further shows that FGF10 signalling might be controlled by a variety of factors. Moreover, Fgf10 is highly overexpressed in a subset of human breast carcinomas and acts as a potent oncogene in mammary epithelial cells (Theodorou et al., 2004). Therefore, generation of FGF10 functioning only through the nucleus, in a proliferation inhibitory fashion, could provide a system limiting cancer formation. However, further studies are required to fully determine the nuclear/intracellular function of the protein.

Part 7.3 Future work

To further elucidate the intracellular distribution and nuclear role of FGF10, a number of investigations could be carried out in the future. Some experiments could be carried out, in order to further clarify the dynamics driving FGF10's nuclear import, others to determine the molecular mechanisms of FGF10's nuclear function.

It should be investigated whether FGF10 is found within cell nucleus with or without its receptor. As shown by the example of FGF2, ligand-receptor complex translocation might have a differential function to the ligand alone (Coleman et al., 2014), which could be determined by immunolabelling of both proteins and assessing their co-localisation in different cell compartments.

In order to fully assess whether the NLS sequences function collectively to drive FGF10 to the cell nucleus, several basic residues could be mutated within both sequences, for example, K143 and K144 of NLS1 and K200 and K201 of NLS2. Other combinations also should be explored. Generating more than 4 mutations at the time might lead to protein misfolding and structural issues. Furthermore, in order to determine whether either of these sequences alone can drive protein's nuclear translocation, NLS1 and NLS2 could be attached to a fluorescent protein and transfected into a cell culture. The fluorescent protein-NLS fusion would be expected to show a high degree of nuclear accumulation. Moreover, it could be explored whether they are able to drive the nuclear import of the fluorescent protein in cooperation. It could be investigated whether fusing two NLSs at the same time strengthens the signal. In FGF10 primary sequence NLS1 and NLS2 are located at a distance from each other, coming in close contact only in protein's 3D structure and without this strategic positioning they might not perform their function in similar fashion to the one they might in FGF10. Nonetheless, the possibility could be explored, whether individually the sequences would show too "weak" to fully target the protein to the nucleus.

Protein nuclear targeting might be strengthened by various PTM. Mutations of previously predicted bioinformatically sites of SUMOylation, glycosylation or phosphorylation, could be carried out and analysed in a context of promoting or preventing FGF10's nuclear transport.

Another element, to fully support the NLS2 transport of the FGF10 would be to determine whether the 4T-NLS2 mutation retains its paracrine function, by binding to the receptor. This could be performed via protein purification and assessing direct protein-protein (4T-NLS2 to FGFR2IIIb) interaction for example, applying yeast two hybrid technique, or through comparison of the epithelial cell stimulation of non-mutated FGF10 and 4T-NLS2 proteins. It would be expected that the mutant shows no/little difference to the wild type FGF10.

To investigate whether FGF10 plays a specific role within the cell nucleus it would be important to determine whether FGF10 interacts with other molecules in the nucleus itself or in the cytoplasm. It would be possible to determine whether the FGF10 possesses any binding partners through performing immunoprecipitation of the protein from the different cell compartments (such as nucleus and cytoplasm) with its putative complex/s. Furthermore, performing this study in a culture of hypothalamic tanycytes, where the intracellular role of FGF10 might be of most significance because of a presumed absence of its paracrine function. List of putative FGF10 binding partners (excluding housekeeping genes, like protein folding chaperones) could significantly help to identify the exact role the protein serves in the nucleus. Moreover, it could provide information about the mechanism of FGF10 nuclear import – either through binding to specific isoform of importin or other chaperone/s.

To fully investigate whether FGF10 possesses and intracellular role, one of the key aspects would be generation of protein that does not become released from the cell. Ablation of the signal peptide (SP) targeting FGF10 to the secretory pathway should result in majority of a protein accumulating in the nucleus. Assuming that the protein would not display any folding or structural issues, it could be used in parallel with the external application of FGF10, testing the paracrine vs intracrine effects of the protein of a cell culture.

Furthermore, it has been hypothesised whether nuclear FGF10 affects cell proliferation. To further investigate this hypothesis, one of the possibilities would be to knock out expression of Fgf10, for example from the hypothalamic cultures of tanycytes, or mesenchymal cell line that typically expresses the protein. Therefore, it could be investigated whether the knockout of FGF10 affected the cell proliferation rate through observation of cell numbers, assessing the number of cells showing expression of cell proliferation markers (e.g. BrdU), and/or assessing the cell death, for example by counting number of cells positive for Trypan Blue reagent.

FGF10 was shown to perform a variety of functions in a cell type dependent manner. Another interesting investigation into the function of FGF10 could be through generation of inducible system, where expression of the protein can be turned on and off. Especially, if the system was able to express different versions of the protein – one paracrine, where the protein would be unable to translocate into cell nucleus, but function solely through the cell secretory pathway (e.g. 4T-NLS2), and second, where the protein would only act in an intracrine manner, by ablation of the SP. Application of this system in a variety of different cell types, including cancer cells could test the specific tissue-dependent FGF10's function. Importantly, the inducible system, where the protein's expression has the potential to be turned on and off would allow to determine whether the expression of Fgf10 causes cell death, which is otherwise difficult to measure if cells are expressing the protein at the time of seeding.

Lastly, application of antibodies reliably detecting the endogenous levels of FGF10 would provide information, whether *in vivo*, FGF10 is translocated into cell nucleus in different cell types.

List of abbreviations

3D	– third dimension
3V	– third ventricle
AER	– apical ectodermal ridge
αIBB	– Impβ1-binding domain
Alk5	– TGFβ type I receptor
Alx4	– aristaless-like homeobox protein
ALSG	– aplasia of lacrimal and salivary glands syndrome
An1	– anosmin-1
ARC	– arcuate nucleus of hypothalamus
Arm	– armadillo
ARPE-19	– human retinal pigment epithelial cells
ATP	– adenosine triphosphate
ATR	– ataxia telangiectasia and Rad3-related protein
B1/CDK1	– isoform of cyclin B1 in a complex with CDK1
Barx2	– homeobox protein
BDNF	– brain-derived neurotrophic factor
βCOP	– coat protein (coatomer) β
β-gal	– β-galactosidase
β-Kap	– β-karyopherin
BLAST	– Basic Local Alignment Search Tool
BLBP	– brain lipid binding protein
BRCA2	– breast cancer type 2 susceptibility protein
BrdU	– 5'bromo 2'deoxyuridine
BSA	– bovine serum albumin
BSC	– back scatter
C-terminal	– protein's carboxyl terminal
C/EBPβ	– CCAAT/enhancer binding protein
CDK1	– cyclin-dependent kinase 1
CEP57	– centrosomal protein of 57 kDa
ChIP	– chromatin immunoprecipitation
CIP	– calf alkaline phosphatase
CK2	– casein kinase 2
c-Myc	– cellular myelocytomatosis protien
CNS	– central nervous system
COS	– acronym of CV-1 Origin with the SV40 genetic material
CRM1	– chromosomal maintenance 1

CSF	– cerebrospinal fluid
D1, D2, D3	– immunoglobulin–like domains of FGFRs
DAG	– diacylglycerol
DFC	– dense fibrillar component
DMN	– dorsomedial nucleus of hypothalamus
DMSO	– dimethyl sulfoxide
DPBS	– Dulbecco's phosphate buffered saline
EBNA-1	– Epstein-Barr virus (EBV) nuclear antigen 1
ECM	– extra-cellular matrix
EGF	– epidermal growth factor
EPD	– Eukaryotic Promoter Database
ER	– endoplasmic reticulum
ERAD	– ER-associated protein degradation
ERK	– extracellular signal-regulated kinases
ERp60	– an isoform of Protein disulphide-isomerase
ETM	– epithelial-to-mesenchyme signalling
EtOH	– Ethanol
FACS	– fluorescence-activated cell sorting
FAST1	– forkhead activin signal transducer-1
FASTA	– a DNA and protein sequence alignment software package
FBS	– foetal bovine serum
FDM	– form deprivation myopia
FGF	– fibroblast growth factor
FGF-BP	– FGF-binding protein
FGFR	– fibroblast growth factor receptor
FHFs	– FGF homologous factors
FIBP	– acidic fibroblast growth factor intracellular-binding protein
FLRT3	– fibronectin leucine-rich transmembrane protein 3
FOXO3	– forkhead box O 3
FSC	– forward scatter
FTC	– familial tumoral calcinosis
GAG	– glycosaminoglycans
GAPDH	– glyceraldehyde 3-phosphate dehydrogenase
GATA3	– trans-acting T-cell-specific transcription factor GATA3
GC box	– guanosine-cytosine rich DNA regions
GDP/GTP	– guanosine diphosphate/ guanosine triphosphate
GFAP	– glial fibrillary acidic protein
GLUT1	– glucose transporter 1

GRB2 – growth factor receptor-bound protein 2
GWAS – Genome Wide Association Studies
H-bond – hydrogen bonds
HA – Hemagglutinin A
HBS – HEPES buffered saline
HEAT – huntingtin, elongation factor 3, protein phosphatase 2A and
TOR1 – serine/threonine-protein kinase
HEK – human embryonic kidney cells
HEPES – 4-(2-hydroxyethyl)-1-piperazineethanesulfonic acid
HMW – high molecular weight
HS – heparan sulfate
Hs6st – 6-*O*-sulfotransferase protein
HSGAGs – heparan sulphate glycosaminoglycans
Hsp90 – heat shock protein 90
HSSE – heparan sulfate-synthesizing enzymes
ICC – immunocytochemistry
IF – intermediate filament
Ig – immunoglobulin
IGF1 – insulin-like growth factor 1
IHP – inositol hexaphosphate
Imp-α – importin-α
Imp-β – importin-β
IP3 – inositol triphosphate
Isl1 – insulin gene enhancer protein 1
KGF – keratinocyte growth factors
L6/TAXREB107 – ribosomal protein
LADD – lacrimo-auriculo-dento-digital syndrome
LEF1 – lymphoid enhancer-binding factor 1
Lfng – lunatic fringe
LHN – lateral hypothalamic nucleus
LHX3 – LIM/homeobox protein3
LMW – low molecular weight
LRRC59 – leucine rich repeat containing 59
MAPK – mitogen-activated protein kinases
MCF-7 – human breast adenocarcinoma cells, acronym of Michigan Cancer Foundation-7
MDS – molecular dynamic simulation
ME – median eminence

MKP – MAP kinase phosphatase
MMPs – matrix metalloproteinases
MSC – mesenchymal stem cells
MSX – Msh homeobox 1 transcription factor
MTE – mesenchymal-to-epithelial signalling
mTOR – mammalian target of rapamycin
N-terminal – protein's amino terminal
NBM – nucleolar binding motifs
NCAM – neural cell adhesion molecules
NCBI – National Center for Biotechnology Information
NDST1 – bifunctional heparan sulfate N-deacetylase/N-sulfotransferase1
NES – nuclear export sequence
NF-κB – nuclear factor kappa-light-chain-enhancer of activated B cells
NGS – normal goat serum
NG2 – neural/glial antigen 2
Nhp6Ap – Non-histone chromosomal protein 6A
NLS – nuclear localisation sequence
NKX – homeobox protein
NoBP – nucleolar binding protein
NPC – nuclear pore complex
NSC – neural stem cells
Nups – nucleoporins
Olig2 – oligodendrocyte transcription factor
P – postnatal day
$p27^{kip1}$ – cyclin-dependent kinase inhibitor
PAGE – polyacrylamide gel electrophoresis
PAX6 – paired box protein 6
PBS – phosphate buffered saline
PBST – phosphate buffered saline with Tween-20
PBX1 – pre-B-cell leukaemia transcription factor 1
PDB – Protein Data Bank
PDGF – platelet-derived growth factor
PDL – poly-D-lysine hydrobromide
PE – Phycoerythrin
PEA3 – polyoma enhancer activator 3
pERK – phospho -ERK
PFA – paraformaldehyde
PI3K – phosphatidylinositol-4,5-bisphosphate 3-kinase

PIP2 – phosphatidylinositol-4,5-biphosphate
PKC – protein kinase C
PLC – phospholipase C
PLC γ1 – is also known as FGFR substrate 1 (FRS1)
PML – promyelocytic leukemia
PNGase F – Peptide -N-Glycosidase F
PNS – peripheral nervous system
PPARγ – peroxisome proliferator activated receptor
PTHrP – parathyroid hormone-related protein
PTM – post-translational modifications
PVN – paraventricular nucleus of hypothalamus
RA – retinoic acid
RAF – acronym for Rapidly Accelerated Fibrosarcoma
RAF1 – RAF proto-oncogene serine/threonine-protein kinase or c-Raf
RanGAP – Ran GTPase-activating protein
RanGEF – Ran guanine nucleotide exchange factor
RMS – rostral migratory stream
ROI – region of interest
RPS19 – ribosomal protein
RT – room temperature
RT-PCR – reverse transcription polymerase chain reaction
SDS – sodium dodecyl sulfate
SE – standard error
SEF – similar expression to *fgf* genes
Sey – small eye phenotype
Shh – sonic hedgehog
Shp2 – aka tyrosine-protein phosphatase non-receptor type 11
SIM – SUMO-interaction motif
SMAD – amalgam of ‘mothers against decapentaplegic’ (MAD) (*Drosophila*) and ‘small body size’ (SMA) (*C.elegants*)
SNP1 – snurportin1
SOS1 – son of sevenless
Sox2 – sex determining region Y (SRY) - box 2
Sox9 – Sry-related HMG box 9
SP – signal peptide
Sp1 – specificity protein 1
SPRY – sprouty family of proteins
STATs – signal transducers and activators of transcription

SUMO – small Ubiquitin-like modifiers
SGZ – subgranular zone
SON – supraoptic nucleus
SOS – sucrose octasulfate
SVZ – subventricular zone
Syo-1 – symportin-1, name derived from “synchronized import”
TAE – Tris base, acetic acid and EDTA buffer solution
TBE – Tris, Borate, EDTA buffer solution
TBX5 – T-box transcription factor 5
TCA – Trichloroacetic acid
TGFβ – transforming growth factor
TGN46 – trans-Golgi network integral membrane protein 2
TK – tyrosine kinase
Tm – melting temperature
Tuj1 – neuronal class III β-tubulin
Txn – tamoxifen
UBF – Upstream binding factor
Ugdh – UDP-glucose dehydrogenase
VMN – ventromedial nucleus of hypothalamus
WB – western blot
Wnt – amalgam of ‘wingless’ (*Drosophila*) and ‘int1’ (mouse)
WT – wild type
X-gal – 5-bromo-4-chloro-3-indolyl-β-D-galactopyranoside

References

ABROUS, D. N., KOEHL, M. & LE MOAL, M. 2005. Adult Neurogenesis: From Precursors to Network and Physiology. *Physiology Reviews,* 85**,** 48.

ABUHARBEID, S., CZUBAYKO, F. & AIGNER, A. 2006. The fibroblast growth factor-binding protein FGF-BP. *Int J Biochem Cell Biol,* 38**,** 1463-8.

ACLAND, P., DIXON, M., PETERS, G. & DICKSON, C. 1990. Subcellular fate of the int-2 oncoprotein is determined by choice of initiation codon. *Nature,* 343**,** 662-5.

AGARWAL, P., WYLIE, J. N., GALCERAN, J., ARKHITKO, O., LI, C., DENG, C., GROSSCHEDL, R. & BRUNEAU, B. G. 2003. Tbx5 is essential for forelimb bud initiation following patterning of the limb field in the mouse embryo. *Development,* 130**,** 623-33.

AL-DEWACHI, H. S., APPLETON, D. R., WATSON, A. J. & WRIGHT, N. A. 1979. Variation in the cell cycle time in the crypts of Lieberkuhn of the mouse. *Virchows Arch B Cell Pathol Incl Mol Pathol,* 31**,** 37-44.

ALTMAN, J. & DAS, G. D. 1965. Post-natal origin of microneurones in the rat brain. *nature* 207**,** 953-6.

ALTSCHUL, S. F., GISH, W., MILLER, W., MYERS, E. W. & LIPMAN, D. J. 1990. Basic local alignment search tool. *Journal of Molecular Biology,* 215**,** 403-410.

ALVAREZ, Y., ALONSO, M. T., VENDRELL, V., ZELARAYAN, L. C., CHAMERO, P., THEIL, T., BOSL, M. R., KATO, S., MACONOCHIE, M., RIETHMACHER, D. & SCHIMMANG, T. 2003. Requirements for FGF3 and FGF10 during inner ear formation. *Development,* 130**,** 6329-38.

ANDERSON, D., BAKER, M., GRIGNOL, G., HU, W., MERCHENTHALER, I. & DUDAS, B. 2010. Distribution and morphology of the juxtapositions between growth hormone-releasing hormone-(ghrh)-immunoreactive neuronal elements. *Growth Horm IGF Res,* 20**,** 356-9.

ANTHONY, T. E., KLEIN, C., FISHELL, G. & HEINTZ, N. 2004. Radial glia serve as neuronal progenitors in all regions of the central nervous system. *Neuron,* 41**,** 881-90.

ANTOINE, M., REIMERS, K., DICKSON, C. & KIEFER, P. 1997. Fibroblast growth factor 3, a protein with dual subcellular localization, is targeted to the nucleus and nucleolus by the concerted action of two nuclear localization signals and a nucleolar retention signal. *J Biol Chem,* 272**,** 29475-81.

ARGENTARO, A., SIM, H., KELLY, S., PREISS, S., CLAYTON, A., JANS, D. A. & HARLEY, V. R. 2003. A SOX9 defect of calmodulin-dependent nuclear import in campomelic dysplasia/autosomal sex reversal. *J Biol Chem,* 278**,** 33839-47.

ARITA, J. & KIMURA, F. 1986. Adenosine 3',5'-cyclic monophosphate stimulates dopamine biosynthesis in the median eminence of rat hypothalamic slices. *Brain Res,* 374**,** 37-44.

ARMELIN, H. A. 1973. Pituitary extracts and steroid hormones in the control of 3T3 cell growth. *Proc Natl Acad Sci U S A,* 70**,** 2702-6.

ARNAUD, E., TOURIOL, C., BOUTONNET, C., GENSAC, M. C., VAGNER, S., PRATS, H. & PRATS, A. C. 1999. A new 34-kilodalton isoform of human fibroblast growth factor 2 is cap dependently synthesized by using a non-AUG start codon and behaves as a survival factor. *Mol Cell Biol,* 19**,** 505-14.

ARNOYS, E. J., ACKERMAN, C. M. & WANG, J. L. 2015. Nucleocytoplasmic shuttling of galectin-3. *Methods Mol Biol,* 1207**,** 465-83.

ASAKI, T., KONISHI, M., MIYAKE, A., KATO, S., TOMIZAWA, M. & ITOH, N. 2004. Roles of fibroblast growth factor 10 (Fgf10) in adipogenesis in vivo. *Mol Cell Endocrinol,* 218**,** 119-28.

ASHIKARI-HADA, S., HABUCHI, H., KARIYA, Y., ITOH, N., REDDI, A. H. & KIMATA, K. 2004. Characterization of growth factor-binding structures in heparin/heparan sulfate using an octasaccharide library. *J Biol Chem,* 279**,** 12346-54.

ATSUMI, T., MIWA, Y., KIMATA, K. & IKAWA, Y. 1990. A chondrogenic cell line derived from a differentiating culture of AT805 teratocarcinoma cells. *Cell Differ Dev,* 30**,** 109-16.

AUDAS, T. E., JACOB, M. D. & LEE, S. 2012. Immobilization of proteins in the nucleolus by ribosomal intergenic spacer noncoding RNA. *Mol Cell,* 45**,** 147-57.

BABU, H., CHEUNG, G., KETTENMANN, H., PALMER, T. D. & KEMPERMANN, G. 2007. Enriched monolayer precursor cell cultures from micro-dissected adult mouse dentate gyrus yield functional granule cell-like neurons. *PLoS One,* 2**,** e388.

BABU, H., CLAASEN, J. H., KANNAN, S., RUNKER, A. E., PALMER, T. & KEMPERMANN, G. 2011. A protocol for isolation and enriched monolayer cultivation of neural precursor cells from mouse dentate gyrus. *Front Neurosci,* 5**,** 89.

BAGAI, S., RUBIO, E., CHENG, J. F., SWEET, R., THOMAS, R., FUCHS, E., GRADY, R., MITCHELL, M. & BASSUK, J. A. 2002. Fibroblast growth factor-10 is a mitogen for urothelial cells. *J Biol Chem,* 277**,** 23828-37.

BARAK, H., HUH, S. H., CHEN, S., JEANPIERRE, C., MARTINOVIC, J., PARISOT, M., BOLE-FEYSOT, C., NITSCHKE, P., SALOMON, R., ANTIGNAC, C., ORNITZ, D. M. & KOPAN, R. 2012. FGF9 and FGF20 maintain the stemness of nephron progenitors in mice and man. *Dev Cell,* 22**,** 1191-207.

BARLOW, A. L., MACLEOD, A., NOPPEN, S., SANDERSON, J. & GUERIN, C. J. 2010. Colocalization analysis in fluorescence micrographs: verification of a more accurate calculation of pearson's correlation coefficient. *Microsc Microanal,* 16**,** 710-24.

BEENKEN, A. & MOHAMMADI, M. 2009. The FGF family: biology, pathophysiology and therapy. *Nat Rev Drug Discov,* 8**,** 235-53.

BEER, H. D., FLORENCE, C., DAMMEIER, J., MCGUIRE, L., WERNER, S. & DUAN, D. R. 1997. Mouse fibroblast growth factor 10: cDNA cloning, protein characterization, and regulation of mRNA expression. *Oncogene,* 15**,** 2211-8.

BELLOSTA, P., TALARICO, D., ROGERS, D. & BASILICO, C. 1993. Cleavage of K-FGF produces a truncated molecule with increased biological activity and receptor binding affinity. *J Cell Biol,* 121**,** 705-13.

BENJAMIN, J. T., CARVER, B. J., PLOSA, E. J., YAMAMOTO, Y., MILLER, J. D., LIU, J. H., VAN DER MEER, R., BLACKWELL, T. S. & PRINCE, L. S. 2010. NF-kappaB activation limits airway branching through inhibition of Sp1-mediated fibroblast growth factor-10 expression. *J Immunol,* 185**,** 4896-903.

BERG, T., ROUNTREE, C. B., LEE, L., ESTRADA, J., SALA, F. G., CHOE, A., VELTMAAT, J. M., DE LANGHE, S., LEE, R., TSUKAMOTO, H., CROOKS, G. M., BELLUSCI, S. & WANG, K. S. 2007. Fibroblast growth factor 10 is critical for liver growth during embryogenesis and controls hepatoblast survival via beta-catenin activation. *Hepatology,* 46**,** 1187-97.

BERGLUND, H., LINDSTROM, P. & SAVIC, I. 2006. Brain response to putative pheromones in lesbian women. *Proc Natl Acad Sci U S A,* 103**,** 8269-74.

BEYER, T. A., WERNER, S., DICKSON, C. & GROSE, R. 2003. Fibroblast growth factor 22 and its potential role during skin development and repair. *Exp Cell Res,* 287**,** 228-36.

BEZ, A., CORSINI, E., CURTI, D., BIGGIOGERA, M., COLOMBO, A., NICOSIA, R. F., PAGANO, S. F. & PARATI, E. A. 2003. Neurosphere and neurosphere-forming cells: morphological and ultrastructural characterization. *Brain Research,* 993**,** 18-29.

BINAME, F. 2014. Transduction of extracellular cues into cell polarity: the role of the transmembrane proteoglycan NG2. *Mol Neurobiol,* 50**,** 482-93.

BIZON, J. L. & GALLAGHER, M. 2003. Production of new cells in the rat dentate gyrus over the lifespan: relation to cognitive decline. *Eur J Neurosci,* 18**,** 215-9.

BLUNDELL, T. L., SIBANDA, B. L., MONTALVAO, R. W., BREWERTON, S., CHELLIAH, V., WORTH, C. L., HARMER, N. J., DAVIES, O. & BURKE, D. 2006. Structural biology and bioinformatics in drug design: opportunities and challenges for target identification and lead discovery. *Philos Trans R Soc Lond B Biol Sci,* 361**,** 413-23.

BOLBOREA, M. & DALE, N. 2013. Hypothalamic tanycytes: potential roles in the control of feeding and energy balance. *Trends Neurosci,* 36**,** 91-100.

BOSSARD, C., LAURELL, H., VAN DEN BERGHE, L., MEUNIER, S., ZANIBELLATO, C. & PRATS, H. 2003. Translokin is an intracellular mediator of FGF-2 trafficking. *Nat Cell Biol,* 5**,** 433-9.

BOTTCHER, R. T., POLLET, N., DELIUS, H. & NIEHRS, C. 2004. The transmembrane protein XFLRT3 forms a complex with FGF receptors and promotes FGF signalling. *Nat Cell Biol,* 6**,** 38-44.

BOUCHE, G., GAS, N., PRATS, H., BALDIN, V., TAUBER, J. P., TEISSIE, J. & AMALRIC, F. 1987. Basic fibroblast growth factor enters the nucleolus and stimulates the transcription of ribosomal genes in ABAE cells undergoing G0----G1 transition. *Proc Natl Acad Sci U S A,* 84**,** 6770-4.

BRAMEIER, M., KRINGS, A. & MACCALLUM, R. M. 2007. NucPred Predicting nuclear localization of proteins. *Bioinformatics,* 23**,** 1159-1160.

BRAUKSIEPE, B., BAUMGARTEN, L., REUSS, S. & SCHMIDT, E. R. 2014. Co-localization of serine/threonine kinase 33 (Stk33) and vimentin in the hypothalamus. *Cell Tissue Res,* 355**,** 189-99.

BUCHTOVA, M., CHALOUPKOVA, R., ZAKRZEWSKA, M., VESELA, I., CELA, P., BARATHOVA, J., GUDERNOVA, I., ZAJICKOVA, R., TRANTIREK, L., MARTIN, J., KOSTAS, M., OTLEWSKI, J., DAMBORSKY, J., KOZUBIK, A., WIEDLOCHA, A. & KREJCI, P. 2015. Instability restricts signaling of multiple fibroblast growth factors. *Cell Mol Life Sci,* 72**,** 2445-59.

BURDINE, R. D., CHEN, E. B., KWOK, S. F. & STERN, M. J. 1997. egl-17 encodes an invertebrate fibroblast growth factor family member required specifically for sex myoblast migration in Caenorhabditis elegans. *Proc Natl Acad Sci U S A,* 94**,** 2433-7.

CAI, X., GONG, P., HUANG, Y. & LIN, Y. 2011. Notch signalling pathway in tooth development and adult dental cells. *Cell Prolif,* 44**,** 495-507.

CAPRA, J. A. & SINGH, M. 2007. Predicting functionally important residues from sequence conservation. *Bioinformatics,* 23**,** 1875-82.

CATEZ, F., ERARD, M., SCHAERER-UTHURRALT, N., KINDBEITER, K., MADJAR, J. J. & DIAZ, J. J. 2002. Unique motif for nucleolar retention and nuclear export regulated by phosphorylation. *Mol Cell Biol,* 22**,** 1126-39.

CAVALLARO, U., NIEDERMEYER, J., FUXA, M. & CHRISTOFORI, G. 2001. N-CAM modulates tumour-cell adhesion to matrix by inducing FGF-receptor signalling. *Nat Cell Biol,* 3**,** 650-7.

CHAICHANA, K., ZAMORA-BERRIDI, G., CAMARA-QUINTANA, J. & QUINONES-HINOJOSA, A. 2006. Neurosphere assays: growth factors and hormone differences in tumor and nontumor studies. *Stem Cells,* 24**,** 2851-7.

CHARLES, C., HOVORAKOVA, M., AHN, Y., LYONS, D. B., MARANGONI, P., CHURAVA, S., BIEHS, B., JHEON, A., LESOT, H., BALOOCH, G., KRUMLAUF, R., VIRIOT, L., PETERKOVA, R. & KLEIN, O. D. 2011. Regulation of tooth number by fine-tuning levels of receptor-tyrosine kinase signaling. *Development,* 138**,** 4063-73.

CHELLAIAH, A., YUAN, W., CHELLAIAH, M. & ORNITZ, D. M. 1999. Mapping ligand binding domains in chimeric fibroblast growth factor receptor molecules. Multiple regions determine ligand binding specificity. *J Biol Chem,* 274**,** 34785-94.

CHEN, L., MA, Y., QIAN, L. & WANG, J. 2013. Sumoylation regulates nuclear localization and function of zinc finger transcription factor ZIC3. *Biochim Biophys Acta,* 1833**,** 2725-33.

CHEN, M. H., BEN-EFRAIM, I., MITROUSIS, G., WALKER-KOPP, N., SIMS, P. J. & CINGOLANI, G. 2005. Phospholipid scramblase 1 contains a nonclassical nuclear localization signal with unique binding site in importin alpha. *J Biol Chem,* 280**,** 10599-606.

CHEN, Y. S., CHEN, C. C. & HORNG, J. C. 2011. Thermodynamic and kinetic consequences of substituting glycine at different positions in a Pro-Hyp-Gly repeat collagen model peptide. *Biopolymers,* 96**,** 60-8.

CHEN, Z., HUANG, J., LIU, Y., DATTILO, L. K., HUH, S. H., ORNITZ, D. & BEEBE, D. C. 2014. FGF signaling activates a Sox9-Sox10 pathway for the formation and branching morphogenesis of mouse ocular glands. *Development,* 141**,** 2691-701.

CHIONI, A. M. & GROSE, R. 2009. Negative regulation of fibroblast growth factor 10 (FGF-10) by polyoma enhancer activator 3 (PEA3). *Eur J Cell Biol,* 88**,** 371-84.

CHO, K. W., CAI, J., KIM, H. Y., HOSOYA, A., OHSHIMA, H., CHOI, K. Y. & JUNG, H. S. 2009. ERK activation is involved in tooth development via FGF10 signaling. *J Exp Zool B Mol Dev Evol,* 312**,** 901-11.

CHOOK, Y. M. & SUEL, K. E. 2011. Nuclear import by karyopherin-betas: recognition and inhibition. *Biochim Biophys Acta,* 1813**,** 1593-606.

CHRISTIE, M., CHANG, C. W., RONA, G., SMITH, K. M., STEWART, A. G., TAKEDA, A. A., FONTES, M. R., STEWART, M., VERTESSY, B. G., FORWOOD, J. K. & KOBE, B. 2015. Structural Biology and Regulation of Protein Import into the Nucleus. *J Mol Biol*.

CHUNG, S. S. & KOH, C. J. 2013. Bladder cancer cell in co-culture induces human stem cell differentiation to urothelial cells through paracrine FGF10 signaling. *In Vitro Cell Dev Biol Anim,* 49**,** 746-51.

CIEMERYCH, M. A., MARO, B. & KUBIAK, J. Z. 1999. Control of duration of the first two mitoses in a mouse embryo. *Zygote,* 7**,** 293-300.

CINGOLANI, G., BEDNENKO, J., GILLESPIE, M. T. & GERACE, L. 2002. Molecular basis for the recognition of a nonclassical nuclear localization signal by importin beta. *Mol Cell,* 10**,** 1345-53.

CINGOLANI, G., PETOSA, C., WEIS, K. & MULLER, C. W. 1999. Structure of importin-beta bound to the IBB domain of importin-alpha. *Nature,* 399**,** 221-9.

CLARKE, W. E., BERRY, M., SMITH, C., KENT, A. & LOGAN, A. 2001. Coordination of fibroblast growth factor receptor 1 (FGFR1) and fibroblast growth factor-2 (FGF-2) trafficking to nuclei of reactive astrocytes around cerebral lesions in adult rats. *Mol Cell Neurosci,* 17**,** 17-30.

CLAUS, P., BRUNS, A. F. & GROTHE, C. 2004. Fibroblast growth factor-2(23) binds directly to the survival of motoneuron protein and is associated with small nuclear RNAs. *Biochem J,* 384**,** 559-65.

CLAUS, P., DORING, F., GRINGEL, S., MULLER-OSTERMEYER, F., FUHLROTT, J., KRAFT, T. & GROTHE, C. 2003. Differential intranuclear localization of fibroblast growth factor-2 isoforms and specific interaction with the survival of motoneuron protein. *J Biol Chem,* 278**,** 479-85.

COLEMAN, S. J., CHIONI, A. M., GHALLAB, M., ANDERSON, R. K., LEMOINE, N. R., KOCHER, H. M. & GROSE, R. P. 2014. Nuclear translocation of FGFR1 and FGF2 in pancreatic stellate cells facilitates pancreatic cancer cell invasion. *EMBO Mol Med,* 6**,** 467-81.

COLES-TAKABE, B. L., BRAIN, I., PURPURA, K. A., KARPOWICZ, P., ZANDSTRA, P. W., MORSHEAD, C. M. & VAN DER KOOY, D. 2008. Don't look: growing clonal versus nonclonal neural stem cell colonies. *Stem Cells,* 26**,** 2938-44.

CONTI, L., POLLARD, S. M., GORBA, T., REITANO, E., TOSELLI, M., BIELLA, G., SUN, Y., SANZONE, S., YING, Q. L., CATTANEO, E. & SMITH, A. 2005. Niche-independent symmetrical self-renewal of a mammalian tissue stem cell. *PLoS Biology,* 3**,** e283.

COPELAND, R. A., JI, H., HALFPENNY, A. J., WILLIAMS, R. W., THOMPSON, K. C., HERBER, W. K., THOMAS, K. A., BRUNER, M. W., RYAN, J. A., MARQUIS-OMER, D. & ET AL. 1991. The structure of human acidic fibroblast growth factor and its interaction with heparin. *Arch Biochem Biophys,* 289**,** 53-61.

CORTES-CAMPOS, C., LETELIER, J., CERIANI, R. & WHITLOCK, K. E. 2015. Zebrafish adult-derived hypothalamic neurospheres generate gonadotropin-releasing hormone (GnRH) neurons. *Biol Open,* 4**,** 1077-86.

CORTÉS-CAMPOS, C., LETELIER, J., CERIANI, R. & WHITLOCK, K. E. 2015. Zebrafish adult-derived hypothalamic neurospheres generate gonadotropin-releasing hormone (GnRH) neurons. *Biology Open,* 4**,** 1077-1086.

COSTES, S. V., DAELEMANS, D., CHO, E. H., DOBBIN, Z., PAVLAKIS, G. & LOCKETT, S. 2004. Automatic and quantitative measurement of protein-protein colocalization in live cells. *Biophys J,* 86**,** 3993-4003.

COUDERC, B., PRATS, H., BAYARD, F. & AMALRIC, F. 1991. Potential oncogenic effects of basic fibroblast growth factor requires cooperation between CUG and AUG-initiated forms. *Cell Regul,* 2**,** 709-18.

CRACKOWER, M. A., HENG, H. H. & TSUI, L. C. 1998. Assignment of mouse fibroblast growth factor 10 (Fgf10) gene to the telomeric region of chromosome 13. *Genomics,* 53**,** 247-8.

CRIVAT, G. & TARASKA, J. W. 2012. Imaging proteins inside cells with fluorescent tags. *Trends Biotechnol,* 30**,** 8-16.

CULAJAY, J. F., BLABER, S. I., KHURANA, A. & BLABER, M. 2000. Thermodynamic characterization of mutants of human fibroblast growth factor 1 with an increased physiological half-life. *Biochemistry,* 39**,** 7153-8.

CURTAIN, M., HEFFNER, C. S., MADDOX, D. M., GUDIS, P., DONAHUE, L. R. & MURRAY, S. A. 2015. A novel allele of Alx4 results in reduced Fgf10 expression and failure of eyelid fusion in mice. *Mamm Genome,* 26**,** 173-80.

CUTRESS, M. L., WHITAKER, H. C., MILLS, I. G., STEWART, M. & NEAL, D. E. 2008. Structural basis for the nuclear import of the human androgen receptor. *J Cell Sci,* 121**,** 957-68.

DALE, N. 2011. Purinergic signaling in hypothalamic tanycytes: potential roles in chemosensing. *Semin Cell Dev Biol,* 22**,** 237-44.

DANILENKO, D. M., RING, B. D., YANAGIHARA, D., BENSON, W., WIEMANN, B., STARNES, C. O. & PIERCE, G. F. 1995. Keratinocyte growth factor is an important endogenous mediator of hair follicle growth, development, and differentiation. Normalization of the nu/nu follicular differentiation defect and amelioration of chemotherapy-induced alopecia. *Am J Pathol,* 147**,** 145-54.

DANOPOULOS, S., PARSA, S., AL ALAM, D., TABATABAI, R., BAPTISTA, S., TIOZZO, C., CARRARO, G., WHEELER, M., BARRETO, G., BRAUN, T., LI, X., HAJIHOSSEINI, M. K. & BELLUSCI, S. 2013. Transient Inhibition of FGFR2b-ligands signaling leads to irreversible loss of cellular beta-catenin organization and signaling in AER during mouse limb development. *PLoS One,* 8**,** e76248.

DE LAPEYRIERE, O., ROSNET, O., BENHARROCH, D., RAYBAUD, F., MARCHETTO, S., PLANCHE, J., GALLAND, F., MATTEI, M. G., COPELAND, N. G., JENKINS, N. A. & ET AL. 1990. Structure, chromosome mapping and expression of the murine Fgf-6 gene. *Oncogene,* 5**,** 823-31.

DE SERANNO, S., D'ANGLEMONT DE TASSIGNY, X., ESTRELLA, C., LOYENS, A., KASPAROV, S., LEROY, D., OJEDA, S. R., BEAUVILLAIN, J. C. & PREVOT, V. 2010. Role of estradiol in the dynamic control of tanycyte plasticity mediated by vascular endothelial cells in the median eminence. *Endocrinology,* 151**,** 1760-72.

DELISE, A. M., STRINGA, E., WOODWARD, W. A., MELLO, M. A. & TUAN, R. S. 2000. Embryonic limb mesenchyme micromass culture as an in vitro model for chondrogenesis and cartilage maturation. *Methods Mol Biol,* 137**,** 359-75.

DELL'ERA, P., PRESTA, M. & RAGNOTTI, G. 1991. Nuclear localization of endogenous basic fibroblast growth factor in cultured endothelial cells. *Exp Cell Res,* 192**,** 505-10.

DENG, W., AIMONE, J. B. & GAGE, F. H. 2010. New neurons and new memories: how does adult hippocampal neurogenesis affect learning and memory? *Nat Rev Neurosci,* 11**,** 339-50.

DERRICK, T., GRILLO, A. O., VITHARANA, S. N., JONES, L., REXROAD, J., SHAH, A., PERKINS, M., SPITZNAGEL, T. M. & MIDDAUGH, C. R. 2007. Effect of polyanions on the structure and stability of repifermin (keratinocyte growth factor-2). *J Pharm Sci,* 96**,** 761-76.

DERSH, D., JONES, S. M., ELETTO, D., CHRISTIANSON, J. C. & ARGON, Y. 2014. OS-9 facilitates turnover of nonnative GRP94 marked by hyperglycosylation. *Mol Biol Cell,* 25**,** 2220-34.

DESAI, M., LI, T. & ROSS, M. G. 2011. Hypothalamic neurosphere progenitor cells in low birth-weight rat newborns: neurotrophic effects of leptin and insulin. *Brain Res,* 1378**,** 29-42.

DICKSON, C., DEED, R., DIXON, M. & PETERS, G. 1989. The structure and function of the int-2 oncogene. *Prog Growth Factor Res,* 1**,** 123-32.

DICKSON, C., FULLER-PACE, F., KIEFER, P., ACLAND, P., MACALLAN, D. & PETERS, G. 1991. Expression, processing, and properties of int-2. *Ann N Y Acad Sci,* 638**,** 18-26.

DIMAURO, I., PEARSON, T., CAPOROSSI, D. & JACKSON, M. J. 2012. A simple protocol for the subcellular fractionation of skeletal muscle cells and tissue. *BMC Research Notes,* 5**,** 1-5.

DINI, G., FUNGHINI, S., WITORT, E., MAGNELLI, L., FANTI, E., RIFKIN, D. B. & DEL ROSSO, M. 2002. Overexpression of the 18 kDa and 22/24 kDa FGF-2 isoforms results in differential drug resistance and amplification potential. *J Cell Physiol,* 193**,** 64-72.

DLUGOSZ, A. A., CHENG, C., DENNING, M. F., DEMPSEY, P. J., COFFEY, R. J., JR. & YUSPA, S. H. 1994. Keratinocyte growth factor receptor ligands induce transforming growth factor alpha expression and activate the epidermal growth factor receptor signaling pathway in cultured epidermal keratinocytes. *Cell Growth Differ,* 5**,** 1283-92.

DONNENBERG, A. D. & DONNENBERG, V. S. 2007. Rare-event analysis in flow cytometry. *Clin Lab Med,* 27**,** 627-52, viii.

DUAN, D. S., WERNER, S. & WILLIAMS, L. T. 1992. A naturally occurring secreted form of fibroblast growth factor (FGF) receptor 1 binds basic FGF in preference over acidic FGF. *J Biol Chem,* 267**,** 16076-80.

DUNN, K. C., AOTAKI-KEEN, A. E., PUTKEY, F. R. & HJELMELAND, L. M. 1996. ARPE-19, a human retinal pigment epithelial cell line with differentiated properties. *Exp Eye Res,* 62**,** 155-69.

ECONOMOU, A., DATTA, P., GEORGIADIS, V., CADOT, S., FRENZ, D. & MACONOCHIE, M. 2013. Gata3 directly regulates early inner ear expression of Fgf10. *Dev Biol,* 374**,** 210-22.

EIFLER, K. & VERTEGAAL, A. C. 2015. SUMOylation-Mediated Regulation of Cell Cycle Progression and Cancer. *Trends Biochem Sci,* 40**,** 779-93.

EL AGHA, E., AL ALAM, D., CARRARO, G., MACKENZIE, B., GOTH, K., DE LANGHE, S. P., VOSWINCKEL, R., HAJIHOSSEINI, M. K., REHAN, V. K. & BELLUSCI, S. 2012. Characterization of a novel fibroblast growth factor 10 (Fgf10) knock-in mouse line to target mesenchymal progenitors during embryonic development. *PLoS One,* 7**,** e38452.

ELLMAN, M. B., YAN, D., AHMADINIA, K., CHEN, D., AN, H. S. & IM, H. J. 2013. Fibroblast growth factor control of cartilage homeostasis. *J Cell Biochem,* 114**,** 735-42.

EMOTO, H. 1997. Structure and Expression of Human Fibroblast Growth Factor-10. *Journal of Biological Chemistry,* 272**,** 23191-23194.

EMOTO, H., TAGASHIRA, S., MATTEI, M. G., YAMASAKI, M., HASHIMOTO, G., KATSUMATA, T., NEGORO, T., NAKATSUKA, M., BIRNBAUM, D., COULIER, F. & ITOH, N. 1997. Structure and expression of human fibroblast growth factor-10. *J Biol Chem,* 272**,** 23191-4.

ENTESARIAN, M., DAHLQVIST, J., SHASHI, V., STANLEY, C. S., FALAHAT, B., REARDON, W. & DAHL, N. 2007. FGF10 missense mutations in aplasia of lacrimal and salivary glands (ALSG). *Eur J Hum Genet,* 15**,** 379-82.

ENTESARIAN, M., MATSSON, H., KLAR, J., BERGENDAL, B., OLSON, L., ARAKAKI, R., HAYASHI, Y., OHUCHI, H., FALAHAT, B., BOLSTAD, A. I., JONSSON, R., WAHREN-HERLENIUS, M. & DAHL, N. 2005. Mutations in the gene encoding fibroblast growth factor 10 are associated with aplasia of lacrimal and salivary glands. *Nat Genet,* 37**,** 125-7.

FEKETE, C. & LECHAN, R. M. 2014. Central regulation of hypothalamic-pituitary-thyroid axis under physiological and pathophysiological conditions. *Endocr Rev,* 35**,** 159-94.

FENG, L., HATTEN, M. E. & HEINTZ, N. 1994. Brain lipid-binding protein (BLBP): a novel signaling system in the developing mammalian CNS. *Neuron,* 12**,** 895-908.

FLORKIEWICZ, R. Z. & SOMMER, A. 1989. Human basic fibroblast growth factor gene encodes four polypeptides: three initiate translation from non-AUG codons. *Proc Natl Acad Sci U S A,* 86**,** 3978-81.

FOLETTI, A., VUADENS, F. & BEERMANN, F. 2003. Nuclear localization of mouse fibroblast growth factor 2 requires N-terminal and C-terminal sequences. *Cell Mol Life Sci,* 60**,** 2254-65.

FONTES, M. R. M., TEH, T. & KOBE, B. 2000. Structural basis of recognition of monopartite and bipartite nuclear localization sequences by mammalian importin-α1. *Journal of Molecular Biology,* 297**,** 1183-1194.

FRAYLING, C., BRITTON, R. & DALE, N. 2011. ATP-mediated glucosensing by hypothalamic tanycytes. *J Physiol,* 589**,** 2275-86.

FREIMAN, R. N. & TJIAN, R. 2003. Regulating the Regulators: Lysine Modifications Make Their Mark. *Cell,* 112**,** 11-17.

FRIEDENSTEIN, A. J., CHAILAKHJAN, R. K. & LALYKINA, K. S. 1970. The development of fibroblast colonies in monolayer cultures of guinea-pig bone marrow and spleen cells. *Cell Tissue Kinet,* 3**,** 393-403.

FRISHBERG, Y., ITO, N., RINAT, C., YAMAZAKI, Y., FEINSTEIN, S., URAKAWA, I., NAVON-ELKAN, P., BECKER-COHEN, R., YAMASHITA, T., ARAYA, K., IGARASHI, T., FUJITA, T. & FUKUMOTO, S. 2007. Hyperostosis-hyperphosphatemia syndrome: a congenital disorder of O-glycosylation associated with augmented processing of fibroblast growth factor 23. *J Bone Miner Res,* 22**,** 235-42.

FRITZ, J. V., DIDIER, P., CLAMME, J. P., SCHAUB, E., MURIAUX, D., CABANNE, C., MORELLET, N., BOUAZIZ, S., DARLIX, J. L., MELY, Y. & DE ROCQUIGNY, H. 2008. Direct Vpr-Vpr interaction in cells monitored by two photon fluorescence correlation spectroscopy and fluorescence lifetime imaging. *Retrovirology,* 5**,** 87.

FU, S. C., HUANG, H. C., HORTON, P. & JUAN, H. F. 2013. ValidNESs: a database of validated leucine-rich nuclear export signals. *Nucleic Acids Res,* 41**,** D338-43.

FU, S. C., IMAI, K. & HORTON, P. 2011. Prediction of leucine-rich nuclear export signal containing proteins with NESsential. *Nucleic Acids Res,* 39**,** e111.

GALY, B., MARET, A., PRATS, A. C. & PRATS, H. 1999. Cell transformation results in the loss of the density-dependent translational regulation of the expression of fibroblast growth factor 2 isoforms. *Cancer Res,* 59**,** 165-71.

GARCEZ, P. P., LOIOLA, E. C., MADEIRO DA COSTA, R., HIGA, L. M., TRINDADE, P., DELVECCHIO, R., NASCIMENTO, J. M., BRINDEIRO, R., TANURI, A. & REHEN, S. K. 2016. Zika virus impairs growth in human neurospheres and brain organoids. *Science*.

GARMY-SUSINI, B., DELMAS, E., GOURDY, P., ZHOU, M., BOSSARD, C., BUGLER, B., BAYARD, F., KRUST, A., PRATS, A. C., DOETSCHMAN, T., PRATS, H. & ARNAL, J. F. 2004. Role of fibroblast growth factor-2 isoforms in the effect of estradiol on endothelial cell migration and proliferation. *Circ Res,* 94**,** 1301-9.

GIL-PEROTIN, S., DURAN-MORENO, M., CEBRIAN-SILLA, A., RAMIREZ, M., GARCIA-BELDA, P. & GARCIA-VERDUGO, J. M. 2013. Adult neural stem cells from the subventricular zone: a review of the neurosphere assay. *Anat Rec (Hoboken),* 296**,** 1435-52.

GOGATE, N., VERMA, L., ZHOU, J. M., MILWARD, E., RUSTEN, R., O'CONNOR, M., KUFTA, C., KIM, J., HUDSON, L. & DUBOIS-DALCQ, M. 1994. Plasticity in the adult human oligodendrocyte lineage. *J Neurosci,* 14**,** 4571-87.

GOLDFARB, M. 2005. Fibroblast growth factor homologous factors: evolution, structure, and function. *Cytokine Growth Factor Rev,* 16**,** 215-20.

GOLDFARB, M., BATES, B., DRUCKER, B., HARDIN, J. & HAUB, O. 1991. Expression and possible functions of the FGF-5 gene. *Ann N Y Acad Sci,* 638**,** 38-52.

GOLDFARB, M., SCHOORLEMMER, J., WILLIAMS, A., DIWAKAR, S., WANG, Q., HUANG, X., GIZA, J., TCHETCHIK, D., KELLEY, K., VEGA, A., MATTHEWS, G., ROSSI, P., ORNITZ, D. M. & D'ANGELO, E. 2007. Fibroblast growth factor homologous factors control neuronal excitability through modulation of voltage-gated sodium channels. *Neuron,* 55**,** 449-63.

GOLZIO, C., HAVIS, E., DAUBAS, P., NUEL, G., BABARIT, C., MUNNICH, A., VEKEMANS, M., ZAFFRAN, S., LYONNET, S. & ETCHEVERS, H. C. 2012. ISL1 directly regulates FGF10 transcription during human cardiac outflow formation. *PLoS One,* 7**,** e30677.

GOODMAN, T. & HAJIHOSSEINI, M. K. 2015. Hypothalamic tanycytes-masters and servants of metabolic, neuroendocrine, and neurogenic functions. *Front Neurosci,* 9**,** 387.

GORLICH, D., PANTE, N., KUTAY, U., AEBI, U. & BISCHOFF, F. R. 1996. Identification of different roles for RanGDP and RanGTP in nuclear protein import. *EMBO J,* 15**,** 5584-94.

GOSPODAROWICZ, D. 1974. Localisation of a fibroblast growth factor and its effect alone and with hydrocortisone on 3T3 cell growth. *Nature,* 249**,** 123-7.

GOULD, E. 2007. How widespread is adult neurogenesis in mammals? *Nature Reviews, Neuroscience* 8**,** 8.

GOVINDARAJAN, V., ITO, M., MAKARENKOVA, H. P., LANG, R. A. & OVERBEEK, P. A. 2000. Endogenous and ectopic gland induction by FGF-10. *Dev Biol,* 225**,** 188-200.

GRAHAM, E. S., TURNBULL, Y., FOTHERINGHAM, P., NILAWEERA, K., MERCER, J. G., MORGAN, P. J. & BARRETT, P. 2003a. Neuromedin U and Neuromedin U receptor-2 expression in the mouse and rat hypothalamus: effects of nutritional status. *Journal of Neurochemistry,* 87**,** 1165-1173.

GRAHAM, V., KHUDYAKOV, J., ELLIS, P. & PEVNY, L. 2003b. SOX2 functions to maintain neural progenitor identity. *Neuron,* 39**,** 749-65.

GRUNWALD, M. & BONO, F. 2011. Structure of Importin13-Ubc9 complex: nuclear import and release of a key regulator of sumoylation. *EMBO J,* 30**,** 427-38.

GUILLEMOT, F. & ZIMMER, C. 2011. From cradle to grave: the multiple roles of fibroblast growth factors in neural development. *Neuron,* 71**,** 574-88.

GUO, L., DEGENSTEIN, L. & FUCHS, E. 1996. Keratinocyte growth factor is required for hair development but not for wound healing. *Genes Dev,* 10**,** 165-75.

HAAN, N., GOODMAN, T., NAJDI-SAMIEI, A., STRATFORD, C. M., RICE, R., EL AGHA, E., BELLUSCI, S. & HAJIHOSSEINI, M. K. 2013. Fgf10-expressing tanycytes add new neurons to the appetite/energy-balance regulating centers of the postnatal and adult hypothalamus. *J Neurosci,* 33**,** 6170-80.

HAAN, N. & HAJIHOSSEINI, M. K. 2009. Fgf10 is a putative marker of quiescent neural stems cells in the adult hypothalamus. *Mechanisms of Development,* 126**,** S276.

HAJIHOSSEINI, M. K., DE LANGHE, S., LANA-ELOLA, E., MORRISON, H., SPARSHOTT, N., KELLY, R., SHARPE, J., RICE, D. & BELLUSCI, S. 2008. Localization and fate of Fgf10-expressing cells in the adult mouse brain implicate Fgf10 in control of neurogenesis. *Mol Cell Neurosci,* 37**,** 857-68.

HAJIHOSSEINI, M. K. & DICKSON, C. 1999. A subset of fibroblast growth factors (Fgfs) promote survival, but Fgf-8b specifically promotes astroglial differentiation of rat cortical precursor cells. *Mol Cell Neurosci,* 14**,** 468-85.

HAJIHOSSEINI, M. K., DUARTE, R., PEGRUM, J., DONJACOUR, A., LANA-ELOLA, E., RICE, D. P., SHARPE, J. & DICKSON, C. 2009. Evidence that Fgf10 contributes to the skeletal and visceral defects of an Apert syndrome mouse model. *Dev Dyn,* 238**,** 376-85.

HAJIHOSSEINI, M. K. & HEATH, J. K. 2002. Expression patterns of fibroblast growth factors-18 and -20 in mouse embryos is suggestive of novel roles in calvarial and limb development. *Mech Dev,* 113**,** 79-83.

HANOVER, J. A., LOVE, D. C., DEANGELIS, N., O'KANE, M. E., LIMA-MIRANDA, R., SCHULZ, T., YEN, Y. M., JOHNSON, R. C. & PRINZ, W. A. 2007. The High Mobility Group Box Transcription Factor Nhp6Ap enters the nucleus by a calmodulin-dependent, Ran-independent pathway. *J Biol Chem,* 282**,** 33743-51.

HARADA, H., KETTUNEN, P., JUNG, H. S., MUSTONEN, T., WANG, Y. A. & THESLEFF, I. 1999. Localization of putative stem cells in dental epithelium and their association with Notch and FGF signaling. *J Cell Biol,* 147**,** 105-20.

HARADA, H., TOYONO, T., TOYOSHIMA, K. & OHUCHI, H. 2002a. FGF10 maintains stem cell population during mouse incisor development. *Connect Tissue Res,* 43**,** 201-4.

HARADA, H., TOYONO, T., TOYOSHIMA, K., YAMASAKI, M., ITOH, N., KATO, S., SEKINE, K. & OHUCHI, H. 2002b. FGF10 maintains stem cell compartment in developing mouse incisors. *Development,* 129**,** 1533-41.

HARMER, N. J., ILAG, L. L., MULLOY, B., PELLEGRINI, L., ROBINSON, C. V. & BLUNDELL, T. L. 2004. Towards a resolution of the stoichiometry of the fibroblast growth factor (FGF)-FGF receptor-heparin complex. *J Mol Biol,* 339**,** 821-34.

HART, A., PAPADOPOULOU, S. & EDLUND, H. 2003. Fgf10 maintains notch activation, stimulates proliferation, and blocks differentiation of pancreatic epithelial cells. *Dev Dyn,* 228**,** 185-93.

HAY, R. T. 2005. SUMO: a history of modification. *Mol Cell,* 18**,** 1-12.

HEESE, O., DISKO, A., ZIRKEL, D., WESTPHAL, M. & LAMSZUS, K. 2005. Neural stem cell migration toward gliomas in vitro. *Neuro Oncol,* 7**,** 476-84.

HEISER, P. W., LAU, J., TAKETO, M. M., HERRERA, P. L. & HEBROK, M. 2006. Stabilization of beta-catenin impacts pancreas growth. *Development,* 133**,** 2023-32.

HEROLD, A., TRUANT, R., WIEGAND, H. & CULLEN, B. R. 1998. Determination of the functional domain organization of the importin alpha nuclear import factor. *J Cell Biol,* 143**,** 309-18.

HOLZMANN, K., GRUNT, T., HEINZLE, C., SAMPL, S., STEINHOFF, H., REICHMANN, N., KLEITER, M., HAUCK, M. & MARIAN, B. 2012. Alternative Splicing of Fibroblast Growth Factor Receptor IgIII Loops in Cancer. *J Nucleic Acids,* 2012**,** 950508.

HOSOKAWA, R., OKA, K., YAMAZA, T., IWATA, J., URATA, M., XU, X., BRINGAS, P., JR., NONAKA, K. & CHAI, Y. 2010. TGF-beta mediated FGF10 signaling in cranial neural crest cells controls development of myogenic progenitor cells through tissue-tissue interactions during tongue morphogenesis. *Dev Biol,* 341**,** 186-95.

HSI, E., CHEN, K. C., CHANG, W. S., YU, M. L., LIANG, C. L. & JUO, S. H. 2013. A functional polymorphism at the FGF10 gene is associated with extreme myopia. *Invest Ophthalmol Vis Sci,* 54**,** 3265-71.

HU, Y., GUIMOND, S. E., TRAVERS, P., CADMAN, S., HOHENESTER, E., TURNBULL, J. E., KIM, S. H. & BOULOUX, P. M. 2009. Novel mechanisms of fibroblast growth factor receptor 1 regulation by extracellular matrix protein anosmin-1. *J Biol Chem,* 284**,** 29905-20.

HUANG, C., DAI, J. & ZHANG, X. A. 2015. Environmental physical cues determine the lineage specification of mesenchymal stem cells. *Biochim Biophys Acta,* 1850**,** 1261-6.

HUANG, Y. M., KANG, M. & CHANG, C. E. 2014. Switches of hydrogen bonds during ligand-protein association processes determine binding kinetics. *J Mol Recognit,* 27**,** 537-48.

HUNTER, C. C., SIEBERT, K. S., DOWNES, D. J., WONG, K. H., KREUTZBERGER, S. D., FRASER, J. A., CLARKE, D. F., HYNES, M. J., DAVIS, M. A. & TODD, R. B. 2014. Multiple nuclear localization signals mediate nuclear localization of the GATA transcription factor AreA. *Eukaryot Cell,* 13**,** 527-38.

IAKOVOU, G., HAYWARD, S. & LAYCOCK, S. 2014. A real-time proximity querying algorithm for haptic-based molecular docking. *Faraday Discuss,* 169**,** 359-77.

IAKOVOU, G., HAYWARD, S. & LAYCOCK, S. D. 2015. Adaptive GPU-accelerated force calculation for interactive rigid molecular docking using haptics. *Journal of Molecular Graphics and Modelling,* 61**,** 1-12.

IBRAHIMI, O. A., YEH, B. K., ELISEENKOVA, A. V., ZHANG, F., OLSEN, S. K., IGARASHI, M., AARONSON, S. A., LINHARDT, R. J. & MOHAMMADI, M. 2005. Analysis of mutations in fibroblast growth factor (FGF) and a pathogenic mutation in FGF receptor (FGFR) provides direct evidence for the symmetric two-end model for FGFR dimerization. *Mol Cell Biol,* 25**,** 671-84.

IGARASHI, M. 1998. Characterization of Recombinant Human Fibroblast Growth Factor (FGF)-10 Reveals Functional Similarities with Keratinocyte Growth Factor (FGF-7). *Journal of Biological Chemistry,* 273**,** 13230-13235.

IMAMURA, T., ENGLEKA, K., ZHAN, X., TOKITA, Y., FOROUGH, R., ROEDER, D., JACKSON, A., MAIER, J. A., HLA, T. & MACIAG, T. 1990. Recovery of mitogenic activity of a growth factor mutant with a nuclear translocation sequence. *Science,* 249**,** 1567-70.

ISHIZAWA, J., KOJIMA, K., HAIL, N., JR., TABE, Y. & ANDREEFF, M. 2015. Expression, function, and targeting of the nuclear exporter chromosome region maintenance 1 (CRM1) protein. *Pharmacol Ther,* 153**,** 25-35.

ITOH, N. & OHTA, H. 2014. Fgf10: a paracrine-signaling molecule in development, disease, and regenerative medicine. *Curr Mol Med,* 14**,** 504-9.

ITOH, N. & ORNITZ, D. M. 2004. Evolution of the Fgf and Fgfr gene families. *Trends Genet,* 20**,** 563-9.

JACOBI, A., LOY, K., SCHMALZ, A. M., HELLSTEN, M., UMEMORI, H., KERSCHENSTEINER, M. & BAREYRE, F. M. 2015. FGF22 signaling regulates synapse formation during post-injury remodeling of the spinal cord. *EMBO J,* 34**,** 1231-43.

JAKEL, S., ALBIG, W., KUTAY, U., BISCHOFF, F. R., SCHWAMBORN, K., DOENECKE, D. & GORLICH, D. 1999. The importin beta/importin 7 heterodimer is a functional nuclear import receptor for histone H1. *EMBO J,* 18**,** 2411-23.

JAROSZ, M., ROBBEZ-MASSON, L., CHIONI, A.-M., CROSS, B., ROSEWELL, I. & GROSE, R. 2012. Fibroblast Growth Factor 22 Is Not Essential for Skin Development and Repair but Plays a Role in Tumorigenesis. *PLoS ONE,* 7**,** e39436.

JASKOLL, T., ABICHAKER, G., WITCHER, D., SALA, F. G., BELLUSCI, S., HAJIHOSSEINI, M. K. & MELNICK, M. 2005. FGF10/FGFR2b signaling plays essential roles during in vivo embryonic submandibular salivary gland morphogenesis. *BMC Dev Biol,* 5**,** 11.

JEAN, J. C., LU, J., JOYCE-BRADY, M. & CARDOSO, W. V. 2008. Regulation of Fgf10 gene expression in murine mesenchymal cells. *J Cell Biochem,* 103**,** 1886-94.

JENSEN, J. B. & PARMAR, M. 2006. Strengths and Limitations of the Neurosphere Culture System. *Molecular Neurobiology,* 34**,** 9.

JIA, S., MOU, C., MA, Y., HAN, R. & LI, X. 2016. Magnesium regulates neural stem cell proliferation in the mouse hippocampus by altering mitochondrial function. *Cell Biol Int,* 40**,** 465-71.

JIN, K., SUN, Y., XIE, L., BATTEUR, S., MAO, X. O., SMELICK, C., LOGVINOVA, A. & GREENBERG, D. A. 2003. Neurogenesis and aging: FGF-2 and HB-EGF restore neurogenesis in hippocampus and subventricular zone of aged mice. *Aging Cell,* 2**,** 175-83.

KARVINEN, S., PASONEN-SEPPANEN, S., HYTTINEN, J. M., PIENIMAKI, J. P., TORRONEN, K., JOKELA, T. A., TAMMI, M. I. & TAMMI, R. 2003. Keratinocyte growth factor stimulates migration and hyaluronan synthesis in the epidermis by activation of keratinocyte hyaluronan synthases 2 and 3. *J Biol Chem,* 278**,** 49495-504.

KATO, K., JEANNEAU, C., TARP, M. A., BENET-PAGES, A., LORENZ-DEPIEREUX, B., BENNETT, E. P., MANDEL, U., STROM, T. M. & CLAUSEN, H. 2006. Polypeptide GalNAc-transferase T3 and familial tumoral calcinosis. Secretion of fibroblast growth factor 23 requires O-glycosylation. *J Biol Chem,* 281**,** 18370-7.

KAWANO, S., SAITO, M., HANDA, K., MOROTOMI, T., TOYONO, T., SETA, Y., NAKAMURA, N., UCHIDA, T., TOYOSHIMA, K., OHISHI, M. & HARADA, H. 2004. Characterization of dental epithelial progenitor cells derived from cervical-loop epithelium in a rat lower incisor. *J Dent Res,* 83**,** 129-33.

KELLEY, M. J., PECH, M., SEUANEZ, H. N., RUBIN, J. S., O'BRIEN, S. J. & AARONSON, S. A. 1992. Emergence of the keratinocyte growth factor multigene family during the great ape radiation. *Proc Natl Acad Sci U S A,* 89**,** 9287-91.

KELLY, R. G., BROWN, N. A. & BUCKINGHAM, M. E. 2001. The Arterial Pole of the Mouse Heart Forms from Fgf10-Expressing Cells in Pharyngeal Mesoderm. *Developmental Cell,* 1**,** 6.

KENEALY, B. P., KEEN, K. L., GARCIA, J. P., RICHTER, D. J. & TERASAWA, E. 2015. Prolonged infusion of estradiol benzoate into the stalk median eminence stimulates release of GnRH and kisspeptin in ovariectomized female rhesus macaques. *Endocrinology,* 156**,** 1804-14.

KESSLER, O., SHRAGA-HELED, N., LANGE, T., GUTMANN-RAVIV, N., SABO, E., BARUCH, L., MACHLUF, M. & NEUFELD, G. 2004. Semaphorin-3F is an inhibitor of tumor angiogenesis. *Cancer Res,* 64**,** 1008-15.

KIEFER, P., ACLAND, P., PAPPIN, D., PETERS, G. & DICKSON, C. 1994a. Competition between nuclear localization and secretory signals determines the subcellular fate of a single CUG-initiated form of FGF3. *EMBO J,* 13**,** 4126-36.

KIEFER, P., ACLAND, P., PAPPIN, D., PETERS, G. & DICKSON, C. 1994b. Competition between nuclear localization and secretory signals determines the subcellular fate of a single CUG-initiated form of FGF3. *EMBO journal,* 13**,** 4126-36.

KIEFER, P. & DICKSON, C. 1995a. Nucleolar association of fibroblast growth factor 3 via specific sequence motifs has inhibitory effects on cell growth. *Mol Cell Biol,* 15**,** 4364-74.

KIEFER, P. & DICKSON, C. 1995b. Nucleolar association of fibroblast growth factor 3 via specific sequence motifs has inhibitory effects on cell growth. *Mol Cell Biol,* 15**,** 4364–4374.

KIM, H. S. & CROW, T. J. 1998. Human proto-oncogene Int-2/FGF-3. Map position 11q13.3-q13.4. *Chromosome Res,* 6**,** 579.

KIRIKOSHI, H., SAGARA, N., SAITOH, T., TANAKA, K., SEKIHARA, H., SHIOKAWA, K. & KATOH, M. 2000. Molecular cloning and characterization of human FGF-20 on chromosome 8p21.3-p22. *Biochem Biophys Res Commun,* 274**,** 337-43.

KIROV, A., KACER, D., CONLEY, B. A., VARY, C. P. & PRUDOVSKY, I. 2015. AHNAK2 Participates in the Stress-Induced Nonclassical FGF1 Secretion Pathway. *J Cell Biochem*.

KISELYOV, V. V., KOCHOYAN, A., POULSEN, F. M., BOCK, E. & BEREZIN, V. 2006. Elucidation of the mechanism of the regulatory function of the Ig1 module of the fibroblast growth factor receptor 1. *Protein Sci,* 15**,** 2318-22.

KITAMURA, R., SEKIMOTO, T., ITO, S., HARADA, S., YAMAGATA, H., MASAI, H., YONEDA, Y. & YANAGI, K. 2006. Nuclear import of Epstein-Barr virus nuclear antigen 1 mediated by NPI-1 (Importin alpha5) is up- and down-regulated by phosphorylation of the nuclear localization signal for which Lys379 and Arg380 are essential. *J Virol,* 80**,** 1979-91.

KLINGENBERG, O., WIDLOCHA, A., RAPAK, A., MUNOZ, R., FALNES, P. & OLSNES, S. 1998. Inability of the acidic fibroblast growth factor mutant K132E to stimulate DNA synthesis after translocation into cells. *J Biol Chem,* 273**,** 11164-72.

KOIVUNEN, P., HELAAKOSKI, T., ANNUNEN, P., VEIJOLA, J., RAISANEN, S., PIHLAJANIEMI, T. & KIVIRIKKO, K. I. 1996. ERp60 does not substitute for protein disulphide isomerase as the beta-subunit of prolyl 4-hydroxylase. *Biochem J,* 316 (Pt 2)**,** 599-605.

KOKOEVA, M. V., YIN, H. & FLIER, J. S. 2005. Neurogenesis in the hypothalamus of adult mice: potential role in energy balance. *Science,* 310**,** 679-83.

KOLPAKOVA, E., WIEDŁOCHA, A., STENMARK, H., KLINGENBERG, O., FALNES, P. O. & OLSNES, S. 1998. Cloning of an intracellular protein that binds selectively to mitogenic acidic fibroblast growth factor. *The Biochemical Journal,* 336**,** 213-222.

KOMI-KURAMOCHI, A., KAWANO, M., ODA, Y., ASADA, M., SUZUKI, M., OKI, J. & IMAMURA, T. 2005. Expression of fibroblast growth factors and their receptors during full-thickness skin wound healing in young and aged mice. *J Endocrinol,* 186**,** 273-89.

KONISHI, M., ASAKI, T., KOIKE, N., MIWA, H., MIYAKE, A. & ITOH, N. 2006. Role of Fgf10 in cell proliferation in white adipose tissue. *Mol Cell Endocrinol,* 249**,** 71-7.

KORSENSKY, L. & RON, D. 2016. Regulation of FGF signaling: recent insights from studying positive and negative modulators. *Semin Cell Dev Biol*.

KOSMAN, J., CARMEAN, N., LEAF, E. M., DYAMENAHALLI, K. & BASSUK, J. A. 2007. Translocation of fibroblast growth factor-10 and its receptor into nuclei of human urothelial cells. *J Cell Biochem,* 102**,** 769-85.

KOSUGI, S., HASEBE, M., MATSUMURA, N., TAKASHIMA, H., MIYAMOTO-SATO, E., TOMITA, M. & YANAGAWA, H. 2009. Six classes of nuclear localization signals specific to different binding grooves of importin alpha. *J Biol Chem,* 284**,** 478-85.

KOVALENKO, D., YANG, X., NADEAU, R. J., HARKINS, L. K. & FRIESEL, R. 2003. Sef inhibits fibroblast growth factor signaling by inhibiting FGFR1 tyrosine phosphorylation and subsequent ERK activation. *J Biol Chem,* 278**,** 14087-91.

KREJCI, P., KRAKOW, D., MEKIKIAN, P. B. & WILCOX, W. R. 2007. Fibroblast growth factors 1, 2, 17, and 19 are the predominant FGF ligands expressed in human fetal growth plate cartilage. *Pediatr Res,* 61**,** 267-72.

KUHN, H. G., DICKINSON-ANSON, H. & GAGE, F. H. 1996. Neurogenesis in the dentate gyrus of the adult rat: age-related decrease of neuronal progenitor proliferation. *J Neurosci,* 16**,** 2027-33.

KUO, C. T., MIRZADEH, Z., SORIANO-NAVARRO, M., RASIN, M., WANG, D., SHEN, J., SESTAN, N., GARCIA-VERDUGO, J., ALVAREZ-BUYLLA, A., JAN, L. Y. & JAN, Y. N. 2006. Postnatal deletion of Numb/Numblike reveals repair and remodeling capacity in the subventricular neurogenic niche. *Cell,* 127**,** 1253-64.

LADIWALA, U., BASU, H. & MATHUR, D. 2012. Assembling neurospheres: dynamics of neural progenitor/stem cell aggregation probed using an optical trap. *PLoS One,* 7**,** e38613.

LAM, Y. W. & TRINKLE-MULCAHY, L. 2015. New insights into nucleolar structure and function. *F1000Prime Rep,* 7**,** 48.

LE BOUFFANT, R., WANG, J. H., FUTEL, M., BUISSON, I., UMBHAUER, M. & RIOU, J. F. 2012. Retinoic acid-dependent control of MAP kinase phosphatase-3 is necessary for early kidney development in Xenopus. *Biol Cell,* 104**,** 516-32.

LEE, B. Y., HAN, J. A., IM, J. S., MORRONE, A., JOHUNG, K., GOODWIN, E. C., KLEIJER, W. J., DIMAIO, D. & HWANG, E. S. 2006. Senescence-associated beta-galactosidase is lysosomal beta-galactosidase. *Aging Cell,* 5**,** 187-95.

LEE, J. E. & KIM, J. H. 2015. SUMO modification regulates the protein stability of NDRG1. *Biochem Biophys Res Commun,* 459**,** 161-5.

LEVINE, J. M., REYNOLDS, R. & FAWCETT, J. W. 2001. The oligodendrocyte precursor cell in health and disease. *Trends Neurosci,* 24**,** 39-47.

LI, A., GUO, H., LUO, X., SHENG, J., YANG, S., YIN, Y., ZHOU, J. & ZHOU, J. 2006. Apomorphine-induced activation of dopamine receptors modulates FGF-2 expression in astrocytic cultures and promotes survival of dopaminergic neurons. *FASEB J,* 20**,** 1263-5.

LI, C., GUO, H., XU, X., WEINBERG, W. & DENG, C. X. 2001. Fibroblast growth factor receptor 2 (Fgfr2) plays an important role in eyelid and skin formation and patterning. *Dev Dyn,* 222**,** 471-83.

LI, C., HU, L., XIAO, J., CHEN, H., LI, J. T., BELLUSCI, S., DELANGHE, S. & MINOO, P. 2005. Wnt5a regulates Shh and Fgf10 signaling during lung development. *Dev Biol,* 287**,** 86-97.

LI, C., SCOTT, D. A., HATCH, E., TIAN, X. & MANSOUR, S. L. 2007. Dusp6 (Mkp3) is a negative feedback regulator of FGF-stimulated ERK signaling during mouse development. *Development,* 134**,** 167-76.

LI, C. Y., PROCHAZKA, J., GOODWIN, A. F. & KLEIN, O. D. 2014a. Fibroblast growth factor signaling in mammalian tooth development. *Odontology,* 102**,** 1-13.

LI, J., TANG, Y. & CAI, D. 2012a. IKKbeta/NF-kappaB disrupts adult hypothalamic neural stem cells to mediate a neurodegenerative mechanism of dietary obesity and pre-diabetes. *Nat Cell Biol,* 14**,** 999-1012.

LI, V. C., BALLABENI, A. & KIRSCHNER, M. W. 2012b. Gap 1 phase length and mouse embryonic stem cell self-renewal. *Proc Natl Acad Sci U S A,* 109**,** 12550-5.

LI, W., LIN, C. Y., SHANG, C., HAN, P., XIONG, Y., LIN, C. J., YANG, J., SELLERI, L. & CHANG, C. P. 2014b. Pbx1 activates Fgf10 in the mesenchyme of developing lungs. *Genesis,* 52**,** 399-407.

LIANG, S., ZHANG, C., LIU, S. & ZHOU, Y. 2006. Protein binding site prediction using an empirical scoring function. *Nucleic Acids Res,* 34**,** 3698-707.

LIN, J., JIN, R., ZHANG, B., CHEN, H., BAI, Y. X., YANG, P. X., HAN, S. W., XIE, Y. H., HUANG, P. T., HUANG, C. & HUANG, J. J. 2008. Nucleolar localization of TERT is unrelated to telomerase function in human cells. *J Cell Sci,* 121**,** 2169-76.

LIN, Z., WILLERS, C., XU, J. & ZHENG, M. H. 2006. The chondrocyte: biology and clinical application. *Tissue Eng,* 12**,** 1971-84.

LISENBEE, C. S., KARNIK, S. K. & TRELEASE, R. N. 2003. Overexpression and mislocalization of a tail-anchored GFP redefines the identity of peroxisomal ER. *Traffic,* 4**,** 491-501.

LIU, F., POGODA, H. M., PEARSON, C. A., OHYAMA, K., LOHR, H., HAMMERSCHMIDT, M. & PLACZEK, M. 2013. Direct and indirect roles of Fgf3 and Fgf10 in innervation and vascularisation of the vertebrate hypothalamic neurohypophysis. *Development,* 140**,** 1111-22.

LO, S. J., LEE, C. C. & LAI, H. J. 2006. The nucleolus: reviewing oldies to have new understandings. *Cell Res,* 16**,** 530-8.

LONDIN, E., YADAV, P., SURREY, S., KRICKA, L. J. & FORTINA, P. 2013. Use of linkage analysis, genome-wide association studies, and next-generation sequencing in the identification of disease-causing mutations. *Methods Mol Biol,* 1015**,** 127-46.

LOUIS, S. A., MAK, C. K. & REYNOLDS, B. A. 2013. Methods to culture, differentiate, and characterize neural stem cells from the adult and embryonic mouse central nervous system. *Methods Mol Biol,* 946**,** 479-506.

LU, W. 1999. Fibroblast Growth Factor-10. A SECOND CANDIDATE STROMAL TO EPITHELIAL CELL ANDROMEDIN IN PROSTATE. *Journal of Biological Chemistry,* 274**,** 12827-12834.

LU, W., LUO, Y., KAN, M. & MCKEEHAN, W. L. 1999. Fibroblast growth factor-10. A second candidate stromal to epithelial cell andromedin in prostate. *J Biol Chem,* 274**,** 12827-34.

LUI, K. & HUANG, Y. 2009. RanGTPase: A Key Regulator of Nucleocytoplasmic Trafficking. *Mol Cell Pharmacol,* 1**,** 148-156.

MAILLEUX, A. A., KELLY, R., VELTMAAT, J. M., DE LANGHE, S. P., ZAFFRAN, S., THIERY, J. P. & BELLUSCI, S. 2005. Fgf10 expression identifies parabronchial smooth muscle cell progenitors and is required for their entry into the smooth muscle cell lineage. *Development,* 132**,** 2157-66.

MAKARENKOVA, H. P., HOFFMAN, M. P., BEENKEN, A., ELISEENKOVA, A. V., MEECH, R., TSAU, C., PATEL, V. N., LANG, R. A. & MOHAMMADI, M. 2009. Differential interactions of FGFs with heparan sulfate control gradient formation and branching morphogenesis. *Sci Signal,* 2**,** ra55.

MAKARENKOVA, H. P., ITO, M., GOVINDARAJAN, V., FABER, S. C., SUN, L., MCMAHON, G., OVERBEEK, P. A. & LANG, R. A. 2000. FGF10 is an inducer and Pax6 a competence factor for lacrimal gland development. *Development,* 127**,** 2563-72.

MALECKI, J., WESCHE, J., SKJERPEN, C. S., WIEDLOCHA, A. & OLSNES, S. 2004. Translocation of FGF-1 and FGF-2 across vesicular membranes occurs during G1-phase by a common mechanism. *Mol Biol Cell,* 15**,** 801-14.

MALECKI, J., WIEDLOCHA, A., WESCHE, J. & OLSNES, S. 2002. Vesicle transmembrane potential is required for translocation to the cytosol of externally added FGF-1. *EMBO J,* 21**,** 4480-90.

MANN, G. B., FOWLER, K. J., GABRIEL, A., NICE, E. C., WILLIAMS, R. L. & DUNN, A. R. 1993. Mice with a null mutation of the TGF alpha gene have abnormal skin architecture, wavy hair, and curly whiskers and often develop corneal inflammation. *Cell,* 73**,** 249-61.

MANSOUR, S. L., GODDARD, J. M. & CAPECCHI, M. R. 1993. Mice homozygous for a targeted disruption of the proto-oncogene int-2 have developmental defects in the tail and inner ear. *Development,* 117**,** 13-28.

MARCHAL, L., LUXARDI, G., THOME, V. & KODJABACHIAN, L. 2009. BMP inhibition initiates neural induction via FGF signaling and Zic genes. *Proc Natl Acad Sci U S A,* 106**,** 17437-42.

MARCHESE, C., FELICI, A., VISCO, V., LUCANIA, G., IGARASHI, M., PICARDO, M., FRATI, L. & TORRISI, M. R. 2001. Fibroblast growth factor 10 induces proliferation and differentiation of human primary cultured keratinocytes. *J Invest Dermatol,* 116**,** 623-8.

MARECHAL, A. & ZOU, L. 2013. DNA damage sensing by the ATM and ATR kinases. *Cold Spring Harb Perspect Biol,* 5.

MARFORI, M., MYNOTT, A., ELLIS, J. J., MEHDI, A. M., SAUNDERS, N. F., CURMI, P. M., FORWOOD, J. K., BODEN, M. & KOBE, B. 2011. Molecular basis for specificity of nuclear import and prediction of nuclear localization. *Biochim Biophys Acta,* 1813**,** 1562-77.

MARICS, I., ADELAIDE, J., RAYBAUD, F., MATTEI, M. G., COULIER, F., PLANCHE, J., DE LAPEYRIERE, O. & BIRNBAUM, D. 1989. Characterization of the HST-related FGF.6 gene, a new member of the fibroblast growth factor gene family. *Oncogene,* 4**,** 335-40.

MARKS, K. M. & NOLAN, G. P. 2006. Chemical labeling strategies for cell biology. *Nat Methods,* 3**,** 591-6.

MASON, J. M., MORRISON, D. J., BASSIT, B., DIMRI, M., BAND, H., LICHT, J. D. & GROSS, I. 2004. Tyrosine phosphorylation of Sprouty proteins regulates their ability to inhibit growth factor signaling: a dual feedback loop. *Mol Biol Cell,* 15**,** 2176-88.

MATSUURA, Y. & STEWART, M. 2005. Nup50/Npap60 function in nuclear protein import complex disassembly and importin recycling. *EMBO J,* 24**,** 3681-9.

MCDONALD, H. Y. & WOJTOWICZ, J. M. 2005. Dynamics of neurogenesis in the dentate gyrus of adult rats. *Neurosci Lett,* 385**,** 70-5.

MCKELVY, J. F., SHERIDAN, M., JOSEPH, S., PHELPS, C. H. & PERRIE, S. 1975. Biosynthesis of thyrotropin-releasing hormone in organ cultures of the guinea pig median eminence. *Endocrinology,* 97**,** 908-18.

MCKENNA, G. J., BURKE, F. M. & MELLAN, K. 2009. Case report: Presentation of lacrimo-auriculodento- digital (LADD) syndrome in a young female patient. *Eur Arch Paediatr Dent,* 10 Suppl 1**,** 35-9.

MELCHIOR, F., SCHERGAUT, M. & PICHLER, A. 2003. SUMO: ligases, isopeptidases and nuclear pores. *Trends Biochem Sci,* 28**,** 612-8.

MEUNIER, S., NAVARRO, M. G., BOSSARD, C., LAURELL, H., TOURIOL, C., LACAZETTE, E. & PRATS, H. 2009. Pivotal role of translokin/CEP57 in the unconventional secretion versus nuclear translocation of FGF2. *Traffic,* 10**,** 1765-72.

MICHAILOVICI, I., HARRINGTON, H. A., AZOGUI, H. H., YAHALOM-RONEN, Y., PLOTNIKOV, A., CHING, S., STUMPF, M. P., KLEIN, O. D., SEGER, R. & TZAHOR, E. 2014. Nuclear to cytoplasmic shuttling of ERK promotes differentiation of muscle stem/progenitor cells. *Development,* 141**,** 2611-20.

MICHALCZYK, K. & ZIMAN, M. 2005. Nestin structure and predicted function in cellular cytoskeletal organisation. *Histol Histopathol,* 20**,** 665-71.

MIETTINEN, P. J., CHIN, J. R., SHUM, L., SLAVKIN, H. C., SHULER, C. F., DERYNCK, R. & WERB, Z. 1999. Epidermal growth factor receptor function is necessary for normal craniofacial development and palate closure. *Nat Genet,* 22**,** 69-73.

MIGAUD, M., BATAILLER, M., SEGURA, S., DUITTOZ, A., FRANCESCHINI, I. & PILLON, D. 2010. Emerging new sites for adult neurogenesis in the mammalian brain: a comparative study between the hypothalamus and the classical neurogenic zones. *Eur J Neurosci,* 32**,** 2042-52.

MIGNATTI, P., MORIMOTO, T. & RIFKIN, D. B. 1992. Basic fibroblast growth factor, a protein devoid of secretory signal sequence, is released by cells via a pathway independent of the endoplasmic reticulum-Golgi complex. *J Cell Physiol,* 151**,** 81-93.

MIKI, T., BOTTARO, D. P., FLEMING, T. P., SMITH, C. L., BURGESS, W. H., CHAN, A. M. & AARONSON, S. A. 1992. Determination of ligand-binding specificity by alternative splicing: two distinct growth factor receptors encoded by a single gene. *Proc Natl Acad Sci U S A,* 89**,** 246-50.

MILUNSKY, J. M., ZHAO, G., MAHER, T. A., COLBY, R. & EVERMAN, D. B. 2006. LADD syndrome is caused by FGF10 mutations. *Clin Genet,* 69**,** 349-54.

MIN, H., DANILENKO, D. M., SCULLY, S. A., BOLON, B., RING, B. D., TARPLEY, J. E., DEROSE, M. & SIMONET, W. S. 1998. Fgf-10 is required for both limb and lung development and exhibits striking functional similarity to Drosophila branchless. *Genes & Development,* 12**,** 3156-3161.

MING, G. L. & SONG, H. 2005. Adult neurogenesis in the mammalian central nervous system. *Annual Review of Neuroscience,* 28**,** 223-50.

MING, G. L. & SONG, H. 2011. Adult neurogenesis in the mammalian brain: significant answers and significant questions. *Neuron,* 70**,** 687-702.

MINGOT, J. M., KOSTKA, S., KRAFT, R., HARTMANN, E. & GORLICH, D. 2001. Importin 13: a novel mediator of nuclear import and export. *EMBO J,* 20**,** 3685-94.

MINTSERIS, J. & WENG, Z. 2005. Structure, function, and evolution of transient and obligate protein-protein interactions. *Proc Natl Acad Sci U S A,* 102**,** 10930-5.

MITROUSIS, G., OLIA, A. S., WALKER-KOPP, N. & CINGOLANI, G. 2008. Molecular basis for the recognition of snurportin 1 by importin beta. *J Biol Chem,* 283**,** 7877-84.

MIYAKE, A., KONISHI, M., MARTIN, F. H., HERNDAY, N. A., OZAKI, K., YAMAMOTO, S., MIKAMI, T., ARAKAWA, T. & ITOH, N. 1998. Structure and expression of a novel member, FGF-16, on the fibroblast growth factor family. *Biochem Biophys Res Commun,* 243**,** 148-52.

MIYAMOTO, M., NARUO, K., SEKO, C., MATSUMOTO, S., KONDO, T. & KUROKAWA, T. 1993. Molecular cloning of a novel cytokine cDNA encoding the ninth member of the fibroblast growth factor family, which has a unique secretion property. *Mol Cell Biol,* 13**,** 4251-9.

MIZUKOSHI, E., SUZUKI, M., LOUPATOV, A., URUNO, T., HAYASHI, H., MISONO, T., KAUL, S. C., WADHWA, R. & IMAMURA, T. 1999. Fibroblast growth factor-1 interacts with the glucose-regulated protein GRP75/mortalin. *The Biochemical Journal,* 343**,** 461-466.

MONSIGNY, M., RONDANINO, C., DUVERGER, E., FAJAC, I. & ROCHE, A. C. 2004. Glyco-dependent nuclear import of glycoproteins, glycoplexes and glycosylated plasmids. *Biochim Biophys Acta,* 1673**,** 94-103.

MORI, H., NINOMIYA, K., KINO-OKA, M., SHOFUDA, T., ISLAM, M. O., YAMASAKI, M., OKANO, H., TAYA, M. & KANEMURA, Y. 2006. Effect of neurosphere size on the growth rate of human neural stem/progenitor cells. *J Neurosci Res,* 84**,** 1682-91.

MULLER, S., LEDL, A. & SCHMIDT, D. 2004. SUMO: a regulator of gene expression and genome integrity. *Oncogene,* 23**,** 1998-2008.

MULLER, W. J., LEE, F. S., DICKSON, C., PETERS, G., PATTENGALE, P. & LEDER, P. 1990. The int-2 gene product acts as an epithelial growth factor in transgenic mice. *EMBO J,* 9**,** 907-13.

MUSTAFA, H., STRASSER, B., RAUTH, S., IRVING, R. A. & WARK, K. L. 2006. Identification of a functional nuclear export signal in the green fluorescent protein asFP499. *Biochem Biophys Res Commun,* 342**,** 1178-82.

NAKAO, Y., MITSUYASU, T., KAWANO, S., NAKAMURA, N., KANDA, S. & NAKAMURA, S. 2013. Fibroblast growth factors 7 and 10 are involved in ameloblastoma proliferation via the mitogen-activated protein kinase pathway. *Int J Oncol,* 43**,** 1377-84.

NARDOZZI, J. D., LOTT, K. & CINGOLANI, G. 2010. Phosphorylation meets nuclear import: a review. *Cell Commun Signal,* 8**,** 32.

NARITA, K., FUJIHARA, K., TAKEI, Y., SUDA, M., AOYAMA, Y., UEHARA, T., MAJIMA, T., KOSAKA, H., AMANUMA, M., FUKUDA, M. & MIKUNI, M. 2012. Associations among parenting experiences during childhood and adolescence, hypothalamus-pituitary-adrenal axis hypoactivity, and hippocampal gray matter volume reduction in young adults. *Hum Brain Mapp,* 33**,** 2211-23.

NAVARRO-LERIDA, I., PELLINEN, T., SANCHEZ, S. A., GUADAMILLAS, M. C., WANG, Y., MIRTTI, T., CALVO, E. & DEL POZO, M. A. 2015. Rac1 nucleocytoplasmic shuttling drives nuclear shape changes and tumor invasion. *Dev Cell,* 32**,** 318-34.

NGUYEN BA, A. N., POGOUTSE, A., PROVART, N. & MOSES, A. M. 2009. NLStradamus: a simple Hidden Markov Model for nuclear localization signal prediction. *BMC Bioinformatics,* 10**,** 202.

NICK PACE, C., SCHOLTZ, J. M. & GRIMSLEY, G. R. 2014. Forces stabilizing proteins. *FEBS Lett,* 588**,** 2177-84.

NICOLAOU, N., MARGADANT, C., KEVELAM, S. H., LILIEN, M. R., OOSTERVELD, M. J., KREFT, M., VAN EERDE, A. M., PFUNDT, R., TERHAL, P. A., VAN DER ZWAAG, B., NIKKELS, P. G.,

SACHS, N., GOLDSCHMEDING, R., KNOERS, N. V., RENKEMA, K. Y. & SONNENBERG, A. 2012. Gain of glycosylation in integrin alpha3 causes lung disease and nephrotic syndrome. *J Clin Invest,* 122**,** 4375-87.

NILSEN, T., ROSENDAL, K. R., SORENSEN, V., WESCHE, J., OLSNES, S. & WIEDLOCHA, A. 2007. A nuclear export sequence located on a beta-strand in fibroblast growth factor-1. *J Biol Chem,* 282**,** 26245-56.

NISHIYAMA, A., KOMITOVA, M., SUZUKI, R. & ZHU, X. 2009. Polydendrocytes (NG2 cells): multifunctional cells with lineage plasticity. *Nat Rev Neurosci,* 10**,** 9-22.

NOMURA, S., YOSHITOMI, H., TAKANO, S., SHIDA, T., KOBAYASHI, S., OHTSUKA, M., KIMURA, F., SHIMIZU, H., YOSHIDOME, H., KATO, A. & MIYAZAKI, M. 2008. FGF10/FGFR2 signal induces cell migration and invasion in pancreatic cancer. *Br J Cancer,* 99**,** 305-13.

NORGAARD, G. A., JENSEN, J. N. & JENSEN, J. 2003. FGF10 signaling maintains the pancreatic progenitor cell state revealing a novel role of Notch in organ development. *Developmental Biology,* 264**,** 323-38.

OH, B. K., YOON, S. M., LEE, C. H. & PARK, Y. N. 2007. Rat homolog of PinX1 is a nucleolar protein involved in the regulation of telomere length. *Gene,* 400**,** 35-43.

OHUCHI, H., HORI, Y., YAMASAKI, M., HARADA, H., SEKINE, K., KATO, S. & ITOH, N. 2000. FGF10 acts as a major ligand for FGF receptor 2 IIIb in mouse multi-organ development. *Biochem Biophys Res Commun,* 277**,** 643-9.

OHUCHI, H., NAKAGAWA, T., ITOH, N. & NOJI, S. 1999. FGF10 can induce Fgf8 expression concomitantly with En1 and R-fng expression in chick limb ectoderm, independent of its dorsoventral specification. *Dev Growth Differ,* 41**,** 665-73.

OHUCHI, H., YASUE, A., ONO, K., SASAOKA, S., TOMONARI, S., TAKAGI, A., ITAKURA, M., MORIYAMA, K., NOJI, S. & NOHNO, T. 2005. Identification of cis-element regulating expression of the mouse Fgf10 gene during inner ear development. *Dev Dyn,* 233**,** 177-87.

OLSEN, S. K., IBRAHIMI, O. A., RAUCCI, A., ZHANG, F., ELISEENKOVA, A. V., YAYON, A., BASILICO, C., LINHARDT, R. J., SCHLESSINGER, J. & MOHAMMADI, M. 2004. Insights into the molecular basis for fibroblast growth factor receptor autoinhibition and ligand-binding promiscuity. *Proc Natl Acad Sci U S A,* 101**,** 935-40.

OLSEN, S. K., LI, J. Y., BROMLEIGH, C., ELISEENKOVA, A. V., IBRAHIMI, O. A., LAO, Z., ZHANG, F., LINHARDT, R. J., JOYNER, A. L. & MOHAMMADI, M. 2006. Structural basis by which alternative splicing modulates the organizer activity of FGF8 in the brain. *Genes Dev,* 20**,** 185-98.

OLSON, M. O., DUNDR, M. & SZEBENI, A. 2000. The nucleolus: an old factory with unexpected capabilities. *Trends Cell Biol,* 10**,** 189-96.

ORNITZ, D. M. 2000. FGFs, heparan sulfate and FGFRs: complex interactions essential for development. *Bioessays,* 22**,** 108-12.

ORNITZ, D. M. & ITOH, N. 2001. Fibroblast growth factors. *Genome Biol,* 2**,** REVIEWS3005.

ORNITZ, D. M. & ITOH, N. 2015. The Fibroblast Growth Factor signaling pathway. *Wiley Interdiscip Rev Dev Biol,* 4**,** 215-66.

ORNITZ, D. M. & MARIE, P. J. 2015. Fibroblast growth factor signaling in skeletal development and disease. *Genes Dev,* 29**,** 1463-86.

ORR-URTREGER, A., BEDFORD, M. T., BURAKOVA, T., ARMAN, E., ZIMMER, Y., YAYON, A., GIVOL, D. & LONAI, P. 1993. Developmental localization of the splicing alternatives of fibroblast growth factor receptor-2 (FGFR2). *Dev Biol,* 158**,** 475-86.

OZAKI, K., MIYAZAKI, S., TANIMURA, S. & KOHNO, M. 2005. Efficient suppression of FGF-2-induced ERK activation by the cooperative interaction among mammalian Sprouty isoforms. *J Cell Sci,* 118**,** 5861-71.

PAN, Y., CARBE, C., POWERS, A., ZHANG, E. E., ESKO, J. D., GROBE, K., FENG, G. S. & ZHANG, X. 2008. Bud specific N-sulfation of heparan sulfate regulates Shp2-dependent FGF signaling during lacrimal gland induction. *Development,* 135**,** 301-10.

PARTANEN, J., MAKELA, T. P., EEROLA, E., KORHONEN, J., HIRVONEN, H., CLAESSON-WELSH, L. & ALITALO, K. 1991. FGFR-4, a novel acidic fibroblast growth factor receptor with a distinct expression pattern. *EMBO J,* 10**,** 1347-54.

PASTRANA, E., SILVA-VARGAS, V. & DOETSCH, F. 2011. Eyes wide open: a critical review of sphere-formation as an assay for stem cells. *Cell Stem Cell,* 8**,** 486-98.

PAULEY, S., WRIGHT, T. J., PIRVOLA, U., ORNITZ, D., BEISEL, K. & FRITZSCH, B. 2003. Expression and function of FGF10 in mammalian inner ear development. *Dev Dyn,* 227**,** 203-15.

PEDERSON, T. 2011. The nucleolus. *Cold Spring Harb Perspect Biol,* 3.

PELLEGRINI, L., BURKE, D. F., VON DELFT, F., MULLOY, B. & BLUNDELL, T. L. 2000. Crystal structure of fibroblast growth factor receptor ectodomain bound to ligand and heparin. *Nature,* 407**,** 1029-1034.

PENCEA, V., BINGAMAN, K. D., WIEGAND, S. J. & LUSKIN, M. B. 2001. Infusion of brain-derived neurotrophic factor into the lateral ventricle of the adult rat leads to new neurons in the parenchyma of the striatum, septum, thalamus, and hypothalamus. *Journal of Neuroscience,* 21**,** 6706-17.

PERETTO, P., DATI, C., DE MARCHIS, S., KIM, H. H., UKHANOVA, M., FASOLO, A. & MARGOLIS, F. L. 2004. Expression of the secreted factors noggin and bone morphogenetic proteins in the subependymal layer and olfactory bulb of the adult mouse brain. *Neuroscience,* 128**,** 685-96.

PEREZ-MARTIN, M., CIFUENTES, M., GRONDONA, J. M., LOPEZ-AVALOS, M. D., GOMEZ-PINEDO, U., GARCIA-VERDUGO, J. M. & FERNANDEZ-LLEBREZ, P. 2010. IGF-I stimulates neurogenesis in the hypothalamus of adult rats. *Eur J Neurosci,* 31**,** 1533-48.

PERUZZO, B., PASTOR, F. E., BLÁZQUEZ, J. L., SCHÖBITZ, K., PELÁEZ, B., AMAT, P. & RODRÍGUEZ, E. M. 2000. A second look at the barriers of the medial basal hypothalamus. *Experimental Brain Research,* 132**,** 10-26.

PETERS, G., BROOKES, S., SMITH, R., PLACZEK, M. & DICKSON, C. 1989. The mouse homolog of the hst/k-FGF gene is adjacent to int-2 and is activated by proviral insertion in some virally induced mammary tumors. *Proc Natl Acad Sci U S A,* 86**,** 5678-82.

PETERSEN, T. N., BRUNAK, S., VON HEIJNE, G. & NIELSEN, H. 2011. SignalP 4.0: discriminating signal peptides from transmembrane regions. *Nat Meth,* 8**,** 785-786.

PINTUCCI, G., QUARTO, N. & RIFKIN, D. B. 1996. Methylation of high molecular weight fibroblast growth factor-2 determines post-translational increases in molecular weight and affects its intracellular distribution. *Mol Biol Cell,* 7**,** 1249-58.

PIRVOLA, U., SPENCER-DENE, B., XING-QUN, L., KETTUNEN, P., THESLEFF, I., FRITZSCH, B., DICKSON, C. & YLIKOSKI, J. 2000. FGF/FGFR-2(IIIb) signaling is essential for inner ear morphogenesis. *J Neurosci,* 20**,** 6125-34.

PORTER, L. A. & DONOGHUE, D. J. 2003. Cyclin B1 and CDK1: nuclear localization and upstream regulators. *Prog Cell Cycle Res,* 5**,** 335-47.

PRESTA, M., GUALANDRIS, A., URBINATI, C., RUSNATI, M., COLTRINI, D., ISACCHI, A., CACCIA, P. & BERGONZONI, L. 1993. Subcellular localization and biological activity of M(r) 18,000 basic fibroblast growth factor: site-directed mutagenesis of a putative nuclear translocation sequence. *Growth Factors,* 9**,** 269-78.

PUK, O., ESPOSITO, I., SOKER, T., LOSTER, J., BUDDE, B., NURNBERG, P., MICHEL-SOEWARTO, D., FUCHS, H., WOLF, E., HRABE DE ANGELIS, M. & GRAW, J. 2009. A new Fgf10 mutation in the mouse leads to atrophy of the harderian gland and slit-eye phenotype in heterozygotes: a novel model for dry-eye disease? *Invest Ophthalmol Vis Sci,* 50**,** 4311-8.

QIAO, J., UZZO, R., OBARA-ISHIHARA, T., DEGENSTEIN, L., FUCHS, E. & HERZLINGER, D. 1999. FGF-7 modulates ureteric bud growth and nephron number in the developing kidney. *Development,* 126**,** 547-54.

QU, X., CARBE, C., TAO, C., POWERS, A., LAWRENCE, R., VAN KUPPEVELT, T. H., CARDOSO, W. V., GROBE, K., ESKO, J. D. & ZHANG, X. 2011. Lacrimal gland development and Fgf10-

Fgfr2b signaling are controlled by 2-O- and 6-O-sulfated heparan sulfate. *J Biol Chem,* 286**,** 14435-44.

QU, X., PAN, Y., CARBE, C., POWERS, A., GROBE, K. & ZHANG, X. 2012. Glycosaminoglycan-dependent restriction of FGF diffusion is necessary for lacrimal gland development. *Development,* 139**,** 2730-9.

QUARTO, N., FINGER, F. P. & RIFKIN, D. B. 1991. The NH2-terminal extension of high molecular weight bFGF is a nuclear targeting signal. *J Cell Physiol,* 147**,** 311-8.

RABALLO, R., RHEE, J., LYN-COOK, R., LECKMAN, J. F., SCHWARTZ, M. L. & VACCARINO, F. M. 2000. Basic fibroblast growth factor (Fgf2) is necessary for cell proliferation and neurogenesis in the developing cerebral cortex. *J Neurosci,* 20**,** 5012-23.

REICHELT, R., HOLZENBURG, A., BUHLE, E. L., JR., JARNIK, M., ENGEL, A. & AEBI, U. 1990. Correlation between structure and mass distribution of the nuclear pore complex and of distinct pore complex components. *J Cell Biol,* 110**,** 883-94.

REIMERS, K., ANTOINE, M., ZAPATKA, M., BLECKEN, V., DICKSON, C. & KIEFER, P. 2001. NoBP, a nuclear fibroblast growth factor 3 binding protein, is cell cycle regulated and promotes cell growth. *Mol Cell Biol,* 21**,** 4996-5007.

RENKO, M., QUARTO, N., MORIMOTO, T. & RIFKIN, D. B. 1990. Nuclear and cytoplasmic localization of different basic fibroblast growth factor species. *J Cell Physiol,* 144**,** 108-14.

RETROSI, G., SEBIRE, N. J., BISHAY, M., KIELY, E. M., ANDERSON, J., DE COPPI, P., RESCA, E., RAMPLING, D., BIER, N., MILLS, K., EATON, S. & PIERRO, A. 2011. Brain lipid–binding protein: a marker of differentiation in neuroblastic tumors. *Journal of Pediatric Surgery,* 46**,** 1197-1200.

REYNOLDS, B. A. & WEISS, S. 1992. Generation of Neurons and Astrocytes from Isolated Cells of the Adult Mammalian Central Nervous System. *Science, New Series,* 255**,** 3.

REYNOLDS, B. A. & WEISS, S. 1996a. Clonal and Population Analyses Demonstrate That an EGF-Responsive Mammalian Embryonic CNS Precursor Is a Stem Cell. *Developmental Biology,* 175**,** 13.

REYNOLDS, B. A. & WEISS, S. 1996b. Clonal and population analyses demonstrate that an EGF-responsive mammalian embryonic CNS precursor is a stem cell. *Dev Biol,* 175**,** 1-13.

ROBINS, S. C., STEWART, I., MCNAY, D. E., TAYLOR, V., GIACHINO, C., GOETZ, M., NINKOVIC, J., BRIANCON, N., MARATOS-FLIER, E., FLIER, J. S., KOKOEVA, M. V. & PLACZEK, M. 2013. alpha-Tanycytes of the adult hypothalamic third ventricle include distinct populations of FGF-responsive neural progenitors. *Nat Commun,* 4**,** 2049.

ROCHAIS, F., STURNY, R., CHAO, C. M., MESBAH, K., BENNETT, M., MOHUN, T. J., BELLUSCI, S. & KELLY, R. G. 2014. FGF10 promotes regional foetal cardiomyocyte proliferation and adult cardiomyocyte cell-cycle re-entry. *Cardiovasc Res,* 104**,** 432-42.

RODRIGUEZ, E., BLAZQUEZ, J., PASTOR, F., PELAEZ, B., PENA, P., PERUZZO, B. & AMAT, P. 2005. Hypothalamic Tanycytes: A Key Component of Brain–Endocrine Interaction. *International Review of Cytology,* 247**,** 89-164.

RODRIGUEZ, E. M., BLAZQUEZ, J. L. & GUERRA, M. 2010. The design of barriers in the hypothalamus allows the median eminence and the arcuate nucleus to enjoy private milieus: the former opens to the portal blood and the latter to the cerebrospinal fluid. *Peptides,* 31**,** 757-76.

ROHMANN, E., BRUNNER, H. G., KAYSERILI, H., UYGUNER, O., NURNBERG, G., LEW, E. D., DOBBIE, A., ESWARAKUMAR, V. P., UZUMCU, A., ULUBIL-EMEROGLU, M., LEROY, J. G., LI, Y., BECKER, C., LEHNERDT, K., CREMERS, C. W., YUKSEL-APAK, M., NURNBERG, P., KUBISCH, C., SCHLESSINGER, J., VAN BOKHOVEN, H. & WOLLNIK, B. 2006. Mutations in different components of FGF signaling in LADD syndrome. *Nat Genet,* 38**,** 414-7.

ROJCZYK-GOLEBIEWSKA, E., PALASZ, A. & WIADERKIEWICZ, R. 2014. Hypothalamic subependymal niche: a novel site of the adult neurogenesis. *Cell Mol Neurobiol,* 34**,** 631-42.

ROMANOV, R. A., ALPAR, A., ZHANG, M. D., ZEISEL, A., CALAS, A., LANDRY, M., FUSZARD, M., SHIRRAN, S. L., SCHNELL, R., DOBOLYI, A., OLAH, M., SPENCE, L., MULDER, J., MARTENS, H., PALKOVITS, M., UHLEN, M., SITTE, H. H., BOTTING, C. H., WAGNER, L., LINNARSSON, S., HOKFELT, T. & HARKANY, T. 2015. A secretagogin locus of the mammalian hypothalamus controls stress hormone release. *EMBO J,* 34**,** 36-54.

RONDANINO, C., BOUSSER, M. T., MONSIGNY, M. & ROCHE, A. C. 2003. Sugar-dependent nuclear import of glycosylated proteins in living cells. *Glycobiology,* 13**,** 509-19.

ROSNER, M. & HENGSTSCHLAGER, M. 2012. Detection of cytoplasmic and nuclear functions of mTOR by fractionation. *Methods Mol Biol,* 821**,** 105-24.

ROUBIN, R., NAERT, K., POPOVICI, C., VATCHER, G., COULIER, F., THIERRY-MIEG, J., PONTAROTTI, P., BIRNBAUM, D., BAILLIE, D. & THIERRY-MIEG, D. 1999. let-756, a C. elegans fgf essential for worm development. *Oncogene,* 18**,** 6741-7.

RUGGIANO, A., FORESTI, O. & CARVALHO, P. 2014. Quality control: ER-associated degradation: protein quality control and beyond. *J Cell Biol,* 204**,** 869-79.

SACHDEV, S., BRUHN, L., SIEBER, H., PICHLER, A., MELCHIOR, F. & GROSSCHEDL, R. 2001. PIASy, a nuclear matrix-associated SUMO E3 ligase, represses LEF1 activity by sequestration into nuclear bodies. *Genes Dev,* 15**,** 3088-103.

SAHARA, S. & O'LEARY, D. D. 2009. Fgf10 regulates transition period of cortical stem cell differentiation to radial glia controlling generation of neurons and basal progenitors. *Neuron,* 63**,** 48-62.

SAHIN, U., LAPAQUETTE, P., ANDRIEUX, A., FAURE, G. & DEJEAN, A. 2014. Sumoylation of human argonaute 2 at lysine-402 regulates its stability. *PLoS One,* 9**,** e102957.

SAKAUE, H., KONISHI, M., OGAWA, W., ASAKI, T., MORI, T., YAMASAKI, M., TAKATA, M., UENO, H., KATO, S., KASUGA, M. & ITOH, N. 2002. Requirement of fibroblast growth factor 10 in development of white adipose tissue. *Genes Dev,* 16**,** 908-12.

SALA, F. G., DEL MORAL, P. M., TIOZZO, C., ALAM, D. A., WARBURTON, D., GRIKSCHEIT, T., VELTMAAT, J. M. & BELLUSCI, S. 2011. FGF10 controls the patterning of the tracheal cartilage rings via Shh. *Development,* 138**,** 273-82.

SALVATIERRA, J., LEE, D. A., ZIBETTI, C., DURAN-MORENO, M., YOO, S., NEWMAN, E. A., WANG, H., BEDONT, J. L., DE MELO, J., MIRANDA-ANGULO, A. L., GIL-PEROTIN, S., GARCIA-VERDUGO, J. M. & BLACKSHAW, S. 2014. The LIM homeodomain factor Lhx2 is required for hypothalamic tanycyte specification and differentiation. *J Neurosci,* 34**,** 16809-20.

SANCHEZ-HERAS, E., HOWELL, F. V., WILLIAMS, G. & DOHERTY, P. 2006. The fibroblast growth factor receptor acid box is essential for interactions with N-cadherin and all of the major isoforms of neural cell adhesion molecule. *J Biol Chem,* 281**,** 35208-16.

SASAK, H., YAMAOKA, T., OHUCHI, H., YASUE, A., NOHNO, T., KAWANO, H., KATO, S., ITAKURA, M., NAGAYAMA, M. & NOJI, S. 2002. Identification of cis-elements regulating expression of Fgf10 during limb development. *Int J Dev Biol,* 46**,** 963-7.

SASAKI, T., ITO, Y., BRINGAS, P., JR., CHOU, S., URATA, M. M., SLAVKIN, H. & CHAI, Y. 2006. TGFbeta-mediated FGF signaling is crucial for regulating cranial neural crest cell proliferation during frontal bone development. *Development,* 133**,** 371-81.

SAVIC, I., BERGLUND, H. & LINDSTROM, P. 2005. Brain response to putative pheromones in homosexual men. *Proc Natl Acad Sci U S A,* 102**,** 7356-61.

SCHECKENBACH, K., BALZ, V., WAGENMANN, M. & HOFFMANN, T. K. 2008. An intronic alteration of the fibroblast growth factor 10 gene causing ALSG-(aplasia of lacrimal and salivary glands) syndrome. *BMC Med Genet,* 9**,** 114.

SCHLESSINGER, J., PLOTNIKOV, A. N., IBRAHIMI, O. A., ELISEENKOVA, A. V., YEH, B. K., YAYON, A., LINHARDT, R. J. & MOHAMMADI, M. 2000. Crystal structure of a ternary FGF-FGFR-heparin complex reveals a dual role for heparin in FGFR binding and dimerization. *Mol Cell,* 6**,** 743-50.

SCHLUMMER, S., VETTER, R., KUDER, N., HENKEL, A., CHEN, Y. X., LI, Y. M., KUHLMANN, J. & WALDMANN, H. 2006. Influence of serine O-glycosylation or O-phosphorylation close to the vJun nuclear localisation sequence on nuclear import. *Chembiochem,* 7**,** 88-97.

SCHMID, R. S., YOKOTA, Y. & ANTON, E. S. 2006. Generation and characterization of brain lipid-binding protein promoter-based transgenic mouse models for the study of radial glia. *Glia,* 53**,** 345-51.

SEDEK, M. & STROUS, G. J. 2013. SUMOylation is a regulator of the translocation of Jak2 between nucleus and cytosol. *Biochem J,* 453**,** 231-9.

SEKINE, K., OHUCHI, H., FUJIWARA, M., YAMASAKI, M., YOSHIZAWA, T., SATO, T., YAGISHITA, N., MATSUI, D., KOGA, Y., ITOH, N. & KATO, S. 1999. Fgf10 is essential for limb and lung formation. *Nature Genetics,* 21**,** 138-41.

SERI, B., GARCIA-VERDUGO, J. M., MCEWEN, B. S. & ALVAREZ-BUYLLA, A. 2001. Astrocytes give rise to new neurons in the adult mammalian hippocampus. *J Neurosci,* 21**,** 7153-60.

SEUFERT, W., FUTCHER, B. & JENTSCH, S. 1995. Role of a ubiquitin-conjugating enzyme in degradation of S- and M-phase cyclins. *Nature,* 373**,** 78-81.

SEYMOUR, P. A., SHIH, H. P., PATEL, N. A., FREUDE, K. K., XIE, R., LIM, C. J. & SANDER, M. 2012. A Sox9/Fgf feed-forward loop maintains pancreatic organ identity. *Development,* 139**,** 3363-72.

SHAMS, I., ROHMANN, E., ESWARAKUMAR, V. P., LEW, E. D., YUZAWA, S., WOLLNIK, B., SCHLESSINGER, J. & LAX, I. 2007. Lacrimo-auriculo-dento-digital syndrome is caused by reduced activity of the fibroblast growth factor 10 (FGF10)-FGF receptor 2 signaling pathway. *Mol Cell Biol,* 27**,** 6903-12.

SHANER, N. C., CAMPBELL, R. E., STEINBACH, P. A., GIEPMANS, B. N., PALMER, A. E. & TSIEN, R. Y. 2004. Improved monomeric red, orange and yellow fluorescent proteins derived from Discosoma sp. red fluorescent protein. *Nat Biotechnol,* 22**,** 1567-72.

SHEN, B., ARESE, M., GUALANDRIS, A. & RIFKIN, D. B. 1998. Intracellular association of FGF-2 with the ribosomal protein L6/TAXREB107. *Biochem Biophys Res Commun,* 252**,** 524-8.

SHENG, Z. 2004. Nuclear and Nucleolar Localization of 18-kDa Fibroblast Growth Factor-2 Is Controlled by C-terminal Signals. *Journal of Biological Chemistry,* 279**,** 40153-40160.

SHENG, Z., LEWIS, J. A. & CHIRICO, W. J. 2004. Nuclear and nucleolar localization of 18-kDa fibroblast growth factor-2 is controlled by C-terminal signals. *J Biol Chem,* 279**,** 40153-60.

SHENG, Z., LIANG, Y., LIN, C. Y., COMAI, L. & CHIRICO, W. J. 2005. Direct regulation of rRNA transcription by fibroblast growth factor 2. *Mol Cell Biol,* 25**,** 9419-26.

SHIFLEY, E. T. & COLE, S. E. 2008. Lunatic fringe protein processing by proprotein convertases may contribute to the short protein half-life in the segmentation clock. *Biochimica et Biophysica Acta (BBA) - Molecular Cell Research,* 1783**,** 2384-2390.

SHIMADA, M. & NAKAMURA, T. 1973. Time of neuron origin in mouse hypothalamic nuclei. *Exp Neurol,* 41**,** 163-73.

SHIMOAKA, T., OGASAWARA, T., YONAMINE, A., CHIKAZU, D., KAWANO, H., NAKAMURA, K., ITOH, N. & KAWAGUCHI, H. 2002. Regulation of osteoblast, chondrocyte, and osteoclast functions by fibroblast growth factor (FGF)-18 in comparison with FGF-2 and FGF-10. *J Biol Chem,* 277**,** 7493-500.

SHIN, M., NOJI, S., NEUBUSER, A. & YASUGI, S. 2006. FGF10 is required for cell proliferation and gland formation in the stomach epithelium of the chicken embryo. *Dev Biol,* 294**,** 11-23.

SHUKUNAMI, C., ISHIZEKI, K., ATSUMI, T., OHTA, Y., SUZUKI, F. & HIRAKI, Y. 1997. Cellular hypertrophy and calcification of embryonal carcinoma-derived chondrogenic cell line ATDC5 in vitro. *J Bone Miner Res,* 12**,** 1174-88.

SHUKUNAMI, C., OHTA, Y., SAKUDA, M. & HIRAKI, Y. 1998. Sequential progression of the differentiation program by bone morphogenetic protein-2 in chondrogenic cell line ATDC5. *Exp Cell Res,* 241**,** 1-11.

SHUKUNAMI, C., SHIGENO, C., ATSUMI, T., ISHIZEKI, K., SUZUKI, F. & HIRAKI, Y. 1996. Chondrogenic differentiation of clonal mouse embryonic cell line ATDC5 in vitro: differentiation-dependent gene expression of parathyroid hormone (PTH)/PTH-related peptide receptor. *J Cell Biol,* 133**,** 457-68.

SIDIBE, A., MULLIER, A., CHEN, P., BARONCINI, M., BOUTIN, J. A., DELAGRANGE, P., PREVOT, V. & JOCKERS, R. 2010. Expression of the orphan GPR50 protein in rodent and human dorsomedial hypothalamus, tanycytes and median eminence. *J Pineal Res,* 48**,** 263-9.

SILVA, P. N., ALTAMENTOVA, S. M., KILKENNY, D. M. & ROCHELEAU, J. V. 2013. Fibroblast growth factor receptor like-1 (FGFRL1) interacts with SHP-1 phosphatase at insulin secretory granules and induces beta-cell ERK1/2 protein activation. *J Biol Chem,* 288**,** 17859-70.

SINGEC, I., KNOTH, R., MEYER, R. P., MACIACZYK, J., VOLK, B., NIKKHAH, G., FROTSCHER, M. & SNYDER, E. Y. 2006. Defining the actual sensitivity and specificity of the neurosphere assay in stem cell biology. *Nat Methods,* 3**,** 801-6.

SKJERPEN, C. S., NILSEN, T., WESCHE, J. & OLSNES, S. 2002. Binding of FGF-1 variants to protein kinase CK2 correlates with mitogenicity. *EMBO journal,* 15**,** 4058-4069.

SLEEMAN, M., FRASER, J., MCDONALD, M., YUAN, S., WHITE, D., GRANDISON, P., KUMBLE, K., WATSON, J. D. & MURISON, J. G. 2001. Identification of a new fibroblast growth factor receptor, FGFR5. *Gene,* 271**,** 171-82.

SMALLWOOD, P. M., MUNOZ-SANJUAN, I., TONG, P., MACKE, J. P., HENDRY, S. H., GILBERT, D. J., COPELAND, N. G., JENKINS, N. A. & NATHANS, J. 1996. Fibroblast growth factor (FGF) homologous factors: new members of the FGF family implicated in nervous system development. *Proc Natl Acad Sci U S A,* 93**,** 9850-7.

SOBUE, T., ZHANG, X., FLORKIEWICZ, R. Z. & HURLEY, M. M. 2001. Interleukin-1 regulates FGF-2 mRNA and localization of FGF-2 protein in human osteoblasts. *Biochem Biophys Res Commun,* 286**,** 33-40.

SORENSEN, V., WIEDLOCHA, A., HAUGSTEN, E. M., KHNYKIN, D., WESCHE, J. & OLSNES, S. 2006. Different abilities of the four FGFRs to mediate FGF-1 translocation are linked to differences in the receptor C-terminal tail. *J Cell Sci,* 119**,** 4332-41.

SOULET, F., AL SAATI, T., ROGA, S., AMALRIC, F. & BOUCHE, G. 2001. Fibroblast growth factor-2 interacts with free ribosomal protein S19. *Biochem Biophys Res Commun,* 289**,** 591-6.

SOUSA-FERREIRA, L., ALVARO, A. R., AVELEIRA, C., SANTANA, M., BRANDAO, I., KUGLER, S., DE ALMEIDA, L. P. & CAVADAS, C. 2011. Proliferative Hypothalamic Neurospheres Express NPY, AGRP, POMC, CART and Orexin-A and Differentiate to Functional Neurons. *PLoS One,* 6**,** 11.

STADLER, C., REXHEPAJ, E., SINGAN, V. R., MURPHY, R. F., PEPPERKOK, R., UHLEN, M., SIMPSON, J. C. & LUNDBERG, E. 2013. Immunofluorescence and fluorescent-protein tagging show high correlation for protein localization in mammalian cells. *Nat Meth,* 10**,** 315-323.

STEINBERG, Z., MYERS, C., HEIM, V. M., LATHROP, C. A., REBUSTINI, I. T., STEWART, J. S., LARSEN, M. & HOFFMAN, M. P. 2005. FGFR2b signaling regulates ex vivo submandibular gland epithelial cell proliferation and branching morphogenesis. *Development,* 132**,** 1223-34.

STORM, E. E., RUBENSTEIN, J. L. & MARTIN, G. R. 2003. Dosage of Fgf8 determines whether cell survival is positively or negatively regulated in the developing forebrain. *Proc Natl Acad Sci U S A,* 100**,** 1757-62.

SUGIMOTO, K., YOSHIDA, S., MASHIO, Y., TOYOTA, N., XING, Y., XU, H., FUJITA, Y., HUANG, Z., TOUMA, M. & WU, Q. 2014. Role of FGF10 on tumorigenesis by MS-K. *Genes Cells,* 19**,** 112-25.

SUN, X., LEWANDOSKI, M., MEYERS, E. N., LIU, Y. H., MAXSON, R. E., JR. & MARTIN, G. R. 2000. Conditional inactivation of Fgf4 reveals complexity of signalling during limb bud development. *Nat Genet,* 25**,** 83-6.

SUNMONU, N. A., LI, K. & LI, J. Y. 2011. Numerous isoforms of Fgf8 reflect its multiple roles in the developing brain. *J Cell Physiol,* 226**,** 1722-6.

SUTHERLAND, D., SAMAKOVLIS, C. & KRASNOW, M. A. 1996. branchless encodes a Drosophila FGF homolog that controls tracheal cell migration and the pattern of branching. *Cell,* 87**,** 1091-101.

SUZUKI, A., HARADA, H. & NAKAMURA, H. 2012. Nuclear translocation of FGF8 and its implication to induce Sprouty2. *Dev Growth Differ,* 54**,** 463-73.

TAKEBAYASHI, H., NABESHIMA, Y., YOSHIDA, S., CHISAKA, O., IKENAKA, K. & NABESHIMA, Y. 2002. The basic helix-loop-helix factor olig2 is essential for the development of motoneuron and oligodendrocyte lineages. *Curr Biol,* 12**,** 1157-63.

TAKEBAYASHI, H., YOSHIDA, S., SUGIMORI, M., KOSAKO, H., KOMINAMI, R., NAKAFUKU, M. & NABESHIMA, Y. 2000. Dynamic expression of basic helix-loop-helix Olig family members: implication of Olig2 in neuron and oligodendrocyte differentiation and identification of a new member, Olig3. *Mech Dev,* 99**,** 143-8.

TANNOUS, A., PISONI, G. B., HEBERT, D. N. & MOLINARI, M. 2015. N-linked sugar-regulated protein folding and quality control in the ER. *Semin Cell Dev Biol,* 41**,** 79-89.

TAO, H., ONO, K., KUROSE, H., NOJI, S. & OHUCHI, H. 2006. Exogenous FGF10 can rescue an eye-open at birth phenotype of Fgf10-null mice by activating activin and TGFalpha-EGFR signaling. *Dev Growth Differ,* 48**,** 339-46.

TAO, H., SHIMIZU, M., KUSUMOTO, R., ONO, K., NOJI, S. & OHUCHI, H. 2005. A dual role of FGF10 in proliferation and coordinated migration of epithelial leading edge cells during mouse eyelid development. *Development,* 132**,** 3217-30.

TASSI, E., AL-ATTAR, A., AIGNER, A., SWIFT, M. R., MCDONNELL, K., KARAVANOV, A. & WELLSTEIN, A. 2001. Enhancement of fibroblast growth factor (FGF) activity by an FGF-binding protein. *J Biol Chem,* 276**,** 40247-53.

TEKIN, M., HISMI, B. O., FITOZ, S., OZDAG, H., CENGIZ, F. B., SIRMACI, A., ASLAN, I., INCEOGLU, B., YUKSEL-KONUK, E. B., YILMAZ, S. T., YASUN, O. & AKAR, N. 2007. Homozygous mutations in fibroblast growth factor 3 are associated with a new form of syndromic deafness characterized by inner ear agenesis, microtia, and microdontia. *Am J Hum Genet,* 80**,** 338-44.

TEMU, T. M., WU, K. Y., GRUPPUSO, P. A. & PHORNPHUTKUL, C. 2010. The mechanism of ascorbic acid-induced differentiation of ATDC5 chondrogenic cells. *Am J Physiol Endocrinol Metab,* 299**,** E325-34.

TERADA, M., SHIMIZU, A., SATO, N., MIYAKAZE, S. I., KATAYAMA, H. & KUROKAWA-SEO, M. 2001. Fibroblast growth factor receptor 3 lacking the Ig IIIb and transmembrane domains secreted from human squamous cell carcinoma DJM-1 binds to FGFs. *Mol Cell Biol Res Commun,* 4**,** 365-73.

TERAO, F., TAKAHASHI, I., MITANI, H., HARUYAMA, N., SASANO, Y., SUZUKI, O. & TAKANO-YAMAMOTO, T. 2011. Fibroblast growth factor 10 regulates Meckel's cartilage formation during early mandibular morphogenesis in rats. *Dev Biol,* 350**,** 337-47.

TERAUCHI, A., JOHNSON-VENKATESH, E. M., TOTH, A. B., JAVED, D., SUTTON, M. A. & UMEMORI, H. 2010. Distinct FGFs promote differentiation of excitatory and inhibitory synapses. *Nature,* 465**,** 783-7.

TERAUCHI, A., TIMMONS, K. M., KIKUMA, K., PECHMANN, Y., KNEUSSEL, M. & UMEMORI, H. 2015. Selective synaptic targeting of the excitatory and inhibitory presynaptic organizers FGF22 and FGF7. *J Cell Sci,* 128**,** 281-92.

TERPE, K. 2003. Overview of tag protein fusions: from molecular and biochemical fundamentals to commercial systems. *Appl Microbiol Biotechnol,* 60**,** 523-33.

THEODOROU, V., BOER, M., WEIGELT, B., JONKERS, J., VAN DER VALK, M. & HILKENS, J. 2004. Fgf10 is an oncogene activated by MMTV insertional mutagenesis in mouse mammary tumors and overexpressed in a subset of human breast carcinomas. *Oncogene,* 23**,** 6047-55.

THEUS, M. H., RICARD, J. & LIEBL, D. J. 2012. Reproducible expansion and characterization of mouse neural stem/progenitor cells in adherent cultures derived from the adult subventricular zone. *Curr Protoc Stem Cell Biol,* Chapter 2**,** Unit 2D 8.

TIOZZO, C., DE LANGHE, S., CARRARO, G., ALAM, D. A., NAGY, A., WIGFALL, C., HAJIHOSSEINI, M. K., WARBURTON, D., MINOO, P. & BELLUSCI, S. 2009. Fibroblast growth factor 10 plays a causative role in the tracheal cartilage defects in a mouse model of Apert syndrome. *Pediatr Res,* 66**,** 386-90.

TOMLINSON, D. C., GRINDLEY, J. C. & THOMSON, A. A. 2004. Regulation of Fgf10 gene expression in the prostate: identification of transforming growth factor-beta1 and promoter elements. *Endocrinology,* 145**,** 1988-95.

TOMLINSON, D. C., L'HOTE, C. G., KENNEDY, W., PITT, E. & KNOWLES, M. A. 2005. Alternative splicing of fibroblast growth factor receptor 3 produces a secreted isoform that inhibits fibroblast growth factor-induced proliferation and is repressed in urothelial carcinoma cell lines. *Cancer Res,* 65**,** 10441-9.

TROPEPE, V., SIBILIA, M., CIRUNA, B. G., ROSSANT, J., WAGNER, E. F. & VAN DER KOOY, D. 1999. Distinct neural stem cells proliferate in response to EGF and FGF in the developing mouse telencephalon. *Dev Biol,* 208**,** 166-88.

TROTTER, J., KARRAM, K. & NISHIYAMA, A. 2010. NG2 cells: Properties, progeny and origin. *Brain Res Rev,* 63**,** 72-82.

TSAI, P. S., BROOKS, L. R., ROCHESTER, J. R., KAVANAUGH, S. I. & CHUNG, W. C. 2011. Fibroblast growth factor signaling in the developing neuroendocrine hypothalamus. *Front Neuroendocrinol,* 32**,** 95-107.

TSANG, M. & DAWID, I. B. 2004. Promotion and attenuation of FGF signaling through the Ras-MAPK pathway. *Sci STKE,* 2004**,** pe17.

TSANG, M., FRIESEL, R., KUDOH, T. & DAWID, I. B. 2002. Identification of Sef, a novel modulator of FGF signalling. *Nat Cell Biol,* 4**,** 165-9.

TSAU, C., ITO, M., GROMOVA, A., HOFFMAN, M. P., MEECH, R. & MAKARENKOVA, H. P. 2011. Barx2 and Fgf10 regulate ocular glands branching morphogenesis by controlling extracellular matrix remodeling. *Development,* 138**,** 3307-17.

TUMMERS, M. & THESLEFF, I. 2003. Root or crown: a developmental choice orchestrated by the differential regulation of the epithelial stem cell niche in the tooth of two rodent species. *Development,* 130**,** 1049-57.

TURNER, N. & GROSE, R. 2010. Fibroblast growth factor signalling: from development to cancer. *Nat Rev Cancer,* 10**,** 116-29.

ULLAH, I., SUBBARAO, R. B. & RHO, G. J. 2015. Human mesenchymal stem cells - current trends and future prospective. *Biosci Rep,* 35.

UMEMORI, H., LINHOFF, M. W., ORNITZ, D. M. & SANES, J. R. 2004. FGF22 and its close relatives are presynaptic organizing molecules in the mammalian brain. *Cell,* 118**,** 257-70.

URBAN, N. & GUILLEMOT, F. 2014. Neurogenesis in the embryonic and adult brain: same regulators, different roles. *Front Cell Neurosci,* 8**,** 396.

URNESS, L. D., BLEYL, S. B., WRIGHT, T. J., MOON, A. M. & MANSOUR, S. L. 2011. Redundant and dosage sensitive requirements for Fgf3 and Fgf10 in cardiovascular development. *Dev Biol,* 356**,** 383-97.

URNESS, L. D., WANG, X., SHIBATA, S., OHYAMA, T. & MANSOUR, S. L. 2015. Fgf10 is required for specification of non-sensory regions of the cochlear epithelium. *Dev Biol,* 400**,** 59-71.

VACCARINO, F. M., SCHWARTZ, M. L., RABALLO, R., NILSEN, J., RHEE, J., ZHOU, M., DOETSCHMAN, T., COFFIN, J. D., WYLAND, J. J. & HUNG, Y. T. 1999. Changes in cerebral cortex size are governed by fibroblast growth factor during embryogenesis. *Nat Neurosci,* 2**,** 246-53.

VASSALLI, A., MATZUK, M. M., GARDNER, H. A., LEE, K. F. & JAENISCH, R. 1994. Activin/inhibin beta B subunit gene disruption leads to defects in eyelid development and female reproduction. *Genes Dev,* 8**,** 414-27.

VIKTOROV, I. V., SAVCHENKO, E. A. & CHEKHONIN, V. P. 2007. Spontaneous neural differentiation of stem cells in culture of human olfactory epithelium. *Bull Exp Biol Med,* 144**,** 596-601.

VOLCKAERT, T. & DE LANGHE, S. 2014. Lung epithelial stem cells and their niches: Fgf10 takes center stage. *Fibrogenesis Tissue Repair,* 7**,** 8.

VON BOHLEN UND HALBACH, O. 2011. Immunohistological markers for proliferative events, gliogenesis, and neurogenesis within the adult hippocampus. *Cell Tissue Res,* 345**,** 1-19.

VON MIKECZ, A., CHEN, M., ROCKEL, T. & SCHARF, A. 2008. The nuclear ubiquitin-proteasome system: visualization of proteasomes, protein aggregates, and proteolysis in the cell nucleus. *Methods Mol Biol,* 463**,** 191-202.

WANG, T. Y., SEN, A., BEHIE, L. A. & KALLOS, M. S. 2006. Dynamic behavior of cells within neurospheres in expanding populations of neural precursors. *Brain Res,* 1107**,** 82-96.

WEI, L. C., SHI, M., CHEN, L. W., CAO, R., ZHANG, P. & CHAN, Y. S. 2002. Nestin-containing cells express glial fibrillary acidic protein in the proliferative regions of central nervous system of postnatal developing and adult mice. *Brain Res Mol Brain Res,* 139**,** 9-17.

WERNER, S., PETERS, K. G., LONGAKER, M. T., FULLER-PACE, F., BANDA, M. J. & WILLIAMS, L. T. 1992. Large induction of keratinocyte growth factor expression in the dermis during wound healing. *Proc Natl Acad Sci U S A,* 89**,** 6896-900.

WESCHE, J., MAŁECKI, J., WIEDŁOCHA, A., EHSANI, M., MARCINKOWSKA, E., NILSEN, T. & OLSNES, S. 2005a. Two Nuclear Localization Signals Required for Transport from the Cytosol to the Nucleus of Externally Added FGF-1 Translocated into Cells. . *Biochemistry,* 44**,** 6071-6080.

WESCHE, J., MAŁECKI, J., WIEDŁOCHA, A., EHSANI, M., MARCINKOWSKA, E., NILSEN, T. & OLSNES, S. 2005b. Two nuclear localization signals required for transport from the cytosol to the nucleus of externally added FGF-1 translocated into cells. *Biochemistry,* 44**,** 6071-80.

WESCHE, J., MALECKI, J., WIEDLOCHA, A., SKJERPEN, C. S., CLAUS, P. & OLSNES, S. 2006. FGF-1 and FGF-2 require the cytosolic chaperone Hsp90 for translocation into the cytosol and the cell nucleus. *J Biol Chem,* 281**,** 11405-12.

WHITE, K. E., CARN, G., LORENZ-DEPIEREUX, B., BENET-PAGES, A., STROM, T. M. & ECONS, M. J. 2001. Autosomal-dominant hypophosphatemic rickets (ADHR) mutations stabilize FGF-23. *Kidney Int,* 60**,** 2079-86.

WIEDŁOCHA, A., SANDVIG, K., FALNES, P. O., MADSHUS, I. H. & OLSNES, S. 1994. Dual Mode of Signal Transduction by Externally Added Acidic Fibroblast Growth Factor. *Cell,* 76**,** 1039-1051.

WILLIAMS, A. R. & HARE, J. M. 2011. Mesenchymal stem cells: biology, pathophysiology, translational findings, and therapeutic implications for cardiac disease. *Circ Res,* 109**,** 923-40.

WILLIAMS, S. E., GARCIA, I., CROWTHER, A. J., LI, S., STEWART, A., LIU, H., LOUGH, K. J., O'NEILL, S., VELETA, K., OYARZABAL, E. A., MERRILL, J. R., SHIH, Y. Y. & GERSHON, T. R. 2015. Aspm sustains postnatal cerebellar neurogenesis and medulloblastoma growth in mice. *Development,* 142**,** 3921-32.

WINEY, M., YARAR, D., GIDDINGS, T. H., JR. & MASTRONARDE, D. N. 1997. Nuclear pore complex number and distribution throughout the Saccharomyces cerevisiae cell cycle by three-dimensional reconstruction from electron micrographs of nuclear envelopes. *Mol Biol Cell,* 8**,** 2119-32.

WOODBURY, M. E. & IKEZU, T. 2014. Fibroblast growth factor-2 signaling in neurogenesis and neurodegeneration. *J Neuroimmune Pharmacol,* 9**,** 92-101.

WRIGHT, T. J. & MANSOUR, S. L. 2003. FGF signaling in ear development and innervation. *Curr Top Dev Biol,* 57**,** 225-59.

XIE, M. H., HOLCOMB, I., DEUEL, B., DOWD, P., HUANG, A., VAGTS, A., FOSTER, J., LIANG, J., BRUSH, J., GU, Q., HILLAN, K., GODDARD, A. & GURNEY, A. L. 1999. FGF-19, a novel fibroblast growth factor with unique specificity for FGFR4. *Cytokine,* 11**,** 729-35.

XIONG, F., GAO, H., ZHEN, Y., CHEN, X., LIN, W., SHEN, J., YAN, Y., WANG, X., LIU, M. & GAO, Y. 2011. Optimal time for passaging neurospheres based on primary neural stem cell cultures. *Cytotechnology,* 63**,** 621-31.

XU, D., GRISHIN, N. V. & CHOOK, Y. M. 2012. NESdb: a database of NES-containing CRM1 cargoes. *Mol Biol Cell,* 23**,** 3673-6.

XU, H., MORISHIMA, M., WYLIE, J. N., SCHWARTZ, R. J., BRUNEAU, B. G., LINDSAY, E. A. & BALDINI, A. 2004. Tbx1 has a dual role in the morphogenesis of the cardiac outflow tract. *Development,* 131**,** 3217-27.

XU, J., LAWSHE, A., MACARTHUR, C. A. & ORNITZ, D. M. 1999. Genomic structure, mapping, activity and expression of fibroblast growth factor 17. *Mech Dev,* 83**,** 165-78.

XU, L. & BLACKBURN, E. H. 2004. Human Rif1 protein binds aberrant telomeres and aligns along anaphase midzone microtubules. *J Cell Biol,* 167**,** 819-30.

XU, L. & MASSAGUE, J. 2004. Nucleocytoplasmic shuttling of signal transducers. *Nat Rev Mol Cell Biol,* 5**,** 209-19.

XU, Y., TAMAMAKI, N., NODA, T., KIMURA, K., ITOKAZU, Y., MATSUMOTO, N., DEZAWA, M. & IDE, C. 2005. Neurogenesis in the ependymal layer of the adult rat 3rd ventricle. *Exp Neurol,* 192**,** 251-64.

YAMAMOTO-SHIRAISHI, Y., HIGUCHI, H., YAMAMOTO, S., HIRANO, M. & KUROIWA, A. 2014. Etv1 and Ewsr1 cooperatively regulate limb mesenchymal Fgf10 expression in response to apical ectodermal ridge-derived fibroblast growth factor signal. *Dev Biol,* 394**,** 181-90.

YAMASAKI, M., MIYAKE, A., TAGASHIRA, S. & ITOH, N. 1996. Structure and Expression of the Rat mRNA Encoding a Novel Member of the Fibroblast Growth Factor Family. *Journal of Biological Chemistry,* 271**,** 15918-15921.

YAMASHITA, T., YOSHIOKA, M. & ITOH, N. 2000. Identification of a novel fibroblast growth factor, FGF-23, preferentially expressed in the ventrolateral thalamic nucleus of the brain. *Biochem Biophys Res Commun,* 277**,** 494-8.

YANG, H. Y., LIESKA, N., SHAO, D., KRIHO, V. & PAPPAS, G. D. 1994. Proteins of the intermediate filament cytoskeleton as markers for astrocytes and human astrocytomas. *Mol Chem Neuropathol,* 21**,** 155-76.

YAO, Y. & WANG, Y. 2013. ATDC5: an excellent in vitro model cell line for skeletal development. *J Cell Biochem,* 114**,** 1223-9.

YEH, B. K., IGARASHI, M., ELISEENKOVA, A. V., PLOTNIKOV, A. N., SHER, I., RON, D., AARONSON, S. A. & MOHAMMADI, M. 2003. Structural basis by which alternative splicing confers specificity in fibroblast growth factor receptors. *Proc Natl Acad Sci U S A,* 100**,** 2266-71.

YOKOHAMA-TAMAKI, T., OHSHIMA, H., FUJIWARA, N., TAKADA, Y., ICHIMORI, Y., WAKISAKA, S., OHUCHI, H. & HARADA, H. 2006. Cessation of Fgf10 signaling, resulting in a defective dental epithelial stem cell compartment, leads to the transition from crown to root formation. *Development,* 133**,** 1359-66.

YOSHIDA, M., MEGURO, A., OKADA, E., NOMURA, N. & MIZUKI, N. 2013. Association study of fibroblast growth factor 10 (FGF10) polymorphisms with susceptibility to extreme myopia in a Japanese population. *Mol Vis,* 19**,** 2321-9.

YOSHIDA, M. C., WADA, M., SATOH, H., YOSHIDA, T., SAKAMOTO, H., MIYAGAWA, K., YOKOTA, J., KODA, T., KAKINUMA, M., SUGIMURA, T. & ET AL. 1988. Human HST1 (HSTF1) gene maps to chromosome band 11q13 and coamplifies with the INT2 gene in human cancer. *Proc Natl Acad Sci U S A,* 85**,** 4861-4.

ZACHERL, S., LA VENUTA, G., MULLER, H. M., WEGEHINGEL, S., DIMOU, E., SEHR, P., LEWIS, J. D., ERFLE, H., PEPPERKOK, R. & NICKEL, W. 2015. A direct role for ATP1A1 in unconventional secretion of fibroblast growth factor 2. *J Biol Chem,* 290**,** 3654-65.

ZAKRZEWSKA, M., KROWARSCH, D., WIEDLOCHA, A. & OTLEWSKI, J. 2004. Design of fully active FGF-1 variants with increased stability. *Protein Eng Des Sel,* 17**,** 603-11.

ZELARAYAN, L. C., VENDRELL, V., ALVAREZ, Y., DOMINGUEZ-FRUTOS, E., THEIL, T., ALONSO, M. T., MACONOCHIE, M. & SCHIMMANG, T. 2007. Differential requirements for FGF3, FGF8 and FGF10 during inner ear development. *Dev Biol,* 308**,** 379-91.

ZHAN, X., HU, X., FRIEDMAN, S. & MACIAG, T. 1992. Analysis of endogenous and exogenous nuclear translocation of fibroblast growth factor-1 in NIH 3T3 cells. *Biochem Biophys Res Commun,* 188**,** 982-91.

ZHANG, K., HANSEN, P. J. & EALY, A. D. 2010a. Fibroblast growth factor 10 enhances bovine oocyte maturation and developmental competence in vitro. *Reproduction,* 140**,** 815-26.

ZHANG, X., BAO, L., YANG, L., WU, Q. & LI, S. 2012. Roles of intracellular fibroblast growth factors in neural development and functions. *Sci China Life Sci,* 55**,** 1038-44.

ZHANG, X., IBRAHIMI, O. A., OLSEN, S. K., UMEMORI, H., MOHAMMADI, M. & ORNITZ, D. M. 2006. Receptor specificity of the fibroblast growth factor family. The complete mammalian FGF family. *J Biochem,* 281**,** 15694-700.

ZHANG, X., WU, M., ZHANG, W., SHEN, J. & LIU, H. 2010b. Differentiation of human adipose-derived stem cells induced by recombinantly expressed fibroblast growth factor 10 in vitro and in vivo. *In Vitro Cell Dev Biol Anim,* 46**,** 60-71.

ZHAO, C., DENG, W. & GAGE, F. H. 2008. Mechanisms and functional implications of adult neurogenesis. *Cell,* 132**,** 645-60.

ZHAO, H., LI, S., HAN, D., KAARTINEN, V. & CHAI, Y. 2011. Alk5-mediated transforming growth factor beta signaling acts upstream of fibroblast growth factor 10 to regulate the proliferation and maintenance of dental epithelial stem cells. *Mol Cell Biol,* 31**,** 2079-89.

ZHAO, L., ERICKSEN, B., WU, X., ZHAN, C., YUAN, W., LI, X., PAZGIER, M. & LU, W. 2012. Invariant gly residue is important for alpha-defensin folding, dimerization, and function: a case study of the human neutrophil alpha-defensin HNP1. *J Biol Chem,* 287**,** 18900-12.

ZHAO, M., MOMMA, S., DELFANI, K., CARLEN, M., CASSIDY, R. M., JOHANSSON, C. B., BRISMAR, H., SHUPLIAKOV, O., FRISEN, J. & JANSON, A. M. 2003. Evidence for neurogenesis in the adult mammalian substantia nigra. *Proc Natl Acad Sci U S A,* 100**,** 7925-30.

ZHAO, Q., XIE, Y., ZHENG, Y., JIANG, S., LIU, W., MU, W., LIU, Z., ZHAO, Y., XUE, Y. & REN, J. 2014. GPS-SUMO: a tool for the prediction of sumoylation sites and SUMO-interaction motifs. *Nucleic Acids Res,* 42**,** W325-30.

ZHENG, W., NOWAKOWSKI, R. S. & VACCARINO, F. M. 2004. Fibroblast growth factor 2 is required for maintaining the neural stem cell pool in the mouse brain subventricular zone. *Dev Neurosci,* 26**,** 181-96.

Appendix 1: Representative data demonstrating similarities of results generated by bioinformatics searches using rat, mouse and human FGF10 protein sequences.

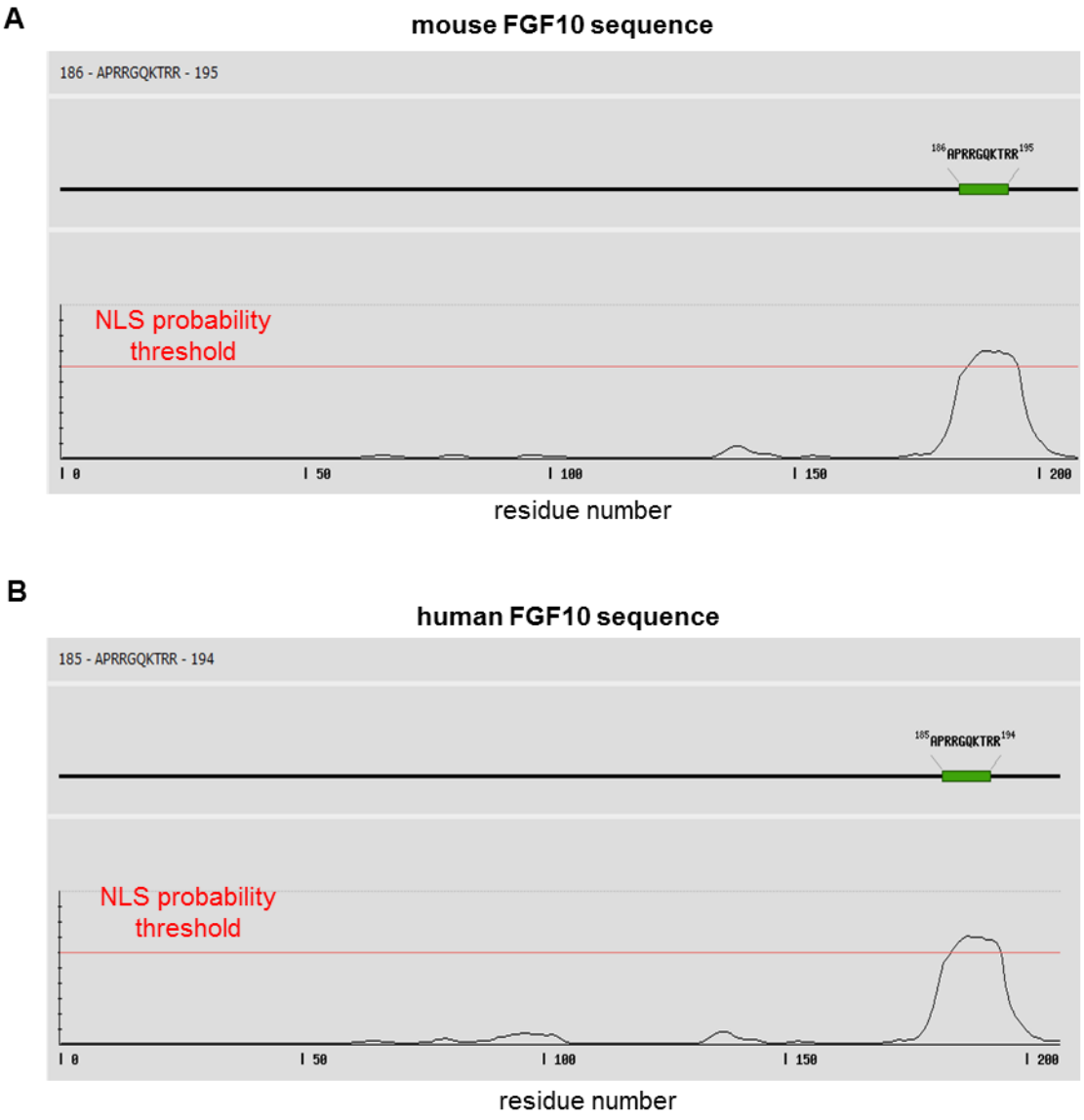

Appendix 1 Results of NLStradamus showing positioning of NLS2 sequence present within mouse (A) and human (B) FGF10 sequences. Note the sequence conservation between the species.

Appendix 2: SUMOylation sites within human and mouse FGF10

A

human FGF10 sequence

ID	Position	Peptide	Score	Cutoff	Type
FGF10_human	91	SFTKYFLKIEKNGKV	26.376	16	Sumoylation

O15520|FGF10_HUMAN Fibroblast growth factor 10 OS=Homo sapiens GN=FGF10 PE=1

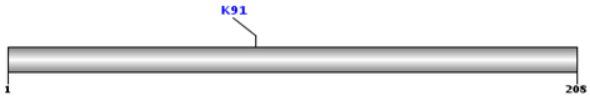

B

mouse FGF10 sequence

Carleton UNIVERSITY Department of Systems and Computer Engineering

PCI-SUMO

PCI-Based Sumo Site Prediction Server

J.R. Green, G.M. Dmochowski, and A. Golshani

Results

mFGF10

Lysine Location	Window of Residues	Sumo/Not Sumo	Confidence	Part of a Motif
3	XXXXXXMWKWILTHCAS	NA	NA	No
88	WRRLFSFTKYFLTIEKN	NotSumo	0.9252	No
95	TKYFLTIEKNGKVSGTK	NotSumo	0.4960	No
98	FLTIEKNGKVSGTKNED	NotSumo	0.5710	No
103	KNGKVSGTKNEDCPYSV	Sumo	0.7085	No
125	VEIGVVAVKAINSNYYL	NotSumo	0.9207	No
137	SNYYLAMNKKGKLYGSK	NotSumo	0.4533	No
138	NYYLAMNKKGKLYGSKE	NotSumo	0.9646	No
140	YLAMNKKGKLYGSKEFN	NotSumo	0.7426	No
145	KKGKLYGSKEFNNDCKL	Sumo	0.3642	No
152	SKEFNNDCKLKERIEEN	Sumo	0.5827	No
154	EFNNDCKLKERIEENGY	Sumo	0.4841	No
184	QMYVALNGKGAPRRGQK	NotSumo	0.8858	No
192	KGAPRRGQKTRRKNTSA	NotSumo	0.0877	No
196	RRGQKTRRKNTSAHFLP	NotSumo	0.7126	No

Appendix 2 A SUMOylation site was predicted within human FGF10 at position K91 (A), but not within mouse protein (B).

Appendix 3: Representative data showing sequencing results of mutated sites within FGF10-HA construct

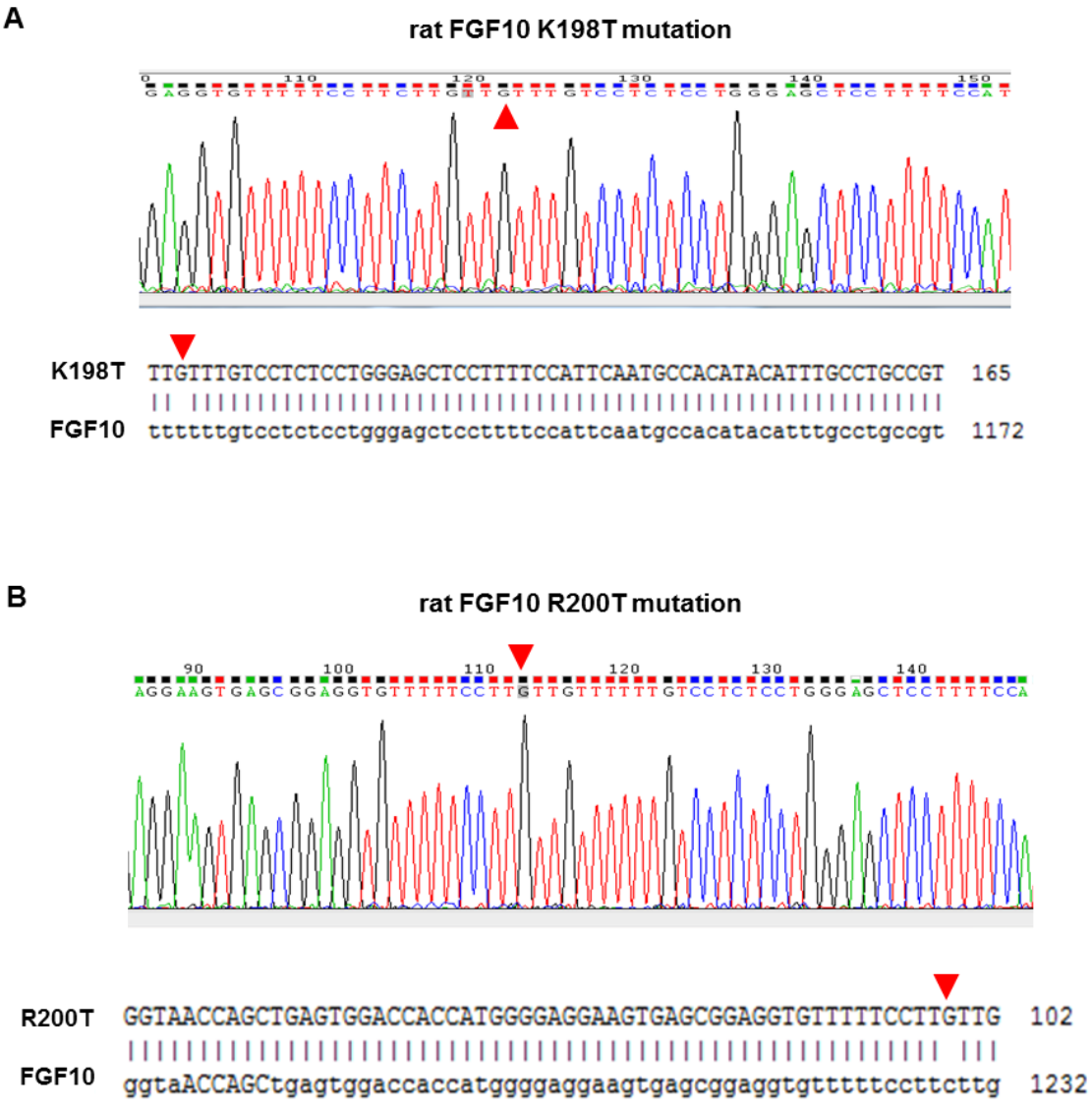

Appendix 3 Each residue substitution causing mutation has been validated through Sanger sequencing and compared to WT FGF10HA sequence. (A) Representative data showing single base substitution causing K198T mutation. (B) Representative data showing single base substitution causing R200T mutation.